VIBRATION AND FLUTTER OF UNSTIFFENED AND ORTHOGONALLY STIFFENED CIRCULAR CYLINDRICAL SHELLS

A Thesis

Submitted for the Degree of

DOCTOR OF PHILOSOPHY

of

LOUGHBOROUGH UNIVERSITY OF TECHNOLOGY

by

S. PARTHAN

Department of Transport Technology

April 1971

Supervisor: Professor D.J. Johns

ACKNOWLEDGEMENTS

It is a pleasure to express my deep sense of gratitude to Professor D.J. Johns for his valuable time and counsel during the course of this study.

Financial support was provided by the Ministry of Technology (U.K.) under contract no: AT/2170/07/STR.

The assistance rendered by Messrs. R. Payne, A. Newbold, N. Randall, J. Court, J.E. Smith, W. Squires and R. Hassett during the experimental work is also gratefully acknowledged.

ABSTRACT

The problem of vibration and flutter analysis of simply-supported unstiffened and orthogonally stiffened circular cylindrical shells which are typical of missile bodies has been developed and programmed for digital computer solution.

An extensive review of the existing literature covering various aspects of the shell flutter problem is given with a critical appraisal of the assumptions made, results obtained, etc. A comprehensive chronological bibliography is also included.

The analysis and the programme which have been developed are capable of handling shells of arbitrary geometrical, modal and flow parameters.

In the case of stiffened shells, the stiffener effects may be treated as 'averaged' ('smeared') or 'discrete' and in each case the influence of eccentricity, inplane and rotary inertias may be studied.

The aerodynamic generalised forces may be calculated using the linear piston theory, the linear piston theory with a correction for curvature, and the exact potential flow solution.

By combining the invacuo-natural vibration analysis and the aerodynamic generalised forces the cylindrical shell flutter problem may be solved and the flutter boundaries may be obtained in each of the above cases.

The procedures have been illustrated with typical examples in each of the above cases and the results discussed. A few shells have been tested using an experimental vibration rig designed and built for the purpose and compared with the theoretically predicted invacuo-natural frequencies and mode shapes.

LIST OF CONTENTS

LIST OF TABLES

LIST OF FIGURES

NOMENCLATURE

Capital letters

A_{uu}, A_{vu}, A_{wu}, etc.	structural operators (see eqn. I-1)
B	matrix elements
D	$\frac{Eh^3}{12(1-\nu^2)}$, flexural rigidity of the shell
E	Young's Modulus
G	Shear modulus
I	Moment of Inertia
J	Torsion constant
(K_r+1)	Total no. of rings
L	Length of the cylindrical shell
$2L_s$	Total no. of stringers
M	Mach number
Q_{mr}	Non-dimensional aerodynamic generalised forces
R	Radius of the cylindrical shell
T	Kinetic energy
U	Free stream velocity; also strain energy

Small letters

a_o	acoustic velocity
d	stringer spacing
g	artificial damping
h	shell thickness
i	$\sqrt{-1}$
k	$\Omega L/_U$, reduced frequency parameter
l	ring spacing
m	number of axial half-waves
n	number of circumferential full waves
p	aerodynamic pressure
q	dynamic pressure; also generalised co-ordinate

r	radial co-ordinate; also streamwise mode no.
s	Laplace transform variable
t	time variable
(u,v,w)	axial, tangential and radial displacements of the middle surface of the shell
$\bar{z}$	distance of the centroid of stiffener cross-section from shell middle surface

Greek letters

α	$\frac{h^2}{12R^2}$
β	$\sqrt{M^2-1}$
$\epsilon_x, \epsilon_y, \gamma_{xy}$	normal strains and shearing strains of the shell middle surface
ν	Poisson's ratio
ρ	material density
ρ_o	air density
Φ	velocity potential of fluid flow
θ	arbitrary spatial angle
ω	circular frequency of shell vibration
Ω	flutter frequency
σ	shell mass per unit area
∇^2	Laplacian operator
Δ	frequency factor $(\frac{\omega^2 mnR^2(1-\nu^2)}{E})$
λ_m	$\frac{m\pi R}{L}$

Subscripts

c, s, r	refer to cylindrical shell, stringers and rings as appropriate
o	refer to quantities referred to a line in the shell middle surface

Superscripts

D	Discrete
S	Smeared

NOTE: i) Other symbols are explained in the text

ii) Some of the above symbols have been used in other contexts when there is no scope for confusion. These symbols are explained in the section where they appear.

CHAPTER I
FLUTTER OF CIRCULAR CYLINDRICAL SHELLS - A REVIEW

Summary

A comprehensive review is given of the aerodynamic and structural assumptions made in the existing cylindrical shell flutter analyses. A review is also given of such analyses for shells of infinite and finite lengths. A critical discussion of analytical and experimental results is included and a comprehensive chronological bibliography is appended.

The intention is to assess the state of the art with regard to shell flutter analyses and indicate the areas where future investigations may usefully be made to add to the existing knowledge.

I.1 INTRODUCTION

Supersonic flutter of thin circular cylindrical shells is one of the important problems in the structural design of flight vehicles such as rockets and missiles.

The term "Panel Flutter" refers to the flutter of a thin plate, shell or membrane when, generally, one of the surfaces is exposed to an airstream and the other to still air. The panel then experiences elastic, inertia and aerodynamic forces which can lead to the dynamic instability of the structure. Extraneous disturbances such as aerodynamic noise, flow turbulence or oscillating shocks may also cause instability but these are not regarded as panel flutter and will not be considered here. The smallest thickness of the panel (shell) required to prevent instability at a given airstream velocity defines the "Flutter Boundary". For a given thickness, the minimum flight speed at which instability can occur is defined as the "Flutter Speed".

On practical aerospace structures the most vulnerable flutter condition often occurs near a point where the highest dynamic pressure is encountered and usually this is also

the point where severe structural loads are imposed. In general, the structural non-linearities tend to limit the flutter amplitudes and therefore cause the modes of structural failure to be related to fatigue rather than explosive fracture of the panel. However, it may be quite dangerous to regard panel flutter only as a fatigue problem. The existence of the flutter phenomenon has been demonstrated in the laboratories and in flight and there is considerable literature available to study the various aspects of the problem. Unfortunately there is no general reliable theoretical formula nor a computer programme of guaranteed accuracy to design against panel flutter for all conditions. The physical features of the problem are simple, the observed oscillations are usually mild but the experimental and theoretical difficulties are enormous.

The geometry and the co-ordinate system for the cylindrical shell are illustrated in Fig. 1(a).

I.2 STRUCTURAL ASSUMPTIONS

The first step in the formulation of the flutter problem is to determine the equations of motion which will adequately describe the invacuo natural vibration characteristics of the complete cylinder. A large number of formulations are available in the literature for the vibration analysis of cylindrical shells. Starting from Love's first approximation, many attempts have been made to refine or simplify the equilibrium equations to handle different situations.

If the components of displacements of the middle surface of the shell are u,v,w in the axial, circumferential and radial (positive outwards) directions respectively, all the various formulations may be written in the general form which expresses the quantities u,v,w in terms of the external loadings of the shell (Ref. 69).

$$\begin{bmatrix} A_{uu} & A_{vu} & A_{wu} \\ A_{uv} & A_{vv} & A_{vw} \\ A_{uw} & A_{vw} & A_{ww} \end{bmatrix} \begin{bmatrix} u \\ v \\ w \end{bmatrix} = \left(\frac{1-\nu^2}{Eh}\right) \cdot \begin{bmatrix} X + N_{yy}\left(\frac{\partial^2 v}{\partial x \partial y} - \frac{1}{R}\frac{\partial w}{\partial x}\right) \\ Y - N_{xx}\frac{\partial^2 v}{\partial x^2} \\ Z + N_{xx}\frac{\partial^2 w}{\partial x^2} + N_{yy}\left(\frac{\partial^2 w}{\partial y^2} + \frac{1}{R}\frac{\partial v}{\partial y}\right) \end{bmatrix} \quad - - - \quad (I.1)$$

where (u,v,w) are implicit functions of x,y,t; h is the shell thickness, R is the radius, E is the Young's modulus and ν is the Poisson's ratio. N_{xx}, N_{yy} are constant mid-plane stress resultants in the shell; the shear stress resultant N_{xy} has been neglected but may easily be included, e.g. Timoshenko (Ref. A17). The terms X Y,Z represent the external loadings in units of pressure and include all aerodynamic and inertia effects. The operators A_{ij} may be written as

$$A_{ij} = B_{ij} + \alpha C_{ij} \quad (I.2)$$

where $\alpha = \frac{h^2}{12R^2}$ is a small quantity. The operators B_{ij} are common to all the usual shell formulations but different formulations do occur in the C_{ij}.

To illustrate the form of equation (I.1) the expressions given below are based on the work of Novozhilov (Ref. A18) and Goldenveizer (Ref. A.9) and are comparable to the set used for linear panel flutter analyses by Voss (Ref. 35) and Johns (Ref. 32)

$$A_{uu} = \frac{\partial^2}{\partial x^2} + \frac{1-\nu}{2}\frac{\partial^2}{\partial y^2} \; ; \; A_{vu} = A_{uv} = \frac{1+\nu}{2}\frac{\partial^2}{\partial x \partial y} \; ; \; A_{wu} = A_{uw} = \frac{-\nu}{R}\frac{\partial}{\partial x}$$

$$A_{vv} = \frac{1-\nu}{2}\frac{\partial^2}{\partial x^2} + \frac{\partial^2}{\partial y^2} + \alpha\left\{2(1-\nu)\frac{\partial^2}{\partial x^2} + \frac{\partial^2}{\partial y^2}\right\}$$

$$A_{wv} = A_{vw} = -\frac{1}{R}\frac{\partial}{\partial y} + \alpha R\left\{(2-\nu)\frac{\partial^3}{\partial x^2 \partial y} + \frac{\partial^3}{\partial y^3}\right\}$$

$$A_{ww} = \frac{1}{R^2} + \alpha R^2 \nabla^4 \quad \text{where} \quad \nabla^4 = \left(\frac{\partial^2}{\partial x^2} + \frac{\partial^2}{\partial y^2}\right)^2$$

\- - - - (I.3)

Edge support conditions can have a pronounced effect on the flutter problem and, in the case of complex structural configurations analytical prediction procedures for the invacuo modes and frequencies can be quite inadequate; recourse should be had to measured values where possible.

The role of structural damping has been examined extensively and Ref. 133 provides a useful summary of the position. It is concluded that structural damping is usually stabilising for damping terms containing no spatial derivatives. Hence there is a distinct advantage in applying dissipative (damping) mechanisms at the panel boundaries. For finite surfaces having damping terms with spatial derivatives it will be extremely likely that a combination of parameters may be chosen to produce a destabilising effect. Therefore, for a cylindrical shell, structural damping may be stabilising or destabilising and it is recommended that theoretical studies should investigate this as a variable. There is no trend in analytical studies towards the sole use of either viscous or hysteric damping and both have been extensively used. For both types of damping the effect is proportionally greatest at higher altitudes when aerodynamic damping is least.

It may be concluded that for the flutter analysis of isotropic circular cylindrical shells the more exact equations be used without simplification, by including explicitly the effects of structural damping. For non-linear analysis alternative formulations are usually used.

I.3 AERODYNAMIC ASSUMPTIONS

I.3.1 General

The determination of aerodynamic forces on an oscillating cylindrical shell is a prerequisite for the study of its aeroelastic stability. Considerable efforts have been expended in recent years to develop aerodynamic theories for such shells.

Basically, the problem is to determine the aerodynamic forces on an oscillating cylindrical shell (of infinite or finite length) with the assumption of inviscid potential flow parallel to the generators of the shell. Mathematically, a solution is sought to the linearised, unsteady partial differential equation

$$\nabla^2 \phi - \frac{1}{a_o^2} \left\{ \frac{\partial^2 \phi}{\partial t^2} + 2U \frac{\partial^2 \phi}{\partial x \partial t} + U^2 \frac{\partial^2 \phi}{\partial x^2} \right\} = 0 \qquad (I.4)$$

with the appropriate boundary conditions depending on whether the shell is of infinite or finite length. In equation (I.4) ϕ is the velocity potential, U is the freestream velocity, a_o is the acoustic velocity and ∇^2 is the two-dimensional Laplacian operator

$$\nabla^2 = \frac{\partial^2}{\partial x^2} + \frac{\partial^2}{\partial y^2} \qquad (I.5)$$

The aerodynamic pressure p on the cylindrical shell is determined from the well-known Bernoulli equation

$$p = - \rho_o \left\{ \frac{\partial \phi}{\partial t} + U \frac{\partial \phi}{\partial x} \right\} \qquad (I.6)$$

I.3.2 Cylindrical Shells of Infinite Length

For a shell of infinite length, Leonard and Hedgepeth (Ref. 8) have determined the air forces by reducing the unsteady flow problem to a steady flow problem by means of a moving co-ordinate system and have obtained results for both subsonic and supersonic flows. Miles (Ref. 13) has made further simplifications in the aerodynamic theory using a plane wave approximation. Dowell (Ref. 87) has carried out a flutter analysis using an exact solution of equation (I.4) without any approximation. Bolotin (Ref. 74) formulated the problem using the full aerodynamic theory but carried out the stability analysis

by approximating the aerodynamic expressions. Dzygadlo and Kaliski (Ref. 36) have generalised the analysis of Miles to stiffened orthotropic shells. Most of these papers have used travelling wave solutions.

Stepanov (Ref. 14) has employed "piston theory" for the aerodynamic forces but this is inadequate for the flutter analysis of infinitely long cylindrical shells with travelling wave motions. This has been discussed by Miles (Ref. 32(a)). Krumhaar (Ref. 68) investigated the applicability of linear piston theory to infinitely long shells by applying the well known asymptotic expansions for cylinder functions to the solution of Leonard & Hedgepeth (Ref. 8) and suggested a first-order improvement to linear piston theory involving the addition of a curvature term in (w/R); thus

$$p = a_o \rho_o \left[a_o M \frac{\partial w}{\partial x} + \frac{\partial w}{\partial t} - \frac{a_o w}{2R} \right] \qquad (I.7)$$

No numerical results have been presented to compare the efficacy of the suggested improvement. However the terms in the asymptotic expansion process show that at least in the following cases

(i) $|M_1| < 1$, $|M_2| < 1$; (ii) $|M_1| < 1$, $|M_2| > 1$,

(iii) $|M_1| > 1$, $|M_2| < 1$

where $M_1 = M - \frac{\omega}{\nu_o a_o}$ and $M_2 = M + \frac{\omega}{\nu_o a_o}$ (with ω as the circular frequency, and ν_o as the wave number) linear piston theory (i.e. with the curvature term in equation (I.7) omitted) cannot be considered as a first order approximation for the determination of the aerodynamic pressure.

I.3.3 Cylindrical Shells of Finite Length

Steady or quasisteady theories in various forms have been used with success in recent years to predict the aerodynamic pressures on oscillating cylindrical shells of finite length; the forms more commonly used are the following:

$$p = - \frac{\rho_o U^2}{\sqrt{M^2-1}} \frac{\partial w}{\partial x} \qquad (I.8)$$

$$p = -\rho_o a_o \left[U \frac{\partial w}{\partial x} + \frac{\partial w}{\partial t}\right] \qquad (I.9)$$

$$p = -\frac{\rho_o U^2}{\sqrt{M^2-1}} \left[\frac{\partial w}{\partial x} + \frac{M^2-2}{M^2-1} \frac{1}{U} \frac{\partial w}{\partial t}\right] \qquad (I.10)$$

$$p = -\frac{\rho_o U^2}{\sqrt{M^2-1}} \left[\frac{\partial w}{\partial x} + \frac{M^2-2}{M^2-1} \frac{1}{U} \frac{\partial w}{\partial t} + \frac{1}{M^2-1} \frac{1}{U} \left(\frac{\partial w}{\partial t}\right)_{x=0}\right] \qquad (I.11)$$

The expression (I.8) is the Ackeret result, and (I.9) is the familiar linear piston theory expression which is valid for high Mach numbers. It is obvious that the expressions (I.10) and (I.11) which are obtained by an asymptotic expansion of an exact solution of equation (I.4) under various assumptions, will fail to give the first order term $\left(\frac{M^2-2}{M^2-1}\right)$ if the Mach number is close to $\sqrt{2}$, for then the coefficient of the aerodynamic damping term tends to zero.

In one of his papers, Fung (Ref. 65) mentions that the static, quasi-static or piston theory approximations of the aerodynamic pressure should not be used for "scallop" modes of flutter of cylindrical shells if the number of circumferential nodes is large (n of the order of 10). But a later investigation by Olson and Fung (Ref. 116) showed that a flutter analysis using piston theory yields results which corresponded more closely to experiment than those using the potential theory solution.

Kopzon (Ref. 12(a)) used an axial source distribution to obtain the aerodynamic loads on the cylinder and employed the Laplace-transform method to solve the resulting integro-differential equation similar to Goland and Luke's (Ref. 2(a)) approach for the case of flat panel. No numerical results are presented.

Refined aerodynamic expressions are obtained by Holt and Strack (Ref. 40) and Strearman (Ref. 76). In both these references a formal mathematical solution is presented in terms of Laplace transformation of the velocity potential for the unsteady flow problem in a manner similar to that used by

Randall (Ref. 19) in his investigation of the steady flow problem. The approximations used by Holt and Strack are rather severe and consist essentially of first reducing the unsteady flow problem to the steady flow problem and then expanding about the limiting case of two-dimensional flow. Only the first two terms of the expansion are retained, the first of which corresponds to the Ackeret result and the second term is a first-order correction to that result. The inherent approach is equivalent to neglecting the out-of-phase time effects and is only justified for oscillations of low frequency.

Dzygadlo (Ref. 57) has carried out an expansion process in a more systematic way. First three terms of the asymptotic expansion (in ascending powers of the inverse Mach number of the undisturbed flow) are retained and unsteady effects are included. The first term of the expansion is equivalent to the piston theory approximation. This expansion process however is not rapidly convergent. In a more recent paper Dzygadlo (Ref. 139) has generalised this approach to study the external or internal flows, for arbitrary time dependent oscillations of the shell.

An improvement to the static approximation of Holt and Strack (Ref. 40) is made by Brown and Holt (Ref. 66 and Ref. 77) by taking into account the first order effects of frequency. This causes a phase shift between the shell displacement and the corresponding pressure or the aerodynamic force coefficient which may decrease the energy transfer to the shell and thereby raise the critical flutter velocity. The phase angle which is a complicated function of the reduced frequency $\omega R/U$, the Mach number M and the axial co-ordinate x is approximated by Li (Ref. 113) who found that the flutter boundary is not lower than that of the static approximation (see Fig. 2).

Anderson (Ref. 112) has made some new observations by introducing an arbitrary spatial angle ψ in the pressure expression but neglecting the frequency effects. The results of a four-mode Galerkin analysis neglecting the

inplane loads are shown in Fig. 3. The curves are symmetric with respect to $\psi = 90^{\circ}$. Divergence is shown to be possible near $\psi = 90^{\circ}$ at very large values of dynamic pressure ratios (λ). If ψ is not exactly 90° then flutter can occur at very much lower values of λ and these values are insensitive to changes in ψ for a wide range (-30° to $+60^{\circ}$). This latter result suggests that for cylindrical shell analyses the details of pressure distribution are not so much of importance in low frequency flutter and that an Ackeret type theory can then probably be used with success.

Randall's method (Ref. 19) for the steady supersonic flow problem has been extended to the unsteady problem by Dowell (Ref. 98) and Davies (Ref. 137). Dowell has reduced the problem analytically to a single integration in terms of a Laplace transformation variable for the aerodynamic generalised forces and the integration is performed using the standard complex variable techniques. In another paper (Ref. 99) Dowell has adopted the Fourier transformation to solve both the supersonic and subsonic flow problems. It was found that for subsonic flow the Laplace transform method is not directly applicable and the Fourier transform method is less efficient for the supersonic flow problem. Dowell has published the first results using the full potential theory for the aerodynamic generalised forces (see Fig. 4). This theory, used in conjunction with an appropriate shell theory in a systematic stability analysis may permit the evaluation of the accuracy of the various existing simplified theories.

Explicit calculations of the generalised forces associated with each mode has been made by Coupry (Ref. 134) starting from the concept of equivalent distributions and an asymptotic expansion of the pressure potential.

In conclusion, it is considered that a need exists for a thorough and systematic study of the variations caused in flutter predictions by the use of different aerodynamic approximations as against exact potential solutions. In particular the analyses of Dowell would form a useful basis for such a comparative study.

I.4 FLUTTER ANALYSIS OF INFINITELY LONG CYLINDRICAL SHELLS

I.4.1 Unstiffened Cylindrical Shells

The aeroelastic stability of infinitely long isotropic cylindrical shells has been analysed by several authors under various assumptions.

Leonard and Hedgepeth (Ref. 8) have studied the flutter of infinitely long circular cylinders by including midplane tensile stresses and a small amount of structural damping. Donnell's equations are used to describe the structural behaviour and linearised unsteady potential theory predicts the aerodynamic pressures. When the number of circumferential waves (n) is small enough to invalidate the formulation, simplified Flügge's equations have been used to check the accuracy of the results. For unstiffened thin shells it is shown that the only instability at subsonic speeds is static divergence. At supersonic speeds flutter seems to be the only possible instability. The conclusion is reached that the second asymmetric mode (n=2) is the most critical with regard to stability on the premise that neither the axisymmetric mode (n=0) nor the first symmetric mode (n=1) involved panel action. Fig. 5 shows the stability boundaries for aluminium cylinders at sea level with no applied membrane stresses. The stability criteria are obtained by including the effects of structural damping and then taking the limit as damping tends to zero. This approach has led to the interesting result that the addition of damping makes the structure more prone to flutter. This may be explained by the fact that a damping force, even though in itself dissipative, can cause phase changes in such a manner as to allow the moving outside air to feed more energy into the structure resulting in a net energy gain.

Miles (Ref. 13) has analysed the same problem by using the Timoshenko shell equations and extending the flat panel analysis to include the curvature effect. The results show that the axisymmetric mode (n=0) generally yields the most critical flutter speed. The instability associated with $n \geq 2$ is shown likely to be much weaker than that associated with n=0, thus contradicting the results of Leonard & Hedgepeth.

Fig. 6 gives the minimum thickness ratio required to prevent flutter of an empty isotropic shell. By a precise examination of the neighbourhood of critical instability it can be concluded that while structural damping is beneficial in this neighbourhood, no finite amount thereof can prevent instability predicted by the linear theory. Axial prestress has the effect of increasing the theoretical flutter speed while the circumferential prestress has no such effect.

Thus, it can be seen from Figures 5 and 6 that both Leonard & Hedgepeth and Miles have obtained results that are practically identical as far as the thickness requirement to prevent flutter is concerned, even though their analyses were based on widely differing assumptions. This may be due to the fact that their aerodynamic approximations closely approximate to each other if the wavelength is small compared to the radius.

A different approach to the infinite length cylinder problem is due to Stepanov (Ref. 14) who has used piston theory aerodynamics in the Donnell's equations as well as in Goldenveizer's equations. The cases $n = 0$ and $n \geqslant 2$ are considered and it is found that the critical speed has a fixed value of h/R (h: thickness and R: radius) when n=0 and has the same minimum for larger values of n (of order 20). The value of critical Mach number obtained differs by unity from the corresponding value of Miles (see Fig. 7) due to the replacement of β by M in the airforce expression. The stability boundary is obtained through a more direct approach by solving an octic equation compared to the Nyquist diagram technique of Miles and Leonard & Hedgepeth. Stepanov has also concluded that the axisymmetric mode (n=0) is the most critical with regard to stability. However, the result is suspect because of the doubtful validity of piston theory to infinite cylinders.

The analysis given by Dowell (Ref. 85) attempts to overcome the limitations of the previous studies and very complete results are given for incompressible and compressible flows. An exact aerodynamic pressure expression is used with Goldenveizer's shell equations. Assuming the deflection in a travelling wave form

$$w = a \exp\left\{\frac{2\pi i}{l}(ct - x)\right\} \cos n\theta$$

$$(n=0,\ 1,\ 2,\ \ldots.) \qquad (I.12)$$

(where θ is the angular co-ordinate, a is the amplitude, l is the wave length and c is the phase velocity) and omitting the midplane inertia forces the flutter problem of an infinitely long cylindrical shell is reduced to the solution of an algebraic equation (which is formally identical to that for an infinite flat plate)

$$c_o^2 - c^2 - \mu F(U - c)^2 = 0 \qquad (I.13)$$

(where c_o is the transverse wave velocity of the panel in vacuum, μ is the mass ratio, U is the freestream velocity and F is the term representing the aerodynamic pressure). F is expressed in terms of Bessel functions thus facilitating the analysis considerably. The axisymmetric mode (n=0) and the asymmetric modes ($n \geqslant 2$) are considered separately. By minimising the critical velocity in each case with respect to (l/R) ratio (R: Radius of the cylinder) it is shown that the most critical configuration for very small structural damping is the asymmetric mode with n=2 and long waves (l/R of order $\sqrt{R/h}$, h: shell thickness) for low Mach numbers ($0 \leqslant M \leqslant M_o > 1$), while it is the axisymmetric mode (n=0) with short waves (l/R of order $\sqrt{h/R}$) for $M \geqslant M_o$. The value of M_o depends upon the mass ratio and the thickness ratio. The mass ratio effect is shown to be important in the transonic and low supersonic regime; the three-dimensional effect is only important in this regime, if in addition, the cylinder is relatively thick $h/R \sim 10^{-1}$. For high Mach numbers neither effect seems significant and the instability is relatively so weak that the low supersonic Mach number range ($M \lesssim 2$) may well prove to be of greater practical significance; even though the thickness required to prevent any instability increases with Mach number. A comparison of the n = 0 and n = 2 modes is made in Fig. 8, for an aluminium cylinder at sea level where the thickness required to prevent flutter is plotted against Mach number. The figure shows that

for $M < 1.52$, the n=2 mode gives the larger thickness requirement whereas for $M > 1.52$ the n=0 gives the largest thickness requirement. Thus either the n=0 or the n=2 mode could be most critical depending on the values of h/R, M, μ. Thus the results of Miles and Leonard & Hedgepeth are reconciled. For the asymmetric mode n=1 the wave length of instability is found to be infinite. However long cylinders at n=1 behave like beams and the model considered should be replaced by that used in the investigation of the stability of pipelines. An important consequence of the asymmetric mode ($n \geq 1$) calculations is the indication that the aerodynamic loadings in these modes are essentially of the 'slender body' types. Therefore compressibility effects seem to be relatively insignificant.

I.4.2 Stiffened Cylindrical Shells

The influence of adding rigid ring stiffeners which prevent radial deflections of unstiffened circular cylindrical shells is considered by Leonard & Hedgepeth (Ref. 8). The stiffeners are assumed not to interfere with the flow of air outside or of fluid inside the cylinder. The conclusion is reached that for ring stiffened shells also flutter is not possible at subsonic Mach numbers and the only possible instability is divergence. Fig. 9 shows the critical divergence boundaries for infinitely long unstressed ring stiffened aluminium cylinders at sea-level. Both panel flutter and divergence seem likely at supersonic Mach numbers but no numerical results are available.

The critical parameters of an eccentrically stiffened orthotropic anelastic shell vibrating in a linearised supersonic flow are determined by Dzygadlo and Kaliski (Ref. 36) including the effects of structural damping. Fig. 10 shows the effect of damping on the stability boundaries for an isotropic shell reinforced by rigid stringers. It has been found for a stringer stiffened shell also that an increase of damping can result in lowering the critical Mach number.

I.4.3 Experimental Studies

Experimental experiences on the flutter of unstiffened thin-walled pressurised and unpressurised cylinders seem to indicate that flutter, if it occurs in practice, is mild

in character and of wave lengths small compared to the radius of the cylindrical shell contrary to the prediction by infinite length shell theory. Well defined flutter has been observed where local buckling of the shell occurs, but in the case of unbuckled shells flutter has seldom been observed. Much more definitive experiment will have to be performed before the shell flutter problem is well understood.

The effects of membrane tension, internal pressure, internal fluid, aelotropic character of the shell material and boundary layer effects have all been theoretically analysed (see refs. 13, 16 and 22) but experimental results are lacking.

I.4.4 Dynamical Equations

All the analyses described so far have used the simplified Donnell's shell equations at some stage or other. These are strictly valid for $n \geqslant 2$ only. As the results seem to indicate that the low 'n' modes are the most critical, the question arises whether or not this equation is sufficiently accurate to describe the structural behaviour of the shell. For the case $n < 2$ more refined shell equations (e.g. Flügge's equations) are available. In addition, the mid-plane (longitudinal and circumferential) inertia forces tend to be more important for low n. However, as the wavelengths become smaller relative to the radius both these effects diminish in importance. Since the critical wavelengths seem to be of the order $\sqrt{\frac{h}{R}}$ it would appear that these effects are relatively unimportant and the use of Donnell's equations may be satisfactory. An analysis by Shulman (Ref. 24) to investigate this point suggest that this is indeed the case.

I.4.5 Applicability of the Analyses of Infinitely Long Shells to Shells of Finite Length

The validity of infinite length shell analyses to practical shell structures of finite length has not been proven and since large values of critical shell thickness result, they must be used with caution.

The results for the infinitely long shells would be applicable to shells of finite length only if the wave lengths

of the flutter modes are small in comparison with the length of the finite shell; but the most critical wavelengths for infinitely long unstiffened cylinders are predicted theoretically to be very large (see Fig. 11). It is conceivable that for a finite shell the flutter modes would tend to settle on the smaller of the two longitudinal wave lengths. However, for higher Mach numbers ($M \gtrsim 5$) even these smaller wave lengths are fairly high; for instance, for n=2 wave lengths from one to three times the radius have been experienced.

The comparison of the results of infinite and finite length shells are rather unrealistic since most of the existing analyses for finite length shells have adopted piston theory aerodynamic expressions which are inadequate for dealing with infinitely long cylindrical shells. Nevertheless, Dowell (Ref. 85) has made a comparison for the axisymmetric mode cases (n=0) since only for this case is the piston theory even qualitatively correct for a long narrow cylinder. It is concluded that the results of infinite length shells are applicable to finite length shells in a qualitative sense, as the aerodynamic damping coefficient g_A and thickness ratio h/R increase (see Fig. 12). Unfortunately the values of h/R which occur in practice may violate the conditions on which this contention is based.

The comparison of the results of infinite and finite length flutter analyses is also difficult in view of the fact that most of the analyses for the former class of problems have used the travelling wave solutions while the standing wave solutions are prevalent for the latter. However, Johns (Ref. 32) has applied the travelling wave solution to a shell of finite length in an axisymmetric (n=0) mode and obtained a value of 144 for the flutter speed parameter $\left(= \frac{24qL^3(1-\nu^2)}{MEh^3}\right)$. This value is more conservative compared to the corresponding value of 274 obtained by the standing wave approach. The inherent method is equivalent to applying the travelling wave analysis to one bay of an infinite shell with added rigid ring stiffeners and applying the boundary condition of zero radial deflections at the ring stiffeners.

I.4.6 Discussion of the Results

The results presented so far yielded the highest value of the thickness to radius ratio for which at least one wave mode will flutter (a wave mode is determined by particular values of n and the longitudinal wavelength) and seem to indicate that the lowest values of n are the most critical. The question of which one of the two wavelengths associated with each n is more critical, remains unsettled, though Miles concludes on the basis of his calculations that the shorter of the wavelengths is more critical. In this case his approximate aerodynamic expressions are probably acceptable.

If the thickness ratio is insufficient to prevent flutter, the degree of instability may be expressed as the number of cycles necessary to double the amplitude or as a logarithmic increment. The degree of instability in a real fluid is seen to be much smaller than that predicted on the basis of linearised potential theory.

I.5 FLUTTER ANALYSIS OF SHELLS OF FINITE LENGTH

I.5.1 General

In the treatment of panel flutter of infinitely long cylindrical shells the aerodynamic forces on the distorted cylinder have been calculated by a travelling wave approach, which are inapplicable for shells of finite length on physical grounds. This may partially account for the fact that the flutter speeds predicted by infinite length analyses are much lower than those observed in flight. Thus it is logical to investigate the analyses which include the effects of finite length. One additional factor which is to be considered for finite shell analyses is the boundary support conditions.

Considerable literature is available for studying the flutter problem of cylindrical shells of finite length to deal with different situations.

I.5.2 Cylindrical Shells with Different Boundary Conditions

Stepanov (Ref. 14) considers the problem of finite length cylinders under the following end support conditions: i) simply supported at both ends; ii) clamped at both ends; iii) simply-supported at one end and rigidly clamped on the other; iv) clamped at one end and free at the other; v) simply supported at one end and free at the other. Table 1 shows the values of the critical velocities for the boundary conditions (i), (ii) and (iii) just mentioned. The results seem to indicate that for all the thickness/radius and radius/length ratios considered, the simple support boundary conditions at both ends yields the minimum critical velocities compared to the others. Piston theory aerodynamics and the medium length shell theory due to Goldenveizer are used to reduce the order of the equations from eight to four and to enable the use of Movchan's method. The effect of this approximation is to neglect the longitudinal bending stiffness of the shell. Since the residual longitudinal stiffness is due solely to the membrane stresses and is inversely proportional to n^4, the result suggests that the flutter speed decreases monotonically with n. This means that there always exists a particular mode (n) for which the shell will flutter at any given speed. This result is obviously unacceptable on physical grounds.

Holt and Strack (Ref. 40) have attempted to improve Stepanov's analysis by introducing more refined expressions for the aerodynamic forces into the Goldenveizer's equations in the hope that the results would be valid for both supersonic and hypersonic flows. The inherent aerodynamic refinements have been discussed in section 3. The resulting equations are solved by a method similar to that used by Hedgepeth and Stepanov. The more realistic aerodynamic term is shown to lead to higher estimates of critical flutter Mach numbers than Stepanov's (see Fig. 13). Although a lower critical shell thickness is obtained, the static approximations for aerodynamics seems unrealistic in discounting the effect of time dependence and also makes it difficult to justify the retention of the inertia terms in the elastic equations which are of the second order in the reduced frequency parameter $\omega R/U$. The critical Mach numbersobtained decrease with the number of circumferential nodes as found by Stepanov.

Fig. 14 shows the thickness requirement curves for steel cylinders of finite length for the case of axisymmetric flutter mode (n=0). The results of Miles for infinite length shells are also shown for comparison and which reveal the considerable influence of finite length. Fig. 15 shows the results of Strack and Holt for the asymmetric flutter modes (n = 4, 7). If this is compared with the curves of Hedgepeth, the effect of finite length is again apparent. A comparison of the scale of ordinates of Figures 15 and 14 shows that the thickness requirement for flutter is far more critical for the axisymmetric mode n=0 and hence this mode was thought initially to be of the greatest interest. The number of circumferential modes n has only a minor effect on the stability of infinitely long shells (see Fig. 5), while their effect has since been shown to be considerable for finite length shells.

The discussion in the previous paragraph refers to the calculations based on the clamped-simple support boundary conditions. The effect of varying the end conditions is to change the values comprising the curves but not their form. Thus the value of the critical parameter H (which is a

function of the dynamic pressure, Mach number and R/h ratio) changes from 480 for the clamped-simple support condition to $(\frac{3}{2})(480)$ in the clamped-clamped case and to $(\frac{1}{4} \times 480)$ for the simple support conditions at both ends case suggesting that the simple support case yields the minimum critical speed.

I.5.3 Influence of Damping and Tangential Inertia Forces

The significance of structural damping, aerodynamic damping and mid-plane inertia (longitudinal and circumferential) forces on the cylindrical shell flutter results was shown by Voss (Ref. 35). He has presented a more exact formulation of the structural problem and has used an aerodynamic theory which can be shown to be similar to that of Stepanov and Strack & Holt, but resulting in a differential equation which suggests a modal solution. Only the 'freely-supported' boundary conditions are considered. A shallow shell analysis based on Reissner's equations revealed that if a modal solution of the cylindrical shell flutter problem is to be used, the determination of natural vibration frequencies should be as accurate as possible and that the formulation should include structural and aerodynamic damping. The expression used for aerodynamic loading at low supersonic speeds (and $M > \sqrt{2}$) is

$$p(x,y,t) = -\frac{2q}{\beta}\left\{\frac{\partial w}{\partial x} + \frac{M^2-2}{M^2-1}\frac{1}{U}\frac{\partial w}{\partial t} + \frac{1}{M^2-1}\frac{1}{U}\left(\frac{\partial w}{\partial t}\right)_{x=0}\right\} \quad (I.14)$$

where q is the dynamic pressure and $\beta = \sqrt{M^2-1}$ while for high supersonic speeds and simple harmonic motion it is

$$p(x,y,t) = -\frac{2q}{\beta}\left\{\frac{\partial w}{\partial x} + i\,\frac{\omega\gamma}{U}\,w\right\} e^{i\omega t} \quad (I.15)$$

where $\frac{q}{\beta}$ tends to $\frac{q}{M}$ for $M > M_1$ and

$$\gamma = \frac{M^2-2}{M^2-1} \quad \text{for} \quad \sqrt{2} < M < M_1$$
$$= 1 \quad \text{for} \quad M > 1 \quad (I.16)$$

and the value of M_1 is left to the user.

It has been shown by Voss that for n=0 the modal frequency spectrum is very dense with varying m and many m-modes are required for convergence but at high n this is not so. (See Figures 16 and 17). This result is particularly significant in the flutter solution wherein the modes are uncoupled spanwise - i.e. separate solutions are considered for each value of n. There are two ranges of critical modes to be considered for the cylinder: the first corresponds to low values of circumferential mode number n but relatively high values of longitudinal mode number m which will be referred to as membrane-type flutter and the second corresponds to high values of n and low values of m which will be referred to as panel-type flutter. Calculations performed on an aluminium cylinder (neglecting aerodynamic damping) of 40 inches diameter, 40 inches long and 0.04 inches thick revealed that for very low structural damping (g = 0.001) the initial instability occurs in the mode n=0 at $\frac{q}{\beta}$ = 5.4 and the next occurs in the mode n=16 at $\frac{q}{\beta}$ = 15.1 (see Figures 18 and 19). However the instability at n=0 is relatively weak by comparison and occurs at a considerably higher frequency. When structural damping was increased to 0.01 the critical condition for n=0 has been nearly trebled while the high n condition was but little affected (see Fig. 20). From figures 18, 19 and 20 it would appear therefore that the addition of aerodynamic damping could also delay the onset of low n instability to somewhat higher dynamic pressures particularly as this damping is strongly dependent on flutter frequency which is high for n=0; while the high n modes are conversely relatively unaffected in shifting the stability boundaries as the flutter frequency (and the lowest invacuo frequencies) are then much lower (see later).

Further, the neglect of tangential inertia forces is justified only for large values of n and/or m.

The correlation of these results with experiments is poor and there is need for further experimental evidence to substantiate these conclusions.

The study of Voss shows that the modal approach is entirely satisfactory for panel-type flutter analysis (i.e. with high number of circumferential modes) while it is not entirely satisfactory for membrane-type flutter due to

the large number of modes required to obtain convergence (up to 16 modes in m were used in the calculations).

The effect of aerodynamic damping has also been considered by by Johns (Ref. 32). His analysis is based on the theories of Love and Novozhilov used in conjunction with linear piston theory for the aerodynamic forces viz:

$$p = -\left\{ \frac{\rho_o U^2}{M} \frac{\partial w}{\partial x} + \frac{\rho_o U}{M} \frac{\partial w}{\partial t} \right\} \qquad \text{(I.17)}$$

For a shell of finite length L, simply supported at both ends, a compatible set of displacement functions used for the displacements u,v,w are:

$$\begin{aligned} u &= e^{i\Omega t} \sum_m \sum_n U_{mn} \cos \frac{ny}{R} \cos \frac{m\pi x}{L} \\ v &= e^{i\Omega t} \sum_m \sum_n V_{mn} \sin \frac{ny}{R} \sin \frac{m\pi x}{L} \qquad \text{(I.18)} \\ w &= e^{i\Omega t} \sum_m \sum_n W_{mn} \cos \frac{ny}{R} \sin \frac{m\pi x}{L} \end{aligned}$$

A two degree of freedom analysis and the Galerkin procedure leads to the following expressions for the flutter speed and frequency respectively:

$$2\sigma\Omega^2 = F_r + F_s \qquad \text{(I.19)}$$

$$4\left(\frac{\rho_o U^2}{L M}\right)^2 \left(\frac{4rs}{r^2 - s^2}\right)^2 = (F_r - F_s)^2 + 4\left(\frac{\rho_o U \Omega}{M}\right)^2 \qquad \text{(I.20)}$$

where $F_m = \frac{Eh}{R^2(1-\nu^2)} \left\{ \frac{\alpha(\lambda_m^2 + n^2)^4 + \lambda_m^4 (1 - \nu^2)}{(\lambda_m^2 + n^2)^2} \right\}$ (I.21)

and m = r,s, with the condition that (r + s) must be odd. The term $\frac{\rho_o U \Omega}{M}$ represents the aerodynamic damping the neglect of which can be justified only when Ω is small (as in the case of plane panels). For cylindrical shells, Ω is much higher because of the curvature effects and is given by

$$\Omega^2 = \tfrac{1}{2}(\Omega_r^2 + \Omega_s^2) = \frac{1}{2\sigma} (F_r + F_s) \qquad \text{(I.22)}$$

where $\Omega_{r,s}$ are the natural frequencies in the r,s modes. To illustrate the significance of the aerodynamic damping terms, table 2 represents the results for a particular shell in which it is assumed that the axisymmetric mode n=0 is the most critical. This analysis has neglected the tangential inertia forces. It is felt that these should be included, the justification for this being that the critical speeds in the absence of aerodynamic damping depend on the quantity $(F_r - F_s)^2$ and thus on the difference in the squares of the natural frequencies. This difference appears to be least when tangential inertia forces are neglected, for n=0, r=2, s=1. This is not so when the tangential inertia forces are included. The analysis of Voss also confirms that this is so.

The simple binary flutter analysis of Johns indicates that the axisymmetric flutter mode is the most critical if the aerodynamic damping is neglected but that this is not in general a justifiable assumption.

The fact that the aerodynamic damping is not negligible is also revealed by the studies of Kobayashi (Ref. 71). Effects of the internal pressure and the axial force on the flutter boundary are also studied. Kobayashi has used the Donnell's equation, quasi-steady aerodynamic force and Galerkin's two-mode approximation to the case of a cylindrical shell which is simply supported at both ends. It is concluded that the aerodynamic damping and internal pressure raise the flutter boundary while the axial compression lowers it. The results for n≠0 cases are given in Fig. 21.

I.5.4 Applicability of the Galerkin Method

The applicability of the Galerkin method to cylindrical shells has been confirmed by Krumhaar (Ref. 42) who has developed 'exact' results for the axisymmetric flutter of a simply supported circular cylindrical shell as presented in Fig. 22. By using linearised Timoshenko shell equations and linear piston theory the problem is reduced to a non-self-adjoint eigenvalue problem. This is rigorously investigated without any further approximations. The following conclusions are drawn from the analysis. Aerodynamic and structural damping

have a considerable stabilising effect as was pointed out by Voss (Ref. 35), while the influence of internal pressure differential is very small. The larger the air stream velocity the more modes one has to employ in the Galerkin method to obtain reliable results. Flutter could not be observed experimentally in the Mach number range predicted by this analysis. The unsatisfactory physical assumptions, piston theory aerodynamic approximation, the neglect of both boundary layer effects and tangential inertia forces are thought to be responsible, at least partially for the disagreement. The results of Krumhaar lead to considerably higher estimates of critical flutter Mach numbers than those of Holt and Strack (see Fig. 23).

The mode shapes in the neighbourhood of the flutter boundaries given by Krumhaar (Ref. 42) are investigated by Müller (Ref. 135). Fig. 24 represents the real parts of the mode shapes for two values of the generalised velocity A belonging to the stable domain ($A < A_{crit}$), the critical value ($A = A_{crit}$) and for two values of A belonging to the unstable domain ($A > A_{crit}$). It can be observed that the maxima are shifted towards the trailing edge of the shell with increasing airstream velocities. These results are consistent with those of Movchan (Ref. 55) for flat panels finite length.

I.55 Influence of the Boundary Layer

The influence of the boundary layer on the flutter of cylindrical shells has been examined by Anderson and Fung (Refs. 54 and 65). A uniform parallel subsonic layer of constant thickness is assumed to exist between the external supersonic flow and the oscillating cylindrical shell. It is inferred that the boundary layer has a large effect with respect to scallop modes of flutter even at high Mach numbers. The effect is to stabilise the high n flutter so that the neglect of boundary layer leads to conservative results (see Fig. 25). For axisymmetric flutter for which structural damping has a large influence, whether the neglect of boundary layer effect is considerable or not is still uncertain.

This problem was re-examined by Olson (Ref. 101) using a somewhat more realistic boundary layer model - that of a

parallel shear flow with a velocity profile given by the mean velocity distribution in a classical turbulent boundary layer. The oscillating shell surface was approximated by an oscillating plane wall whose deflection was sinusoidal in both plane directions. Viscous effects were neglected with respect to flow perturbation quantities and the resulting equations were linearised. The final equations admitted solutions with exponential dependence on time and the inplane co-ordinate directions but had to be integrated numerically in the direction normal to the plane. The results from this study and the results of the later work by Anderson (Ref. 90) indicated that the influence of the boundary layer may have been overpredicted by an order of magnitude in the earlier work (Ref. 54).

The main parameter that governs influence of boundary layer in the linearised problem is the ratio of the boundary layer thickness to the axial wave length of the wall deflection. The boundary layer thickness decreases as this parameter decreases. For cylindrical shell flutter with a large number of circumferential waves the pertinent axial wave lengths of interest are very large with respect to the boundary layer thickness (at least for the experimental configurations reported by Olson and Fung (Ref. 116)) so that the influence of boundary layer is probably negligible. Intuitively it is understandable that this might be so since in the boundary layer theory it is shown that the transverse pressure variation is of second order and in practical calculations the pressure inside the boundary layer is always taken to be the same as that of the outside potential flow. Therefore the aerodynamic force on the shell should not differ too much from that of the potential flow if a boundary layer exists at all (also see Ref. 113).

I.5.6 Experimental Investigations and Flutter Criteria

The first successful experimental observation of cylindrical shell flutter was observed at the NASA Ames 8-x7-ft. supersonic tunnel in May 1962 (Refs. 53 and 65). The flutter condition formulated in linearised theories (an exponential increase of amplitude with increasing time) was

unobservable in the experiments. Hence an experimental definition of flutter was suggested by Fung (Ref. 65) leading to the criterion

$$\left(\frac{q}{E\beta}\right)^{\frac{1}{3}} \left(\frac{R}{h}\right) \approx 7 \qquad \text{(I.23)}$$

which seems to be independent of the length of the shell. Additional tests on the same shels by Olson (Ref. 86) confirm this equation. Since the shells tested were of the same length, this criterion needs further confirmation. The tests of Stearman (Ref. 53) and Olson (Ref. 86) for $L/_R = 2$ show that the value of n_{crit} is in the range 14 to 25 (see Fig. 26). It is of interest to note that for n = 25 the effective $L/_W$ for each shell element between the streamwise nodal lines is about 16 and for n = 14, $L/_W \approx 9$, Equation (I.23) may be rewritten as

$$\left(\frac{\beta E}{q}\right)^{\frac{1}{3}} \left(\frac{h}{L}\right) \approx \frac{1}{7} \frac{R}{L} \qquad \text{(I.24)}$$

and if this equation with $L/_R = 2$ is compared with Fig. 27 for unswept flat panels (Ref. 51) it can be seen that the agreement is good for $L/_W$ in the range 9-16. Thus it would appear that for the high-n flutter of cylindrical shells the individual panels between longitudinal nodal lines behave similarly to flat rectangular panels and equation (I.23) could be interpreted as a special case of the general results shown in Fig. 27.

For the high-n case Voss (Ref. 35) has indicated that aerodynamic damping should not modify the flutter boundaries significantly presumably because the flutter frequencies are then much lower than for the n=0 case where the aerodynamic damping is known to be most important.

If the two-mode (m=2,1) closed form solutions of Johns (Ref. 32) are analysed for the high-n case with the aerodynamic damping neglected, it can be shown that for

Ref. 96) $n^2 >> \lambda_m^2$ (with $\lambda_m = \frac{2\pi R}{L}$),

$$n^6_{crit} = 5\left(\frac{1-\nu^2}{\alpha}\right)\left(\frac{\pi R}{L}\right)^2 \qquad (I.25)$$

This result is also derived by Shulman (Ref. 24) who has shown that the value of n_{crit} is not necessarily equal to the value of n for the minimum in-vacuo frequency. The corresponding expression for the critical dynamic pressure parameter is

$$\left(\frac{q}{E\beta}\right)^{\frac{1}{3}}\left(\frac{R}{L}\right) \approx 0.912 \left\{n^2_{crit}\frac{R}{L}\right\}^{\frac{1}{3}} \qquad (I.26)$$

Substitution of eqn. (I.25) into (I.26) leads to a criterion of the form

$$\left(\frac{q}{\beta E}\right) = 6.2\left(\frac{h}{R}\right)^{7/3}\left(\frac{R}{L}\right)^{5/3} \qquad (I.27)$$

and it is seen that length L appears explicitly as a parameter.

Inserting the shell data of Stearman et al (Ref. 53) into eqns. (I.25) and (I.26) gives the results

$$n_{crit} = 31 \qquad (I.28)$$

$$\left(\frac{q}{E\beta}\right)^{\frac{1}{3}}\left(\frac{R}{L}\right) \approx 7.2 \qquad (I.29)$$

Although the estimate of n_{crit} is in error, the agreement of equation (I.29) with (I.23) is remarkably good. However, because of the inherent assumptions made in deriving equations (I.27) to (I.29), these cannot be taken as general.

A semi-empirical criterion to determine the flutter boundary of simply-supported cylinders which also includes the length of the shell as a parameter and is applicable for a wide range of $L/_R$ and $R/_h$ is given by Dixon and Hudson (Ref. 141) as

$$\lambda^* = \begin{cases} \dfrac{\lambda_R}{(1-\nu^2)}\left(\dfrac{h}{R}\right)^x & \text{for } L/_R \geq 1 \\ \dfrac{\lambda_R}{1-\nu^2}\left(\dfrac{h}{R}\right)^x\left(\dfrac{L}{R}\right)^3 & \text{for } L/_R < 1 \end{cases} \qquad (I.30)$$

where $\lambda_R = (1 - \nu^2) \left(\frac{R}{h} \right)^x f\left(\frac{L}{R} \right)$, $x = \tanh \left(\frac{0.5L}{R} \right)$.

Table 3 gives the average calculated values of λ^* for no aerodynamic damping for a range of values of $\left(\frac{L}{R} \right)$. The variation of λ^* with $L/_R$ is indicated in Fig. 28, showing good agreement with other theoretical and experimental results. This also reveals that length is a very significant factor in cylinder flutter, thus indicating that theoretical solutions of infinite shells would be of little value in predicting the results for finite cylinders.

Also shown on Fig. 28 is the two-mode result of eqn. (I.27) and interestingly the agreement is reasonable at $L/_R = 0$ and $L/_R = 2$ with the experimental and theoretical results. The two mode result is unconservative for $L/_R > 2.2$

Circumferentially travelling wave type of flutter in Olson's experiments (Ref. 86) were observed to be critical in high n modes (of order 20) while standing waves in the longitudinal direction were more critical with zero, one or two, circumferential nodal lines. It was found (in qualitative agreement with theory) that small amounts of internal pressurisation were very stabilising but moderate amounts reduced stability to the unpressurised level. On the other hand, contrary to theory, large amounts of pressurisation completely stabilised the shells, independent of axial loading or previous buckling conditions.

Olson and Fung (Ref. 116) assumed that flutter occurs with a large value of n and, by using Donnell's fourth order cylinder equations, have derived equations for $\hat{\lambda}$ and n_{crit} similar to those discussed in equations (I.23) to (I.29). On the basis of these two mode analyses with aerodynamic damping neglected it was concluded that a static internal pressure differential has no effect on the flutter boundary. However, the modal frequencies which couple to produce scallop mode flutter increase rapidly with internal pressurewhen n is large and so, also, does the flutter frequency. As a result it becomes no longer valid to neglect the aerodynamic damping when the internal pressure is large. Therefore the critical

flutter boundary is raised, as indicated in Fig. 29. It should be emphasized that the internal pressure was not of the hydrostatic type as this would presumably have been immediately stabilising due to the axial tensile stresses introduced. Corresponding results are also shown in Fig. 29 for four and six mode analyses employing, respectively, piston theory and Ref.8 potential theory, as well as from experiments. The potential solution flutter boundaries are seen to be somewhat higher than the piston theory boundaries which are higher than, but closer to, the experimental results. Both the aerodynamic theories seem to predict the same stabilising influence of the internal pressure but interestingly the more refined aerodynamic theories seem to yield unconservative results.

Critical flutter speeds for a shell have also been computed by Shveiko (Ref. 34) using piston theory in a Galerkin analysis. The modes of vibration corresponding to the critical flutter speed is found to have at least six waves around the circumference. Increase of damping leads to higher critical Mach numbers but the wave number seems to decrease slightly. No experimental results are available to compare these results. In a later paper, Shveiko (Ref. 83) has considered the effect of a liquid filler contained within the shell and found that the hydrostatic pressure of the liquid increased the critical velocity but the value of n_{crit} was not modified when the shell was completely filled.

I.5.7 Non-linear theories

An attempt to analyse the non-linear effects which strongly influence the experimental phenomena has been made by Olson and Fung (Ref. 65). They have presented a non-linear flutter analysis based on a two-mode, piston theory approximation in a Galerkin procedure to obtain an approximate limit cycle solution. The results which are of a qualitative character, indicate that for practical purposes, cylindrical shell flutter in a standing wave mode does not occur below the stability boundary predicted by linear theory for infinitesimal disturbances and that the limit cycle amplitudes seem to agree well with those observed experimentally. The interesting result is reported that for high asymmetric mode flutter, the critical

mode may jump from one circumferential wave to another as one penetrates into the flutter regime. On Fig. 30 the peak limit cycle versus dynamic pressure curve is shown schematically. A reversal in the slope of the curve can be observed. Olson has determined the two portions of the curve as stable and unstable regimes respectively. Presumably as one reaches λ_b the critical flutter mode jumps from n=23 to a neighbouring flutter curve, which has a stable limit cycle with, say, n=22. Olson cites some indications of such a behaviour from his experiments.

A more detailed and refined non-linear analysis is presented by Olson and Evenson (Ref. 115) by using the non-linear Donnell's shell theory, the linear piston theory and the Galerkin procedure. The limit cycle solution is obtained by the method of harmonic balance. Two types of limit cycle flutter are obtained i) two-mode standing wave flutter and ii) four-mode circumferentially travelling wave flutter. It has been demonstrated that the circumferentially travelling wave flutter, which has been observed experimentally, can be predicted from a non-linear analysis. Fig. 31 illustrates the limit cycle amplitudes for values of n varying from 17 to 27 and for zero structural damping. The analysis indicates that flutter can occur at aerodynamic pressures below the linear flutter boundary - which may explain some of the unconservatism in the linear theory.

Some other refinements are introduced into the structural aspects of the shell flutter analysis by Carter and Stearman (Ref. 111) in an attempt to explain the discrepancies between experimental and theoretical results. The analysis utilizes the non-linear Donnell shell theory coupled with a linear potential flow theory approximation for the aerodynamic loading. The axisymmetric preflutter deformation due to internal pressurisation and axial loading and the aerodynamic loading induced by this preflutter deformation are included in the analysis. However, the flutter solutions are obtained by Galerkin's technique applied to the linearised equations. The calculations show that the predeformation state due to static loading conditions does not appreciably affect the flutter boundaries

for the range of parameters employed in the experiments (see Fig. 32). In particular it tends to stabilise the shell and hence, its neglect in a design analysis would be conservative. The fact that a large number of terms are needed to obtain convergence in the Galerkin procedure, particularly at higher values of shell internal pressure is revealed in Fig. 33. The conclusion is also reached that the flutter boundaries are sensitive to the type of structural boundary conditions and that the agreement between theory and experiment becomes progressively worse as the amount of preloading is increased.

Barr and Stearman (Ref. 126) have extended the analysis of Carter and Stearman by incorporating initial geometric imperfections and radial edge constraint and prestability deformation. The combined influence of initial imperfections and prestability deformation is found to be strongly destabilising probably due to the induced curvature of the middle surface over the central portion of the shell. The results show excellent correlation with the band of the experiment data plotted in Fig. 29, for all values of shell internal pressure. In a more recent paper (Ref. 142), Barr and Stearman have studied the influence of an external supersonic flow field on the critical buckling load of a finite shell subjected to axial compressive loading and internal pressure. They conclude that the critical buckling load and circumferential wave number of the static instability are not significantly influenced by the supersonic flow field. This has also been demonstrated by Fung (Ref. 92).

Librescu and Malaiu (Ref. 138) have obtained the non-linear flutter equations using an infinite number of modes in the Galerkin method. The shells are considered to be hetrogeneous and orthotropic and the non-linearities are considered to be geometrical and aerodynamic in nature. In the case of a large geometric non-linearity the excitation of flutter on the boundary of the instability domain results in the fact that a small increment of the critical velocity is shown to correspond to small amplitude increases, making the critical flutter boundary "non-dangerous" while for an increase of Mach number when the aerodynamic non-linearity is

prevalent the critical flutter boundary tends to be "dangerous".

I.6 CONCLUSIONS AND SCOPE OF THE PROPOSED INVESTIGATIONS

It is apparent from the review that the shell flutter problem has been approached from both the linear and the non-linear formulations. On the linear formulation the aim has been to determine the flutter boundaries. The investigations carried out in this field differ either as regards the physical aspects (such as different shell equations, influence of inertia forces, structural damping, etc., from the structural viewpoint; different approximations for the aerodynamic forces, the role of aerodynamic damping, boundary layer effects, etc., from the aerodynamic point of view), or as regards the mathematical manner of approaching the problem. On the non-linear approach the aim has been to determine the conditions in which the critical flutter speed can be exceeded without an immediate failure of the structure (i.e. the flutter is mild) or the case in which the flutter is violent; the character of the non-linearities themselves may be important in such analyses.

It is also clear that most of the analyses reviewed have tended to use the simplest structural and aerodynamic theories that yield acceptable results for Mach numbers and shell geometries of interest. The structural equations usually used are those due to Donnell, Goldenveizer, Novozhilov, etc., with different approximations or additions such as mid-plane inertia terms, structural damping, etc. The aerodynamic expressions are available from the simplest solution (such as the Ackeret Result or the linear piston theory) to the exact potential flow solution for an oscillating cylindrical shell of finite length, with various intermediate approximations. However the choice of a particular aerodynamic theory for application to shell flutter is usually based on the order of magnitude considerations or on the success achieved in previous flutter investigations and yet no shell flutter calculations appear to have been performed using any of the existing exact aerodynamic theories.

The range of aerodynamic assumptions and the flutter

predictions which result have shown a great need for a comparative study to be made of the influence of aerodynamic approximations in shell flutter. (Ref. 144)

Whilst experimental data on unstiffened shell flutter is scanty and evidenceof full-scale incidents apparently non-existent, there remains a strong possibility that high n mode flutter may occur on longitudinally stiffened shell structures for which the stiffener effect can be minimised by a correspondance of stiffener-spacing and nodal pattern. Hence there is a need for further studies to be made of the influence of stiffeners (including eccentricity effects) on the flutter.

The following aspects have been investigated in the studies conducted for the Ministry of Technology of which this review is a part.

i) A simple analytical method has been developed for the invacuo-natural vibration analysis of simply-supported circular cylindrical shells which are stiffened by an orthogonal set of stringers and/or rings, to include the effects of eccentricity, inplane and rotary inertias, by a) treating the stiffener effects as "smeared" or averaged over the surface of the shell and b) treating the stiffeners as discrete members of the structure. A few such shells have been tested in an experimental rig, designed and built during the course of this study, to verify the theoretical results for these natural vibration modes and frequencies. (Refs. A36, A37)

ii) The aerodynamic generalised forces obtained from a form of linear piston theory are compared with those from exact potential flow solutions for a harmonically oscillating circular cylindrical shell with a view to having an indication of the areas of agreement (or otherwise) between the two theories. (Ref. A38)

iii) The flutter problem is formulated in terms of the invacuo-natural frequency factor of the cylindrical shell and the aerodynamic generalised forces for a multi-degree of freedom system (i.e. for a given circumferential

modal pattern and the interaction of any number of axial modes), and programmed for digital computer solution. The influence of eccentric stiffening has also been included in the frequency expressions. (Ref. A38)

iv) Flutter boundaries for unstiffened shells are obtained for a two-mode Galerkin solution for a range of shell geometries of various lengths/radii and thickness/radii ratios and compared with higher order solutions using up to ten axial modes to assess the convergence of the solutions. Comparison is also made of these boundaries with the flutter boundaries obtained using aerodynamic generalised forces derived from the exact potential flow solution. (Ref. A38)

v) Flutter boundaries for stringer stiffened shells are obtained for a two mode Galerkin solution using the linear piston theory for a range of eccentricities, a range of shell geometries of different length/radius and thickness/radius ratios and compared with higher order solutions up to ten to assess the convergence. (Ref. A39)

CHAPTER 2
VIBRATION ANALYSIS - THEORY

Summary

A simple analytical method is developed for free vibration analysis of simply-supported circular cylindrical shells which are stiffened by an orthogonal set of stringers and/or rings, to include the effects of eccentricity, inplane and rotary inertias, with stiffeners treated as i) discrete elements and ii) 'smeared' over the surface of the shell.

The intention was to eventually develop a program using the information presented in this section for supersonic shell flutter analysis. To that end it was decided at an early stage that the generalised aerodynamic forces would be more easily determined using the single, simple trigonometric mode chosen than from a more complex set of normal modes. Such a set could be obtained from a vibration analysis involving many degrees of freedom as in Ref. A22 but this has not been attempted here.

II.1 GENERAL

The first step in the formulation of the flutter problem is to determine the equations of motion which will adequately describe the invacuo-natural vibration characteristics of the structure. In this study the structure is a missile body which can be idealised to a circular cylindrical shell. A large number of different formulations is available in the literature for determining the natural frequencies of such shells.

II.2 UNSTIFFENED CYLINDRICAL SHELLS

The problem of determining the vibration characteristics of circular cylindrical shells of finite length has been of interest to engineers and scientists for over a century. This interest is maintained in the aerospace industry and elsewhere when the structural response to dynamic loads must be predicted with extreme accuracy.

Starting from Love's first approximation many attempts have been made to refine or simplify the equilibrium equations for cylindrical shells. The literature is too numerous to give a complete survey of all the work done in this field. In general, it can be said that the wide variety of the resulting equations arise basically from small differences in the formulation of the strain-displacement relationships, and the discrepancies occur only in those terms which have little numerical significance. As long as the limitations of thin shell theory are observed, all the different formulations generally give numerical results within about three to four per cent. An excellent account of this fact is given by Warburton (Ref. A23) where it is remarked that for a wide range of parameters the effect of various shell theories is very small. An extensive review of shell dynamics can be found in Ref. A24.

The procedures for the determination of the natural frequencies of unstiffened cylindrical shells can be combined, basically, into two broad groups: i) By considering the equilibrium of an element of the shell, three differential equations containing the displacements (u, v, w) as unknowns can be derived. The exact solution of a dynamical problem requires the determination of (u,v,w) to satisfy the equilibrium equations and the boundary conditions. For most practical end conditions it would be rather difficult to obtain the solution this way. Alternatively the Galerkin method may be applied to these differential equations to obtain an approximate solution. ii) Alternatively, the strain and kinetic energies of the shell element can be written and integrated over the volume of the shell. This method forms the basis of the Rayleigh-Ritz procedure and is usually considered to be approximate. The success of this method and of the Galerkin Method depends on the choice of appropriate functions for the displacements (u,v,w).

Considering the basic point of simplicity and accuracy

of the various shell theories, the only comprehensive results are the natural frequencies of cylindrical shells with simply supported ends. With this end support condition the energy method gives exact results since the assumed mode shapes are exact solutions of the equilibrium equations. Simple support conditions are typical of missile bodies between two stiffening rings and also one bay of, say, a tall chimney between two heavy intermediate rings.

II.3 STIFFENED CYLINDRICAL SHELLS

The vibration analysis of stiffened cylindrical shells is of considerable interest in the design of various types of structures in air, space and water craft. Theoretical investigations of this problem may be divided into two broad classes: i) those in which the stiffener effects are averaged or 'smeared' over the entire surface of the shell - this effectively amounts to replacing the stiffened shell by an equivalent monocoque shell with orthotropic properties, and ii) those in which the stiffeners are treated as discrete members of the structure.

As in the case of unstiffened shells, solutions have been obtained in the literature by the differential equations approach and the energy method, for this class of problems also. However, in order to represent the stiffener effects accurately with a minimum of effort the energy approach is considered to provide a sufficiently accurate formulation. An excellent bibliography of literature related to stiffened shells is contained in Ref. A25.

Several methods have been developed in recent years for studying the vibration characteristics of stiffened cylindrical shells, with various assumptions. Hoppmann (Refs. A26, A27) replaced the stiffened shell by an equivalent orthotropic shell of some uniform thickness, having the equivalent stiffness characteristics and verified his theoretical results with experiment for the simple support boundary conditions. Consequently the effects of eccentricity, rotary inertia and stiffener con-

figuration are not explicitely discussed. The analysis of McElman, et al (Refs. A28, A29) considers the eccentricity effects by averaging ("smearing") the stiffener effects over the shell surface and neglecting the inplane and rotary inertias. Egle and Sewall (Ref. A22) have presented a solution for stiffened shells by treating the stiffeners as discrete elements and considering the symmetric and anti-symmetric modes separately, leading to the evaluation of a large determinant. Schnell and Heinrischbeuer (Ref. A30) compare the results obtained by smeared and discrete solutions with experiments. The method of Scruggs, et al (Ref. A31) relaxes the requirement of large wavelength to spacing ratio by providing for the effects of inter-stiffener deformations.

The purpose of the present investigation is to develop a simple, comprehensive vibration analysis to include the effects of eccentricity, inplane and rotary inertias; to examine the efficacy of i) the stiffener discreteness as compared to stiffener smearing, and ii) stiffener configuration; and to study the influence of various inertia terms on the natural frequencies of vibration of stiffened cylindrical shells. The mode shapes corresponding to simple support boundary conditions of the unstiffened shell are assumed to describe also the mode shapes of the stiffened shell. The Rayleigh-Ritz technique is adopted to derive the frequency equation. Numerical results are presented for three specific cases and are compared with existing experimental and theoretical results.

II.4 ANALYSIS

A vibration analysis is developed, based on the energy approach. Expressions for the strain energy and kinetic energy of the shell and stiffeners are derived in terms of the axial, circumferential and radial displacements (u,v,w) of the shell middle surface, with due allowance for eccentricity, inplane and rotary inertias. Vibration modes appropriate to the simple support boundary condition are assumed. For this boundary condition the energy approach

is exact in the case of unstiffened shells because the assumed mode shapes are exact solutions of the equilibrium equations.

II.5 BASIC RELATIONSHIPS

The displacements (u', v', w') of any point of the shell or stiffeners can be expressed in terms of the shell middle surface displacements (u, v, w) as

$$\begin{aligned} u' &= u - z\frac{\partial w}{\partial x} \\ v' &= v - z\frac{\partial w}{\partial y} \\ w' &= w \end{aligned} \qquad \text{(II.1)}$$

The strains (ϵ'_x, ϵ'_y, γ'_{xy}) at a distance z from the shell middle surface are given by the linear Donnell-type relations

$$\begin{aligned} \epsilon'_x &= \epsilon_x - z\frac{\partial^2 w}{\partial x^2} \\ \epsilon'_y &= \epsilon_y - z\frac{\partial^2 w}{\partial y^2} \\ \gamma'_{xy} &= \gamma_{xy} - 2z\frac{\partial^2 w}{\partial x \partial y} \end{aligned} \qquad \text{(II.2)}$$

Where the middle surface strains (ϵ_x, ϵ_y, γ_{xy}) are defined as

$$\begin{aligned} \epsilon_x &= \frac{\partial u}{\partial x} \\ \epsilon_y &= \frac{\partial v}{\partial y} + \frac{w}{R} \\ \gamma_{xy} &= \frac{\partial u}{\partial y} + \frac{\partial v}{\partial x} \end{aligned} \qquad \text{(II.3)}$$

The stress-strain relations are

$$\begin{aligned} \sigma'_x &= \frac{E}{1-\nu^2}(\epsilon'_x + \nu\epsilon'_y) \\ \sigma'_y &= \frac{E}{1-\nu^2}(\epsilon'_y + \nu\epsilon'_x) \end{aligned} \qquad \text{(II.4)}$$

$\tau_{xy} = G\gamma'_{xy}$

where $G = \frac{E}{2(1+\nu)}$ is the shear modulus, E is the Young's

modulus of the shell and ν is the Poisson's ratio.

II.6 SHELL STRAIN ENERGY

An element of a cylindrical shell of mean radius R, uniform thickness h and length L is considered. The thickness ratio h/R is assumed to be small in order to be able to apply thin shell theory. As for thin plates, the stresses σ_z, τ_{xz} and τ_{yz} are zero at the free surfaces $z = \pm h/2$ and it is assumed that for a thin shell these stresses are zero throughout the thickness. Shells of finite length have modes of vibration in which both axial and circumferential nodes exist. In such cases the assumption that the middle surface is inextensible is not valid. Consequently both bending and stretching of the middle surface should be considered. At a distance z from the middle surface, the strain is equal to the appropriate middle surface strain plus the strain due to change in curvature (twist).

The total strain energy of the deformed cylindrical shell (subscript c), neglecting the stresses that have been assumed to be zero and neglecting the trapezoidal form of the faces of the element perpendicular to the x-axis, may be expressed as

$$U_c = \int_0^{2\pi R} \int_0^{L} \int_{-h/2}^{h/2} \tfrac{1}{2} (\sigma_x' \epsilon_x' + \sigma_y' \epsilon_y' + \tau_{xy}' \gamma_{xy}') dx dy dz \qquad - - - \quad (II.5)$$

Substituting equations (II.2), (II.3), (II.4) into (II.5) and performing the integration with respect to z, the strain energy expression reduces to,

$$U_c = \int_0^{2\pi R} \int_0^{L} \frac{Eh}{2(1-\nu^2)} \left[\left(\frac{\partial u}{\partial x}\right)^2 + \left(\frac{\partial v}{\partial y} + \frac{w}{R}\right)^2 + 2\nu \frac{\partial u}{\partial x}\left(\frac{\partial v}{\partial y} + \frac{w}{R}\right) + \frac{1-\nu}{2} \left(\frac{\partial u}{\partial y} + \frac{\partial v}{\partial x}\right)^2 \right] dx dy$$

$$+ \frac{D}{2} \int_0^{2\pi R} \int_0^{L} \left[\left(\frac{\partial^2 w}{\partial x^2} \right)^2 + \left(\frac{\partial^2 w}{\partial y^2} \right)^2 + 2\nu \frac{\partial^2 w}{\partial x^2} \frac{\partial^2 w}{\partial y^2} + 2(1-\nu) \left(\frac{\partial^2 w}{\partial x \partial y}\right)^2 \right] dx\, dy \qquad (II.6)$$

where $D = \frac{Eh^3}{12(1-\nu^2)}$ is the flexural rigidity of the cylindrical shell.

II.7 STIFFENERS

The shell is reinforced by a set of equally spaced uniform stringers and/or rings; the co-ordinate system for which is shown in Fig. 1(c).

Stiffeners are assumed to be integrally attached to the shell surface. The displacements of the stiffeners are taken to be equal to the displacements of the shell at points of attachment, thus satisfying compatibility. The width of the stringer and/or ring is assumed to be small compared to the shell radius and/or length. It is also assumed that the cross sections of the stiffeners do not deform. Stiffener twisting is accounted for in an approximate matter. The effects of joints in the stiffener framework are ignored.

II.8 STRINGER STRAIN ENERGY

An element of a stringer, having cross-sectional area dA_s, torsional stiffness G_sJ_s is considered. The strain energy per unit length, due to bending about the y and z axes, and torsion about the x axis, stretching along the x axis, of the i^{th} stringer (suffix si) are $\frac{1}{2} E_{si}\epsilon_x'^2$ per unit area, and $\frac{1}{2} G_{si}J_{si}(\frac{\partial^2 w}{\partial x \partial y})^2$ respectively, where E_{si} is the Young's modulus, G_{si} is the shear modulus and J_{si} is the torsion constant, of the i^{th} stringer. The total strain energy of the $2L_s$ stringers (subscript 's') considered as discrete elements (superscript D) is,

$$U_s^{(D)} = \sum_{i=1}^{2L_s} \int_0^L \int_{A_s} \frac{E_{si}\epsilon_x'^2}{2} dA_{si}dx + \frac{G_{si}J_{si}}{2} \int_0^L (\frac{\partial^2 w}{\partial x \partial y})^2 dx \qquad (II.7)$$

As the cross-sections are assumed to be uniform, the integrations over the stringer cross-sectional area can be performed. The strain energy of the $2L_s$ stringers (equation (II.7) can be expressed in terms of shell middle surface

strains by using the first of equations (II.2) as

$$U_s^{(D)} = \sum_{i=1}^{2L_s} \int_0^L \left[\frac{E_{si}}{2} \left\{ \left(\frac{\partial u}{\partial x}\right)^2 A_{si} - 2\bar{z}_{si} A_{si} \frac{\partial u}{\partial x} \frac{\partial^2 w}{\partial x^2} + I_{o_{si}} \left(\frac{\partial^2 w}{\partial x^2}\right) \right\} \right.$$

$$\left. + \frac{G_{si} J_{si}}{2} \left(\frac{\partial^2 w}{\partial x \partial y}\right)^2 \right] dx \qquad \text{(II.8)}$$

where A_{si} is the area, $\bar{z}_{si}$ is the centroid measured from the shell middle surface (positive, zero or negative according to external, symmetric or internal attachment respectively) and I_{osi} is the second moment of area about an axis in the middle surface of the shell, of the i^{th} stringer cross section.

If the stringer effects are averaged or 'smeared' (superscript S) over the circumference of the shell, the finite sum appearing in equation (II.8) can be replaced by the appropriate integral. The result is

$$U_s^{(S)} = \frac{1}{d} \int_0^{2\pi R} \int_0^L \left[\frac{E_s}{2} \left\{ A_s \left(\frac{\partial u}{\partial x}\right)^2 - 2\bar{z}_s A_s \frac{\partial u}{\partial x} \frac{\partial^2 w}{\partial x^2} \right.\right.$$

$$\left.\left. + I_{os} \left(\frac{\partial^2 w}{\partial x \partial y}\right)^2 \right\} + \frac{G_s J_s}{2} \left(\frac{\partial^2 w}{\partial x \partial y}\right)^2 \right] dx dy$$

$$- - \qquad \text{(II.9)}$$

where d is the stringer spacing.

II.9 RING STRAIN ENERGY

The strain energy of a ring is composed of bending about the x and z axes, stretching along the circumference and torsion about the y axis. By considering an element of the ring and proceeding in a manner similar to that for stringers, the total strain energy of the K_r+1 rings (subscript r) considered as discrete elements (superscript D) is

$$U_r^{(D)} = \sum_{j=0}^{K_r} \int_0^{2\pi R} \left[\frac{E_{rj}}{2} \left\{ A_{rj} \left(\frac{\partial v}{\partial y} + \frac{w}{R}\right)^2 \right.\right.$$

$$\left.\left. - 2\bar{z}_{rj} A_{rj} \left(\frac{\partial v}{\partial y} + \frac{w}{R}\right) \frac{\partial^2 w}{\partial y^2} + I_{orj} \left(\frac{\partial^2 w}{\partial y^2}\right)^2 \right\} + \right.$$

$$+ \frac{G_{rj}J_{rj}}{2}\left(\frac{\partial^2 w}{\partial x \partial y}\right)^2\Bigg] dy \qquad \text{(II.10)}$$

where A_{rj} is the area, $\bar{z}_{rj}$ is the centroid (positive, aero or negative according as external, symmetric or internal attachment respectively) and I_{orj} is the second moment of area about an axis in the middle surface of the shell, of the j^{th} ring cross-section. This analysis assumes that the rings are equally spaced such that a ring is attached to each end of the shell (x=0 and x=L).

If the ring effects are smeared (superscript S) over the length of the shell the finite sum appearing in equation (II.10) can be replaced by the appropriate integral.

The result is

$$U_r^{(S)} = \frac{1}{l}\int_0^{2\pi R}\int_0^{L}\Bigg[\frac{E_r}{2}\Bigg\{A_r\left(\frac{\partial v}{\partial y}+\frac{\partial w}{\partial R}\right)^2 - 2\bar{z}_r A_r\left(\frac{\partial v}{\partial y}+\frac{\partial w}{R}\right)\frac{\partial^2 w}{\partial y^2} + I_{or}\left(\frac{\partial^2 w}{\partial y^2}\right)^2\Bigg\} + \frac{G_r J_r}{2}\left(\frac{\partial^2 w}{\partial x \partial y}\right)^2\Bigg] dxdy$$

$$- - - \qquad \text{(II.11)}$$

where l is the ring spacing.

II.10 SHELL KINETIC ENERGY

By considering an element of the shell the total kinetic energy of the cylindrical shell (subscript C) can be written in terms of the axial, circumferential and radial displacements (u', v', w') as

$$T_c = \frac{1}{2}\int_0^{2\pi R}\int_0^{L}\int_{-h/2}^{h/2} \rho_c h\left[\left(\frac{\partial u'}{\partial t}\right)^2 + \left(\frac{\partial v'}{\partial t}\right)^2 + \left(\frac{\partial w'}{\partial t}\right)^2\right] dxdydz$$

$$- - - \qquad \text{(II.12)}$$

where ρ_c is the mass density of the material of the cylindrical shell.

On using equations (II.1) and integrating with respect to z, equation (II.12) can be expressed in terms of the shell middle-surface displacements (u, v, w) as

$$T_c = \tfrac{1}{2} \int_0^{2\pi R} \int_0^{L} \left[\rho_c h \left\{ \left(\frac{\partial u}{\partial t}\right)^2 + \left(\frac{\partial v}{\partial t}\right)^2 + \left(\frac{\partial w}{\partial t}\right)^2 \right\} + \rho_c I_{oc} \left\{ \left(\frac{\partial^2 w}{\partial x \partial t}\right)^2 + \left(\frac{\partial^2 w}{\partial y \partial t}\right)^2 \right\} \right] dx dy \quad \text{(II.13)}$$

where I_{oc} is the moment of inertia of the shell element. Equation (II.13) exhibits the inclusion of inplane (axial and tangential) inertias and rotary inertia of the shell in addition to the radial inertia.

II.11 STRINGER KINETIC ENERGY

By considering an element of a stringer, the total kinetic energy of the $2L_s$ stringers (subscript s) treated as discrete elements (superscript D) can be written, in terms of the axial, circumferential and radial displacements (u', v', w') as

$$T_s^{(D)} = \tfrac{1}{2} \sum_{i=1}^{2L_s} \int_0^{L} \int_{A_s} \rho_{si} \left\{ \left(\frac{\partial u'}{\partial t}\right)^2 + \left(\frac{\partial v'}{\partial t}\right)^2 + \left(\frac{\partial w'}{\partial t}\right)^2 \right\} dx \, d A_{si} \quad \text{(II.14)}$$

where ρ_{si} is the mass density of the material of the i^{th} stringer.

On using equations (II.1) and integrating with respect to z, equation (II.14) can be expressed in terms of the shell middle surface displacements (u , v , w) as

$$T_s^{(D)} = \tfrac{1}{2} \sum_{i=1}^{2L_s} \int_0^{L} \left[\rho_{si} A_{si} \left\{ \left(\frac{\partial u}{\partial t}\right)^2 + \left(\frac{\partial v}{\partial t}\right)^2 + \left(\frac{\partial w}{\partial t}\right)^2 \right\} - 2\rho_{si} A_{si} \bar{z}_{si} \left\{ \frac{\partial u}{\partial t} \frac{\partial^2 w}{\partial x \partial t} + \frac{\partial v}{\partial t} \frac{\partial^2 w}{\partial y \partial t} \right\} + \rho_{si} I_{osi} \left\{ \left(\frac{\partial^2 w}{\partial x \partial t}\right)^2 + \left(\frac{\partial^2 w}{\partial y \partial t}\right)^2 \right\} \right] dx \quad \text{(II.15)}$$

where I_{osi} is the moment of inertia of the i^{th} stringer

cross-sectional area about an axis in the middle surface of the shell. Equation (II.15) exhibits the inclusion of inplane (axial and tangential) and rotary inertia of the stringer, in addition to the radial inertia.

If the stringer effects are smeared (superscript S) over the circumference, equation (II.15) reduces to the form

$$T_s^{(S)} = \frac{1}{2}\int_0^L \int_0^{2\pi R} \left[\frac{\rho_s A_s}{d}\left\{\left(\frac{\partial u}{\partial t}\right)^2+\left(\frac{\partial v}{\partial t}\right)^2+\left(\frac{\partial w}{\partial t}\right)^2\right\} - \frac{2\rho_s A_s}{d}\bar{z}_s\left\{\frac{\partial u}{\partial t}\frac{\partial^2 w}{\partial x \partial t}+\frac{\partial v}{\partial t}\frac{\partial^2 w}{\partial y \partial t}\right\} + \frac{\rho_s I_{os}}{d}\left\{\left(\frac{\partial^2 w}{\partial x \partial t}\right)^2+\left(\frac{\partial^2 w}{\partial y \partial t}\right)^2\right\}\right] dxdy \qquad (II.16)$$

II.12 RING KINETIC ENERGY

By considering an element of a ring and proceeding in a manner similar to that for the stringers, the total kinetic energy of the (K_r+1) rings (subscript r), considered as discrete elements (superscript D) can be written in terms of shell middle surface displacements, to include the effects of inplane and rotary inertias as

$$T_r^{(D)} = \frac{1}{2}\sum_{j=0}^{K_r}\int_0^{2\pi R} \left[\rho_{rj} A_{rj}\left\{\left(\frac{\partial u}{\partial t}\right)^2+\left(\frac{\partial v}{\partial t}\right)^2+\left(\frac{\partial w}{\partial t}\right)^2\right\} - 2\rho_{rj}A_{rj}\bar{z}_{rj}\left\{\frac{\partial u}{\partial t}\frac{\partial^2 w}{\partial x \partial t}+\frac{\partial v}{\partial t}\frac{\partial^2 w}{\partial y \partial t}\right\} + \rho_{rj} I_{orj}\left\{\left(\frac{\partial^2 w}{\partial x \partial t}\right)^2+\left(\frac{\partial^2 w}{\partial y \partial t}\right)^2\right\}\right] dy \qquad (II.17)$$

If the ring effects are smeared (superscript S) over the length of the shell, equation (II.17) reduces to the form

$$T_r^{(S)} = \frac{1}{2}\int_0^{2\pi R}\int_0^L \left[\frac{\rho_r A_r}{l}\left\{\left(\frac{\partial u}{\partial t}\right)^2+\left(\frac{\partial v}{\partial t}\right)^2+\left(\frac{\partial w}{\partial t}\right)^2\right\} - 2\left(\frac{\rho_r A_r}{l}\right)\bar{z}_r\left\{\frac{\partial u}{\partial t}\frac{\partial^2 w}{\partial x \partial t}+\frac{\partial v}{\partial t}\frac{\partial^2 w}{\partial y \partial t}\right\} + \frac{\rho_r I_{or}}{l}\left\{\left(\frac{\partial^2 w}{\partial x \partial t}\right)^2+\left(\frac{\partial^2 w}{\partial y \partial t}\right)^2\right\}\right] dxdy \qquad (II.18)$$

II.13 FUNCTIONS REPRESENTING THE MODE SHAPES

The integrations with respect to x and y can be performed in the foregoing equations only when the vibration forms for the displacements (u,v,w) have been assumed.

Displacements which satisfy the simple support boundary conditions at both ends of the shell (x = 0 and x = L) are taken as

$$u = \bar{u} \cos \frac{m\pi x}{L} \cos \frac{ny}{R} \sin \omega t$$

$$v = \bar{v} \sin \frac{m\pi x}{L} \sin \frac{ny}{R} \sin \omega t \qquad \text{(II.19)}$$

$$w = \bar{w} \sin \frac{m\pi x}{L} \cos \frac{ny}{R} \sin \omega t$$

where $(\bar{u},\bar{v},\bar{w})$ are the modal amplitudes, ω is the circular frequency of harmonic oscillation, m is the number of axial half waves and n is the number of circumferential full waves. The integers m and n define the nodal petterns of the shell.

The tangential and radial displacements (v and w) are zero and the axial force and moment are zero at both ends of the shell with this particular choice of modal functions.

For the discrete stiffener case, the $2L_s$ stringers are located at positions determined by

$$\frac{y_i}{R} = \frac{(2i-1)\pi}{2L_s}, \quad i = 1,2,.....2L_s \qquad \text{(II.20)}$$

and the (K_r+1) rings at positions determined by

$$\frac{x_j}{L} = \frac{j}{K_r} \quad j = 0,1,2,....K_r \qquad \text{(II.21)}$$

The appropriate co-ordinate system is shown in Fig. 1(c).

Thus, the functions representing the displacements corresponding to discrete stringers are evaluated by means of equations (II-19) at $y = y_i$ as

$$\left.\begin{aligned} u = (u)_{y=y_i}, \quad v = (v)_{y=y_i}, \quad w = (w)_{y=y_i} \\ \left(\frac{\partial w}{\partial y}\right) = \left(\frac{\partial w}{\partial y}\right)_{y=y_i} \end{aligned}\right\} \; i=1,2,..2L_s \qquad \text{(II.22)}$$

and those corresponding to discrete rings at $x = x_j$ as

$$\left.\begin{aligned} u = (u)_{x=x_j},\ v = (v)_{x=x_j},\ w = (w)_{x=x_j} \\ \left(\frac{\partial w}{\partial x}\right) = \left(\frac{\partial w}{\partial x}\right)_{x=x_j} \end{aligned}\right\} j=1,2,..K_r \quad - - \text{(II.23)}$$

for the discrete stiffener case, this type of stiffener distribution has the advantage that i) their axial and radial displacements are zero when the circumferential nodes are a multiple of the number of stringers and ii) their circumferential and radial displacements are zero when the axial nodes are a multiple of the number of rings. Simple support boundary conditions are satisfied by this choice of stiffener distribution.

For the smeared stiffener case, equations (II.19) are used for the displacements occuring in the strain and kinetic energy expressions for the shell and for the stiffeners.

II.14 DERIVATION OF THE FREQUENCY EQUATION FOR THE DISCRETE STIFFENER CASE

For the composite structure consisting of the shell and the stiffeners, the total strain and kinetic energy are given by

$$\begin{aligned} U^{(D)}_{max} &= U_{c\ max} + U^{(D)}_{s\ max} + U^{(D)}_{r\ max} \\ T^{(D)}_{max} &= T_{c\ max} + T^{(D)}_{s\ max} + T^{(D)}_{r\ max} \end{aligned} \qquad \text{(II.24)}$$

where the relevant expressions are given in appendix 1.

Equating the maximum strain and kinetic energies yields an equation for ω^2. The Rayleigh-Ritz condition applied in the form

$$\frac{\partial(\omega^2)}{\partial \bar{u}} = \frac{\partial(\omega^2)}{\partial \bar{v}} = \frac{\partial(\omega^2)}{\partial \bar{w}} = 0 \qquad \text{(II.25)}$$

leads to three characteristic equations for the frequency. This can be written in matrix form as

$$\left[A^{(D)}_{ij} + \Delta\ B^{(D)}_{ij} \right] \left\{ \bar{q} \right\} = 0, (i,j=1,2,3) \qquad \text{(II.26)}$$

where $\{\bar{q}\}$ is the column vector of modal amplitudes $(\bar{u}, \bar{v}, \bar{w})$ and Δ is the frequency factor defined as

$$\Delta = \frac{\rho_c R^2 (1-\nu^2)\omega^2}{E} \qquad \text{(II.27)}$$

The expressions for the matrix elements $(A_{ij}^{(D)}, B_{ij}^{(D)})$ are given in appendix 2. The finite trigonometric sums involved in these expressions can be replaced by their equivalent values (see appendix 3).

II.15 DERIVATION OF THE FREQUENCY EQUATION FOR THE SMEARED STIFFENER CASE

When the stiffeners are smeared over the surface of the shell, the finite sums are replaced by the values of the appropriate integrals (see appendix 3). The corresponding frequency equation is

$$\left[A_{ij}^{(S)} + \Delta\, B_{ij}^{(S)}\right] \{\bar{q}\} = 0 \qquad \text{(II.28)}$$

The matrix elements are defined in appendix 4. If the inplane and rotary inertias are neglected, it can be shown that equation (II.28) reduces exactly to equation (42) of Ref. (A29) and to eqn. (2.3) of Ref. (34) with certain modifications*.

II.16 DISCUSSION OF THE FREQUENCY EQUATIONS

The frequencies can be obtained from the characteristic equations (II.26) and (II.28) by setting the determinant of the matrix to zero. The determinant, when expanded, leads to the following cubic equation in the frequency factor Δ :

$$\Delta^3 - K_2\Delta^2 + K_1\Delta - K_o = 0 \qquad \text{(II.29)}$$

where the coefficients K_o, K_1, K_2 are functions of the matrix elements (A_{ij}, B_{ij}). In turn, these elements are functions of many parameters such as thickness ratio (h/R), stiffener areas (A_s, A_r), number of axial and circumferential waves (2m, n), Poisson's ratio ν, density ratios

* Ref. 34 is based directly on Goldenveiser's equilibrium equations whereas Ref. A29 has used an energy approach.

(ρ_s/ρ_c, ρ_r/ρ_c), etc.

For a specific set of values of these parameters, it is found that the cubic equation (29) yields three real, distinct and positive values for Δ and consequently three frequencies are obtained. These three frequencies correspond essentially to axial, circumferential and radial vibrations, with the radial frequency much lower than the other two.

If the inplane (longitudinal and tangential) inertias are neglected, the frequency equation will be linear. Consequently, only one value for the frequency is obtained for each value of m and n. This eigenvalue is an approximation to the lowest of the three frequencies just mentioned.

The effects of eccentricity of stiffeners are reflected in the terms involving $\bar{z}_r$, $\bar{z}_s$.

II.17 DISCUSSION OF NUMERICAL RESULTS AND COMPARISON WITH EXISTING EXPERIMENTAL AND THEORETICAL RESULTS

In order to investigate the effects of inplane and rotary inertias as well as discrete and smeared stiffening on the natural frequencies of stiffened shells, calculations were performed for three shell geometries for which experimental and/or theoretical results were already available. Their properties are given in Table 4.

Table 5 gives the comparison between the results obtained for the unstiffened shell analysed by Voss in Ref. 35, i) by the present analysis with and without various inertia terms, ii) the analysis of Voss neglecting inplane inertia terms and iii) results of Voss. Inplane inertias can have more significant effects as compared to rotary inertia.

Table 6 gives the comparison of minimum frequencies for an eccentrically stiffened shell (of Ref. A28) with various stiffening configurations. Eccentricity alters the frequencies considerably. Of all the possible configurations studied, internal rings yield a much higher frequency compared to the others. The influence of inplane and

rotary inertias seems to be more significant for stiffened shells than for unstiffened shells. Fig. 34 illustrates the influence of stiffener configuration. The frequency spectrum is given in Fig. 35 for the shell with a particular stiffener configuration to illustrate the influence of inplane and rotary inertia for various values of n.

Stringers, when attached internally or symmetrically yield frequencies which are lower than the corresponding unstiffened shell, probably because the stringer contribution to the kinetic energy is greater than its contribution to the strain energy for low values of m. With larger values of m, however, increase of stiffness prevails over that of mass, resulting in higher frequencies, as shown in references A22 and A30. Also included in Table 6 are the minimum frequencies of the shell when stiffeners are treated as discrete elements. These results show very good agreement with those for smeared stiffeners.

Table 7 gives the comparison of frequencies of the shell with four internal stringers analysed by Egle and Sewall in Reference A22, by Schnell and Heinrichbeuer in Reference A30 and by the present analysis, for increasing values of n.* The results from the present analysis are somewhat lower than those of Egle and Sewall. This is probably due to the fact that the inplane inertias were neglected in the numerical calculations presented in Ref. A22. Surprisingly, there is very good agreement whether the stringers, even when they are few in number, are treated as smeared or discrete, particularly for the minimum frequency. Thus the assumption of discrete stiffening seems to have little advantage over smeared stiffening whether the stiffeners are densely spaced or sparsely spaced. In fact the frequencies by smeared and discrete analyses are identical for odd values of n while there is only a small difference for even values of n. This phenomenon can be explained as follows.

Taking the particular shell under consideration for illustration, we see that the spacing with four stringers

---

* Comparable results are given for the same shell with 60 external stringers in Table 8.

$= d = 2\pi R/4 = \frac{\pi R}{2}$. Hence the integrals for the smeared case which appear in appendix 3 have the value 2 for all values of n and are independent of the radius while the summations for the discrete case have the following values.

$$\sum_{i=1}^{2L_s} \cos^2 \frac{(2i-1)n\pi}{2L_s} = \sum_{i=1}^{2L_s} \sin^2 \frac{(2i-1)n\pi}{2L_s} = 2, \text{ for } n=1,3,5,7..$$

$$\sum_{i=1}^{2L_s} \cos^2 \frac{(2i-1)n\pi}{2L_s} = 0; \quad \sum_{i=1}^{2L_s} \sin^2 \frac{(2i-1)n\pi}{2L_s} = 4 \text{ for } n=2,6,10..$$

$$\sum_{i=1}^{2L_s} \cos^2 \frac{(2i-1)n\pi}{2L_s} = 4; \quad \sum_{i=1}^{2L_s} \sin^2 \frac{(2i-1)n\pi}{2L_s} = 0 \text{ for } n=4,8,12,..$$

Consequently, the frequency spectrum, which is smooth in the smeared case, has a slight wavy appearance if the stringers are treated as discrete elements. This is illustrated in Fig. 36.

II.18 CONCLUSIONS

A simple analysis has been presented for determining the natural frequencies of vibration of stiffened cylindrical shells. A one term solution, with a proper choice of stiffener distribution and including inplane and rotary inertia terms yields results which are in good agreement with existing more complicated analyses and experimental data. Numerical results show that inplane and rotary inertias can have significant effect on the frequencies. The efficacy of i) stiffener configuration, ii) treating stiffeners as discrete or smeared and iii) omission or inclusion of any particular term can be easily studied by means of a single computer programme.

CHAPTER III
VIBRATION ANALYSIS - EXPERIMENT

Summary

Experimental vibration analysis has been performed on unstiffened, and stringer stiffened circular cylindrical shells which are simply-supported at both the ends. The experimental results are compared with an analysis which utilises the modes of the unstiffened shell in a Rayleigh-Ritz solution to the problem. Good agreement was found between theoretically predicted results and experimental results for the shells tested.

III.1 INTRODUCTION

An experimental rig was designed and built to determine the modes and frequencies of unstiffened and stringer stiffened circular cylindrical shells. The apparatus consists of a shell fixture, an excitation system and a shell modal pattern sensing system. The details of design and instrumentation are described below and can be seen in Figs. 37 - 39.

III.2 CONSTRUCTION OF THE SHELLS

It would be ideal to have a seamless shell machined out of a tubular stock material. But, for the type of geometries that it was intended should be tested, it would be almost impossible to construct shells this way. Hence, a successful attempt was made to fabricate circular cylindrical shells from commercially available aluminium sheets. These sheets can be obtained with very good tolerance on the thickness distribution over the entire sheet. Thesheet is rolled into the desired form and joined by one or two seams along a generatrix of the shell. Shells of any desired length/radius ratio can be easily and inexpensively made by this process. The seams can be joined either by seam or spot welding or with a strong adhesive. Either type of welded seam has the disadvantage of leaving the joint non-uniform and

can produce localised discontinuities of shape or stiffness and hence the seams were joined using adhesives. There is still some discontinuity effect due to the seams but these are considered to be minimal.

Stiffeners of rectangular section have been added to the shell by bonding stripsof the same material on to the shell at equal intervals. Eccentricity of the stiffeners can be varied by adding additional layers of strips to the stiffeners.

III.3 END SUPPORT CONDITIONS

The object here has been to simulate the simple-support end conditions in accordance with the theoretical assumptions. Each end of the shell was provided with a smooth fitting, light aluminium plate accurately machined to fit the bore of the cylinder and shaped to provide as near as possible line contact with the inner surface of the shell. Slackness of fit in the end plates was found to produce inconsistent results and when this occurred suitable packing was introduced.

Some cut-outs were introduced into the end plates as shown in Figure 37 to give access to instrumentation inside the shell and reduce the weight of the end plates. The cylinder, with the end-plates in place was supported between centres by a central shaft so that it could freely be rotated and the shaft is mounted on stanchions resting on a solid base. Various lengths of the shell can be accommodated by adjusting the distance between the stanchions. An air bearing was provided between the endplate and the central shaft to reduce any inherent restraint against longitudinal motion of the shell due to friction in the end supports.

III.4 MODEL EXCITATION DEVICE

Initially, an oscillator, amplifier and loud speakers were used as the input power source to excite the shell. This was thought to have the advantage that the excitation

system was non-contacting but the instrumentation output signals were swamped by the excessive noise generated by the speakers. This difficulty was overcome by substituting for the loud speakers an electromechanical shaker. The shaker was suspended on rubber chords to excite the shell radially by action/reaction and to reduce the inertia introduced by the shaker armature. The shaker was allowed to rest against the shell and, in this configuration it was found that a more uniform vibration pattern was produced with all the anti-nodes vibrating at near-equal amplitude. The shaker is powered by an oscillator and amplifier. The oscillator is a precision decade oscillator (Muirhead-Wigan type D-890-A Decade Oscillator) which can be varied in 0.1Hz steps making the detection of resonances more accurate. The amplifier used has a 50 watt output which directly powers the shaker.

III.5 INSTRUMENTATION

An instrumentation set up was developed to detect the nodal patterns and frequencies and record them in a suitable form (Fig. 38).

The sensors used for the purpose could be contacting or non-contacting types. The former type very often influences the nodal preference and hence the non-contacting type sensors were preferred. Two types of transducers have been tried, viz. i) Capacity probes and ii) pressure transducers and the comments on their behaviour are recorded below. In the first instance the vibration was measured with a Wayne Kerr vibration meter which is a capacity-type transducer. It was found on application that due to the slight non-circularity of the shell the distance of the probe head from the shell surface exceeded the maximum allowable range. The results obtained were inaccurate and hence their use was abandoned.

Next, a pressure transducer was tried. A Kistler differential transducer was fitted inside the shell to scan the shell surface axially and circumferentially. But, due

to the excessive noise generated by the acoustic exciters used with it, the recorded nodal patterns were swamped by the input signals.

Finally a successful attempt has been made to detect the resonances by scanning the inside of the shell with a microphone mounted in a perspex holder. (Fig. 39)

The block diagram of the resonance detection and excitation system is shown in Fig. 40.

The microphone (Acos MIC 43-3) was used in preference to the Kistler because of its small size, cheapness and availability. The inlet to the microphone to detect the pressure variations due to the vibration of the shell wall is via a 1" long, $\frac{1}{8}$" diameter base steel tube, this tube is to confine to a small area that portion of the shell being monitored. The electric output from the microphone is fed to the input of the wave analyser via a screened cable. The Muirhead wave analyser, filters the input at the excitation frequency and, by careful tuning the exact vibration frequency can be verified. The instrument is fitted with a pair of output terminals which monitor the filtered signal. This output has a maximum peak to peak value of 8v. An attenuating network has been added to reduce the signal to one tenth of its initial value to produce a signal suitable for feeding into the AC-DC converter. The converter used is a Dawe Engine Roughness measuring instrument which takes the AC signal and converts to a DC voltage which is proportional to the peak to peak value of the input signal. The instrument in normal use displays the output on a meter but it has been modified so that theoutput is brought to and monitored on a Sanborn two-channel chart recorder. A typical recording is shown in Fig. 41.

III.6 SCANNING SYSTEM

The microphone is attached to an arm which is mounted on the central shaft. The arm is capable of axial and circumferential scan. The axial traverse is by means of a

lead screw and nut. The lead screw is capable of being rotated by a small motor which acts as an actuator and the arm can be driven in either direction by a push button and a direction switch. The circumferential scan is driven by a $1/_{15}$ horsepower electric motor through a stepped belt. On depressing the scan-initiate button the microphone will scan 360^{o} and then stop. On redepressing it will scan 360^{o} in the other direction, the change in direction being to avoid winding up the microphone lead.

III.7 GENERAL TEST PROCEDURE

The clarity of the mode shapes is affected by the position of the shaker. Best results are usually obtained when the shaker is positioned in the centre of the shell, on the seam to detect the circumferential modes corresponding to m = 1. Thecircumferential scan for the m=2 modes were best excited by placing the shaker roughly a quarter of the way along the shell. Similarly the shaker is positioned at a point of maximum amplitude, corresponding to the higher m modes.

Having placed the shaker in a suitable position all the instruments are switched on and one of the limit switches is closed in order to energise one of the relays. The microphone is adjusted to be as close as possible to the shell wall such that it does not touch the shell during a circumferential scan.

Starting with the lowest predicted frequency, the oscillator is adjusted in steps of 10Hz until a response is produced from the shell. The oscillator is then adjusted to produce a maximum amplitude on the oscilloscope. At each step, the output from the microphone which is monitored through the wave analyser is adjusted to the frequency giving the maximum amplitude and the resonant frequency. A scan is then taken, the frequency and any mode shape information produced noted on the chart record. The frequency is then increased until the next resonant mode is encountered and so on. When all the detectable m=1 modes had been

accounted for, the shaker was moved and as many of the m=2 modes found as possible.

III.8 RESULTS AND CONCLUSIONS

The experimental results are compared with theory in Tables 9 to 14. The response of each mode is described as very good, good, moderate, poor and inconclusive. In terms of the apparatus these mean as follows:

Very good response:	Clearly defined peak of amplitudes. The trace has mainly regular peaks.
Good response:	Easily detectable peak of amplitude, few irregularities in the trace present.
Moderate response:	Low amplitude or peak hard to find, possibility of nodes missing from the trace.
Poor response:	Amplitude almost nil or no definite peak, irregular trace with nodes missing.
Inconclusive:	Almost completely swamped by another mode or almost nil amplitude, many nodes missing from the trace, could be a different mode from that specified.

The most successful shell was made of 0.052"thick aluminium sheets, 28" long, 28" diameter. For a stringer-stiffened shell 0.25" wide strips were cut from the same sheet and bonded to the shell to form 12 equal stringers.

Good agreement has been shown, in general, between the experimental results and theoretical predictions. The detection of high circumferential resonances is possible due to the low vibration amplitudes. Modes with a few circumferential nodes cannot be detected with the present vibrator as it appears that the shell cannot be excited sufficiently. A good representation has been achieved for excitation frequencies between approximately 100 to 1000Hz which encompasses n numbers between about 8 and 20.

It has not been possible to detect the axial modes

corresponding to $m > 2$ probably because they were beyond the scope of the equipment.

For the case of shells stiffened with external stringers very good response was achieved when the number of nodes was a multiple of the number of stringers.

CHAPTER IV
GENERALISED AERODYNAMIC FORCES

Summary

The aerodynamic generalised forces based on the most commonly used form of linear piston theory expression and the exact potential flow solutions are examined for a harmonically oscillating circular cylindrical shell, with a view to adapt them in the formulation of the flutter equations in terms of the invacuo-natural frequencies corresponding to the assumed modes for a multi-degree of freedom system.

IV.1 GENERAL

In the assumed mode approach to the flutter problem the aerodynamic quantities directly involved in the flutter equations are the generalised forces and not the corresponding pressure distributions themselves.

A considerable economy of effort may be accomplished by dealing directly with the generalised forces, particularly when using the exact potential flow solution. The general aerodynamic assumptions have already been discussed in the literature survey.

IV.2 LINEAR PISTON THEORY APPROXIMATION

Piston theory was introduced into supersonic aeroelastic analyses by Ashley and Zartarian as a handy tool in 1956 (Ref. 10). The term piston theory as used here, refers to any method of calculating the supersonic aerodynamic loads on surfaces in which the local pressure generated by the body's motion is related to the local normal component of fluid velocity in the same way that these quantities are related to the face of a piston moving in a one-dimensional channel. The expression for the pressure difference (between the instantaneous pressure and the pressure at infinity) can be written as

$$p = \rho_o a_o \left[U \frac{\partial w}{\partial x} + \frac{\partial w}{\partial t} \right] \qquad \text{(IV.1)}$$

where w is the normal (radial) deflection, $(\frac{\partial}{\partial t} + U \frac{\partial}{\partial x})$ represents the substantial derivative of a fluid particle in unsteady motion in the linearised form and U is the free stream velocity.

In general it is believed that linear piston theory may be employed for large flight Mach numbers or high reduced frequencies of unsteady motion, whenever the surface involved is plane or nearly plane and not inclined too sharply to the flow. Linear piston theory has been widely used with success in supersonic plane panel flutter analysis. Because of the previous lack of appropriate simple expressions for the aerodynamic pressures on a vibrating shell, it has also been used in the flutter analysis of such cylindrical shells.

The non-dimensional aerodynamic generalised forces are defined, in the usual way, as,

$$Q_{mr} = \frac{1}{\rho_o U^2} \iint_S p_{mn}(\tfrac{x}{L}, \theta) w_{rn}(\tfrac{x}{L}, \theta) d(\tfrac{x}{L}) d\theta \qquad \text{(IV.2)}$$

where p_{mn} is the aerodynamic pressure due to a deflection

$$w_{mn}(\tfrac{x}{L}, \theta) = \cos n\theta * \sin \frac{\lambda_m x}{R} \qquad \text{(IV.3)}$$

and $\lambda_m = \frac{m\pi R}{L}$. This deflection w_{mn} corresponds to the assumed flutter mode of a simply supported cylindrical shell (see Eqn. I.18)

Phsyically, a generalised force Q_{mr} equals the work that would be done by a pressure field p_{mn} per unit deflection, w_{rn}.

If equations (IV.1) and (IV.3) are used in (IV.2) and integrated over the surface of the cylinder, the non-dimensional aerodynamic generalised forces corresponding to linear piston theory are obtained as

$$Q_{mr} = \frac{1}{M} \frac{mr}{m^2 - r^2} \left[1-(-1)^{m+r}\right] \quad \text{for } m \neq r$$

and

$$Q_{mm} = \frac{ik}{2M} \qquad \text{(IV.4)}$$

where $M = \frac{U}{a_o}$ is the free stream Mach number and $k = \frac{\Omega L}{U}$ is the non-dimensional frequency parameter.

IV.3 EXACT POTENTIAL FLOW SOLUTION

Randall (Ref. 19) has developed an exact solution to the steady potential flow equation in terms of Laplace transformation. The solution is based on the linearised small perturbation theory of supersonic flow and involves Bessel functions of imaginary arguments to be evaluated numerically. Holt and Strack (Ref. 40) have suggested an extension of this method to obtain the pressures on an oscillating cylindrical shell and derived the general solution to the problem. Dowell (Ref. 98) and Davies (Ref. 137) have gone a stage further to determine the aerodynamic generalised forces using the exact solution. The approach of Dowell (Ref. 98) has been adopted here as it leads directly to the formulation of the shell flutter equations and is explained below.

The cylindrical shell of length L and radius R is assumed to be performing small oscillations around its mean position in the presence of an external supersonic potential flow field parallel to its axis. The radial component of the shell deflection is denoted by $w(x, \theta, t)$ and the radial co-ordinate of a point on its middle surface is given by

$$r = R + w(x, \theta, t) \qquad \text{(IV.5)}$$

The perturbation velocity potential ϕ induced by the shell deformation satisfies the differential equation

$$\nabla^2\phi - \frac{1}{a_\infty^2}\left[\frac{\partial^2\phi}{\partial t^2} + 2U\frac{\partial^2\phi}{\partial x\partial t} + U^2\frac{\partial^2\phi}{\partial x^2}\right] = 0 \qquad \text{(IV.6)}$$

The problem is to solve this equation subject to the following boundary conditions: i) the normal component of velocity should vanish everywhere on the cylinder surface.

$$\text{i.e.} \quad \left(\frac{\partial\phi}{\partial r}\right)_{r=R} = \left[\frac{\partial w}{\partial t} + U\frac{\partial w}{\partial x}\right] \quad \text{for } 0 < x < L$$
$$= 0 \quad \text{for} \quad x < 0 \qquad \text{(IV.7)}$$

ii) the appropriate conditions at infinity should be satisfied that a) the fluid is undisturbed at an infinite distance from the shell ($\phi \to 0$ as $r \to \infty$ for $x > 0$) and b) the

disturbance is only confined to the Mach cone at any given point ($\phi = 0$ for $x \leq 0$).

The radial displacement w and the potential function ϕ (so also the corresponding aerodynamic pressure p) are assumed to have periodic variation with time and it is assumed that the circumferential (n) modes are decoupled from the axial modes (m). With these assumptions the following equations can be written:

$$\left.\begin{aligned} w(x,\theta,t) &= W(x)\cos n\theta\, e^{i\Omega t} \\ \phi(x,r,\theta,t) &= \bar{\Phi}(x,r)\cos n\theta\, e^{i\Omega t} \\ p(x,\theta,t) &= P(x)\cos n\theta\, e^{i\Omega t} \end{aligned}\right\} \qquad \text{(IV.8)}$$

The differential equation (IV.6) and the boundary conditions (IV.7) now become

$$\frac{\partial^2\bar{\Phi}}{\partial x^2} + \frac{\partial^2\bar{\Phi}}{\partial r^2} + \frac{1}{r}\frac{\partial\bar{\Phi}}{\partial r} - n^2\bar{\Phi} + \frac{1}{a_o^2}\left[-\Omega^2\bar{\Phi} + 2i\Omega U\frac{\partial\bar{\Phi}}{\partial x} + U^2\frac{\partial^2\bar{\Phi}}{\partial x^2}\right] = 0 \qquad \text{(IV.9)}$$

$$\left.\begin{aligned} \left(\frac{\partial\bar{\Phi}}{\partial r}\right)_{r=R} &= U\frac{\partial W(x)}{\partial x} + i\Omega W(x) \qquad \text{for } 0 < x < L \\ &= 0 \qquad \text{for } x < 0 \end{aligned}\right\} \qquad \text{(IV.10)}$$

By using the Laplace transform with respect to the streamwise variable x, the above equations can be solved for $\bar{\Phi}$ as

$$\bar{\Phi}_{r=R} = \frac{RU}{L}\int_0^x\left[\frac{1}{2\pi i}\int_{-i\infty}^{i\infty}\frac{K_n(\zeta)}{\zeta K_n'(\zeta)}\, e^{s(x-\xi)}ds\right]\left(\frac{\partial}{\partial\xi} + ik\right)W(\xi)d\xi \qquad \text{(IV.11)}$$

where K_n is the modified Bessel function of order n and K_n' its derivative, with the complex argument ζ given by

$$\zeta^2 = (R/L)^2\left[M^2(s+ik)^2 - s^2\right] \quad \text{and} \quad k = \frac{\Omega L}{U} \qquad \text{(IV.12)}$$

The aerodynamic pressure is determined from $\bar{\Phi}$ using Bernoulli's equation. The generalised force is determined from equation (IV.2) which for this case is

$$Q_{mr} = \left(-\frac{R}{L}\right)\frac{1}{2\pi i}\int_{-i\infty}^{i\infty}\frac{K_n(\zeta)}{\zeta K_n'(\zeta)}\, G_{mr}(s)ds \qquad \text{(IV.13)}$$

where the function $G_{mr}(s)$ represents the influence of coupling between the axial modes m and r. If sinusoidal

axial modes (eqn. IV.3) are assumed for the cylinder deflection, closed form expressions are available for the function $G_{mr}(s)$ depending on whether or not m and r are equal (Ref.98).

i) If $m = r$,

$$G_{mm}(s) = \frac{(s+ik)^2}{2}\left\{\frac{-s}{s^2+(m\pi)^2} + \frac{2(m\pi)^2}{[s^2+(m\pi)^2]^2}\left[1-(-1)^m e^s\right]\right\} + \frac{s+2ik}{2} \qquad \text{(IV.14)}$$

ii) If $m \neq r$

$$G_{mr}(s) = (s+ik)^2 \frac{rm}{r^2-m^2}\left\{\frac{-1}{(r\pi)^2+s^2}\left[1-(-1)^r e^s\right] + \frac{(-1)^{m+r}\left[1-(-1)^m e^s\right]}{(m\pi)^2+s^2}\right\} + \left[1-(-1)^{m+r}\right]\frac{rm}{r^2-m^2}$$

The integral (IV.13) has been evaluated around the contour shown in Fig. 42. By taking the contributions to the integral along the various branches of the contour it can be shown that it reduces to the form:

$$Q_{mr} = -\left(\frac{L}{R}\right)\sum_j \frac{G_{mr}(s_j)\,\zeta_j^2}{\left[s_j(M^2-1)+ikM^2\right]\left[\zeta_j^2+n^2\right]}$$

$$- \left(\frac{R}{L}\right)\frac{1}{2\pi i}\left\{\int_{-\infty+s_o}^{s_o} G_{mr}\left[\frac{K_n(re^{-i\pi})}{re^{-i\pi}K_n'(re^{-i\pi})} - \frac{K_n(re^{i\pi})}{re^{i\pi}K_n'(re^{i\pi})}\right]ds\right.$$

$$+ \int_{s_1}^{s_o} G_{mr}\left[\frac{K_n(re^{i\pi})}{re^{i\pi}K_n'(re^{i\pi})} - \frac{K_n(r)}{rK_n'(r)}\right]ds$$

$$\left. + \int_{s_o}^{s_2} G_{mr}\left[\frac{K_n(re^{-i\pi})}{re^{-i\pi}K_n'(re^{-i\pi})} - \frac{K_n(r)}{rK_n'(r)}\right]ds\right\} \qquad \text{(IV.15)}$$

where r is the modulus of ζ, ζ_j are the zeros of $K_n'(\zeta)$ and the corresponding s_j are determined by solving equation (IV.12):

$$s_j = \frac{-ikM^2}{M^2-1} + \frac{\left[\zeta_j^2(L/R)^2(M^2-1)-k^2M^2\right]^{\frac{1}{2}}}{M^2-1}$$

Randall (Ref. 19) has tabulated the ζ_j for n=1 - 10 and Dzygadlo (Ref. 139) has extended this up to 25. The function $K_n'(\zeta)$ has all its zeros to the left of the imaginary axis and the number of zeros is the nearest even integer to $(n+\frac{1}{2})$. Thus, $K_o'(\zeta)$ has no zero, $K_1'(\zeta)$ and $K_2'(\zeta)$ each have two zeros, $K_3'(\zeta)$ and $K_4'(\zeta)$ each have four zeros, and

so on. These zeros are reproduced in Table 15 for n=1 to 25.

It is a fairly straight forward procedure to compute the various terms of equation (IV.16) and hence the aerodynamic generalised forces.

IV.4 NUMERICAL RESULTS AND CONCLUSIONS

Numerical results have been obtained for various values of the cylindrical shell and flow parameters. The generalised forces using exact aerodynamic theory are functions of six parameters (M, k, L/R, n, m, r), whereas the linear piston theory generalised forces are only functions of four parameters (M, k, m, r). In other words the latter are independent of the circumferential wave number (n) and the length to radius ratio (L/R). The comparisons are listed in Tables 16 to 20 to cover a wide range of the parameters involved. It is very difficult to give a general realistic comparison between the two theories. In fact, according to the linear piston theory expressions (Equations IV.4) when the axial coupling between the modes m and r are equal, Q_{mm} is a purely imaginary quantity; it is only a function of the two parameters M and k; it is always positive and is independent of the axial modes. When m is differemt from r, Q_{mr} is a function of three parameters (m, r, M); it is invariant with the frequency parameter k; it is purely real and is non-zero only if (m+r) is odd. These are not so in general for the exact generalised forces. Looking at Tables 16 to 20, bearing all the foregoing remarks in mind suggests that linear piston theory can be expected to be a reasonable approximation only for short shells vibrating with large number of circumferential modes.

CHAPTER V
FLUTTER ANALYSIS

Summary

The flutter problem of a simply-supported circular cylindrical shell oscillating harmonically in supersonic flow is formulated in terms of the invacuo-natural frequency factors of the shell and the aerodynamic generalised forces for a multi-degree of freedom system in the assumed modes. The problem is ultimately reduced to a complex eigenvalue problem and programmed for digital computer solution, via the well-known "U-g method". Flutter boundaries are obtained for unstiffened and stringer stiffened shells using linear piston theory for a two mode solution. These results are compared with the higher order solutions up to ten to assess the convergence of the two-mode solution. Results using the exact aerodynamic theory have also been obtained for specific cases and convergence of the solutions established. A range of i) shell geometries (i.e. L/R and h/R ratios), ii) eccentricities (in the case of stringer-stiffened shells), iii) circumferential modal patterns; have been considered.

V.1 GENERAL FORM OF THE AEROELASTIC EQUATIONS

The most general form of aeroelastic equations of dynamical systems (in the absence of external forces) can be expressed (Ref. A35) symbolically by equating the elastic force ($\mathcal{S}$) to the aerodynamic (A) and inertia (I) forces in terms of the generalised displacements q.

$$\mathcal{S}(q) = A(q) + I(q) \qquad (V.1)$$

The term generalised displacement is used because the co-ordinates used to describe the system analytically need not necessarily have the dimensions of length; some of them may be angles or even quantities with no direct observable physical significance at all.

The flutter problem is to solve the equation (V.1) and determine the conditions of sustained self-excited oscillations of constant amplitude in the presence of an external

supersonic flow field.

If A(q) = 0, the problem reduces to that of determining the invacuo-natural vibration characteristics of the structure.

For a majority of applications to flight vehicle structures it may not be possible to solve equation (V.1) exactly and hence various approximate numerical solutions have been developed. Most of the approximate methods can be broadly divided into two steps: first the space configuration of the deformed structure, which is actually an infinite degree of freedom system, is approximated by an equivalent system with finite degrees of freedom. The equations of the continuous system are thus reduced to systems simultaneous equations. The second step is to solve the simultaneous equations and determine the critical parameters of the problem.

One of the most commonly accepted ways of deriving the flutter equations of a structure is the Rayleigh-Ritz or the Galerkin method in which the deformed shape of the structure is assumed to consist of a superposition of a finite number of pre-assigned mode shapes. The prescribed displacement boundary conditions of the structure must be satisfied by these mode shapes. The displacements of the structure (u,v,w) can then be expressed in terms of the assumed mode shapes and the generalised co-ordinates q, (which are as many in number as the desired degrees of freedom). In some cases it may be possible to describe the displacement functions as the natural mode shapes which satisfy the boundary conditions exactly. In such cases the natural mode shapes are orthogonal functions and the generalised co-ordinates are the same as the normal co-ordinates. The term normal co-ordinate implies a co-ordinate which expresses the displacement in a natural mode of motion.

By writing the expressions for kinetic andpotential energies of the system and applying Lagrange's equations the aeroelastic equations are derived.

V.2 FLUTTER EQUATIONS FOR A CYLINDRICAL SHELL

The circular cylindrical shells considered here have simple-support end conditions and hence the displacement functions in a given mode can be conveniently chosen as the natural mode shapes appropriate to unstiffened circular cylindrical shells.

$$u_{mn} = \bar{u}_{mn} \cos \frac{m\pi x}{L} \cos n\theta$$

$$v_{mn} = \bar{v}_{mn} \sin \frac{m\pi x}{L} \sin n\theta \qquad (V.2)$$

$$w_{mn} = \bar{w}_{mn} \sin \frac{m\pi x}{L} \cos n\theta$$

The expressions for the displacements (u,v,w) can be written in terms of the normal co-ordinates q_{mn} as

$$u = \sum_m u_{mn} q_{mn}, \quad v = \sum_m v_{mn} q_{mn}, \quad w = \sum_m w_{mn} q_{mn} \qquad (V.3)$$

There are as many terms in these equations as the number of axial modes (degrees of freedom) chosen, since the axial (m) and circumferential (n) motions are assumed decoupled and a particular value of n is chosen for investigation.

The general expressions for the kinetic and potential energy can be written for an unstiffened shell as

$$T = \tfrac{1}{2} \sum_m M_{mn} \dot{q}_{mn}^2$$

$$\bar{U} = \tfrac{1}{2} \sum_m M_{mn} q_{mn}^2 \omega_{mn}^2 \qquad (V.4)$$

where $M_{mn} = \int_s (u_{mn}^2 + v_{mn}^2 + w_{mn}^2) \sigma \, ds$ is the generalised mass, ω_{mn} is the invacuo-natural frequency of the shell in the mode (m,n) and σ is the mass per unit area of the shell surface s.

Lagrange's equation is applied in the form

$$\frac{d}{dt} \left(\frac{\partial T}{\partial \dot{q}_{mn}} \right) + \frac{\partial \bar{U}}{\partial q_{mn}} = \bar{Q}_m^{(n)} \qquad (V.5)$$

where $\bar{Q}_m^{(n)}$ is the m^{th} (dimensional) generalised force ($= \rho_o U^2 Q_{mr}$) and equals the work done by the external force

field per unit displacement q_{mn}. In the present application the external force field consists of the aerodynamic pressures acting on the surface of the vibrating cylinder and is equal to the sum of the pressures induced by each of the individual axial modes assumed.

Hence

$$\bar{Q}_m^{(n)} = \int_s \left[(p)_1 + (p)_2 + \ldots + (p)_{m'} \right] w_{mn} ds = \sum_{r=1}^{m'} \rho_o U^2 Q_{mr} q_{rn} w_{mn} \quad - - \quad (V.6)$$

where $(p)_1$, $(p_2)\ldots$ are the pressure distributions resulting from the motions $w_{1n}q_{1n}$, $w_{2n}q_{2n}, \ldots w'_{mn}q'_{mn}$ and m' is the maximum number of axial modes chosen (degrees of freedom).

Since neutral stability is under investigation, each generalised co-ordinate can be assumed to have the form $\bar{q}_{mn}e^{i\Omega_n t}$ and, using equations (V.4,5,6), the flutter equations for a cylindrical shell can be written as

$$\left[(\Omega_n^2 - \omega_{mn}^2) T_{mn} \sigma + \rho_o U^2 Q_{mm} \right] \bar{q}_{mn} \bar{w}_{mn} + \sum_{r=1}^{m'} \rho_o U^2 Q_{mr} \bar{q}_{rn} \bar{w}_{rn} = 0$$

$$m = 1, 2, \ldots\ldots m'$$

$$\text{where } T_{mn} = \left(\frac{\bar{u}_{mn}}{\bar{w}_{mn}}\right)^2 + \left(\frac{\bar{v}_{mn}}{\bar{w}_{mn}}\right)^2 + 1 \quad - - - \quad (V.7)$$

The equations (V.7) are written in terms of $\bar{w}_{mn}$ implying that the radial modes are more predominant, which is usually the case. The term T_{mn} can be considered as a correction to the generalised mass which arises due to the coupling of the in-plane modes with the predominantly radial mode. Equations (V.7) may be written more conveniently in terms of the frequency factors

$$\Delta_{mn} \left(= \frac{\omega_{mn}^2 R^2 \rho_c (1-\nu^2)}{E}\right) \text{ and } \Delta \left(= \frac{\Omega_n^2 R^2 \rho_c (1-\nu^2)}{E}\right)$$

in the matrix form as (with $T_{mn}=1$),

$$\begin{bmatrix} (\Delta_{1n}+k_1Q_{11}-\Delta) & k_1Q_{12} & k_1Q_{13}\cdots & k_1Q_{1m'} \\ k_1Q_{21} & (\Delta_{2n}+k_1Q_{22}-\Delta) & k_1Q_{23} & k_1Q_{2m'} \\ = & = & = & = \\ k_1Q_{m'1} & k_1Q'_{m2}\cdots\cdots\cdots & & (\Delta_{m'n}+k_1Q'_{m'm'}-\Delta) \end{bmatrix} \begin{bmatrix} q_{1n} \\ q_{2n} \\ \vdots \\ q'_{mn} \end{bmatrix} = 0$$

$$- \quad - \quad - \quad (V.8)$$

where $k_1 = \frac{2(1-\nu^2)}{E}\left(\frac{R}{L}\right)\left(\frac{R}{h}\right)\rho_o U^2$ is a non-dimensional aerodynamic stiffness ratio parameter and Q_{mr} are the non-dimensional aerodynamic generalised forces defined already. By setting the determinant of the complex matrix in eqn. (V.8) to zero, for a given n, there will be a set of solution frequencies equal in number to the number of axial modes (m') assumed, each with its associated damping ratio. The flutter stability boundary can be fixed by the vanishing of the damping ratio for one of the modes.

The expressions for the generalised forces appearing in equation (V.8) are given by equation (IV.4) and (IV.5) corresponding to a linear piston theory and the exact aerodynamic theory respectively.

For a simply-supported cylindrical shell stiffened by an orthogonal set of stringers and rings the in-vacuo-natural frequencies can be determined from the expressions given in Appendix 4. These are illustrated in a few cases below.

V.3 NATURAL FREQUENCIES OF VIBRATION OF CYLINDRICAL SHELLS

a) Unstiffened Shells

The characteristic determinant to determine the natural frequencies of an unstiffened shell, can be derived from appendix 4 by setting the terms corresponding to stringers and rings to zero, and only retaining the frequency parameter for radial inertias,

$$\begin{vmatrix} \lambda_m^2 + \frac{1-\nu}{2}n^2 & -\frac{1+\nu}{2}\lambda_m n & -\lambda\nu \\ -\frac{1+\nu}{2}\lambda_m n & \frac{1-\nu}{2}\lambda_m^2+n^2 & n \\ -\lambda_m\nu & n & \frac{h^2}{12R^2}(n^2+\lambda_m^2)^2+1-\Delta \end{vmatrix} = 0$$

$$- \quad - \quad (V.9)$$

which on expansion yields a simple expression for the natural frequency factor

$$\Delta_{mn} \quad (= \frac{\rho_c \omega_{mn}^2 R^2 (1-\nu^2)}{E})$$

as

$$\Delta_{mn} = \frac{h^2}{12R^2} (\lambda_m^2+n^2)^2 + \frac{\lambda_m^4 (1-\nu^2)}{(\lambda_m^2 + n^2)^2} \qquad (V.10)$$

b) Stringer-Stiffened Shells

The characteristic determinant to determine the natural frequencies of a stringer-stiffened shell, neglecting inplane and rotary inertias, and assuming the stringer effects to be 'smeared', can be derived from appendix 4 by setting the terms corresponding to rings to zero, i.e.

$$\begin{vmatrix} \lambda_m^2(1-\bar{s}) + \frac{1-\nu}{2} n^2 & -(\frac{1+\nu}{2})\lambda_m n & -\lambda\left[\nu + \lambda_m^2 \frac{\bar{z}_s}{R} \bar{s}\right] \\ -\frac{(1+\nu)}{2}\lambda_m n & \frac{1-\nu}{2}\lambda_m^2 + n^2 & n \\ -\lambda\left[\nu + \lambda_m^2 \frac{\bar{z}_s}{R} \bar{s}\right] & n & A_{33} - (1+f_s)\Delta \end{vmatrix} = 0$$

$$- \quad - \quad - \quad (V.11)$$

where

$$A_{33} = \frac{h^2}{12R^2} \lambda_m^4 \left[(1 + \bar{\beta}^2) + \left\{\frac{E_s I_s}{Dd} + \bar{\beta}^2 \frac{G_s J_s}{Dd}\right\}\right]$$

$$+ \lambda_m^4 (\frac{\bar{z}_s}{R})^2 \bar{s} + 1$$

$$f_s = \frac{\text{mass of stringers}}{\text{mass of shell}} \simeq (\frac{A_s}{hd})$$

and $\bar{z}_s = \frac{h_s+h}{2}$, ($h_s$ = depth of the stringer)

The determinant (V.11) when expanded, yields the explicit expression for the frequency factor $\Delta_{mn}^{(S)}$ as

$$\Delta_{mn}^{(S)} = \frac{1}{(1+f_s)} \frac{h^2}{12R^2} \left[(\lambda_m^2+n^2) + \lambda_m^4 (1-\nu^2) f_s (\frac{b_s}{h})^2 \right.$$

$$\left. + \frac{\lambda_m^2 n^2 \frac{9}{5} (1-\nu) f_s^3 (\frac{b_s}{h})^2}{f_s^2 + (\frac{b_s}{h})^4 (\frac{h}{R})^2 (\frac{L_s}{\pi})^2} \right] +$$

$$+\frac{1}{(1+f_s)}(1-\nu^2)\lambda_m^4\left[\frac{1+f_s\left\{1+2\left(\frac{\bar{z}_s}{R}\right)\left[n^2-\nu\lambda_m^2\right]+\left(\frac{\bar{z}_s}{R}\right)^2\left(\lambda_m^2+n^2\right)^2\right\}}{\left(\lambda_m^2+n^2\right)^2+f_s(1+\nu)\lambda_m^2\left[2n^2+(1-\nu)\lambda_m^2\right]}\right]$$

$$- - \quad (V.12)$$

V.4 SOLUTION OF THE SHELL FLUTTER EQUATIONS

The flutter equations (V.8) may be looked upon as an eigenvalue problem of the form

$$(A - \Delta I)Q = 0 \qquad (V.13)$$

where the elements of the matrix A are complex numbers composed of generalised inertial, elastic and aerodynamic forces, I is the unit matrix, Δ is the eigenvalue and Q is the corresponding eigenvector. In general, the aerodynamic forces are transcendental functions of the eigenvalue itself and hence it may not be possible to solve the eigenvalue problem uniquely.

However, the problem may be reduced to an algebraic eigenvalue problem by calculating the aerodynamic generalised forces for constant (assumed) values of Mach number M_a and frequency parameter k_a. For each pair of values of (M_a, k_a), the set of eigenvalues Δ can be predicted by any of the available methods (e.g. Ref. A33). Using the relation

$$k_a = \frac{\Omega_n L}{U}$$

a predicted Mach number $M_p (= \frac{U}{a_o})$ may be determined.

Physically, flutter condition is reached only if Δ is real and positive and M_p is equal to M_a. But, for arbitrarily assumed values of (M_a, k_a) this is generally not the case. Therefore, the generalised aerodynamic forces have to be calculated for various assumed pairs of values of (M_a, k_a) and the eigenvalue problem is to be solved for each pair until a positive real eigenvalue is obtained. In order not to miss a possible flutter case M_a and k_a have to be varied in small steps involving a large number of different matrices and their solutions. This is the effect of reducing the original transcendental eigenvalue problem to an algebraic one.

For arbitrarily assumed values of (M_a, k_a) the real part of the eigenvalue determines a predicted frequency factor and the ratio of the imaginary part to the real part can be thought of as an artificial damping inherent in the system, i.e.

$$g_p = \frac{Im\ (\Delta)}{Rl\ (\Delta)} \qquad (V.14)$$

For each of a series of pre-assigned Mach numbers M_a the critical speed M_p is determined using one of the standard methods such as the U-g method (Ref. A34). Once this is done, a plot of M_p vs M_a can be drawn and the point where this curve meets the line $M_p = M_a$ determines the critical flutter speed M_f for the geometry under investigation. Also then found is the critical value of the flutterfrequency parameter k_f.

V.5 CLOSED FORM SOLUTIONS FOR A TWO-MODE (BINARY) FLUTTER ANALYSIS USING THE LINEAR PISTON THEORY

V.5(a) Unstiffened shells

If the linear piston theory generalised forces (equations IV.4) are used with the frequency expression (V.10) in a binary analysis (coupling between the two axial modes r and s), the flutter determinant (V.8) can easily expand to yield explicit expressions for the flutter frequency factor Δ_F and the flutter Mach number M_f as

$$\Delta_F = \tfrac{1}{2}\left[\Delta_{rn} + \Delta_{sn}\right]$$

$$M_F = \left(\frac{r^2-s^2}{4rs}\right) \frac{E}{2\rho_o a_o^2(1-\nu^2)} \left(\frac{L}{R}\right)\left(\frac{h}{R}\right)\left[(\Delta_{rn}-\Delta_{sn})^2 + 4\left(\frac{\rho_o}{\rho_c}\right)\frac{\rho_o a_o^2(1-\nu^2)}{E}\left(\frac{R}{h}\right)^2\left(\frac{\Delta_{rn}+\Delta_{sn}}{2}\right)\right]^{\frac{1}{2}} \qquad (V.15)$$

with the condition that (r+s) is an odd integer.

V.5(b) Stringer-stiffened shells

If the linear piston theory generalised forces (equations IV.4) are combined with the frequency expression (V.12) in a binary analysis, the following expressions are obtained for the flutter frequency factor $\Delta_F^{(S)}$ and flutter

Mach number $M_F^{(S)}$ corresponding to a stringer-stiffened shell. (The stringer effects are assumed to be smeared in this case)

$$\Delta_F^{(S)} = \tfrac{1}{2}\left[\Delta_{rn}^{(S)} + \Delta_{sn}^{(S)}\right]$$

$$M_F^{(S)} = \left(\frac{r^2-s^2}{4rs}\right)\frac{E}{2\rho_o a_o^2(1-\nu^2)}\left(\frac{L}{R}\right)\left(\frac{h}{R}\right)\left[\left(\Delta_{rn}^{(S)} - \Delta_{sn}^{(S)}\right)^2 + 4\left(\frac{\rho_o}{\rho_c}\right)\frac{\rho_o a_o^2(1-\nu^2)}{E}\left(\frac{R}{h}\right)^2\left(\frac{\Delta_{rn}^{(S)} + \Delta_{sn}^{(S)}}{2}\right)\right]^{\frac{1}{2}} \quad - - - \quad (V.16)$$

with the condition that (r+s) is an odd integer.

V.5(c) Krumhaar Correction.

If the Krumhaar Correction (Ref. 64) is included in the linear piston theory expression as given by equation (I.7), the (non-dimensional) generalised forces are

$$Q_{mm} = \frac{ik}{2M} - \left(\frac{L}{R}\right)\frac{1}{4M^2}$$

and $$Q_{mr} = \frac{1}{M}\frac{mr}{m^2-r^2}\left[1-(-1)^{m+r}\right] \quad \text{for} \quad m \neq r \qquad (V.17)$$

The effect of this correction is to introduce an aerodynamic stiffness term in the leading diagonal of the flutter determinant. In a binary analysis, the inclusion of Krumhaar correction leads to the following explicit expressions for the flutter frequency factor and Mach number.

$$\Delta_F = \left(\frac{\Delta_{rn}+\Delta_{sn}}{2}\right) - \left(\frac{R}{h}\right)\frac{(1-\nu^2)\rho_o a_o^2}{2E}$$

$$M_F = \left(\frac{r^2-s^2}{4rs}\right)\frac{E}{2\rho_o a_o^2(1-\nu^2)}\left(\frac{L}{R}\right)\left(\frac{h}{R}\right)\left(\Delta_{rn}-\Delta_{sn}\right)^2 + 4\left(\frac{\rho_o}{\rho_c}\right)\frac{\rho_o a_o^2(1-\nu^2)}{E}\left(\frac{R}{h}\right)^2\left\{\frac{\Delta_{rn}+\Delta_{sn}}{2} - \left(\frac{R}{h}\right)\frac{(1-\nu^2)}{2E}\rho_o a_o^2\right\}\Bigg]^{\frac{1}{2}} \qquad (V.18)$$

The condition that (r+s) is odd applies.

It is interesting to note that the correction term is inde-

pendent of M, k and n.

V.5(d) Divergence Criterion for an Unstiffened Shell Resulting from the Krumhaar Correction

Putting $\Omega = 0$ in the binary flutter determinant including the Krumhaar correction leads to the following criterion for the divergence of an unstiffened shell.

$$\begin{vmatrix} \left(\frac{Eh\,\Delta_{rn}}{R^2(1-\nu^2)} - \frac{\rho_o a_o^2}{2R}\right) & \frac{\rho_o U^2}{LM}\cdot\frac{4rs}{s^2-r^2} \\ -\frac{\rho_o U^2}{LM}\frac{4rs}{s^2-r^2} & \frac{Eh\,\Delta_{sn}}{R^2(1-\nu^2)} - \frac{\rho_o a_o^2}{2R} \end{vmatrix} = 0 \quad (V.19)$$

which on expansion gives the following expression for the critical divergence speed:

$$M_{div} = \frac{E}{\rho_o a_o^2(1-\nu^2)}\left(\frac{L}{R}\right)\left(\frac{h}{R}\right)\left(\frac{r^2-s^2}{4rs}\right)\left[\frac{\rho_o a_o^2(1-\nu^2)}{2E}\left(\frac{R}{h}\right)(\Delta_{rn}+\Delta_{sn}) - \left\{\Delta_{rn}\Delta_{sn} + \left(\frac{R}{h}\,\frac{\rho_o a_o^2(1-\nu^2)}{2E}\right)^2\right\}\right]^{\frac{1}{2}} \quad (V.20)$$

A single degree of freedom divergence criterion may be obtained by setting any of the leading diagonal terms of the determinant (eqn. V.19) to zero, i.e.

$$\Delta_{rn} = \frac{\rho_o a_o^2(1-\nu^2)}{2E}\left(\frac{R}{h}\right) \quad (V.21)$$

V.6 NUMERICAL RESULTS

The shell flutter problem has been programmed for digital computer solution and numerical results have been obtained for various values of cylindrical shell and flow parameters. The following numerical data (Ref. 71) is common to all the shells considered for flutter analysis:

Material of the shell: Steel, $E = 2.04 \times 10^4 Kg/mm^2$

$\rho_c g = 7.8 \times 10^{-6} Kg/mm^3$, $\nu = 0.3$

Flight altitude: sea-level,

Static pressure of undisturbed flow =

$p_o = 1.03 \cdot 10^{-2} Kg/mm^2$

$\rho_o g = 1.225 \cdot 10^{-9} Kg/mm^3$

Ratio of specific heats = $\gamma = 1.4$

V.6(a) Two Mode (Binary) Flutter Analysis of Unstiffened Shells using Linear Piston Theory

The most critical combination of modes r and s giving the lowest critical Mach numbers was found to be r = 2 and s = 1, and accordingly, critical flutter Mach numbers have been obtained for a range of length to radius (L/R) and thickness to radius (h/R) ratios. Fig. 43 shows the variation of critical Mach numbers as a function of circumferential mode number n for a particular thickness ratio. The pattern of these curves is very similar to the invacuo-natural frequency spectrum in that the minimum critical speed does not correspond to the minimum circumferential mode number suggesting that the asymmetric flutter could be more critical than the axisymmetric flutter. For short shells (L/R ~2.0) the critical speed may occur at values of n higher than 17. For longer shells, however, the critical circumferential mode numbers can be considerably less (as low as 4 for L/R ~ 20). The dotted lines correspond to the critical Mach numbers obtained by neglecting the influence of aerodynamic damping. This leads to the conclusion that the neglect of aerodynamic damping may in certain circumstances lead to very pessimistic results.

In Fig. 44 the variation of the invacuo-natural frequency factors corresponding to L/R = 2.0, h/R =0.002, m = 1,2 is compared with the flutter frequency factor which is the arithmetic mean of these two invacuo frequency factors (see equation V.15). The value of n_{crit} corresponding to M_{crit} could be very different from that corresponding to Δ_F (e.g. for L/R = 2.0 M_{crit} occurs at n_{crit} = 17 while the minimum flutter frequency corresponds to n = 10). The effect of increasing the (L/R) is to reduce the value of

n corresponding to the minimum natural frequency and also that corresponding to M_{crit}. The former is illustrated in Fig. 45 for the case m = 1 and h/R = 0.002, and the latter is apparent from Table 26. The curves of critical Mach numbers as a function of the (h/R) ratio is drawn in Fig. 46 for cylinders of various values of (L/R) vibrating at particular circumferential modes. It appears that the influence of thickness on the flutter boundary is very significant for short shells as compared with very long shells. The influence of aerodynamic damping is again apparent. The values of M_{crit} and the corresponding n_{crit} are listed in Table 26 for a range of (L/R) and (h/R).

It was found over a very wide range of L/R, h/R, and n the Krumhaar correction did not significantly affect the critical Mach numbers or the frequency factors (see equation V.18) and hence the results are not presented here.

It was found also over the same wide range of parameters that equation (V.20) yields imaginary divergence speeds suggesting that divergence may not be possible for a cylindrical shell in the supersonic flow field.

It is to be noted that the single degree of freedom divergence criterion (Eqn. V.20) does not yield a critical divergence speed since the aerodynamic stiffness terms introduced by the Krumhaar correction in the leading diagonal terms of the determinant are independent of the flow parameters M and k. Once the shell material and the flight altitude are fixed the right side of equation (V.21) varies inversely as the thickness ratio (h/R), and is independent of m, n, L/R, h/R. The values of (L/R) which yield minimum values of Δ_{rn} equal to the right hand side of equation (V.21) are plotted against (h/R) for steel shells at sea level in Fig. 47. This figure may be considered as a 'divergence' boundary derived from a single degree of freedom system. The corresponding curve for aluminium is also included in the same figure.

V.6(b) Multi-mode Flutter Analysis of Unstiffened Shells Using the Linear Piston Theory

The determination of flutter Mach numbers and flutter frequency factors of an unstiffened shell becomes very tedious when the number of axial modes is more than two. It is not possible to derive simple explicit expressions such as equations (V.15) applicable to a multi-mode system. Hence the indirect procedure described in Section V.4 is followed. The flutter Mach number and the flutter frequency factor given by the binary analysis may be used as a useful guide to choose the assumed initial values of M_a and k_a and to reduce the computational labour.

The procedure is illustrated for a cylindrical shell with L/R = 10.0, h/R = 0.002 for which the critical Mach number and frequency parameter derived from the binary are: M_{crit} = 1.397 and k_{crit} = 2.384, corresponding to n_{crit} = 6. The chosen value of L/R is not typical of missile bodies but is selected for the following reasons:

i) It was intended to compare these results with the flutter boundaries derived from the exact aerodynamic theory. The programme to calculate the exact aerodynamic generalised forces was restricted to values of n up to 10 due to limitations on computer time and storage whereas the critical Mach numbers for short shells were beyond this range for most of the thickness ratios considered (see Table 26).

ii) The variation of critical Mach numbers with thickness ratio in the range of the latter considered is so rapid for short shells that one has to consider Mach numbers of unrealistic magnitudes (of the order of M ~ 100; see Table 26).

The various steps involved in the calculation of flutter Mach number and flutter frequency factor are as follows:

i) Data: Material - E, ρ_c, ν
Shell - (h/R), (L/R)
Mode - m, n
Airflow - ρ_o, a_o

ii) Invacuo-natural frequency factors $\Delta \left(= \frac{\rho_c \omega^2 R^2 (1-\nu^2)}{E}\right)$

are determined using the above data in eqn. (V.10).

iii) A pair of assumed initial values (M_a, k_a) is chosen and the aerodynamic generalised forces are determined from eqn. (IV.4).

iv) The elements of the complex matrix in equation (V.8) are formed. The order of the matrix would be equal to the number of axial modes chosen.

v) The eigenvalues and eigenvectors of the complex matrix are determined using Ref. A33.

Results:

a) The real part of the eigenvalue is a predicted frequency factor Δ and $\Omega R = \sqrt{\frac{E\,\Delta}{\rho_c(1-\nu^2)}}$ where Ω is the predicted frequency corresponding to the assumed values of (M_a, k_a).

b) $k_a = \frac{\Omega L}{U} = \frac{\Omega R}{U}\left(\frac{L}{R}\right)$ by definition and hence the predicted Mach number corresponding to (M_a, k_a) is

$$M_p = \frac{U}{a_o} = \frac{\Omega R}{k_a a_o}\left(\frac{L}{R}\right)$$

c) Artificial damping $g_p = \frac{Im(\Delta)}{Rl(\Delta)}$

The calculations are repeated with different pairs of (M_a, k_a) until a positive, real eigenvalue is obtained.

Sample results are presented for some values of M_a and k_a in Table 21 in which 2 to 10 axial modes were considered.

The conventional U-g plots leading to the critical Mach number and frequency parameter are given in Fig. 48 corresponding to 10 axial modes. Figs. (48)a,b,c correspond to the assumed Mach numbers of 1.7, 1.8, 1.9 respectively, each yielding a predicted Mach number of 1.84, 1.8, 1.775. These values are plotted in Fig. 48(d) and the point where the $M_p \sim M_a$ curve intersects the 45^o line is the flutter Mach number. The real parts of the eigenvalues are plotted against M_a in Fig. 48(e) and the point where

this curve meets the M_F line corresponds to the flutter frequency factor.

Table 22 shows the comparison of the two mode solution with various higher order solutions up to 10. It can be seen that for the cases analysed the convergence of the Galerkin solution is reached by taking six or seven axial modes. The invacuo-natural frequency factors for the first ten axial modes and the flutter frequency factors by taking the first two, three,... ten axial modes are given in Table 23. An increase in the number of axial modes does not seem to alter the flutter frequency factors considerably, most of them being closer to the invacuo frequency factor corresponding to m=2. An examination of the eigenvector components corresponding to the flutter solution also suggests the most predominant influence of the second axial mode and the significant influence of the first and the third axial modes respectively. This is a possible justification for considering the coupling of the first few modes only for flutter analysis.

V.6(c) Flutter Analysis of Unstiffened Shells Using the Exact Aerodynamic Theory

The generalised forces using the exact aerodynamic theory are implicit functions of the Mach number and the frequency parameter. Consequently, it is not possible to derive explicit expressions for the flutter speed and frequency, even for a binary, if the exact aerodynamic theory is used. The procedure to determine the critical Mach numbers is exactly the same as listed in Section V.6(b) except that now the aerodynamic generalised forces are determined from equations (IV.14) and (IV.15). The amount of computer time involved in the calculation of the exact aerodynamic generalised forces is so large that the results have only been obtained for specific cases. In Table 24 the flutter Mach numbers using the exact aerodynamic theory are compared with those using the linear piston theory for a two-mode solution. It was

concluded from Tables 16 to 20 that the linear piston theory generalised forces are closer to the exact theory for large n and small L/R at high Mach numbers. It can be seen in Table 24 that the comparison between the two theories is very good for small L/R, large n and M but gets progressively worse for longer L/R, smaller n and M. Surprisingly the difference in the critical Mach numbers between the two theories is very much less when the thickness ratio is doubled, even though the (L/R) ratio is large.

The convergence of the Galerkin solution can be seen by comparing the two mode results with higher mode results. From Table 22 it appears that increasing the number of modes does not appreciably change the results when exact aerodynamic theory is used.

There is as yet no definite method of determining the severity of the flutter condition. However, the rate of change of damping inherent in the system may give an indication of the severity of flutter. In Table 25 the inherent damping predicted by the exact aerodynamic theory is presented along with that predicted by the linear piston theory for one set of parameters. A negative damping may be thought of as corresponding to instability and a positive damping as that corresponding to stability. This Table suggests that the damping predicted by the exact theory is much higher than that by the linear piston theory implying the stabilising influence of the exact aerodynamic theory. The results presented here are typical of the observed trend in all the cases analysed.

V.6(d) Two-mode (Binary) Flutter Analysis of Stringer-stiffened Shells Using Linear Piston Theory

In Tables 26 and 27 the critical Mach numbers are presented for shells stiffened internally or externally with stringers, using the linear piston theory in a binary analysis. The total mass of the stringers has been assumed to be equal to the total mass of the shell in each of the cases analysed. The effect of doubling the mass of a given shell by

distributing the additional mass in the form of ten equal stringers of rectangular cross-section is studied and the following conclusions may be inferred from the results.

For all the (L/R) and (h/R) ratios considered, the shells stiffened with external stringers appear to yield much higher critical Mach numbers compared to the shells stiffened with internal stringers of the same eccentricity, (see Tables 26 and 27). Eccentric stiffening appears to yield higher critical Mach numbers for short shells provided that the eccentricity is sufficiently large (i.e. the ratio of the stiffener depth/shell thickness = $h_s/h > 5.0$ for external stringers and about 8.0 for internal stringers). If the stiffener eccentricity is small, however, it seems that a monocoque shell of double the thickness yields critical Mach numbers higher than the corresponding stringer-stiffened shell of the same mass. As the (L/R) ratio is increased, the effectiveness of eccentric stiffening over the monocoque shell of the same mass in increasing the critical Mach numbers may be felt only if the eccentricity is very high.

Table 28 shows the convergence of the Galerkin solution for a stringer-stiffened shell. Comparison is also given of the results corresponding to a monocoque shell of the same mass. The converged solution seems to indicate that for this case the shell stiffened with stringers is only marginally better than the monocoque shell of the same mass.

V.7 CONCLUSIONS

Due to the multiplicity of the parameters involved it is very difficult to draw general conclusions applicable to the whole range of geometrical, modal and flow parameters. The results obtained so far at least confirm the rather conservative nature of the results derived previously from binary analysis using linear piston theory and also that one has to adopt at least six or seven axial modes to obtain a realistic estimate of the flutter boundary. If the exact aerodynamic theory is used the results seem to indicate that the instability is milder than that predicted by the

linear pistom theory. The amount of computer time involved to produce meaningful results using exact aerodynamic theory is so large that it prohibits very extensive calculations over a wide range of parameters. However the results obtained from linear piston theory may be refined at least for particular cases of interest, by having the closed form binary solutions as a useful guide to reduce the computational labour.

VI GENERAL CONCLUSIONS

The problem of vibration and flutter analysis of simply-supported unstiffened and orthogonally stiffened circular cylindrical shells which are typical of missile bodies has been developed and programmed for digital computer solution. The analysis and the programme are capable of handling shells of arbitrary lengths to radius (L/R) and thickness to radius (h/R) ratios.

In the case of stiffened shells, the stiffener effects may be treated as 'smeared' or 'discrete' and in each case the effects of eccentricity, inplane and rotary inertias could be studied.

The aerodynamic generalised forces may be calculated using the linear piston theory, with or without the Krumhaar correction and also using the exact aerodynamic theory.

By combining the invacuo-vibration analysis and the aerodynamic generalised forces the flutter boundaries may be obtained in each of the above cases for a binary involving only two axial modes and the accuracy may be improved by increasing the axial modal combinations to produce a converged solution.

The following general conclusions may be drawn from this study:

i) A one term solution which corresponds to that of a simply-supported, unstiffened cylindrical shell when used with a proper choice of stiffener distribution yields the invacuo-natural frequencies which are in good agreement with the existing more complicated analytical and experimental results.

ii) Inplane and rotary inertia of the stiffeners can have significant influence on the frequencies of a shell depending on their mass and eccentricity .

iii) The assumption of treating the stiffeners as 'discrete' members of the structure seems to have little advantage over that of treating them as 'smeared' if a proper stiffener distribution can be made.

iv) The theoretical predictions of natural frequencies can be verified against carefully conducted experiments to give more confidence in the use of the theoretical results.

v) Good agreement in the aerodynamic generalised forces between the linear piston theory and the exact aerodynamic theory appear to exist only for short shells vibrating at a large number of circumferential waves in a supersonic stream at high Mach numbers.

vi) The simple closed form solution obtained by combining the linear piston theory in a two-mode Galerkin (binary) analysis may be used as a useful guide to produce flutter boundaries of unstiffened and orthogonally stiffened cylindrical shells.

vii) The convergence of the Galerkin solution and the corresponding critical flutter modes may be established by including more axial modes and studying the critical Mach numbers, flutter frequencies and eigenvectors. The Binary results may be used as a useful initial guide in the choice of (M_a, k_a) to reduce the computational labour involved in the determination of critical parameters via the well-known U-g method. It has been found that six or seven axial modes may be sufficient to give a reasonable estimate of the critical Mach numberwhich is close to the converged solution.

viii) Exact aerodynamic theory may be used to further refine the calculations and determine the severity of the flutter condition. The influence of using the exact aero theory is to predict flutter of shells as a mild instability.

REFERENCES

a) Chronological Bibliography of Cylindrical Shell Panel Flutter

1. Ward, G.N. "The Approximate External and Internal Flow Past a Quasi-Cylindrical Tube Moving at Supersonic Speeds" Quarterly Journal of Mechanics and Applied Mathematics, Vol. 1, No. 2, June 1948, pp. 225-245.
2. Miles, J.W. "On the Reduction of Unsteady Supersonic Flow Problems to Steady Flow Problems" Journal of Aeronautical Sciences, Vol. 17, January 1950, pp. 64.

2.(a) Goland, M. and Luke, Y.L. "An Exact Solution for Two-Dimensional Linear Panel Flutter at Supersonic Speeds" Journal of Aeronautical Sciences, Vol. 21, No. 4, 1954, pp. 275-276.

3. Miles, J.W. "Supersonic Flutter of a Cylindrical Shell" I- General Theory. The Ramo-Wooldridge Corporation, Report AM5-2, August 19, 1955.
4. Miles, J.W. "Supersonic Flutter of a Cylindrical Shell" II- Pressurisation and Internal Fluid Effects, The Ramo-Wooldridge Corporation, Report AM 5-11, November 14, 1955.
5. Miles, J.W. "Supersonic Flutter of a Cylindrical Shell" III- Aelotropic Shells, The Ramo-Wooldridge Corporation, Report AM 5-12, December 2, 1955.
6. Miles, J.W. "Supersonic Flutter of a Cylindrical Shell" IV- Effects of Non-Uniform Steady Flow, The Ramo-Wooldridge Corporation, Report AM-16, December 7, 1955.
7. Bolotin, V.V. "Vibrations and Stability of Circular Cylindrical Shells in a Compressible Fluid Flow" (in Russian), Injenernyi Jurnal, Vol. 24, No. 3, 1956.
8. Leonard R.W., and Hedgepeth, J.M. "On Panel Flutter and Divergence of Infinitely Long Unstiffened and Ring-Stiffened Thin-walled Circular Cylinders" NACA TN 3638, April 1956, NACA Report 1302, 1957.
9. Miles, J.W. "On the Aerodynamic Instability of Thin Panels" The Ramo-Wooldridge Corporation Report, AM 5-2A, May 20, 1955; Journal of the Aeronautical Sciences, Vol. 23, No. 8, August 1956, pp. 771-780.
10. Ashley, H. and Zartarian, G. "Piston Theory - A New Aerodynamic Tool for the Aeroelastician" Journal of the Aeronautical Sciences, Vol. 23, No. 12, December 1956, pp. 1109-1118.

11. Kaplan, A., Miles, J.W., and Fung, Y.C. "Experiments on Supersonic Flutter of Thin Cylinders under Internal Pressure" Tecnnical Report No. AM 6-3, Space Technology Laboratories, 1956.

12. Bolotin, V.V. "Vibrations and Stability of an Elastic Cylindrical Shell in Supersonic Flow" (in Russian), Engineering Transactions, Inzhener Shornik Akad. Nauk., Vol. 24, 1956.

12.(a) Kopzon, G.I. "Vibration of Thin-walled Elastic Bodies in a Gas Stream" (in Russian) Doklady Akad. Nauk., 107, 2, 1956, pp. 217-220; (Applied Mechanics Reviews, 10, Rev. 33, 1957).

13. Miles, J.W. "Supersonic Panel Flutter of a Cylindrical Shell" Journal of the Aeronautical Sciences, Vol. 24, No. 2, February 1957, pp. 107-118.

14. Stepanov, R.D. "On the Flutter of Cylindrical Shells and Panels moving in a Flow of Gas" Prikladnaia Mathematika i Mekhanika, Vol. 21, No. 5, 1957 (Translated and issued as NACA TM 1438, September 1958).

15. Luke, Y.L., and St. John, A. "Supersonic Panel Flutter" Midwest Research Institute, WADC Technical Report 57-252, 1957.

16. Miles, J.W. "Supersonic Panel Flutter of a Cylindrical Shell - II" Journal of the Aeronautical Sciences, Vol. 25, No. 5, May 1958, pp. 312-316.

17. Volkov, A.N. "Vibration of a Cylindrical in the Stream of an Ideal Fluid" (in Czech.), Aplik. Mat. Cesko-Akad. Ved., Vol. 3(3), 1958, pp. 161.

18. Holt, M. "Aerodynamic Forces on a Cylindrical Shell in Panel Flutter" Brown University, AFOSR TN-58-474, AD 205548, 1958.

19. Randall, D.G. "Supersonic Flow past Quasi-Cylindrical Bodies of Almost Circular Cross Section" British Ministry of Supply, ARC R&M No. 3067, 1958.

20. Johns, D.J. "Some Panel Flutter Studies using Piston Theory" Journal of the Aeronautical Sciences, Vol. 25, No. 11, November 1958, pp. 679-684, (Errata: Vol. 26, March 1959).

21. Shen, S.F. "An Approximate Analysis of Non-linear Flutter Problems" Journal of Aerospace Sciences, Vol. 26, January 1959, pp. 25.

22. Miles, J.W. "On Panel Flutter in the Presence of Boundary Layer" Journal of Aerospace Sciences, Vol. 26, No. 2, February 1959, pp. 81-93.

23. Strack, S.L., and Holt, M. "Supersonic Panel Flutter of a Cylindrical Shell of Finite Length" AFOSR TN 59-547, Brown University, May 1959.

24. Shulman, Y. "Vibration and Flutter of Cylindrical and Conical Shells" MIT Report TR-74-2, AFOSR TR 59-776, June 1959.

25. Rattayya, J.V., and Goodman, L.E. "Bibliographical Review of Panel Flutter and Effects of Aerodynamic Noise", WADC TR 59-70, ASTIA Document No. 215448, University of Minnesota, June 1959.

26. Stepanov, R.D. "Flutter of Cylindrical Panels Moving in a Gas" (in Russian), Inzhener Shornik. Akad. Nauk., Vol. 25, 1959, pp. 92.

27. Bolotin, V.V. "Some New Problems in the Dynamics of Shells" (in Russian), Translation "Strength Calculations" No. 4, Mashgis 1959.

28. Rabinovich, B.I. "On Small Harmonic Oscillations of a Cylindrical Shell along the Axis of which an Ideal Gas flows with Supersonic Velocity" Prikladnaia Mathematika i Mekhanika, Vol. 23(5), 1959, pp. 1255.

29. Movchan, A.A. "On the Influence of Aerodynamic Damping in the Supersonic Flutter of Shells" (in Russian), Izvetsia Akad. Nauk. SSSR (OTN Mekh. i Mashino), No. 1, January-February 1960.

30. Fung, Y.C.B., "A Summary of The Theories and Experiments on Panel Flutter" AGARD Manual on Aeroelasticity, Vol. 3, Chapter 7; Also GALCIT Report AFOSR TN-60-224, May 1960.

31. Johns, D.J. "Supersonic Flutter of a Cylindrical Panel in an Axisymmetric Mode" Journal of the Royal Aeronautical Society, Vol. 64, June 1960, pp. 362-363.

32. Johns, D.J. "Supersonic Flutter of Cylindrical Shells" C.O.A., Note No. 104, July 1960.

32.(a) Miles, J.W. "On Supersonic Flutter of Long Panels" Journal of Aerospace Sciences, Vol. 27, 1960, pp. 476.

33. Johns, D.J. "Panel Flutter and Divergence Criteria" Aircraft Engineering, Vol. 32, July 1960, pp. 203.

34. Shveiko, Iu., Iu., "Stability of Circular Cylindrical Shells in Gas Flow" (in Russian), Izvestsia Akad. Nauk., USSR, (OTN Mekh. i Mashino), No. 6, November-December 1960, pp. 74.

35. Voss, H.M. "The Effect of an External Supersonic Flow on the Vibration Characteristics of Thin Cylindrical Shells" IAS Paper No. 60-45, Presented at the IAS 28th Annual Meeting, New York, January 25-27, 1960 (Also, Journal of the Aerospace Sciences, Vol. 28, (12), December 1961, pp. 945-956).

36. Dzygadlo, Z., and Kaliski, S. "Self-excited Vibrations of a Stiffened Cylindrical Orthotropic Inelastic Shell in a Linearised Supersonic Flow" Proceedings of Vibration Problems, (Polish Academy of Sciences) Vol. 1(3), 1960, pp. 3-33.

37. Bolotin, V.V. "Non-linear Flutter of Plates and Shells" (in Russian), Engineering Transactions, Inzhener Shornik. Akad.Nauk., SSSR, Vol. 29, 1960, pp. 55.

38. Kacprzynski, J. and Kaliski, S. "Flutter of a Deformable Rocket in Supersonic Flow" Proceedings of the International Aeronautical Congress, Zurich, 1960.

39. Bolotin, V.V. "On the Application of Piston Theory for the Determination of Aerodynamic Forces Acting on an Oscillating Shell" (in Russian), Izvetsia Akad. Nauk. (OTN Mekh. i Mashino) No. 1, January-February 1961, pp. 159.

40. Holt, M. and Strack, S. "Supersonic Panel Flutter of a Cylindrical Shell of Finite Length" Journal of the Aerospace Sciences, Vol. 28, No. 3, March 1961, pp. 197-208.

41. Nayler, G.H.F. "Flutter of Circular Panels in Supersonic Flow" Thesis (unpublished) submitted to the College of Aeronautics (U.K.), June 1961.

42. Krumhaar, H. "Supersonic Flutter of a Circular Cylindrical Shell of Finite Length in an Axisymmetrical Mode", GALCIT, AFOSR TN 1574, October 1961. (Also, International Journal of Solids and Structures, Vol. 1, pp. 23-57, 1965).

43. Librescu, L. "Vibrations of Non-homogeneous, Circular Cylindrical Shells in Supersonic Fluid Flow" (in French) Revue de Mecanique Applique, Vol. 6(5), 1961.

44. Niesytto, J., and Sep. Z., "The Vibration of a Cylindrical Shell of Finite Length with a Supersonic Inside Flow" Proceedings of Vibration Problems, Polish Academy of Sciences, Vol. 2(3), 1961, pp. 251-264.

45. Dzygadlo, Z. "Linearised Supersonic Flow Past a Vibrating Surface of a Body of Revolution" Proceedings of Vibration Problems, Polish Academy of Sciences, Vol. 2(3), 1961, pp. 265.

46. Shveiko, Iu, Iu., "On the Influence of Supersonic Gas Flow on the Lower Critical Force for a Cylindrical Panel" (in Russian), Izvetsia Akad. Nauk., USSR (OTN Mekh. i Mashino), Vol. 4, 1961.

47. Shveiko, Iu,Iu, "Flutter of Circular Cylindrical Shells" (in Russian), Trudi Konferentsii po Toreii Plastin i Obolocek, Kazan, 1961, pp. 414.

48. Miles, J.W. "Remarks on 'Supersonic Panel Flutter of a Cylindrical Shell of Finite Length'" (and Reply of Authors - Strack and Holt), Jour. of Aerospace Sciences, Vol. 29, January 1962, pp. 115.

49. Librescu, L. "Vibrations and Aeroelastic Stability of Thin, Non-homogeneous Cylindrical Shells in a Compressible Fluid Flow", Mecan. Appl. Vol. 13 (4), 1962, pp. 911 (From English abstracts of Selected articles from Soviet Block and Mainland China Technical Journals, Ser. 4, No. 26, March 1963. - see Applied Mechanics Reviews 4885, August 1963).

50. Krumhaar, H. "Formulas for the Determination of the Material Damping of a Cylindrical Shell by a Decaying Free Vibration" AFOSR Report 2995, GALCIT Aeroelasticity and Structural Dynamics Report SM 62-31, June 1962.

51. Mirowitz, L.I., Zimmerman, N.H., and Schweiker, J.W. "Panel Flutter Survey and Design Criteria" ATC Report No: ARTC-32, Aerospace Industries Association of America, August 7, 1962.

52. Hess, R.W., and Gibson, F.W. "Experimental Investigation of the Effects of Compressive Stress on the Flutter of a Curved Panel and a Flat Panel at Supersonic Mach Numbers" NASA TN D-1386, October 1962.

53. Stearman, R., Lock, M., and Fung, Y.C., "Ames Tests on the Flutter of Cylindrical Shells", GALCIT Aeroelasticity and Structural Dynamics Report SM 62-37, CALTECH, Graduate Aeronautical Laboratories, December 1962.

54. Anderson, W.J., and Fung, Y.C., "The Effect of an Idealised Boundary Layer on the Flutter of Cylindrical Shells in Supersonic Flow" GALCIT Structural Dynamics Report SM 62-49, December 1962.

55. Movchan, A.I., and Movchan, A.A. "Travelling Waves in the Supersonic Flutter Problem of Panels of Finite Length" International Council of the Aeronautical Sciences Congress, Stockholm, 1962, Proceedings A-65-15539-06-34, Washington, pp. 723-735, Spartan Books).

56. Novichkov, Iu.N., "On the Solution of the Equations of Steady Flutter of Cylindrical Panels" (in Russian), Ingh. Zh., Vol. 2(4), 1962, pp. 352.

57. Dzygadlo, Z. "Self-excited Vibration of a Cylindrical Shell of Finite Length in a Supersonic Flow" Proceedings of Vibration Problems, Polish Academy of Sciences, Vol. 3 (1), 1962, pp. 69-88.

58. Bolotin, V.V. "Behaviour of Heated Plates and Shells in a Gas Flow" (in Russian), Inzh. Zh., Vol. 2(3), 1962.

59. Johns, D.J. "Some Structural Design Aspects of Space Vehicles" Advances in Space Technology, Edited by J.L. Nayler, Newnes, London, 1962, pp. 123.

60. Bagadsaryan, Zh.E., "Stability of An Anisotropic Cylindrical Shell in a Supersonic Stream of Gas" (in Russian), Fiz.Mat.Git.Ser.Izv.Akad.Nauk., SSSR, Vol. 15(6), 1962, pp.3.

61. Kaliski, S., and Solarz, L. "Aeroelastic Vibrations and Stability of a Deformable Rotating Rocket in a Linearised Flow" Proceedings of Vibration Problems, Vol. 3, No. 1(10), 1962, pp. 57-68.

62. Saunders, H. "Determination of Supersonic Panel Flutter of CylindricalShells with In-plane Stresses" AIAA Journal, Vol. 1, January 1963, pp. 209.

63. Mitchell, R.R. "Supersonic Flutter of a Cylindrical Shell with Application to the Container Interstage Adapter" General Dynamics/Convair Report, NASA CR 54542, January 1963.

64. Krumhaar, H. "The Accuracy of Applying Linear Piston Theory to Cylindrical Shells" GALCIT Aeroelasticity and Structural Dynamics Report SM 62-50, February 1963.

65. Fung, Y.C. "Some Recent Contributions to Panel Flutter Research" AIAA Journal, Vol. 1(4), April 1963, pp. 898-909.

66. Brown, R.A., and Holt, M. "Calculations of Aerodynamic Forces on Cylindrical Shells in Unsteady Supersonic Flow" University of California, Berkley Report AS-63-1, AFOSR-268-63, April 1963.

67. Bublik, B.M. "Vibrations and Stability of a Ribbed Cylindrical Shell in a Flow of a Compressible Liquid" (in Russian), Dokl. Akad.Nauk.Ukr., Vol. 2 (1963), p. 178, (In English: Air Systems Command FDT-TT-63-647/1, Ohio, June 1963).

68. Krumhaar, H. "The Accuracy of Linear Piston Theory when Applied to Cylindrical Shells" AIAA Journal, Vol. 1, No. 6, June 1963, pp. 1448-1449.

69. Johns, D.J. "Some Panel Aeroelastic Instabilities" AGARD Report 474, September 1963.

70. Shirk, M.H., and Olson, J.J. "Recent Panel Flutter Research and Applications" AGARD Report 475, September 1963.

71. Kobayashi, S. "Supersonic Panel Flutter of Unstiffened Circular Cylindrical Shells having Simply Supported Ends" Transactions of the Japan Society for Aeronautical and Space Sciences, Vol. 6, No. 9, 1963, pp. 27-35.

72. Librescu, L. "Aeroelastic Vibrations and Stability of Non-homogeneous Cylindrical Shells in a Compressible Fluid Flow" (in French) Revue de Mecanique Applique, Vol. 8 (2), 1963.

73. Lamper, R.E., Shandarov, L.G. "Analysis and Experimental Investigation of Self-Vibrations of Cylindrical Shells and Panels in a Gas Flow" (in Russian), Izv. An. USSR, (OTN Mekh. i Mashino) No. 3, 1963 (Also, transactions of the Conference on Theory of Shells and Plates, Izv. Akad. Nauk. Armarm, USSR, Erevan: 407, 1964).

74. Bolotin, V.V. "Non-conservative Problems of the Theory of Elastic Stability" Pergamon Press, 1963.

75. Librescu, L. "Vibrations et Stabilite Aero-elastique des Structures Cylindriques nonhomogenes Placees dans un Courant Fluide Compressible" Revuew Mec. Appl. Buc. 8, 2, 1963, pp. 251.

76. Stearman, R. "Research on the Panel Flutter of Cylindrical Shells" Midwest Research Institute, AFOSR Final Scientific Report 64-0074, January 1964.

77. Brown, R., and Holt, M. "Frequency Effects in Panel Flutter of Cylindrical Shells" University of California, Berkley, Inst. of Engineering Res., Rep. No. AS 64-6, (AD-603981), March 1964.

78. Bartolozzi, G. "Panel Flutter of Thin-walled Circular Cylindrical Shells in Supersonic Flow" Fourth Congress of International Council of Aeronautical Sciences, Paris, August 1964.

79. Livanov, K.J. "Axially Symmetric Oscillations of Cylindrical Shells in Supersonic Flow of Gas" Translation in Joint Publications Research Service (Washington D.C.) Engineering Journal, August 1964, pp. 208.

80. Stearman, R. "Flutter of a Ring of Panels" AIAA Journal, Vol. 2, No. 8, August 1964, pp. 1441-1448.

81. Johns, D.J. "The Present Status of Panel Flutter" AGARD Report 484, October 1964.

82. Dzygadlo, Z. "The Problem of Aeroelasticity of a Cylindrical Panel and a Plate Strip Taking Into Consideration the Transversal Coupling" Proceedings of Vibration Problems,

82. Polish Academy of Sciences, Warsaw, 2, 5, 1964.
83. Shveiko, Iu, Iu., "Stability of a Cylindrical Shell with a Liquid Filler in a Gas Flow" (in Russian), Izv. An., USSR (OTN Mekh. i Mashino), No. 5, 1964, pp. 112-116.
84. Bagdasaryan, G.E. "The Stability of an Orthotropic Cylindrical Shell Situated in a Supersonic Flow of Gas" (in Russian), Dokl. Akad. Nauk. Arm., USSR, Vol. 39(5), 1964, pp. 217.
85. Dowell, E.H. "The Flutter of an Infinitely Long Cylindrical Shell" Aeroelastic and Structures Laboratory, MIT, ASRL TR 112-3; Also, AFOSR 65-0639, January 1965.
86. Olson, M.H. "Supersonic Flutter of Circular Cylindrical Shells Subjected to Internal Pressure and Axial Compression" GALCIT Report SM 65-7 (AFOSR 65-0599) April, 1965.
87. Dowell, E.H. "Flutter of Infinitely Long Plates and Shells" Part II - Cylindrical Shell, AIAA Symposium, Boston, August 1965; (Also AIAA Journal Vol. 4, No. 9, Sept. 1966, pp. 1510-1518).
88. Anderson, W.J. "Oscillatory Pressures in an Idealised Boundary Layer with an Application to the Panel Flutter of Cylindrical Shells", AIAA Symposium, Boston, August 1965 (Also, AIAA Journal, Vol. 4, 1966, pp. 865-872).
89. Johns, D.J. "Review of Panel Flutter at Low Supersonic Speeds" Journal of the Royal Aeronautical Society, Vol. 69, Sept. 1965, pp. 627 (Also NPL Aero Report 1102, April 1964).
90. Anderson, W.J. "Supersonic Wind Tunnel Tests on Wavy Walled Cylinders", U.S. Airforce Aerospace Research Lab., Wright-Patterson Airforce Base, Ohio, TDR 65-203, October 1965; (Also AIAA Journal, Vol. 5, No. 3, March 1967, pp. 595).
91. Platzer, M., Bernneck, R., and Saunders, L. "On Some Aerodynamic Aspects of the Panel Flutter Problem" NASA TM X-53389, Marshall Space Flight Centre, October 1965.
92. Fung, Y.C. "Interaction of Mechanical and Aeroelastic Instabilities of a Circular Cylindrical Shell" International Conference on Dynamic Stability of Structures, North Western University, Illinois, October 1965; (Also Dynamic Stability

92. of Structures, Pergamon Press, Oxford and New York, 1966).

93. Johns, D.J. "A Survey on Panel Flutter" AGARD Report 1, November 1965.

94. Dzygadlo, Z. "Linearised Supersonic Flow in an Axially Symmetric Duct with a Vibrating Wall" Proceedings of Vibration Problems, Polish Academy of Sciences, Vol. 6, No. 1, 1965, pp. 33.

95. Grigoliuk, E.I., Lamper, R.E., and Sandarov, L.G. "Flutter of Panels and Shells" Itogi Nauk., i Mekhanika, Moskva, 1965.

96. Johns, D.J., "Cylindrical Shell Flutter - Theory and Experiment" Journal of the Royal Aeronautical Society, April 1966.

97. Librescu, L. "Aeroelastic Stability of Thin Circular Cylindrical Multi-layered Structures of Finite Length in the Vicinity of the Flutter Boundary" Paper presented to the 7th Anniversary Symposium on the 'Theory of Shells', University of Houston, April 1966.

98. Dowell, E.H., and Windall, S.E. "Generalised Aerodynamic Forces on an Oscillating Cylindrical Shell " Quarterly of Applied Mathematics, Vol. 24, No. 1, April 1966, pp. 1-17.

99. Dowell, E.H., and Windall, S.E., "Generalised Aerodynamic Forces on an Oscillating Cylindrical Shell: Subsonic and Supersonic Flow" AIAA Journal, Vol. 4, No. 4, April 1966, pp. 607-610.

100. Olson, M.D., and Fung, Y.C., "Supersonic Flutter of Circular Cylindrical Shells Subjected to Internal Pressure and Axial Compression" AIAA Journal, Vol. 4, No. 5, April 1966, pp. 858-864.

101. Olson, M. "On Comparing Theory and Experiment for the Supersonic Flutter of Circular Cylindrical Shells" GALCIT Report AFOSR 66-0944, June 1966.

102. Carter, L.L., and Stearman, R.O., "A Theoretical Investigation of the Aeroelastic Stability of Isotropic Cylindrical Shells at both the High and Low Supersonic Mach Numbers" AFOSR Final Technical Report 66-1930, October 1966.

103. Bagdasaryan, G., and Belubekian, M., "Flutter of a Cylindrical Shell in the Flow of a Compressible Conducting Fluid in the Presense of a Magnetic Field" Inz-Zhurnal Mekh. Tverdogo-Tela, November-December 1966, p. 50.

104. Stearman, R.O., "An Experimental Study on the Aeroelastic Stability of Thin Cylindrical Shells at the Lower Supersonic Mach Numbers" AFOSR Final Technical Report 66-2828, December 1966, (Also ARL 67-0006).

105. Paidoussis, M.P., "Dynamics of Flexible Cylinders in Axial Flow" Jour. of Fluid Mechanics, Vol. 26, December 1966, pp. 717.

106. Woroszyl, S., "Coupled Local and Integral Flutter of a Cylindrical shell in Linearised Supersonic Flow" Proceedings of Vibration Problems, Polish Academy of Science, Vol. 1(1), 1966, p. 67.

107. Brusilovskii, A., Melinkova, L., and Shveiko, Iu, Iu., "Vibration and Stability of Cylindrical Shells in a Gas Flow" (in Russian), Inj. Zhurnal Mekhanika, Iverdogotela, 1, 1966, p. 67.

108. Kaliski, S., and Woroszyl, S., "The Flutter Problem of a Cylindrical Shell Immersed in Gas" Proceedings of Vibration Problems, Polish Academy of Sciences, Vol. 7 (2), 1966, pp. 155.

109. Carter, L., "A Theoretical Study of Cylindrical Shell Panel Flutter", Ph.D. Thesis, University of Kansas, 1966.

110. Gontkevich, V., and Ponomarenko, V., "Natural Oscillations of Cylindrical Shells in a Hypersonic Fluid Flow" Publ. 'Dynamics and Durability of Machines', Kharkov University, 1966.

111. Carter, L.L., and Stearman, R., "Some Aspects of Cylindrical Shell Panel Flutter" AIAA Paper No. 67-78, February 1967; (Also AIAA Journal, Vol. 6, No. 1, January 1968, pp. 37-43).

112. Anderson, W.J., "Aeroelastic Stability of Plates and Cylinders" NACA CR 89183, February 1967.

113. Li, T.M., "First Order Frequency Effects in Supersonic Panel Flutter of Finite Cylindrical Shells" AFOSR Report No. AS-67-16, August 1967.

114. Korbut, B., and Konditsuia, E., "Flutter of Two Cylindrical Panels Joined by an Elastic Filler" Prikladnaia Mekhanika, Vol. 3, August 1967, p. 70.

115. Evenson, D.A., and Olson, M.D., "Non-Linear Flutter of a Circular Cylindrical Shell in Supersonic Flow" Aero Report LR-486, NRC of Canada, September 1967; Also NASA TND-4265, September 1967.

116. Olson, M.D., and Fung, Y.C., "Comparing Theory and Experiments for the Supersonic Flutter of Circular Cylindrical Shells", AIAA Journal, Vol. 5, No. 10, October 1967, pp. 1849-1856.

117. Dowell, E.H., "Non-linear Analysis of the Flutter of Plates and Shells" ASME Symposium on Fluid Solid Interaction, November 1967.

118. Guji, B., "Flutter in a Sector of a Cylindrical Shell in Supersonic Flow" (in Russian), Bull-Wojsk Akad. Techn., Vol. 15, (6), 41, 1966, RZM No. 5, 1967.

119. Derbentsev, D., "Vibrations of a Circular Cylindrical Shell with a Gas Flowing Within It" Translated from Russian: Prikladnaia Mekhanika Akad. Nauk.,RSR (Kiev) Vol. 3(3), 14, 1967 - (Lockheed Missiles and Space Co., Palo Alto, California, N67-27721).

120. Skurlatov, E., "On the Stability of a Circular Cylindrical Shell in a Supersonic Gas Flow" (Translated from Russian) Lockheed Missiles and Space Co., Sunnyvale, California, 1967 ('STAR' N67-30060).

121. Windall, D.E., and Dowell, E.H., "Aerodynamic Forces on an Oscillating Cylindrical Duct with an Internal Flow" Jour. of Sound and Vibration (1), 6, 1967, pp. 113-127.

122. Coupry, G., "Sur le Calcul du Potentiel des Vitesses d'un ecoulement supersonique en Presence des Vibrations de Respiration Asymptotiques d'un Cylindre"C.R.Ac.Sc. Tome 265, A, 1967, pp. 873-875.

123. Platzer, M.F., "Unsteady Aerodynamics" Research Achievements Review, Vol. 1, NASA Huntsville, 1967.

124. Librescu, L., "Aeroelastic Stability of Orthotropic Hetrogeneous Thin Panels in the Vicinity of the Flutter Critical Boundary (Part II), Journal Mecanique, Vol. 6,

124. No. 1, 1967, p. 113.

125. Anderson, W.J., and Hsu, K.H., "Engineering Estimates for Supersonic Flutter of Curved Shell Segments" AIAA/ASME 9th Structures, Structural Dynamics and Materials Conference, Paper No. 68-284, April 1-3, 1968.

126. Barr, G.W., and Stearman, R.O., "Aeroelastic Stability Characteristics of Cylindrical Shells Considering Imperfections and Edge Constraint" AIAA Paper No. 68-285, AIAA/ASME 9th Structures, Structural Dynamics and Materials Conference, April 1-3, 1968.

127. Plaut, R.H., "A Stability Criterion for Flutter of a Cylindrical Panel" AIAA Journal, Vol. 6, No. 6, June 1968, p. 1205.

128. Plaut, R.H., "Comment on 'Further Study on a Stability Criterion for Panel Flutter via the Second Method of Liapunov" AIAA Journal, Vol. 6, No. 7, July 1968, p. 1437.

129. Stearman, R.O., "An Experimental Study on the Stability of Thin Cylindrical Shells" Abstracts of the 12th International Congress of Applied Mechanics, Stanford University, August 1968.

130. Evenson, D.A., and Olson, M.D., "Circumferentially Travelling Wave Flutter of a Circular Cylindrical Shell" AIAA Journal, Vol. 6, No. 8, August 1968, p. 1522-1527.

131. Dowell, E.H., "Generalised Aerodynamic Forces on a Flexible Cylindrical Shell Undergoing Transient Motion" Quarterly of Applied Mathematics, Vol. 26, No. 3, October 1968, pp. 343-353.

132. Platzer, M.F., Hoffmann, G.H., and Liu, D.D., "First and Second Order Theories for Supersonic and Transonic Flow Past Oscillating Bodies of Revolution" 3rd Technical Workshop on Dynamic Stability Problems, NASA Ames Research Centre, November 4-7, 1968.

133. Ellen, C.H., "Influence of Structural Damping on Panel Flutter" AIAA Journal, Vol. 6, No. 11, November 1968, pp. 2169-2174.

134. Coupry, G., "Unsteady Supersonic Flow around a Thin Circular Cylinder" (in French) La Recherche Aerospatiale No. 127, ONERA, November-December 1968.

135. Müller, P., "A Note on the Axisymmetrical Flutter of Circular Cylindrical Shells of Finite Length", International Journal of Solids and Structures, Vol. 4, 1968 pp. 833-835.

136. Kaliski, S., and Woroszyl, S., "Centrifugal and Coriolis Force Effect on the Flutter of Rotating Cylindrical Shell Immersed in a Gas" Acad. Polon. des Sciences, Bulletin Serie des Sciences Tech. Vol. 16(1), 1968, p.1.

137. Davies, D.E., "Generalised Airforces on a Cylindrical Shell Oscillating Harmonically in a Uniform Flow" ARC R&M No. 3534, 1968.

138. Librescu, L., and Malaiu, E., "Supersonic Flutter of Circular Cylindrical Hetrogeneous Orthotropic Thin Panels of Finite Length" Jour. of Sound & Vibration, Vol. 8, No. 3, 1968, pp. 494-512.

139. Dzygadlo, Z., "Pressure on a Cylindrical Shell Performing Oscillation in External or Internal Linearised Supersonic Flow" Proceedings of Vibration Problems, Vol. 2, No. 9, Polish Academy ofSciences, 1968, pp. 130-146.

140. Stearman, R.O., "Aeroelastic Stability and Response Problems Associated with Thin Shell Structures" Interim Scientific Report, Grant No. AF-AFOSR-1234-67, A, March 1969.

141. Dixon, S.C., and Hudson, M.L., "Flutter Boundary for Simply Supported Unstiffened Cylinders" AIAA Journal, Vol. 7, No. 7, July 1969, pp. 1390-1391.

142. Barr, G.W., and Stearman, R.O., "The Influence of a Supersonic Flow Field on the Elastic Stability of Cylindrical Shells".

143. Johns, D.J., "A Panel Flutter Review" Chapter 5 of AGARD Manual of Aeroelasticity, 1969.

144. Parthan, S., and Johns,D.J., "Flutter of Circular Cylindrical Shells - A Review", Loughborough University of Technology Report TT 6917, November 1969, pp.1-89.

b) Other References

A1. Donnell, L.H., "Stability of Thin-walled Tubes under Torsion" NACA Report 479, 1933.

A2. Flugge, W., "Statik und Dynamik der Schalen" Julius Springer, Berlin, 1939.

A3. Batdorf, S.B., "A Simplified Method of Elastic-Stability Analysis for Thin Cylindrical Shells" NACA Report 874, 1947, (Formerly included in NACA-TN 1341 and -TN-1342).

A4. Vlasov, V.Z., "A General Theory of Shells" Moscow, 1949.

A5. Miles, J.W., "On the Reduction of Unsteady Supersonic-Flow Problems to Steady-flow Problems" Jour. of the Aeronautical Sciences, Vol. 17, January 1950, p. 64.

A6. Vlasov, V.S., "Basic Differential Equations in General Theory of Elastic Shells" NACA TM 1241, 1951.

A7. Dugungi, "A Nyquist Approach to Flutter" AMR-6(53) 611, Journal of the Aeronautical Sciences, Vol. 19, No. 6, June 1952.

A8. Junger, M.C., "The Physical Interpretation of the Expression for an Outgoing Wave in Cylindrical Co-ordinates" Journal of the Acousticsl Society of America, Vol. 25, No. 1, January 1953, pp. 40-47.

A9. Goldenveizer, A.L., "Theory of Thin Elastic Shells" GTL, Moscow, 1953.

A10. Kempner, J., "Remarks on Donnell's Equations" Journal of Applied Mechanics, Vol. 22, No. 1, March 1955, pp. 117-118.

A11. Hoff, N.J., "The Accuracy of Donnell's Equations" Journal of Applied Mechanics, Vol. 22, No. 3, September 1955, pp. 329-334.

A12. Jordan, P.F., "The Physical Nature of Panel Flutter" Aero-Digest, February 1956, pp. 34-38.

A13. Movchan, A.A., "On the Stability of a Panel Moving in a Gas" Prikladnaia Mathematika i Mekhanika, Vol. 21, No. 2, 1957 (Translated and issued as NASA RE 11-21-58W).

A14. Pines, S., "An Elementary Explanation of the Flutter Mechanism" Proceedings of the National Specialists Meeting on Dynamics and Aeroelasticity, I.A.S., November 1958, pp. 52-58.

A.15 Franklin, J.N., "On the Numerical Solution of Characteristic Equations in Flutter Analysis" Journal for the Association of Computing Machinery, Vol. 5, 1958, pp. 45-51.

A16. Morley, L.S.D., "An Improvement on Donnell's Approximation for Thin-walled Circular Cylinders" Quarterly Journal of Mechanics and Applied Mathematics, Vol. 12, No.1, 1959, pp. 89-99.

A17. Timoshenko, S.H., and Wiqnowsky-Kreiger, S., "Theory of Plates and Shells" Second Edition, McGraw-Hill Book Co., 1959.

A18. Novozhilov, V.V., "The Theory of Thin Shells," Noordhoff Ltd., 1959.

A19. Movchan, A.A., "Behaviour of Complex Eigenvalues in Panel Flutter Problem" Akademia Nauk SSSR, Inzhenernyi Sbornik, Moscow, Vol. 27, 1960, pp. 70-76.

A20. Forsberg, K., "A Review of Analytical Methods used to Determine the Modal Characteristics of Cylindrical Shells" Technical Report, Lockheed Missile and Space Company, Presented at the 7th International Aeronautical Congress, Paris, France, 14-17th June, 1965.

A21. Love, A.E.H., "The Mathematical Theory of Elasticity" Dover Publications.

A22. Egle & Sewall, J.L., "An Analysis of Free Vibration of Orthogonally Stiffened Cylindrical Shells with Stiffeners Treated as Discrete Elements"AIAA Jnl.,Vol.6,No.3,March 1968.

A23. Warburton, G.B., "Comments on 'Vibration Studies of a Ring-stiffened Circular Cylindrical Shell" J.Sound & Vibration, Vol. 9, No. 2, 1969, pp.349-352.

A24. Warburton, G.B., "Dynamics of Shells" Symposium on Structural Dynamics, Vol. 1, Paper A.1, March 1970, pp.1-34.

A25. Egle, D.M., & Soder, K.E., "A Theoretical Analysis of the Free Vibration of Discretely Stiffened Cylindrical Shells with Arbitrary End Conditions" AIAA Structural Dynamics & Aeroelasticity Specialist Conference, New Orleans, Apr.16-17, 1969, pp. 262-274.

A26. Hoppmann, W.H.II, "Some Characteristics of the Flexural Vibrations of Orthogonally Stiffened Cylindrical Shells" Jnl. of Acoustical Soc. of America, Vol. 30, 1958, pp.77-82.

A27. Hoppmann, W.H.II, "Flexural Vibrations of Orthogonally Stiffened Cylindrical Shells" Proceedings of 9th Intnl. Congress of Applied Mechanics, Bruxelles, 1956, pp. 225-237.

A28. McElman, J.A., Mikulas, M.M.Jr., Stein, M., "Static and Dynamic Effects of Eccentric Stiffening of Plates and Shells", AIAA Jnl., Vol. 4, No. 5, May 1966, pp.887-894.

A29. Mikulas, M.M.Jr., McElman, J.A., "On the Free Vibration of Eccentrically Stiffened Cylindrical Shells and Flat Plates", TN-D 3010, Sept. 1965, NASA.

A30. Schnell, W., Heinrichbauer, F., "The Determination of Free Vibrations of Longitudinally-Stiffened, Thin-Walled, Circular Cylindrical Shells", TT F-8856, April 1964, NASA.

A31. Scruggs, R.M., Pierce, C.V., Reese, J.R., "An Analytical and Experimental Study of the Vibration of Orthogonally Stiffened Cylindrical Shells" AIAA/ASME 9th Structures, Structural Dynamics and Materials Conference, April 1-3, 1968., AIAA Paper No. 68-349, pp.1-10.

A32. Miller, P.R., "Free Vibrations of a Stiffened Cylindrical Shell" R&M No. 3154, May 1957.

A33. Morrow, T.B., Parthan, S., "Determination of Eigen-Values and Eigenvectors of Arbitrary-Complex Matrices" Translated from German Rept. (Ref. not available).

A34. Bisplinghoff, R.L., Ashley, H., Halfman, R.L., "Aeroelasticity" Addison-Wesley Pub.Co., Inc., 1957.

A35. Bisplinghoff, R.L., Ashley, H., "Principles of Aero-elasticity" John Wiley & Sons, Incs., 1962.

A36. Parthan, S., and Johns, D.J., "Effect of Inplane and Rotary Inertia on the Frequencies of Eccentrically-Stiffened Cylindrical Shells", AIAA Structural Dynamics and Aeroelasticity Specialist Conference, New Orleans, April 16-17, 1969; Also AIAA Journal, March 1970, pp. 592-595

A37. Johns, D.J., Sharma, C.B., Parthan, S., and Brave-Boy, G.K., "On Wind-Induced Instabilities of Open-Ended Circular Cylindrical Shells" International Association for Shell Structures, Conference on Tower-Shaped Structures, The Hague, April 24-26, 1969, pp. 185-212.

A38. Parthan, S., and Johns, D.J., "Determination of Generalised Aerodynamic Forces on an Oscillating Cylindrical Shell and Their Application to Shell Flutter", Aeronautical Society of India Conference, Kanpur, February 26-28, 1971, pp. 1-28.

A39. Parthan, S., and Johns, D.J., "Supersonic Flutter of Stringer-Stiffened Cylindrical Shells (to be published).

APPENDIX 1: Expressions for U_{max} and T_{max}

Displacements are substituted from Equations (II.19) (22) and (23) into (6), (8), (10), (13), (15), (17) and integrations are performed. After some manipulation, the maximum strain and kinetic energy expressions become as follows:

$$U_{C_{max}} = \frac{Eh\pi L}{4R(1-\nu^2)} \left[\lambda_m^2 \bar{u}^2 + (n\bar{v}+\bar{w})^2 - 2\nu\lambda_m \bar{u}(n\bar{v}+\bar{w}) \right.$$

$$\left. + \frac{1-\nu}{2} (\lambda_m \bar{v} - n\bar{u})^2 + \alpha^2 \lambda_m^4 (1+\bar{\beta}^2)^2 \bar{w}^2 \right] \qquad (A1.1)$$

$$U_{S_{max}}^{(D)} = \sum_{i=1}^{2L_s} \left[\frac{LE_{si}}{4} \left\{ \lambda_m^2 \frac{A_{si}}{R^2} (\bar{u} - \frac{\bar{z}_{si}}{R} \lambda_m \bar{w})^2 \right.\right.$$

$$\left. + \frac{I_{si} \lambda_m^4}{R^4} \bar{w}^2 \right\} \cos^2 \frac{(2i-1)n\pi}{2L_s}$$

$$\left. + L \frac{G_{si} J_{si}}{4R^4} \lambda_m^2 n^2 \bar{w}^2 \sin^2 \frac{(2i-1)n\pi}{2L_s} \right] \qquad (A1.2)$$

$$U_{r_{max}}^{(D)} = \sum_{j=0}^{K_r} \left[\frac{\pi R E_{rj}}{2} \left\{ \frac{A_{rj}}{R^2} (n\bar{v} + \bar{w}\{1+n^2 \frac{\bar{z}_{rj}}{R}\})^2 \right.\right.$$

$$\left. + \frac{I_{rj}}{R^4} n^4 \bar{w}^2 \right\} \sin^2 \frac{m\pi j}{K_r}$$

$$\left. + \frac{\pi R G_{rj} J_{rj}}{2R^4} n^2 \lambda_m^2 \bar{w}^2 \cos^2 \frac{m\pi j}{K_r} \right] \qquad (A1.3)$$

$$T_{C_{max}} = \frac{\omega^2}{4} \pi RL \left[\rho_c h(\bar{u}^2+\bar{v}^2+\bar{w}^2) + \frac{\rho_c I_{oc}}{R^2} \lambda_m^2 (1+\bar{\beta}^2)\bar{w}^2 \right] \qquad (A1.4)$$

$$T_{S_{max}}^{(D)} = \frac{L\omega^2}{4} \sum_{i=1}^{2L_s} \left[\rho_{si} A_{si} \left\{ (\bar{u}^2+\bar{w}^2)\cos^2 \frac{(2i-1)n\pi}{2L_s} \right.\right.$$

$$\left. + \bar{v}^2 \sin^2 \frac{(2i-1)n\pi}{2L_s} \right\}$$

$$- 2\rho_{si} A_{si} \frac{\bar{z}_{si}}{R} \lambda_m \bar{w} (\bar{u}\cos^2 \frac{(2i-1)n\pi}{2L_s} - \bar{v}\sin^2 \frac{(2i-1)n}{2L_s}) +$$

$$+ \rho_{si} \frac{I_{o_{si}}}{R^2} \lambda_m^2 \bar{w}^2 \left(\cos^2 \frac{(2i-1)n\pi}{2L_s} + \bar{\beta}^2 \sin^2 \frac{(2i-1)n\pi}{2L_s}\right)$$

$$T^{(D)}_{r_{max}} = \frac{\pi R \omega^2}{4} \sum_{j=0}^{K_r} \left[\rho_{rj} A_{rj} \left\{\bar{u}^2 \cos^2 \frac{m\pi j}{K_r} \right. \right. \qquad - - \quad (A1.5)$$

$$+ (\bar{v}^2 + \bar{w}^2) \sin^2 \frac{m\pi j}{K_r}$$

$$- 2\rho_{rj} A_{rj} \frac{\bar{z}_{rj}}{R} \lambda_m \bar{w} \left(\bar{u} \cos^2 \frac{m\pi j}{K_r} + \bar{\beta}^2 \sin^2 \frac{m\pi j}{K_r}\right) \quad (A1.6)$$

where

$$\alpha = \frac{h^2}{12R^2}, \quad \lambda_m = \frac{m\pi R}{L}, \quad \bar{\beta} = \frac{Ln}{m\pi R},$$

$$I_{o_{si}} = I_{si} + \bar{z}_{si}^2 A_{si} \qquad (A1.7)$$

$$I_{o_{rj}} = I_{rj} + \bar{z}_{rj}^2 A_{rj}$$

with I_{si}, I_{rj} as the moments of inertia of the stringer and ring cross sections about an axis through the centroid perpendicular to their planes respectively.

For the smeared stiffener case, the summations are replaced by the appropriate integrals (see Appendix 3).

APPENDIX 2: Matrix Elements $A_{ij}^{(D)}$ and $B_{ij}^{(D)}$

$$A_{11}^{(D)} = \lambda_m^2 \left(1 + \sum_{i=1}^{2L_s} \bar{S}_i \cos^2 \frac{(2i-1)n\pi}{2L_s}\right) + \frac{1-\nu}{2} n^2$$

$$A_{12}^{(D)} = -\frac{(1+\nu)}{2} \lambda_m n$$

$$A_{13}^{(D)} = -\lambda_m \left[\nu + \lambda_m^2 \sum_{i=1}^{2L_s} \bar{S}_i \cos^2 \frac{(2i-1)n\pi}{2L_s} \right]$$

$$A_{21}^{(D)} = A_{12}^{(D)}$$

$$A_{22}^{(D)} = \frac{1-\nu}{2} \lambda_m^2 + n^2 \left(1 + \sum_{j=0}^{K_r} \bar{R}_j \sin^2 \frac{m\pi j}{K_r}\right)$$

$$A_{23}^{(D)} = n \left[1 + \sum_{r=1}^{K_r} \left(1 + n^2 \frac{\bar{z}_{rj}}{R}\right) \bar{R}_j \sin^2 \frac{m\pi j}{K_r} \right]$$

$$A_{31}^{(D)} = A_{13}^{(D)}$$

$$A_{32}^{(D)} = A_{23}^{(D)}$$

$$A_{33}^{(D)} = \alpha\lambda_m^2 \left[\left(1 + \bar{\beta}^2\right)^2 + \sum_{i=1}^{2L_s} \left\{ \frac{E_{si} I_{si}}{\pi RD} \cos^2 \frac{(2i-1)n\pi}{2L_s} \right.\right.$$

$$+ \bar{\beta}^2 \frac{G_{si} J_{si}}{\pi RD} \sin^2 \frac{(2i-1)n\pi}{2L_s}$$

$$+ \sum_{j=0}^{K_r} \bar{\beta}^2 \left\{ \frac{G_{rj} J_{rj}}{DL/2} \cos^2 \frac{m\pi j}{K_r} + \bar{\beta}^2 \frac{E_{rj} I_{rj}}{DL/2} \sin^2 \frac{m\pi j}{K_r} \right.$$

$$\left.\left.\left. + \lambda_m^4 \sum_{l=1}^{2L_s} \bar{S}_i \frac{\bar{z}_{si}^2}{R^2} \cos^2 \frac{(2i-1)n\pi}{2L_s} + \sum_{j=0}^{K_r} \bar{R}_j \left(1 + n^2 \frac{\bar{z}_{rj}}{R}\right)^2 \sin^2 \frac{m\pi j}{K_r} + 1 \right] \right.$$

$$B_{11}^{(D)} = -\left[1 + \sum_{i=1}^{2L_s} m_{si} \cos^2 \frac{(2i-1)n\pi}{2L_s} + \sum_{j=0}^{K_r} m_{rj} \cos^2 \frac{m\pi j}{K_r} \right]$$

$$B_{12}^{(D)} = 0$$

$$B_{13}^{(D)} = \lambda_m \left[\sum_{i=1}^{2L_s} m_{si} \frac{\bar{z}_{si}}{R} \cos^2 \frac{(2i-1)n\pi}{2L_s} + \sum_{j=0}^{K_r} m_{rj} \frac{\bar{z}_{rj}}{R} \cos^2 \frac{m\pi j}{K_r} \right]$$

$$B_{21}^{(D)} = B_{12}^{(D)}$$

$$B_{22}^{(D)} = -\left[1 + \sum_{i=1}^{2L_s} m_{si}\sin^2\frac{(2i-1)n\pi}{2L_s} + \sum_{j=0}^{K_r} m_{rj}\sin^2\frac{m\pi j}{K_r}\right]$$

$$B_{23}^{(D)} = -n\left[\sum_{i=1}^{2L_s} m_{si}\frac{\bar{z}_{si}}{R}\sin^2\frac{(2i-1)n\pi}{2L_s} + \sum_{j=0}^{K_r} m_{rj}\frac{z_{rj}}{R}\sin^2\frac{m\pi j}{K_r}\right]$$

$$B_{31}^{(D)} = B_{13}^{(D)}$$

$$B_{32}^{(D)} = B_{23}^{(D)}$$

$$B_{33}^{(D)} = -\left[\left\{1+\sum_{i=1}^{2L_s} m_{si}\cos^2\frac{(2i-1)n\pi}{2L_s} + \sum_{j=0}^{K_r} m_{rj}\sin^2\frac{m\pi j}{K_r}\right\}\right.$$

$$+\lambda_m^2\left\{I_c+\sum_{i=1}^{2L_s} I_i\left(\cos^2\frac{(2i-1)n\pi}{2L_s} + \bar{\beta}^{-2}\sin^2\frac{(2i-1)n\pi}{2L_s}\right)\right.$$

$$\left.\left.+\sum_{j=0}^{K_r}\left(\cos^2\frac{m\pi j}{K_r} + \bar{\beta}^2\sin^2\frac{m\pi j}{K_r}\right)\right]\right.$$

where

$$\Delta = \frac{\rho_c R^2(1-\nu^2)\omega^2}{E}$$

$$\bar{S}_i = \frac{E_{si}A_{si}(1-\nu^2)}{Eh\pi R}$$

$$\bar{R}_j = \frac{E_{rj}A_{rj}(1-\nu^2)}{Eh\,L/2}$$

$$m_{si} = \frac{\rho_{si}A_{si}}{\rho_c h\pi R}$$

$$m_{rj} = \frac{\rho_{rj}A_{rj}}{\rho_c h\,L/2}$$

$$I_i = \frac{\rho_{si}I_{osi}}{\rho_c h\pi R^3}$$

$$I_j = \frac{\rho_{rj}I_{orj}}{\rho_c hR^2L/2}$$

APPENDIX 3: Trigonometric Sums

If the stiffeners are assumed to be identical, the finite trigonometric sums in Appendix 2 can be replaced by their equivalent values (Ref.32)

$$\sum_{j=0}^{K_r} \cos^2 \frac{m\pi j}{K_r} = \begin{cases} \frac{K_r}{2} + 1 & \text{if } m \neq 0, K_r, 2K_r, \ldots \\ K_r + 1 & \text{if } m = 0, K_r, 2K_r, \ldots \end{cases}$$

$$\sum_{j=0}^{K_r} \sin^2 \frac{m\pi j}{K_r} = \begin{cases} K_r/2 & \text{if } m \neq 0, K_r, 2K_r, \ldots \\ 0 & \text{if } m = 0, K_r, 2K_r, \ldots \end{cases}$$

$$\sum_{i=1}^{2L_s} \cos^2 \frac{(2i-1)n\pi}{2L_s} = \begin{cases} L_s & \text{if } n \neq L_s, 2L_s, 3L_s, \ldots \\ 0 & \text{if } n = L_s, 3L_s, 5L_s, \ldots \\ 2L_s & \text{if } n = 2L_s, 4L_s, 6L_s, \ldots \end{cases}$$

$$\sum_{i=1}^{2L} \sin^2 \frac{(2i-1)n\pi}{2L_s} = \begin{cases} L_s & \text{if } n \neq L_s, 2L_s, 3L_s, \ldots \\ 2L_s & \text{if } n = L_s, 3L_s, 5L_s, \ldots \\ 0 & \text{if } n = L_s, 2L_s, 4L_s, 6L_s, \ldots \end{cases}$$

For the smeared case, these summations are replaced by the following appropriate integrals:

$$\int_0^a \cos^2 \frac{m\pi x}{L} \frac{dx}{l} = \frac{L}{2l}$$

$$\int_0^{2\pi R} \cos^2 \frac{(2i-1)n\pi}{2L_s} \frac{dy}{d} = \frac{\pi R}{d}$$

APPENDIX 4: Matrix Elements $A_{ij}^{(S)}$, $B_{ij}^{(S)}$

$$A_{11}^{(S)} = \lambda_m^2 (1 + \bar{S}) + \frac{1 - \nu}{2} n^2$$

$$A_{12}^{(S)} = - \frac{(1+\nu)}{2} \lambda_m n$$

$$A_{13}^{(S)} = - \lambda_m \left[\nu + \lambda_m^2 \frac{\bar{z}_s}{R} \bar{S} \right]$$

$$A_{21}^{(S)} = A_{12}^{(S)}$$

$$A_{22}^{(S)} = \frac{1 - \nu}{2} \lambda_m^2 + n^2 (1 + \bar{R})$$

$$A_{23}^{(S)} = n \left[1 + (1 + n^2 \frac{\bar{z}_r}{R}) \bar{R} \right]$$

$$A_{31}^{(S)} = A_{13}^{(S)}$$

$$A_{32}^{(S)} = A_{23}^{(S)}$$

$$A_{33}^{(S)} = \propto \lambda_m^4 \left[(1 + \bar{\beta}^2)^2 + \left\{ \frac{E_s I_s}{Dd} + \bar{\beta}^2 \left(\frac{G_s J_s}{Dd} + \frac{G_r J_r}{Dl} \right) + \bar{\beta}^4 \frac{E_r I_r}{Dl} \right\} \right]$$

$$+ \left[\lambda_m^4 \frac{\bar{z}_s^2}{R^2} \bar{S} + (1 + n^2 \frac{\bar{z}_r}{R})^2 \bar{R} + 1 \right]$$

$$B_{11}^{(S)} = -\bar{M}, \quad B_{12}^{(S)} = 0, \quad B_{13}^{(S)} = \propto M_1$$

$$B_{21}^{(S)} = B_{12}^{(S)} \quad B_{22}^{(S)} = - \bar{M}, \quad B_{23}^{(S)} = -nM_1$$

$$B_{31}^{(S)} = B_{13}^{(S)} \quad B_{32}^{(S)} = B_{23}^{(S)} \quad B_{33}^{(S)} = -\left[\bar{M} + \lambda_m^2 \bar{I} (1 + \bar{\beta}^2) \right]$$

with

$$\bar{S} = \frac{E_s A_s (1-\nu^2)}{Eh\,d}, \qquad \bar{R} = \frac{E_r A_r (1-\nu^2)}{Ehl}$$

$$\bar{M} = (1 + \frac{\rho_s A_s}{\rho_c hd} + \frac{\rho_r A_r}{\rho_c hl}), \quad M_1 = (\frac{\rho_s A_s}{\rho_c hd} \frac{\bar{z}_s}{R} + \frac{\rho_r A_r}{\rho_c hl} \frac{\bar{z}_r}{R})$$

$$\bar{I} = (I_{oc} + \frac{\rho_s I o_s}{\rho_c hdR^2} + \frac{\rho_r I o_r}{\rho_c hlR^2})$$

TABLE 1

VALUE OF THE CRITICAL VELOCITIES (m/sec) OF FLOW FOR CLOSED CYLINDRICAL SHELLS

(Shells simply supported on the ends (I); clamped on one end and simply supported on the other (II); and clamped on both ends (III))

$\frac{h}{R}$	$\frac{R}{l}$	Exact			By the variational method					
					2nd approximation			3rd approximation		
		I	II	III	I	II	III	I	II	III
$\frac{1}{200}$	$\frac{1}{6}$	14,067	19,182	26,642	12,278	16,883	22,132	14,770	20,448	29,040
	$\frac{1}{8}$	5,934	9,092	11,239	5,203	7,141	9,352	6,332	8,869	11,880
	$\frac{1}{10}$	3,038	4,143	5,754	2,708	3,686	4,812	3,369	4,238	6,134
	$\frac{1}{12}$	1,758	2,397	3,330	1,648	2,186	2,822	1,999	2,656	3,526
$\frac{1}{300}$	$\frac{1}{6}$	9,378	12,788	17,761	8,197	11,266	14,765	9,847	13,939	19,360
	$\frac{1}{8}$	3,956	5,396	7,493	3,484	4,775	6,249	4,308	5,913	7,920
	$\frac{1}{10}$	2,025	2,769	3,836	1,687	2,475	3,225	2,246	3,314	4,089
	$\frac{1}{12}$	1,172	1,598	2,220	1,120	1,444	1,902	1,390	2,014	2,539

TABLE 1

cont.

$\frac{h}{R}$	$\frac{R}{l}$	Exact			By the variational method					
					2nd approximation			3rd approximation		
		I	II	III	I	II	III	I	II	III
$\frac{1}{400}$	$\frac{1}{6}$	7,033	9,591	13,321	6,160	8,461	11,085	7,385	10,723	14,879
	$\frac{1}{8}$	2,968	4,048	5,623	2,629	3,596	4,701	3,233	4,437	5,943
	$\frac{1}{10}$	1,520	2,072	2,879	1,378	1,874	2,436	1,685	2,533	3,069
	$\frac{1}{12}$	879	1,199	1,666	861	1,130	1,447	1,043	1,626	1,976
$\frac{1}{500}$	$\frac{1}{6}$	5,656	7,673	10,656	4,940	6,781	8.880	5,908	8,578	11,903
	$\frac{1}{8}$	2,375	3,238	4,498	2,119	2,892	3,776	2,586	3,549	4,754
	$\frac{1}{10}$	1,216	1,658	2,303	1,129	1,512	1,968	1,348	2,026	2,595
$\frac{1}{750}$	$\frac{1}{6}$	3,751	5,115	7,104	3,322	4,548	5.946	3,938	5,718	7,367
	$\frac{1}{8}$	1,583	2,159	2,999	1,450	1,964	2,552	1,890	2,366	3,169
	$\frac{1}{10}$	810	1,105	1,535	796	1,056	1,354	1,025	1,350	1,636

TABLE 2.

Critical Mach Number for Axisymmetric Flutter of a Light Alloy Cylindrical Shell at Sea Level

$$\frac{h}{L} = 6 \times 10^{-3}; \quad \frac{L}{R} = 2; \quad L = 2ft; \quad n = 0$$
$$X = 0$$

Elastic Equations	4 Mode Solution m = 1,2,3,4	2-Mode Solution m = 1,2	2-Mode Solution (No Aero Damping) m = 1,2
Flugge	9.5	11.2	2.5
Novozhilov	9.6	11.2	2.6

TABLE 3

Average Calculated Values of λ^* (for no aerodynamic damping)

L/R	0	0.75	1	2	4	6	10
λ^*	374.7^{10}	1408	1190	40.41	4.063	1.844	0.723

TABLE 4: Properties of Shells for Numerical Examples to Determine the Invacuo-natural Frequencies

	Ref. 38	Ref. A28	Ref. A22	
Length = L in.	40	23.75	24.00	38.85
Radius = R in.	20	9.55	9.537	7.657
Thickness = h in.	0.04	0.028	0.0256	0.0182
Young's Modulus = E $= E_s = E_r$ (p.s.i.)	10×10^6	10.5×10^6	10×10^6	29×10^6
density = ρ_c $= \rho_s = \rho_r$ (lb/in.^{3})	0.0998	0.095	0.0975	0.2819
Poisson's ratio = ν	0.3	0.3	0.315	0.3
Stringer/Ring breadth $b_s = b_r$ (in.)	-	0.096	0.1118	0.0409
Stringer/Ring depth $h_s = h_r$ (in.)	-	0.302	0.2262	0.3981
No. of Stringers = $2L_s$	-	60	60	4
No. of Rings = (K_r+1)	-	25	-	-
Stringer Spacing = d	-	1		
Ring Spacing = l	-	1	-	-

TABLE 5: Calculated Natural Frequencies (Hz) for an Unstiffened Shell With and Without Various Inertia Terms*

n	Present Analysis			Ref. 36	Ref. 36
	(i)	(i)(iii)	(i)(ii)(iii)	(i)	(i)(ii)
2	3741.24	3741.23	3354.00	3741.17	3362
4	1314.71	1314.70	1271.00	1314.16	1270
6	669.12	669.11	659.30	666.97	657
8	536.76	536.74	532.40	532.22	527
10	652.35	652.31	649.00	646.66	643

* (i) radial inertia, (ii) in-plane inertia, (iii) rotary inertia

TABLE 6: Minimum Frequencies (Hz) For a Cylindrical Shell with Various Stiffening Configurations (m=1)*

No.	Case	n	S(i)	S(i)(iii)	S(i) (ii) (iii)	D(i) (ii) (iii)
1	Unstiffened	6	185.35	185.34	182.68	182.68
2	Stringers - External	7	205.40	202.41	202.08	204.75
3	Stringers - Symmetric	7	169.50	168.97	165.57	167.56
4	Stringers - Internal	6	150.49	149.03	146.61	147.00
5	Rings - External	3	480.79	479.91	452.57	450.33
6	Rings - Symmetric	3	417.12	416.95	393.71	390.99
7	Rings - Internal	3	509.98	509.05	482.01	480.04
8	Stringers & Rings - External	3	484.28	483.11	458.85	457.89
9	Stringers & Rings - Symmetric	4	375.60	375.22	363.68	366.32
10	Stringers & Rings - Internal	3	436.28	435.22	411.94	411.681
11	Stringers - Internal Rings - External	3	435.75	434.70	408.20	407.84
12	Stringers - External Rings - Internal	3	473.01	471.87	451.04	450.05

"S" = Smeared, D = Discrete, (i) radial inertia, (ii) Inplane inertia, (iii) Rotary inertia

TABLE 7: Frequencies (Hz) of a Shell Stiffened with 4 Internal Stringers

n	Present		Expt	Egle & Sewall (Ref.A22) Discrete		Unstiffened
	Discrete	Smeared		Symmetric	Unsymmetric	
2	314.61	315.31	-	-	-	-
3	158.72	158.72	-	169	169	171
4	100.27	102.21	100	103	108	108
5	93.09	93.09	87	94.7	94.7	98.1
6	115.00	113.91	104	109	116	117
7	144.00	144.00	137	145	145	151
8	179.71	185.26	176	183	192	194
9	233.26	233.26	224	236	236	243
10	296.81	287.38	295	278	297	300

TABLE 8: Frequencies (Hz) or a Shell Stiffened with 60 External Stringers

n	Present Discrete	Egle & Sewall (Ref.A22 Discrete	Shnell & Heinrichbeur Smeared
2	666.98	736.5	736.3
3	424.89	445.3	445.1
4	297.10	304.0	303.9
5	229.56	231.8	231.8
6	197.13	197.70	197.9
7	187.83	188.2	188.6
8	194.77	196.0	196.7
9	213.33	216.1	217.0
10	240.41	245.2	246.3

TABLE 9: Experimental Results for an Unstiffened Shell

n	m = 1			m = 2		
	Measured Freq (Hz)	Pred. Freq (Hz)	Remarks	Measrd. Freq(Hz)	Pred. Freq(Hz)	Remarks
5		207	Not Found		624	Not Found
6		170	Interferred with by n=7,8 modes		486	" "
7	148.0	166	Poor Response	-	397	Swamped by ^{n}=12,m=1 mode
8	177.0	184	Moderate Response but hard to separate	-	347	*Swamped by Vibration
9	219.6	218	Very Good Response	-	330	
10	265.8	261	" " "	-	338	
11	315.4	311	" " "	358	367	Good Response
12	370	367	" " "	407	409	" "
13	437	429	" " "	460	463	" "
14	503	496	Good Response	529	525	Moderate Response
15	578	569	" "	598	594	Poor Trace
16	657	646	" "	677	669	Moderate Response
17	743	729	" "	759	750	" "
18	833	816	*Almost Swamped by Vibration	856	837	Inconclusive
19	927	909	Moderate Response	940	929	"
20	1028	1006	" "	-	1026	Untraceable

*Untraceable Vibrations at 329Hz and 827Hz - source unknown.

TABLE 10: Experimental Results for a Stringer Stiffened Shell (2 Strips)

n	m = 1			m = 2		
	Measured Freq.(Hz)	Predicted Freq(Hz)	Remarks	Measured Freq.(Hz)	Pred. Freq(Hz)	Remarks
5		207	Not Found		617	Not Found
6		171	" "	490	486	Inconclusive*
7	154	164	Inconclusive		399	
8	174.8	181	Moderate Response		350	
9	214	213	Good Response		332	Interferred with one another
10	255.5	254	" "		339	
11	--	302	Swamped by Untraceable Vibrations*		364	
12	354	346	Very Good Response	389	394	Very Good Response
13	427	417	Good Response	449	455	Good Response
14	--	482	Swamped by Strong 490Hz Vibrations*	521	515	" "
15	564	551	Good Response	587	581	Moderate Response
16	640	626	" "	--	653	Interferred with by m=1 mode
17	724	706	Moderate Response	748	731	Just Detectable
18		818	Too High for Shaker		844	Too High for Shaker
19		880	" " " "		904	" " " "
20		975	" " " "		998	" " " "

*There were very strong responses at 312Hz and again at 490Hz. The 490Hz vibration seemed to indicate m=2, n=6, but proof of m=2 was inconclusive.

TABLE 11: Experimental Results for a Stringer Stiffened Shell (3 Strips)

n	m = 1			m = 2		
	Observd Freq (Hz)	Pred. Freq (Hz)	Remarks	Observd Freq (Hz)	Pred. Freq (Hz)	Remarks
5		208	Swamped by n=9 mode		618	Undetectable
6		172	Integral with n=8 mode		489	"
7	178	165	Moderate Response		405	"
8	-	181	Interferred with n=6 mode		358	Interferred with n=9, 10, 11
9	212.4	212	Good Response		340	" " n=8, 10, 11
10	259.5	252	" "	350	346	Moderate Response
11	-	300	Swamped by Vibration*		370	Interferred with n=8, 9, 10
12	370	336	Very Good Response	378	393	Moderate
13	420	412	" " "	441	458	Moderate Response
14	-	476	Swamped by Vibration*		516	Swamped by Vibration*
15	557	545	Poor Response	580	581	Inconclusive
16	633	619	Moderate Response		652	Undetectable
17	715	697	" "		728	"
18	-	822	Undetectable		857	"
19	-	969	"		898	"
20	-	962	"		990	"

* There were very powerrul vibrations at 319Hz and again at 490Hz. These swamped the n=11, 14, m=1 modes and the n=14, m=2 mode.

TABLE 12: Experimental Results for a Stringer Stiffened Shell (4 Strips)

n	m = 1			m = 2		
	Measured Freq.(Hz)	Predicted Freq.(Hz)	Remarks	Measured Freq.(Hz)	Predicted Freq.(Hz)	Remarks
5		210	Undetectable		620	Undetectable
6		175	"		492	"
7	172.1	167	Moderate Response		415	"
8	182.7	183	Good Response		369	"
9	209.3	213	" "		351	"
10	254.2	252	" "		357	"
11		298	Swamped by Vibration*		381	"
12	340.0	328	Very good Response	374	396	Moderate Response
13	418	409	" " "	447	466	" "
14		472	Swamped by Vibration*		522	Undetectable
15	552	539	Good Response		585	"
16	627	612	Moderate Response		654	"
17	708	689	" "		729	"
18		827	Swamped by 828Hz Vibration		876	"
19	891	858	Very Weak		895	"
20		950	Undetectable		986	"

*The n=11, m=1, mode was swamped by an untraceable vibration at 296 and 303Hz.
The n=14, m=1, mode was swamped by a vibration of 482Hz.

TABLE 13: Experimental Results for a Stringer Stiffened Shell (7 Strips)

n	m = 1			m = 2		
	Measured Freq.(Hz)	Predicted Freq.(Hz)	Remarks	Measd. Freq(Hz)	Predicted Freq.(Hz)	Remarks
5	224.6	231	Poor Response		672	Not Found
6		192	Not Found		519	
7	171.6	189	Poor Response		509	
8		200	Appeared to Interfere with one another		474	
9		225			461	
10	257.8	259	Poor Response		465	*Swamped by Vibration
11		300	*Swamped by Vibration		482	
12		302	" " "		480	
13	409	400	Good Response		549	Untraceable
14		458	*Swamped by Vibration		595	"
15	538	520	Very Poor Trace		648	"
16		586			708	"
17		657	*Swamped by Vibration		773	"
18	881	861	Moderate Response		999	"
19		813	Untraceable		920	"
20		897	"		1000	"

*Strong Vibrations at 659Hz, 311Hz and at 470Hz, 823Hz

TABLE 14: Experimental Results for a Stringer-Stiffened Shell (10 Strips)

	m = 1			m = 2		
n	Measured Freq.(Hz)	Predictd Freq(Hz)	Remarks	Measd. Freq(Hz)	Predicted Freq.(Hz)	Remarks
4		307	Not Found		829	
5		233	" "		681	
6		194	" "		522	
7	156.8	192	Poor Response		522	
8	178.4	203	Good Response		488	
9	195.0	227	" "		475	
10	242.6	261	Very Good Response		479	
11		301	*Swamped by Vibration		495	
12		301	" " "		495	
13	401	400	Moderate Response		561	
14		457	*Swamped by Vibration		606	
15	526	518	Moderate Response		658	
16	590	584	" "		716	
17		655	*Swamped by Vibration		780	
18		864	Untraceable		924	
19		808	*Swamped by Vibration		1011	

*Strong Vibrations at 280Hz, 304Hz, 460Hz, 659Hz, 829Hz

TABLE 15: Zeroes of K_n' $(-\alpha_j \pm i\beta_j)$ for n = 1 to 25 inclusive

n	j	α_j	β_j	n	j	α_j	β_j	n	j	α_j	β_j
1	1	-0.64355	0.50118	14	1	-1.66183	13.00682	21	1	-1.90932	19.86895
2	1	-0.83455	1.43444		2	-4.67488	10.48267		2	-5.54430	17.08581
3	1	-0.96756	2.37386		3	-6.39619	8.47718		3	-7.76070	14.92601
	2	-1.98162	0.44080		4	-7.57868	6.61123		4	-9.41256	12.94699
4	1	-1.07279	3.32208		5	-8.39903	4.81167		5	-10.70086	11.06073
	2	-2.44093	1.32259		6	-8.93364	3.04796		6	-11.71626	9.23047
5	1	-1.16125	4.27689		7	-9.22047	1.30319		7	-12.50886	7.43664
	2	-2.80372	2.21193	15	1	-1.70167	13.98474		8	-13.10922	5.66727
	3	-3.30981	0.43637		2	-4.81647	11.41990		9	13.53672	3.91421
6	1	-1.23832	5.23662		3	-6.62004	9.39079		10	-13.80353	2.17142
	2	-3.10823	3.10944		4	-7.88181	7.50804		11	-13.91669	0.43402
	3	-3.83945	1.31040		5	-8.78277	5.69612	22	1	-1.93986	20.85183
7	1	-1.30706	6.20016		6	-9.40221	3.92362		2	-5.65015	18.03583
	2	-3.37302	4.01420		7	-9.78092	2.17340		3	-7.92542	15.85587
	3	-4.28713	2.18909		8	-9.93986	0.43416		4	-9.63207	13.86164
	4	-4.63643	0.43515	16	1	-1.73976	14.96359		5	-10.97383	11.96325
8	1	-1.36941	7.16673		2	-4.95117	12.35946		6	-12.04274	10.12315
	2	-3.60873	4.92518		3	-6.83234	10.30729		7	-12.88990	8.32132
	3	-4.67840	3.07328		4	-8.16837	8.40792		8	-13.54668	6.54555
	4	-5.19993	1.30647		5	-9.14415	6.58356		9	-14.03331	4.78760
9	1	-1.42666	8.13579		6	-9.84144	4.80185		10	-14.36289	3.04143
	2	-3.82205	5.84153		7	-10.30328	3.04535		11	-14.54355	1.30227
	3	-5.02799	3.96283		8	-10.55323	1.30283	23	1	-1.96948	21.83521
	4	-5.69437	2.18088	17	1	-1.77628	15.94327		2	-5.75255	18.98717
	5	-5.96254	0.43465		2	-5.07975	13.30114		3	-8.08454	16.78747
					3	-7.03445	11.22645		4	-9.84381	14.77826
					4	-8.44039	9.31068		5	-11.23675	12.86787
					5	-9.48609	7.47384		6	-12.35669	11.01794

n	j	α_j	β_j
10	1	-1.47974	9.10691
	2	-4.01755	6.76252
	3	-5.34530	4.85737
	4	-6.13752	3.05918
	5	-6.54609	1.30470
11	1	-1.52933	10.07980
	2	-4.19846	7.68757
	3	-5.63673	5.75647
	4	-6.54075	3.94149
	5	-7.07040	2.17695
	6	-7.28842	0.43440
12	1	-1.57595	11.05421
	2	-4.36716	8.61620
	3	-5.90688	6.65971
	4	-6.91185	4.82774
	5	-7.54847	3.05207
	6	-7.88525	1.30376
13	1	-1.62001	12.02993
	2	-4.52549	9.54802
	3	-6.15916	7.56673
	4	-7.25644	5.71773
	5	-7.98920	3.93030
	6	-8.43037	2.17475
	7	-8.61418	0.43425
17	6	-10.25545	5.68266
	7	-10.79349	3.91930
	8	-11.12546	2.17250
	9	-11.26550	0.43410
18	1	-1.81137	16.92371
	2	-5.20286	14.24476
	3	-7.22748	12.14807
	4	-8.69954	10.21613
	5	-9.81095	8.36683
	6	-10.64753	6.56600
	7	-11.25577	4.79538
	8	-11.66281	3.04359
	9	-11.88437	1.30258
19	1	-1.84517	17.90484
	2	-5.32103	15.19016
	3	-7.41236	13.07197
	4	-8.94721	11.12410
	5	-10.12071	9.26239
	6	-11.02031	7.45180
	7	-11.69397	5.67364
	8	-12.17012	3.91634
	9	-12.46594	2.17187
	10	-12.59111	0.43405
20	1	-1.87778	18.88660
	2	-5.43471	16.13722
	3	-7.58987	13.99800
	4	-9.18455	12.03444
	5	-10.41686	10.16040
	6	-11.37595	8.33999
	7	-12.11088	6.55407
	8	-12.65122	4.79087
	9	-13.01536	3.04235
	10	-13.21437	1.30240
23	7	-13.25563	9.20804
	8	-13.96571	7.42571
	9	-14.50785	5.66260
	10	-14.89595	3.91263
	11	-15.13900	2.17108
	12	15.24226	0.43400
24	1	-1.99824	22.81906
	2	-5.85177	19.93975
	3	-8.23850	17.72070
	4	10.04843	15.69674
	5	-11.49047	13.77447
	6	-12.65921	11.91476
	7	-13.60749	10.09675
	8	14.36810	8.30774
	9	-14.96261	6.53924
	10	-15.40557	4.78514
	11	-15.70670	3.04074
	12	-15.87211	1.30217
25	1	-2.02622	23.80334
	2	-5.94803	20.89350
	3	-8.38769	18.65547
	4	-10.24647	16.61698
	5	-11.73573	14.68296
	6	-12.95127	12.81351
	7	-13.94669	10.98737
	8	-14.75538	9.19159
	9	-15.39950	7.41755
	10	-15.89414	5.65906
	11	-16.24965	3.91142
	12	-16.47285	2.17082
	13	-16.56781	0.43398

M	Q_{11}^R	Q_{11}^I	Q_{12}^R	Q_{12}^I	Q_{22}^R	Q_{22}^I
2.0	-0.2523	0.2766	0.8597	-0.0090	-0.3890	0.2625
	0	0.2500	0.6667	0	0	0.2500
3.0	-0.1313	0.1991	0.5740	0.0135	-0.2176	0.2183
	0	0.1667	0.4444	0	0	0.1667
4.0	-0.0910	0.1587	0.4431	0.0127	-0.1540	0.1773
	0	0.1250	0.3333	0	0	0.1250
5.0	-0.0702	0.1328	0.3652	0.0106	-0.1190	0.1486
	0	0.1000	0.2666	0	0	0.1000
6.0	-0.0573	0.1147	0.3121	0.0089	-0.0965	0.1280
	0	0.0834	0.2222	0	0	0.0834

TABLE 16: Aerodynamic Generalised Forces Q_{mr} for small Values of L/R and n

L/R = 1.0, n = 2, k = 1.0, m = 2, r = 1

Upper values: Exact Theory.

Lower values: Linear Piston Theory.

M	Q_{11}^R	Q_{11}^I	Q_{12}^R	Q_{12}^I	Q_{22}^R	Q_{22}^I	k
10.0	-0.0285	0.0028	0.1490	-0.00035	0.00075	0.0023	
	0	0.0025	0.1333	0	0	0.0025	
12.0	-0.0162	0.0022	0.1202	-0.00026	0.0054	0.0019	
	0	0.0021	0.1112	0	0	0.0021	0.05
14.0	-0.0096	0.0019	0.1004	-0.00020	0.0073	0.0016	
	0	0.0018	0.0952	0	0	0.0018	
16.0	-0.0056	0.0016	0.0860	-0.00016	0.0080	0.0014	
	0	0.0016	0.0833	0	0	0.0016	
10.0	-0.0284	0.0056	0.1490	-0.00069	0.00075	0.0045	
	0	0.0050	0.1333	0	0	0.0050	
12.0	-0.0162	0.0045	0.1202	-0.00051	0.0054	0.0037	
	0	0.0042	0.1112	0	0	0.0042	0.10
14.0	-0.0096	0.0037	0.1004	-0.00039	0.0073	0.0032	
	0	0.0036	0.0952	0	0	0.0036	
16.0	-0.0056	0.0032	0.0860	-0.00032	0.0080	0.0027	
	0	0.0031	0.0833	0	0	0.0031	
10.0	-0.0284	0.0083	0.1490	-0.0010	0.00074	0.0068	
	0	0.0075	0.1333	0	0	0.0075	
12.0	-0.0162	0.0067	0.1202	-0.00077	0.0054	0.0056	
	0	0.0063	0.1112	0	0	0.0063	0.15
14.0	-0.0095	0.0056	0.1004	-0.00059	0.0073	0.0048	
	0	0.0054	0.0952	0	0	0.0054	
16.0	-0.0056	0.0048	0.0860	-0.00048	0.0080	0.0041	
	0	0.0047	0.0833	0	0	0.0047	
10.0	-0.0284	0.0100	0.1490	-0.0012	0.00073	0.0082	
	0	0.0090	0.1333	0	0	0.0090	
12.0	-0.0162	0.0081	0.1202	-0.00092	0.0054	0.0067	
	0	0.0075	0.1112	0	0	0.0075	0.18
14.0	-0.0095	0.0067	0.1004	-0.00071	0.0073	0.0057	
	0	0.0064	0.0952	0	0	0.0064	
16.0	-0.0056	0.0058	0.0860	-0.00057	0.0080	0.0049	
	0	0.0056	0.0833	0	0	0.0056	

TABLE 17: Aerodynamic Generalised Forces Q_{mr} for medium values of L/R, Large values of n, and very high Mach numbers for a range of frequency parameters.

L/R = 2.0, n = 9. m = 2, r = 1

Upper values: Exact theory; Lower values: Linear piston theory.

M	Q_{11}^R	Q_{11}^I	Q_{12}^R	Q_{12}^I	Q_{22}^R	Q_{22}^I	k
0.0	-0.0294	0.0111	0.1490	-0.0014	0.00072	0.0091	
	0	0.01	0.1333	0	0	0.01	
2.0	-0.0162	0.0090	0.1202	-0.0010	0.00538	0.0075	
	0	0.0083	0.1112	0	0	0.0083	0.2
4.0	-0.0095	0.0075	0.1004	-0.00079	0.0072	0.0063	
	0	0.0071	0.0952	0	0	0.0071	
6.0	-0.0056	0.0064	0.0860	-0.00064	0.0080	0.0055	
	0	0.0063	0.0833	0	0	0.0063	
0.0	-0.0282	0.0277	0.1487	-0.0034	0.00049	0.0227	
	0	0.025	0.1333	0	0	0.0250	
2.0	-0.0160	0.0224	0.1200	-0.0025	0.0052	0.0187	
	0	0.0209	0.1112	0	0	0.0209	0.5
4.0	-0.0094	0.0187	0.1003	-0.0019	0.0071	0.0159	
	0	0.0179	0.0952	0	0	0.0179	
6.0	-0.0055	0.0160	0.0859	-0.0016	0.0079	0.0138	
	0	0.0157	0.0833	0	0	0.0157	
0.0	-0.0273	0.0554	0.1478	-0.0067	-0.00035	0.0456	
	0	0.05	0.1333	0	0	0.0500	
2.0	-0.0154	0.0447	0.1194	-0.0049	0.0045	0.0375	
	0	0.0417	0.1112	0	0	0.0417	1.0
4.0	-0.0089	0.0374	0.0998	-0.0038	0.0065	0.0319	
	0	0.0357	0.0952	0	0	0.0357	
6.0	-0.0051	0.0321	0.0855	-0.0031	0.0074	0.0276	
	0	0.0313	0.0833	0	0	0.0313	
0.0	-0.0259	0.0828	0.1464	-0.0097	-0.0016	0.0689	
	0	0.075	0.1333	0	0	0.0750	
2.0	-0.0144	0.0670	0.1184	-0.0071	0.0035	0.0567	
	0	0.0626	0.1112	0	0	0.0626	1.5
4.0	-0.0082	0.0560	0.0990	-0.0055	0.0057	0.0481	
	0	0.0536	0.0952	0	0	0.0536	
6.0	-0.0045	0.0480	0.0849	-0.0044	0.0067	0.0417	
	0	0.0470	0.0833	0	0	0.0470	

TABLE 17:Continued.

M	Q^R_{11}	Q^I_{11}	Q^R_{12}	Q^I_{12}	Q^R_{22}	Q^I_{22}	k
.5	-0.1405	0.0002	0.00135	0.00784	-0.5700	0.00066	
	0	0.0333	0.8889	0	0	0.0333	
.0	-0.1414	0.0003	0.00246	0.00806	-0.5852	0.00099	
	0	0.0250	0.6667	0	0	0.0250	0.1
.0	-0.1430	0.0006	0.00015	0.00952	-0.6581	0.00473	
	0	0.0167	0.4444	0	0	0.0167	
.0	-0.1502	0.0011	0.01935	0.01321	-0.7188	0.0216	
	0	0.0125	0.3333	0	0	0.0125	
.5	-0.1417	0.0005	0.00138	0.0235	-0.5714	0.00197	
	0	0.1000	0.8889	0	0	0.1000	
.0	-0.1427	0.0009	0.00242	0.0242	-0.5870	0.00299	
	0	0.0750	0.6667	0	0	0.0750	0.3
.0	-0.1444	0.0017	0.00009	0.0286	-0.6615	0.0144	
	0	0.0500	0.4444	0	0	0.0500	
.0	-0.1521	0.0034	0.0212	0.0396	-0.7180	0.0648	
	0	0.038	0.3333	0	0	0.0375	
.0	-0.1437	0.0012	0.0024	0.0323	-0.5886	0.0040	
	0	0.1000	0.6667	0	0	0.1000	
.0	-0.1538	0.0046	0.0229	0.0527	-0.7174	0.0863	
	0	0.0500	0.3333	0	0	0.0500	0.4
.0	-0.1594	0.0240	0.1603	0.0213	-0.3527	0.0703	
	0	0.0333	0.2222	0	0	0.0333	
.0	-0.1163	0.0266	0.1785	0.0038	-0.1423	0.0386	
	0	0.0250	0.1666	0	0	0.0250	
.0	-0.1451	0.0015	0.0024	0.0404	-0.5906	0.0051	
	0	0.1250	0.6667	0	0	0.1250	
.0	-0.1560	0.0058	0.0250	0.0657	-0.7166	0.0179	
	0	0.0625	0.3333	0	0	0.0625	0.5
.0	-0.1603	0.0300	0.1617	0.0265	-0.3506	0.0877	
	0	0.0417	0.2222	0	0	0.0417	
.0	-0.1164	0.0333	0.1789	0.0047	-0.1415	0.0482	
	0	0.0313	0.1666	0	0	0.0313	

TABLE 13: Aerodynamic Generalised Forces Q_{mr} for large values of L/R, n, Medium to High Mach Numbers for a range of k. L/R = 4.0, n = 9, m = 2, r = 1

Upper values: Exact Theory; Lower values: Linear piston theory.

M	Q_{11}^R	Q_{11}^I	Q_{12}^R	Q_{12}^I	Q_{22}^R	Q_{22}^I	k
.0	-0.1468	0.0018	0.0023	0.0485	-0.5931	0.0061	
	0	0.1500	0.6667	0	0	0.1500	
.0	-0.1586	0.0072	0.0275	0.0787	-0.7156	0.1295	
	0	0.0750	0.3333	0	0	0.0750	0.6
.0	-0.1614	0.0362	0.1635	0.0316	-0.3482	0.1050	
	0	0.0500	0.2222	0	0	0.0500	
.0	-0.1166	0.0400	0.1794	0.0056	-0.1406	0.0577	
	0	0.0375	0.1666	0	0	0.0375	
.0	-0.1511	0.0024	0.0022	0.0648	-0.5993	0.0084	
	0	0.2000	0.6667	0	0	0.2000	
.0	-0.1654	0.0102	0.0341	0.1044	-0.7130	0.1728	
	0	0.1000	0.3333	0	0	0.1000	0.8
.0	-0.1641	0.0487	0.1678	0.0415	-0.3420	0.1391	
	0	0.0667	0.2222	0	0	0.0667	
.0	-0.1171	0.0535	0.1806	0.0072	-0.1382	0.0765	
	0	0.0500	0.1666	0	0	0.0500	
.5	-0.1553	0.0016	0.0017	0.0785	-0.5870	0.0065	
	0	0.3333	0.8889	0	0	0.3333	
.0	-0.1566	0.0029	0.0021	0.0812	-0.6073	0.0107	
	0	0.2500	0.6667	0	0	0.2500	1.0
.0	-0.1603	0.0056	-0.00081	0.0981	-0.6993	0.0555	
	0	0.1667	0.4444	0	0	0.1667	
.0	-0.1740	0.0138	0.0425	0.1297	-0.7096	0.2160	
	0	0.1250	0.3333	0	0	0.1250	
.5	-0.1637	0.0020	0.0018	0.0982	-0.5968	0.0081	
	0	0.4167	0.8889	0	0	0.4167	
.0	-0.1653	0.0036	0.0021	0.1019	-0.6197	0.0139	
	0	0.3125	0.6667	0	0	0.3125	1.25
.0	-0.1703	0.0070	0.00034	0.1246	-0.7217	0.0751	
	0	0.2083	0.4444	0	0	0.2083	
.0	-0.1873	0.0193	0.0555	0.1605	-0.7042	0.2701	
	0	0.1563	0.3333	0	0	0.1563	

TABLE 18: Continued.

M	Q_{11}^R	Q_{11}^I	Q_{12}^R	Q_{12}^I	Q_{22}^R	Q_{22}^I	k
.0	-0.1233	0.00006	-0.0031	0.0178	-0.5148	0.0010	
	0	0.0417	0.6667	0	0	0.0417	0.25
.0	-0.1336	0.0023	0.0151	0.0265	-0.6147	0.0369	
	0	0.0312	0.3333	0	0	0.0312	
.0	-0.1399	0.0108	0.1135	0.0154	-0.3831	0.0396	
	0	0.0208	0.2222	0	0	0.0208	
.0	-0.1129	0.0135	0.1444	0.0056	-0.1972	0.0253	
	0	0.0156	0.1667	0	0	0.0156	
.0	-0.1311	0.00017	-0.0033	0.0571	-0.5258	0.0035	
	0	0.2000	0.6667	0	0	0.2000	
.0	-0.1447	0.0081	0.0236	0.0843	-0.6160	0.1189	
	0	0.1000	0.3333	0	0	0.1000	0.8
.0	-0.1463	0.0354	0.1220	0.0480	-0.3732	0.1254	
	0	0.0667	0.2222	0	0	0.0637	
.0	-0.1153	0.0437	0.1481	0.0175	-0.1918	0.0802	
	0	0.0500	0.1667	0	0	0.0500	
.0	-0.1360	0.0002	-0.0034	0.0716	-0.5326	0.0046	
	0	0.2500	0.6667	0	0	0.2500	
.0	-0.1516	0.0107	0.0289	0.1050	-0.6168	0.1491	
	0	0.1250	0.3333	0	0	0.1250	1.0
.0	-0.1503	0.0449	0.1272	0.0591	-0.3671	0.1557	
	0	0.0833	0.2222	0	0	0.0833	
.0	-0.1167	0.0586	0.1503	0.0214	-0.1884	0.0996	
	0	0.0625	0.1667	0	0	0.0625	

TABLE 19: Aerodynamic Generalised Forces Q_{mr} for very large values of L/R and Medium values of n, Medium to High Mach Numbers for a range of k.
L/R = 10.0, n = 4, m = 2, r = 1
Upper values: Exact theory.
Lower Values: Linear Piston Theory.

M	Q_{11}^R	Q_{11}^I	Q_{12}^R	Q_{12}^I	Q_{22}^R	Q_{22}^I	k
.5	-0.0825	-0.0001	-0.00079	0.0220	-0.3264	-0.00036	
	0	0.1667	0.8889	0	0	0.1667	
.0	-0.0830	-0.00006	-0.0012	0.0224	-0.3317	-0.00005	
	0	0.1250	0.6667	0	0	0.1250	0.5
.0	-0.0842	0.00019	-0.0017	0.0236	-0.3469	0.0014	
	0	0.0833	0.4444	0	0	0.0833	
.0	-0.0860	0.00081	-0.0012	0.0253	-0.3689	0.0047	
	0	0.0625	0.3333	0	0	0.0625	
.5	-0.0887	-0.00022	-0.0009	0.0440	-0.3330	-0.00073	
	0	0.3333	0.8889	0	0	0.3333	
.0	-0.0893	-0.00013	-0.0013	0.0449	-0.3889	-0.000098	
	0	0.2500	0.6667	0	0	0.2500	1.0
.0	-0.0909	0.00036	-0.0018	0.0475	-0.3561	0.0030	
	0	0.1667	0.4444	0	0	0.1667	
.0	-0.0932	0.0016	-0.0016	0.0512	-0.3828	0.0104	
	0	0.1250	0.3333	0	0	0.1250	
.5	-0.0991	-0.00037	-0.0011	0.0661	-0.3440	-0.0011	
	0	0.5000	0.8889	0	0	0.5000	
.0	-0.09990	-0.00023	-0.0015	0.0674	-0.3509	-0.00015	
	0	0.3750	0.6667	0	0	0.3750	1.5
.0	-0.1021	0.0005	-0.0021	0.0716	-0.3715	0.0049	
	0	0.2500	0.4444	0	0	0.2500	
.0	-0.1052	0.0023	-0.0022	0.0782	-0.4060	0.0184	
	0	0.1875	0.3333	0	0	0.1875	
.5	-0.1135	-0.00056	-0.0013	0.0882	-0.3595	-0.0015	
	0	0.6667	0.8889	0	0	0.6667	
.0	-0.1147	-0.00037	-0.0017	0.0901	-0.3677	-0.0002	
	0	0.5000	0.6667	0	0	0.5000	2.0
.0	-0.1179	0.0006	-0.0024	0.0963	-0.3933	0.0072	
	0	0.3333	0.4444	0	0	0.3333	
.0	-0.1224	0.0031	-0.0027	0.1068	-0.4385	0.0301	
	0	0.2500	0.3333	0	0	0.2500	

TABLE 2: Aerodynamic Generalised Forces Q_{mr} for Very Large Values of L/λ. Large Values of n. L/λ = 10.0, n = 6, m = 2, r =1
Upper Values: Exact Theory, Lower Values: Linear Piston Theory.

M	Q_{11}^R	Q_{11}^I	Q_{12}^R	Q_{12}^I	Q_{22}^R	Q_{22}^I	k
.5	-0.1322	-0.00081	-0.0016	0.1104	-0.3794	-0.0020	
	0	0.8333	0.8889	0	0	0.8333	
.0	-0.1339	-0.00056	-0.0020	0.1130	-0.3894	-0.00024	
	0	0.6250	0.6667	0	0	0.6250	2.5
.0	-0.1385	0.00070	-0.0027	0.1216	-0.4215	0.0099	
	0	0.4167	0.4444	0	0	0.4167	
.0	-0.1451	0.0038	-0.0026	0.1376	-0.4801	0.0470	
	0	0.3125	0.3333	0	0	0.3125	
.5	-0.1551	-0.0011	-0.0019	0.1328	-0.4038	-0.0025	
	0	1.000	0.8889	0	0	1.000	
.0	-0.1573	-0.00082	-0.0024	0.1362	-0.4161	-0.00028	
	0	0.7500	0.6667	0	0	0.7500	3.0
.0	-0.1639	0.0008	-0.0029	0.1477	-0.4566	0.0134	
	0	0.5000	0.4444	0	0	0.5000	
.0	-0.1736	0.0048	-0.0012	0.1713	-0.5302	0.0709	
	0	0.3750	0.3333	0	0	0.3750	
.5	-0.1821	-0.0015	-0.0024	0.1552	-0.4326	-0.0030	
	0	1.1667	0.8889	0	0	1.1667	
.0	-0.1851	-0.0011	-0.0029	0.1596	-0.4479	-0.00031	
	0	0.8750	0.6667	0	0	0.8750	3.5
.0	-0.1943	0.0009	-0.0032	0.1748	-0.4991	0.0177	
	0	0.5833	0.4444	0	0	0.5833	
.0	-0.2085	0.0063	0.0022	0.2082	-0.5877	0.1037	
	0	0.4375	0.3333	0	0	0.4375	
.5	-0.2133	-0.0020	-0.0029	0.1778	-0.4661	-0.0037	
	0	1.3333	0.8889	0	0	1.3333	
.0	-0.2174	-0.0016	-0.0034	0.1835	-0.4848	-0.0003	
	0	1.0000	0.6667	0	0	1.0000	4.0
.0	-0.2300	0.0011	-0.0033	0.2033	-0.5494	0.0234	
	0	0.6667	0.4444	0	0	0.6667	
.0	-0.2504	0.0087	0.0090	0.2486	-0.6512	0.1473	
	0	0.5000	0.3333	0	0	0.5000	

TABLE 20: Continued.

TABLE 21: Intermediate Results for Illustration of U-g Method
Linear Piston Theory - 2 to 10 Axial Modes

M_a	No.of Axial Modes	k_a	2.0		2.05	
		$\Delta_R * 10^3$	M_p	g_p	M_p	g_p
1.7	2	0.4949	1.6656	-0.0529	1.6249	-0.0474
	3	0.6765	1.9473	0.0172	1.9000	0.0213
	4	0.5755	1.7962	-0.0049	1.7524	-0.0001
	5	0.5828	1.8075	0.0052	1.7634	0.0099
	6	0.5810	1.8045	0.0020	1.7607	0.0067
	7	0.5817	1.8059	0.0032	1.7618	0.0079
	8	0.5815	1.8055	0.0026	1.7615	0.0073
	9	0.5817	1.8057	0.0029	1.7617	0.0076
	10	0.5816	1.8056	0.0028	1.7616	0.0075
1.8	2	0.4949	1.6656	-0.0585	1.6249	-0.0526
	3	0.6866	1.9619	-0.0472	1.9140	-0.0429
	4	0.5849	1.8107	-0.0111	1.7665	-0.0062
	5	0.5945	1.8255	0.0005	1.7809	0.0053
	6	9.5920	1.8217	-0.0033	1.7773	0.0016
	7	0.5930	1.8232	-0.0019	1.7787	0.0030
	8	0.5926	1.8227	-0.0025	1.7782	0.0024
	9	0.5928	1.8229	-0.0022	1.7785	0.0027
	10	0.5928	1.8228	-0.0024	1.7784	0.0025

L/R = 10.0, h/R = 0.002, n = 6

Δ_R = Real part of the eigenvalue

M_p = predicted } Mach number

M_a = assumed } Mach number

k_a = assumed frequency parameter

g_p = predicted inherent damping corresponding to (M_a, k_a)

TABLE 22: Critical Mach Numbers for a Long (Unstiffened) Shell

	h/R	NUMBER OF AXIAL MODES								
		2	3	4	5	6	7	8	9	10
LINEAR PISTON THEORY	0.002	1.4	1.73	1.67	1.82	1.8	1.8	1.8	1.8	1.8
	0.004	2.82	3.48	3.60	3.75	3.70	3.75	3.75	3.75	3.75
EXACT AERODY-NAMIC THEORY	0.004	3.10	3.12	3.13	3.2	3.2	3.2	3.2	3.2	3.2

L/R = 10.0, n = 6; Convergence of the Galerkin's Solution

TABLE 23:

(a) Frequency Factors for an Unstiffened Shell

m	$\Delta_m * 10^3$ IN VACUO
1	0.4412
2	0.5486
3	0.9812
4	2.0776
5	4.2372
6	7.8647
7	13.3186
8	20.8728
9	30.6932
10	42.8315

No.of axial modes	$\Delta_F * 10^3$ FLUTTER
2	0.4949
3	0.5748
4	0.5849
5	0.5945
6	0.5920
7	0.5930
8	0.5926
9	0.5928
10	0.5928

(b) Components of the Non-Dimensional Eigenvector Corresponding to the Eigenvalue which Leads to the Flutter Solution with 10 Axial Modes

m	Eigenvector Components	
	Real Part	Imaginary Part
1	425.7	314.5
2	617.1	-7.881
3	317.9	-85.32
4	90.5	-15.67
5	29.2	-3.299
6	11.0	-0.517
7	5.3	-0.364
8	2.7	-0.034
9	1.6	-0.093
10	1.0	0.000

L/R = 10.0, m = 6, h/R = 0.002

TABLE 24: Critical Mach Numbers Using Exact Theory and Linear Piston Theory Using a Two-mode Solution For an Unstiffened Shell

L/R	h/R	n	M_{CRIT} (EXACT THEORY)	M_{CRIT} (LINEAR PISTON THEORY)
2.0	0.002	9	12.2	12.13
4.0	0.002	9	4.2	3.29
10.0	0.002	6	2.7	1.4
10.0	0.004	6	3.10	2.82

No. of Axial Modes	g Exact Theory	g Linear Piston Theory.
2	0.005333	-0.0168
3	0.032779	-0.0239
4	0.040811	-0.0002
5	0.040443	0.0049
6	0.040913	0.0032
7	0.040897	0.0038
8	0.040967	0.0035
9	0.040965	0.0037
10	0.040983	0.0036

TABLE 25: Damping Inherent in the System for a Particular Shell Using Exact Theory and Linear Piston Theory.

$L/R = 10.0$, $h/R = 0.004$, $n = 6$, $M = 4.0$, $k = 2.0$

TABLE 26: Critical Mach Numbers for Unstiffened and Internally Stringer-Stiffened Cylindrical Shells: Binary Analysis r = 2, s = 1; Linear Piston Theory

L/R	h_s/h	UNSTIFFENED		STRINGERS - INTERNAL									
		0		1.0		3.0		5.0		8.0		10.0	
	h/R	n_{crit}	M_{crit}	n_{crit}	M_{crit}	n_{crit}	M_{crit}	n_{crit}	M_{crit}	n_{crit}	M_{crit}	n_{crit}	M_{crit}
2.0	0.002	16	3.352	16	2.374	13	5.064	11	9.103	9	16.13	8	21.1
	0.004	14	14.11	13	9.874	10	24.58	8	44.99	7	77.59	7	97.7
	0.006	12	35.64	11	24.79	8	63.62	7	115.5	6	193.7	6	236.8
	0.008	11	69.35	10	48.09	7	125.8	6	227.5	5	377.4	5	457.8
	0.010	10	116.2	9	80.74	7	212.7	6	388.7	5	623.8	5	777.0
	0.012	9	178.9	8	124.6	6	329.5	5	596.8	5	964.8	5	1234.
4.0	0.002	11	1.984	11	1.461	10	2.018	9	3.194	8	5.417	7	6.944
	0.004	10	5.374	10	3.892	8	8.345	7	14.66	6	24.29	6	28.82
	0.006	10	12.01	9	8.664	7	20.66	6	36.37	5	57.18	5	62.33
	0.008	9	22.54	8	16.38	7	40.31	6	70.36	5	98.60	5	105.4
	0.010	8	37.47	8	26.78	6	65.66	5	112.0	5	153.9	5	163.2
	0.012	8	57.34	7	40.67	6	101.6	5	167.0	4	221.1	4	234.4

TABLE 26 continued

L/R	h_s/h	UNSTIFFENED				STRINGERS - INTERNAL							
		0		1.0		3.0		5.0		8.0		10.0	
	h/R	n_{crit}	M_{crit}	n_{crit}	M_{crit}	n_{crit}	M_{crit}	n_{crit}	M_{crit}	n_{crit}	M_{crit}	n_{crit}	M_{crit}
6.0	0.002	8	1.637	8	1.263	8	1.448	8	1.927	7	2.995	7	3.809
	0.004	8	3.700	8	2.759	7	4.668	6	7.998	6	13.04	5	15.22
	0.006	8	7.003	8	5.182	7	11.21	6	19.55	5	29.02	5	31.58
	0.008	8	12.34	7	9.142	6	20.93	5	35.95	5	51.74	5	53.23
	0.010	7	19.66	7	14.45	5	35.65	5	59.15	4	75.73	4	74.19
	0.012	7	29.72	7	22.03	5	52.20	4	88.47	4	101.9	4	99.40
10.0	0.002	6	1.397	6	1.084	6	1.138	6	1.277	6	1.654	6	1.983
	0.004	6	2.822	6	2.125	6	2.644	5	3.899	5	5.889	5	6.998
	0.006	6	4.572	6	3.418	6	5.529	5	8.774	4	13.31	4	13.95
	0.008	6	6.881	6	5.142	5	9.634	4	16.87	4	22.02	4	21.76
	0.010	6	10.04	6	7.534	4	15.89	4	26.04	4	32.61	4	30.62
	0.012	5	14.36	6	10.85	4	24.64	4	38.09	4	44.72	4	40.60

TABLE 27: Critical Mach Numbers for Unstiffened and Externally Stringer-Stiffened Cylindrical Shells: Binary Analysis, r=2, s=1, Linear Piston Theory

L/R	h_s/h	UNSTIFFENED		STRINGERS - EXTERNAL									
		0		1.0		3.0		5.0		8.0		10.0	
	h/R	n_{crit}	M_{crit}	n_{crit}	M_{crit}	n_{crit}	M_{crit}	n_{crit}	M_{crit}	n_{crit}	M_{crit}	n_{crit}	M_{crit}
2.0	0.002	16	3.352	18	3.427	15	8.245	12	15.28	10	27.75	10	36.47
	0.004	14	14.11	15	16.19	11	43.24	9	79.83	8	139.0	7	175.5
	0.006	12	35.64	13	42.67	10	114.7	8	207.7	7	348.5	6	427.5
	0.008	11	69.35	11	85.28	8	228.3	7	406.2	6	657.2	6	806.1
	0.010	10	116.2	10	145.9	8	388.4	6	677.6	5	1074.	5	1327.
	0.012	9	117.9	10	226.1	7	595.2	5	1029.0	5	1613.	4	2021.
4.0	0.002	11	1.984	11	1.717	11	2.699	10	4.546	9	8.090	8	10.53
	0.004	10	5.347	11	5.245	9	12.48	8	22.86	7	39.71	7	49.30
	0.006	10	12.01	10	12.56	8	32.58	7	59.55	6	98.03	6	115.0
	0.008	9	22.54	9	24.60	7	65.19	6	117.3	6	182.0	6	207.1
	0.010	8	37.47	9	41.72	7	110.7	6	195.9	6	293.3	6	328.0
	0.012	8	57.34	8	64.40	6	172.1	6	300.9	5	426.0	6	481.0

TABLE 27 continued

L/R	h_s/h	UNSTIFFENED		STRINGERS - EXTERNAL									
		0		1.0		3.0		5.0		8.0		10.0	
	h/R	n_{crit}	M_{crit}	n_{crit}	M_{crit}	n_{crit}	M_{crit}	n_{crit}	M_{crit}	n_{crit}	M_{crit}	n_{crit}	M_{crit}
6.0	0.002	8	1.637	9	1.386	9	1.740	8	2.487	8	4.100	7	5.226
	0.004	8	3.700	9	3.342	8	6.284	7	11.17	6	19.21	6	23.42
	0.006	8	7.003	9	6.835	7	15.87	6	28.80	6	47.22	6	54.50
	0.008	8	12.34	8	12.34	7	31.69	6	56.58	5	85.22	5	94.20
	0.010	7	19.66	8	20.63	6	53.08	5	94.02	5	133.2	5	144.0
	0.012	7	29.72	7	31.36	6	82.46	5	141.0	5	191.5	5	205.0
10.0	0.002	6	1.397	6	1.140	6	1.256	6	1.470	6	1.974	6	2.390
	0.004	6	2.822	6	2.344	6	3.175	6	4.858	5	7.916	5	9.469
	0.006	6	4.572	6	3.958	6	6.868	5	11.82	5	18.75	5	21.18
	0.008	6	6.881	6	6.196	5	13.22	5	22.68	4	34.35	5	36.53
	0.010	6	10.04	6	9.303	5	21.55	4	38.54	4	51.88	4	54.17
	0.012	5	14.36	6	13.52	5	31.03	4	56.60	4	72.49	4	74.53

TABLE 28: Critical Mach Numbers (a) Unstiffened (h/R = 0.004), (b) Stiffened with 10 Internal Stringers (h/R = 0.002)

NUMBER OF AXIAL MODES	M_{CRIT}	
	(b).	(a)
2	1.98	2.82
3	2.75	3.48
4	3.00	3.60
5	3.60	3.75
6	3.65	3.70
7	3.85	3.75
8	3.80	3.75
9	3.90	3.75
10	3.80	3.75

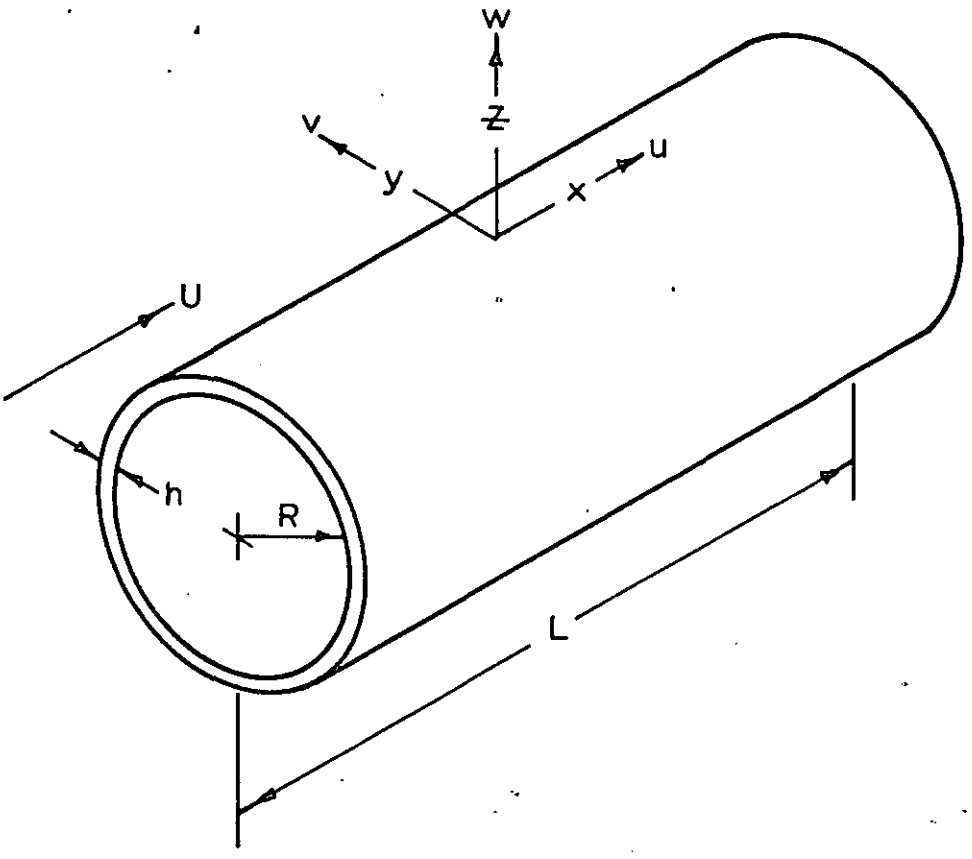

FIG. 1a CO-ORDINATE SYSTEM FOR THE CIRCULAR CYLINDRICAL SHELL.

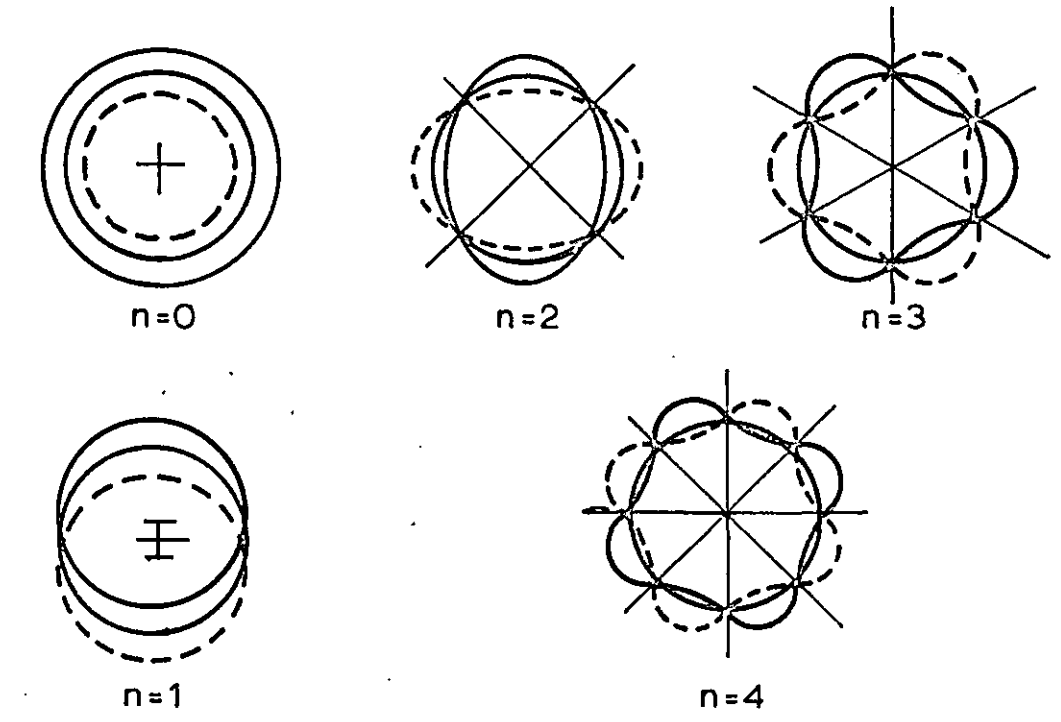

CIRCUMFERENTIAL NODAL PATTERN

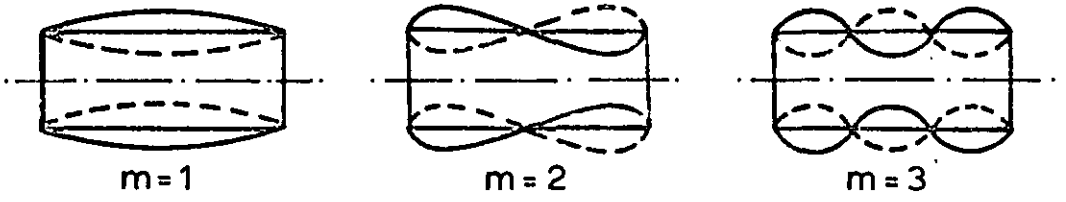

AXIAL NODAL PATTERN

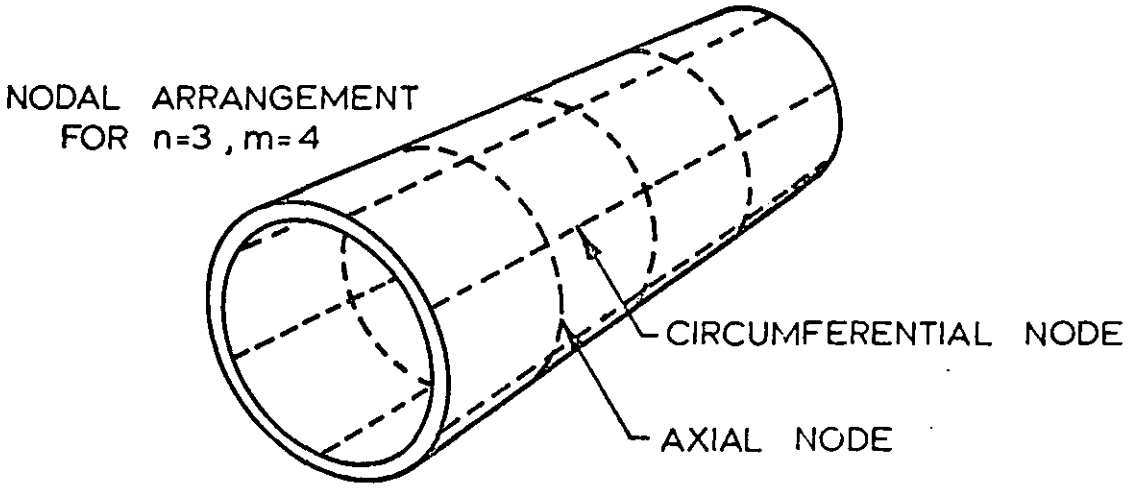

FIG. 1 b NODAL PATTERNS

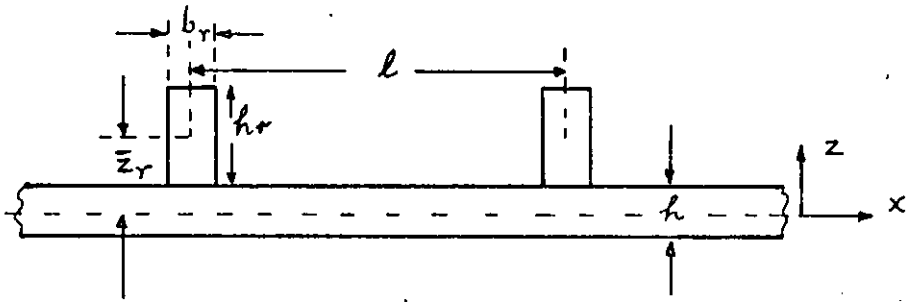

RING DETAIL.

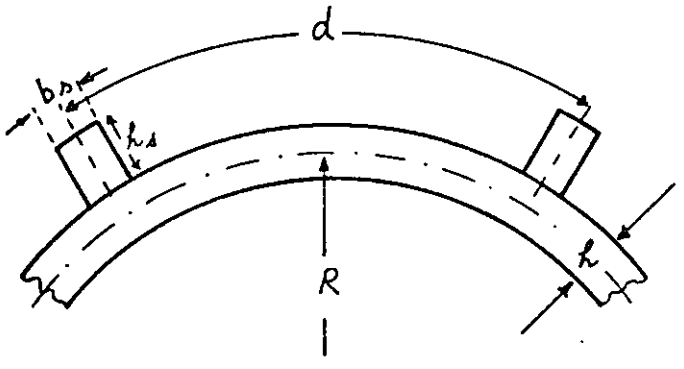

STRINGER DETAIL.

FIG. 1(c) STIFFENER NOTATION

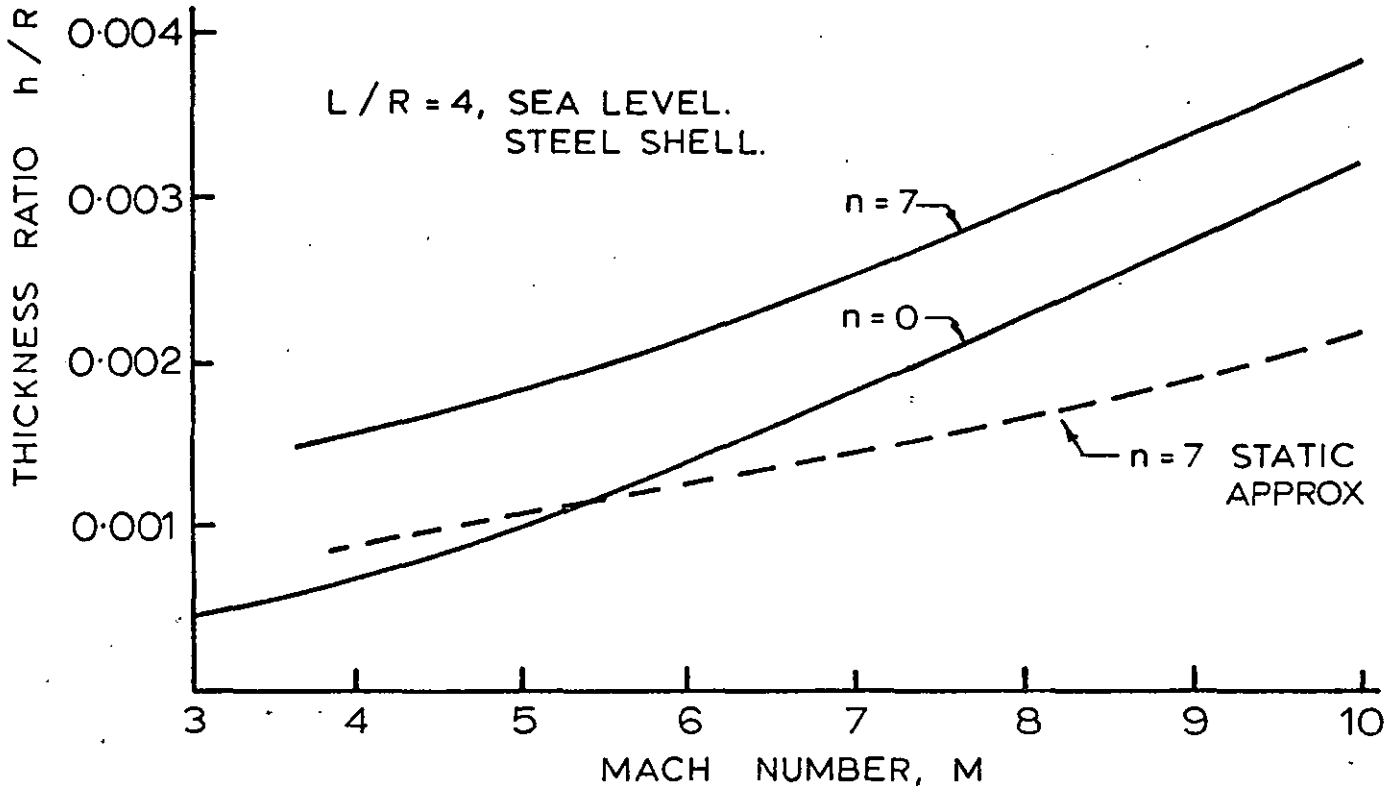

FIG. 2 COMPARISON OF THE FLUTTER BOUNDARY WITH THAT OF STATIC APPROXIMATION. (REF. 113)

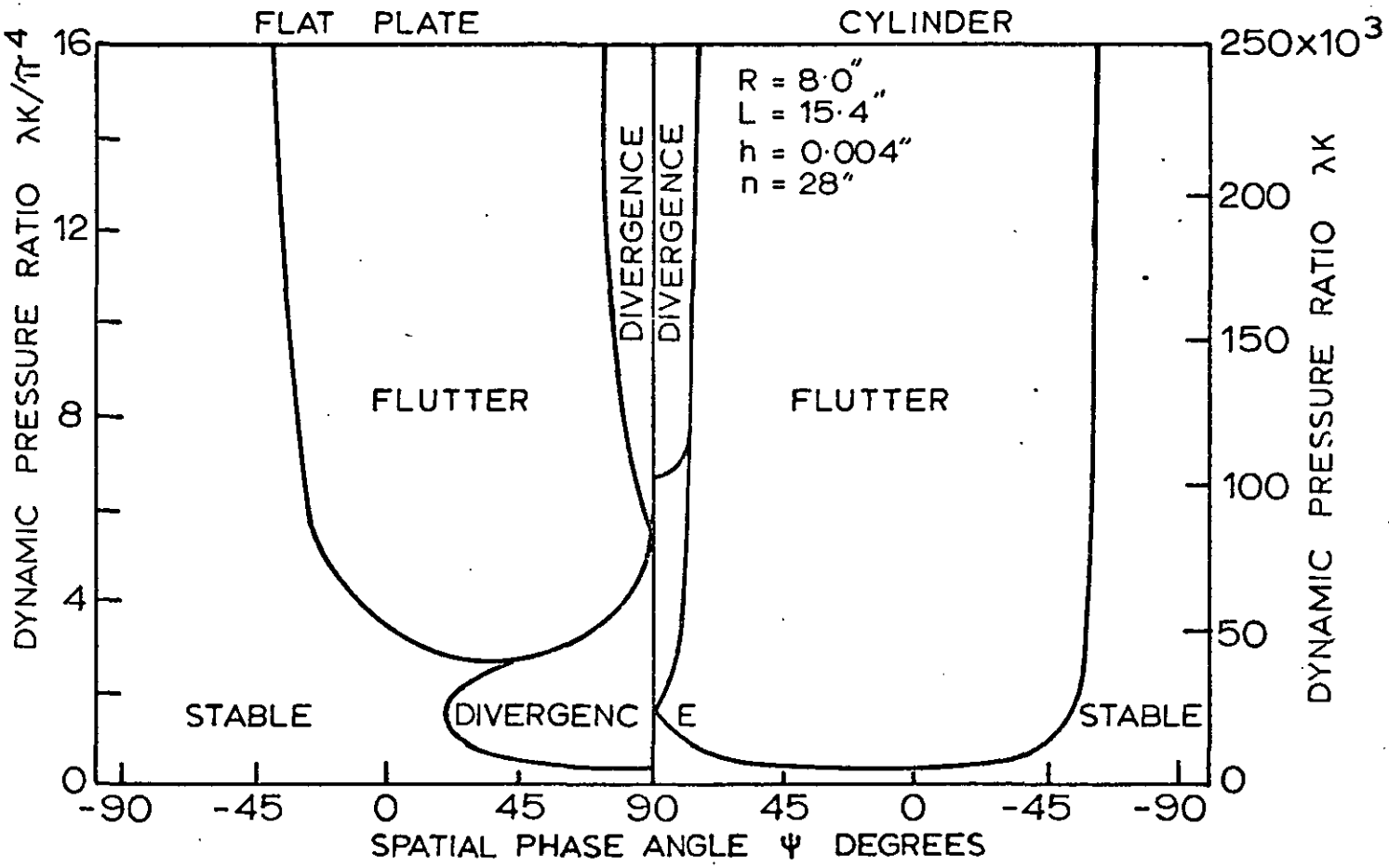

FIG. 3 STABILITY BOUNDARIES FOR A FLAT PLATE & A CYLINDRICAL SHELL (REF. 112). ($\lambda = \frac{\rho_0 U^2}{\beta E(1-\nu^2)} \left(\frac{R}{h}\right)^3$; K = the aerodynamic pressure constant in eqn (5) of Ref. 112).

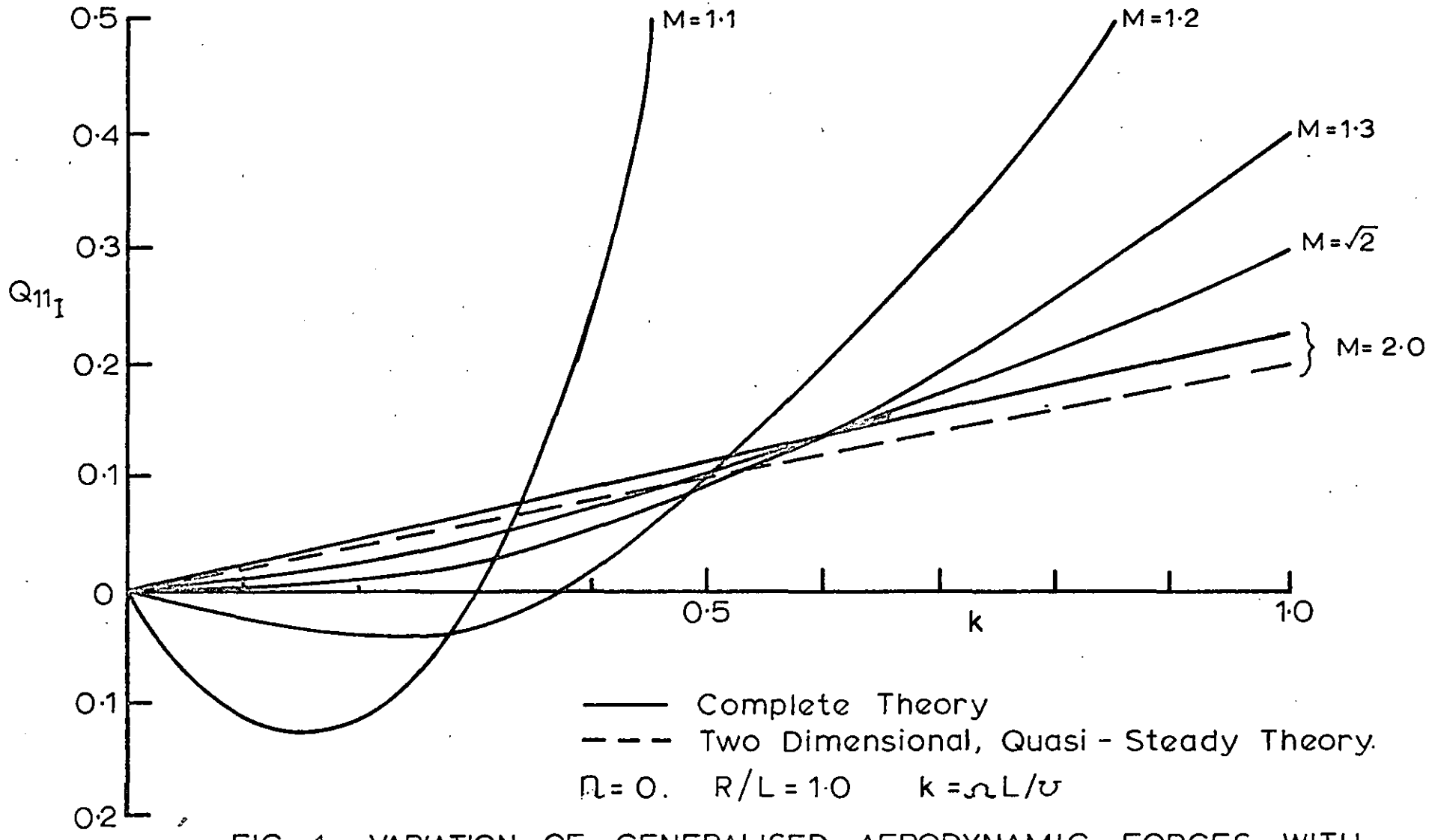

FIG. 4. VARIATION OF GENERALISED AERODYNAMIC FORCES WITH THE REDUCED FREQUENCY. (REF. 98).

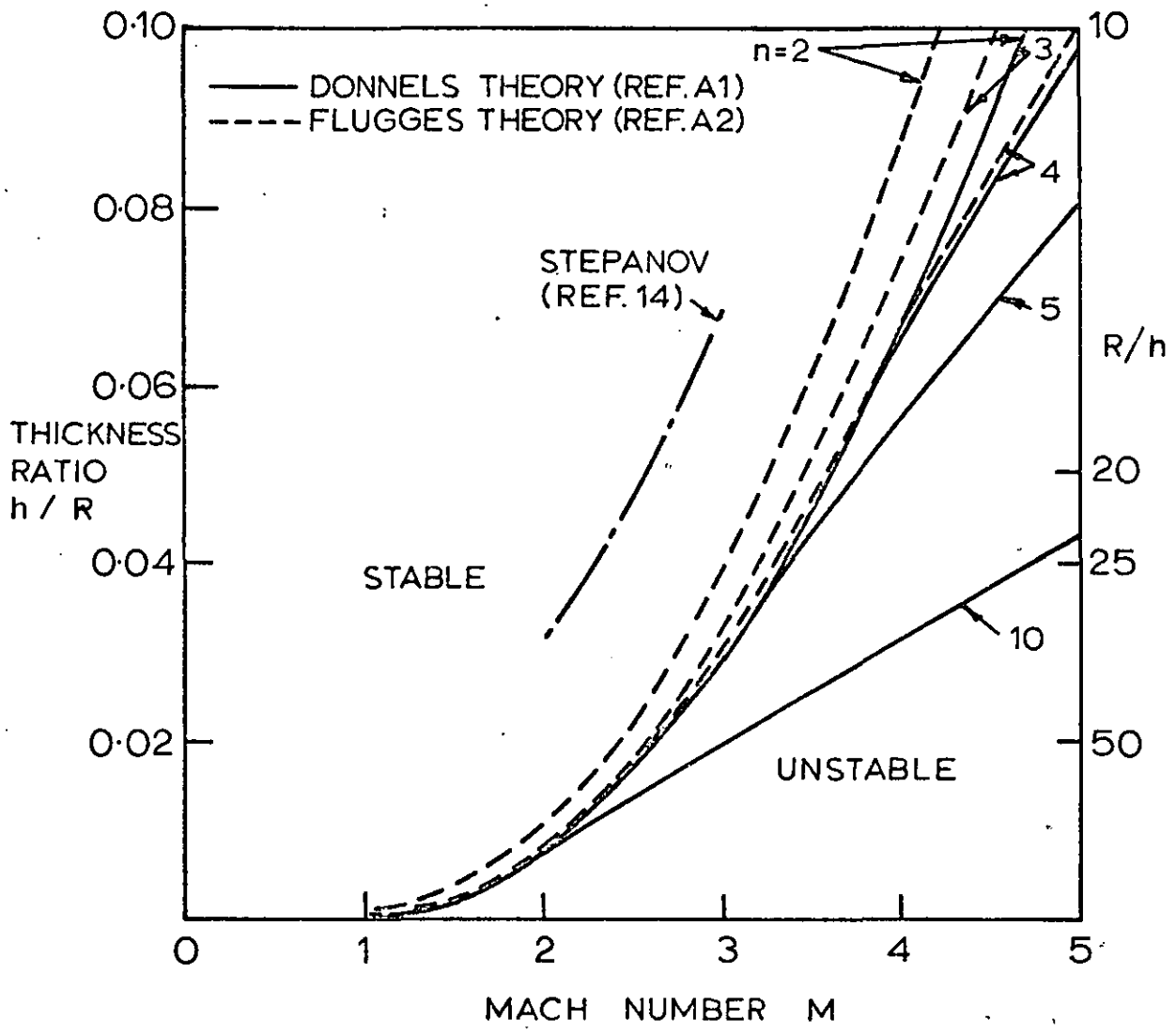

FIG. 5 FLUTTER BOUNDARIES FOR AN EMPTY, INFINITELY LONG, UNSTIFFENED ALUMINIUM CYLINDER AT SEA LEVEL WITH NO APPLIED MEMBRANE STRESSES (REF. 8)

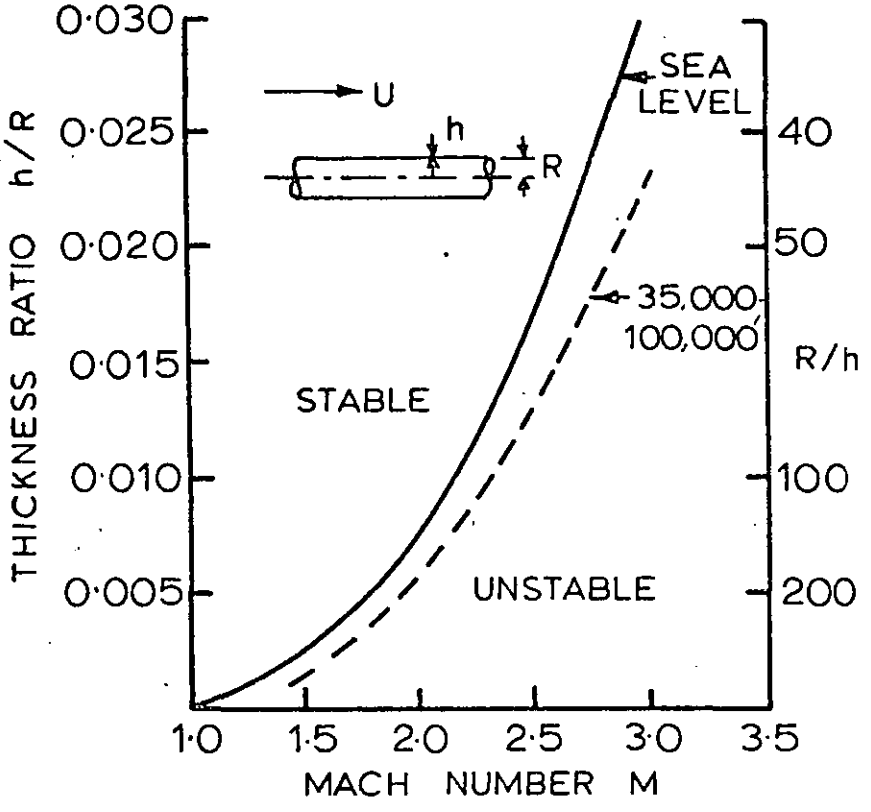

FIG. 6 FLUTTER BOUNDARIES FOR AN EMPTY INFINITELY LONG, UNSTIFFENED CYL-INDRICAL SHELL WITH NO APPLIED MEMBRANE STRESSES. (REF. 13)

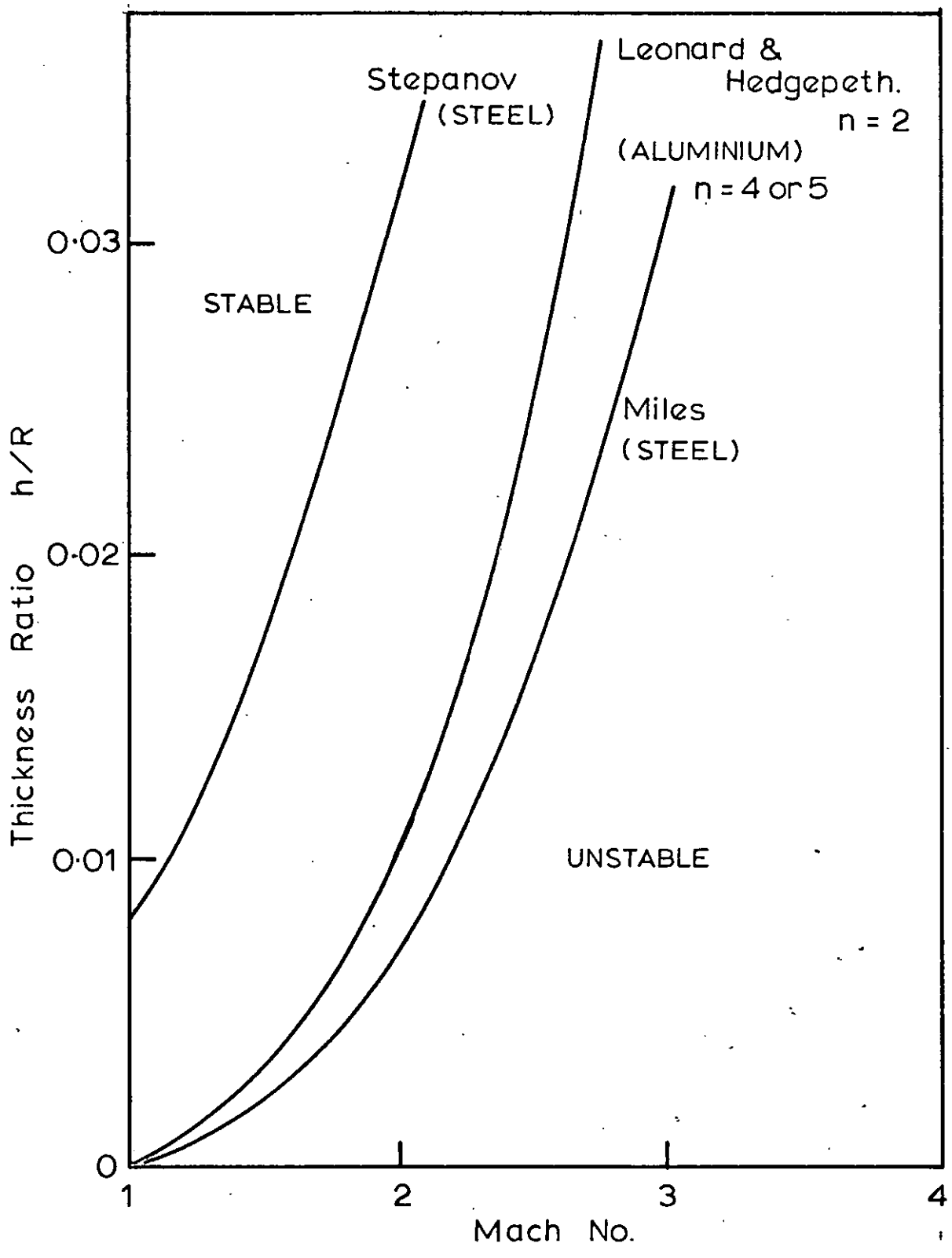

FIG. 7. FLUTTER BOUNDARIES FOR AN EMPTY INFINITELY LONG ISOTROPIC CYLINDRICAL SHELL. (REF. 40).

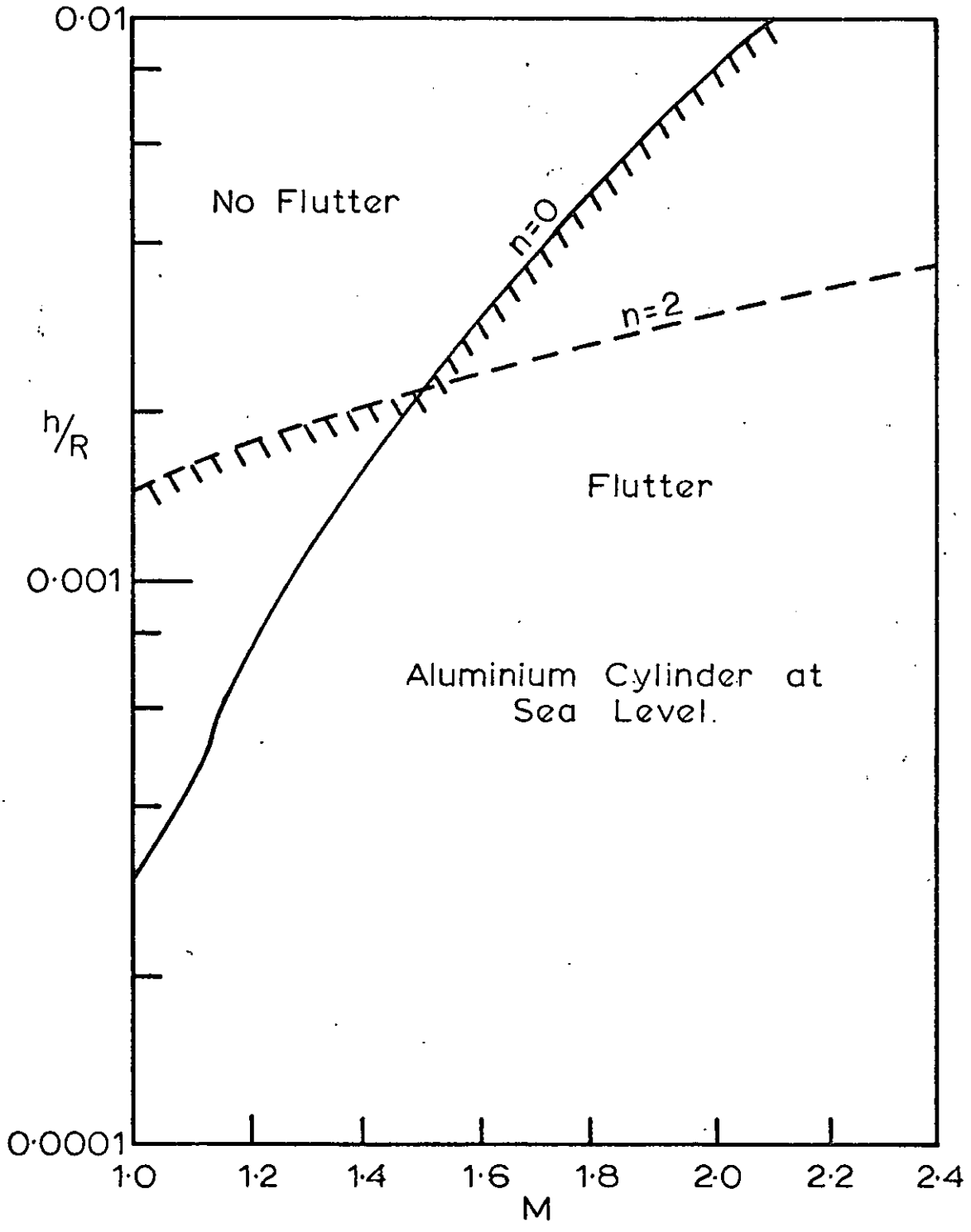

FIG. 8. COMPARISON OF FLUTTER BOUNDARIES FOR INFINITELY LONG CYLINDRICAL SHELL IN AN AXISYMMETRIC AND ASYMMETRIC MODE. (REF. 99).

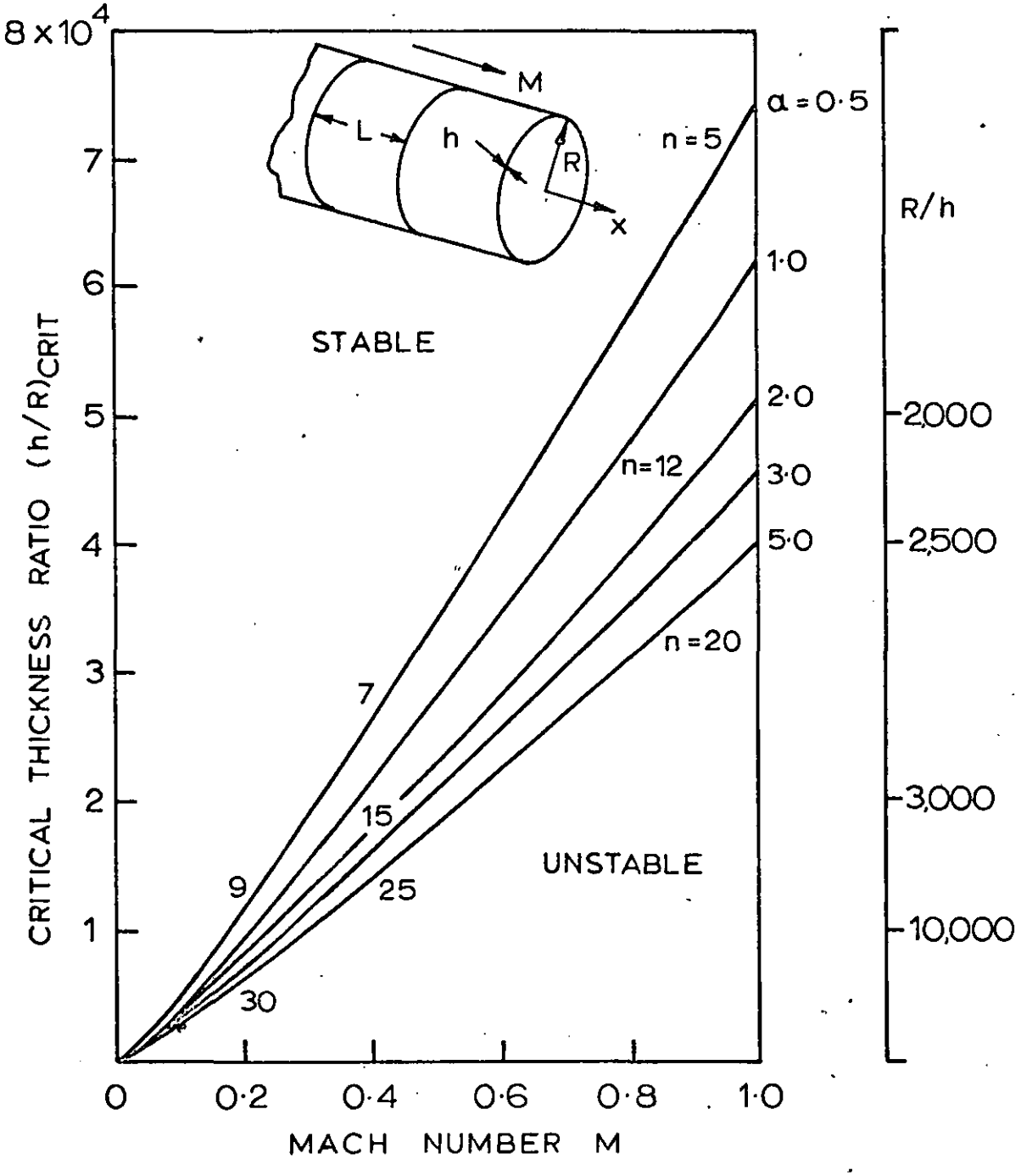

FIG. 9 CRITICAL DIVERGENCE BOUNDARIES FOR AN INFINITELY LONG, UNSTRESSED, RING-STIFFENED ALUMINIUM CYLINDER AT SEA LEVEL. ($\alpha = \pi R / L$) (REF. 8)

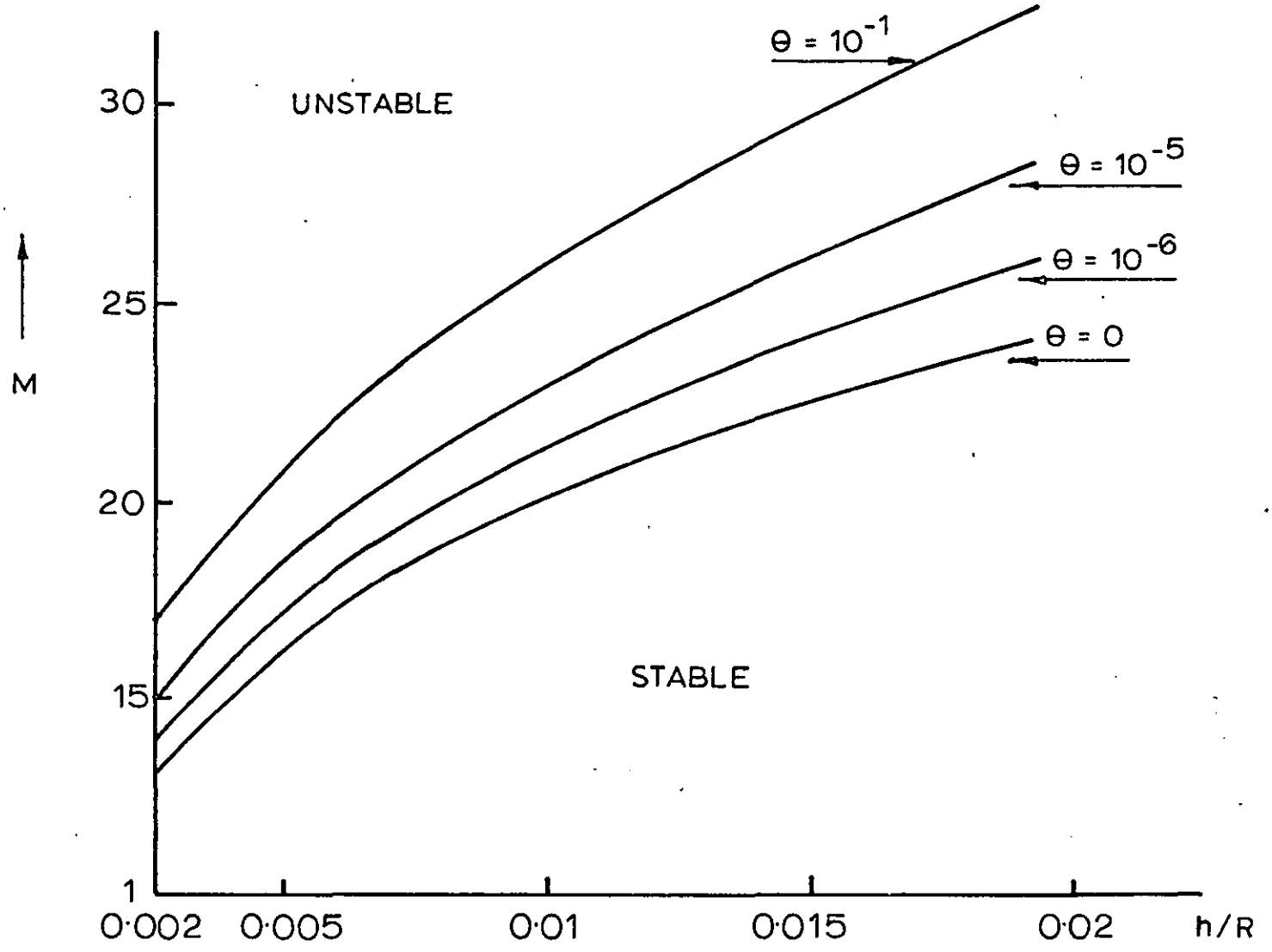

FIG. 10. INFLUENCE OF DAMPING ON THE FLUTTER BOUNDARY OF AN INFINITELY LONG STEEL SHELL. (REF. 36).

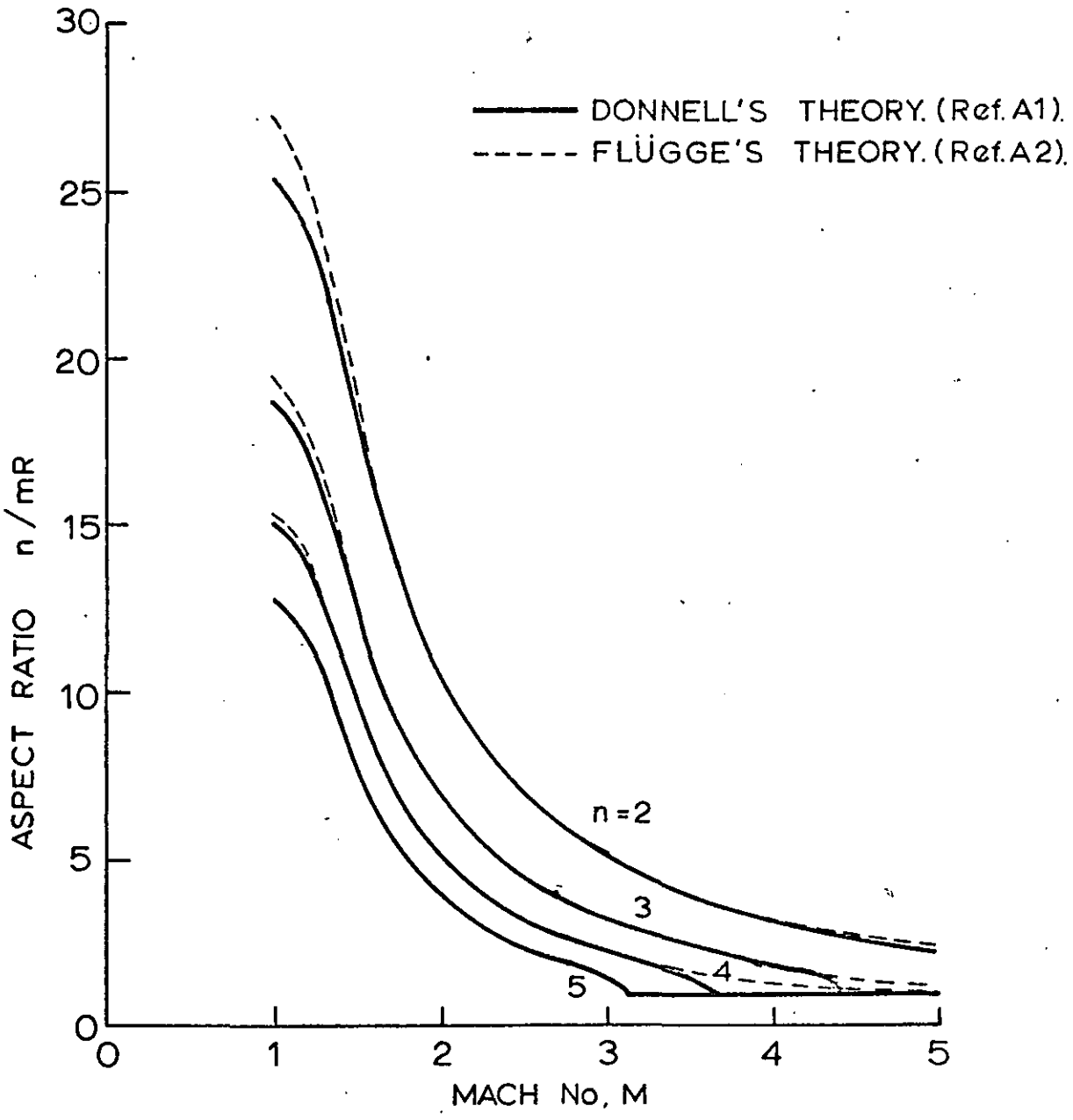

FIG. 11. PANEL ASPECT RATIO OF THE CRITICAL FLUTTER MODE FOR AN EMPTY, INFINITELY LONG UNSTIFFENED ALUMINIUM CYLINDER AT SEA LEVEL WITH NO APPLIED MEMBRANE STRESSES. (REF. 8)

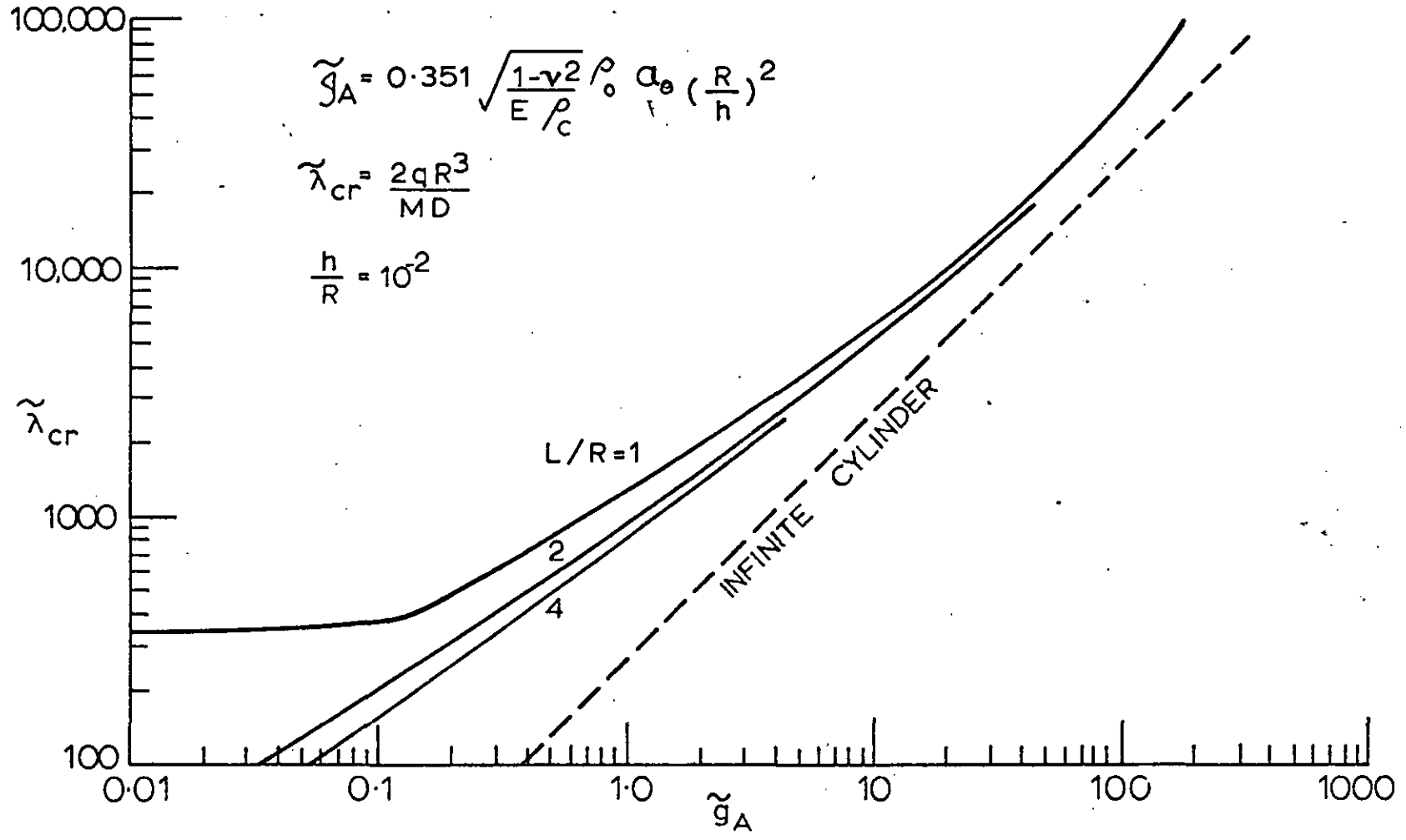

FIG. 12 FLUTTER DYNAMIC PRESSURE VERSUS AERODYNAMIC DAMPING FOR CYLINDRICAL SHELLS IN AXISYMMETRIC MODES. (REF. 85).

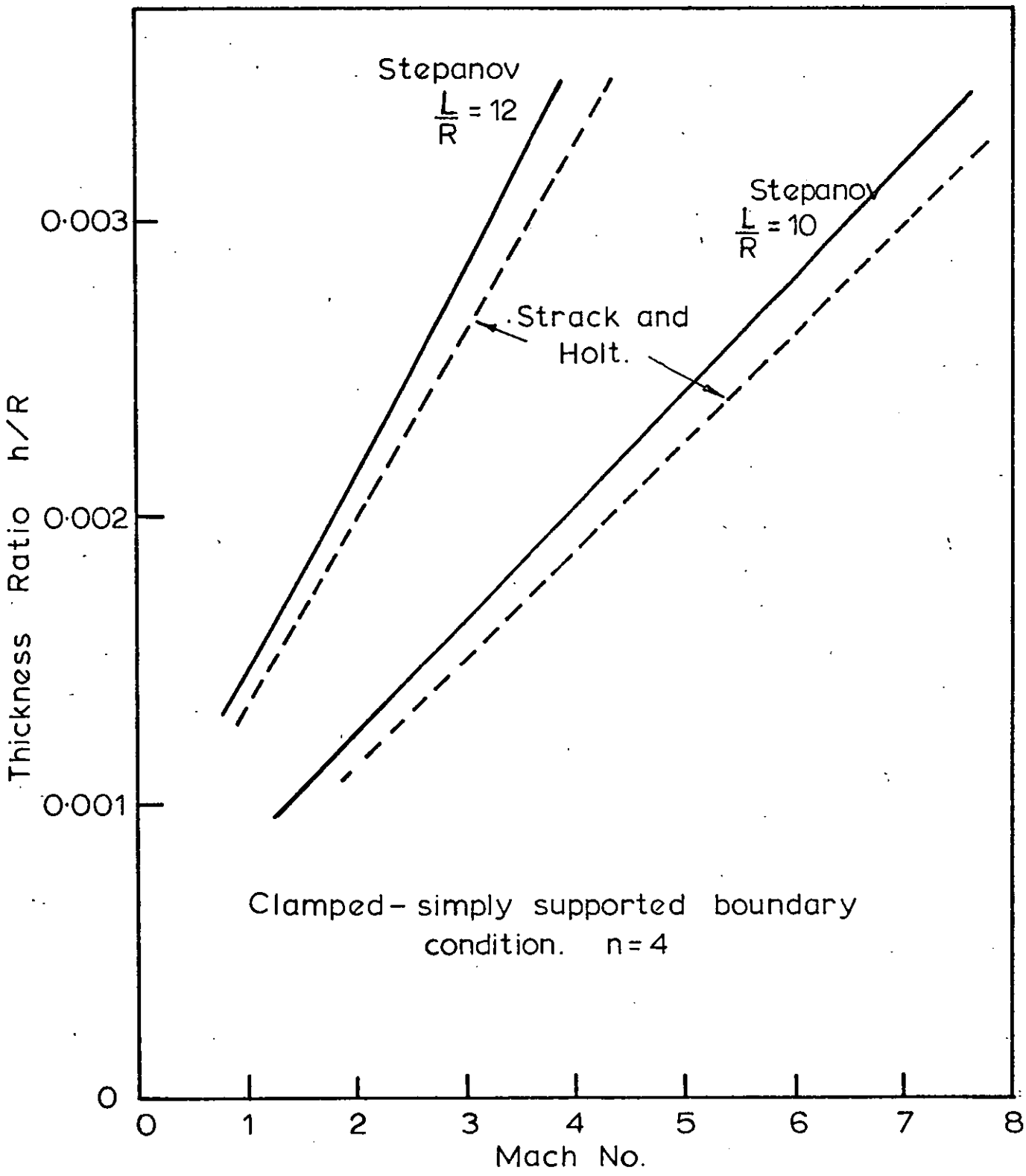

FIG. 13. FLUTTER BOUNDARIES FOR AN EMPTY ISOTROPIC CYLINDRICAL SHELL. (REF. 40).

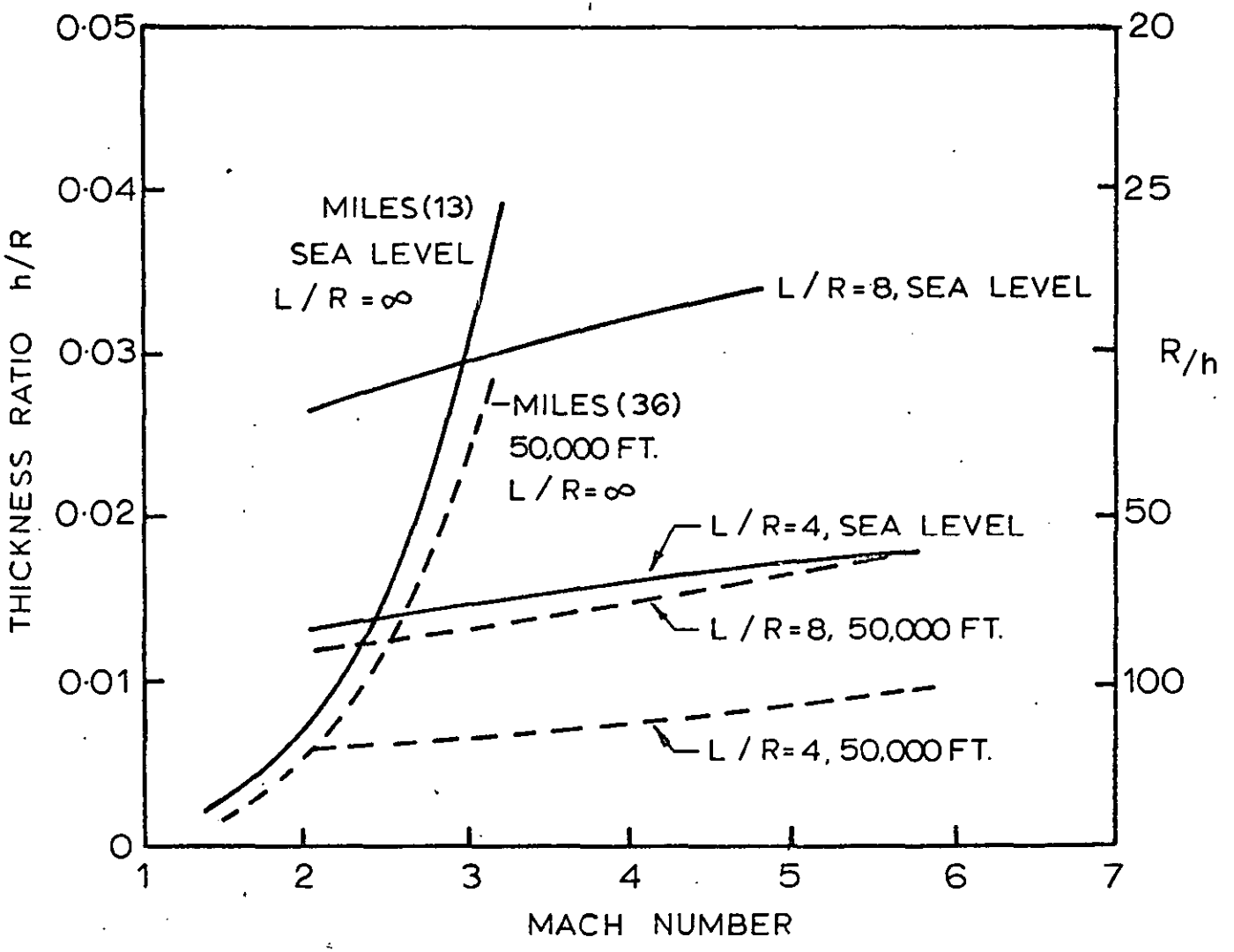

FIG. 14 FLUTTER BOUNDARIES FOR AN EMPTY STEEL CYLINDER IN THE AXISYMMETRIC MODE. (REF. 40)

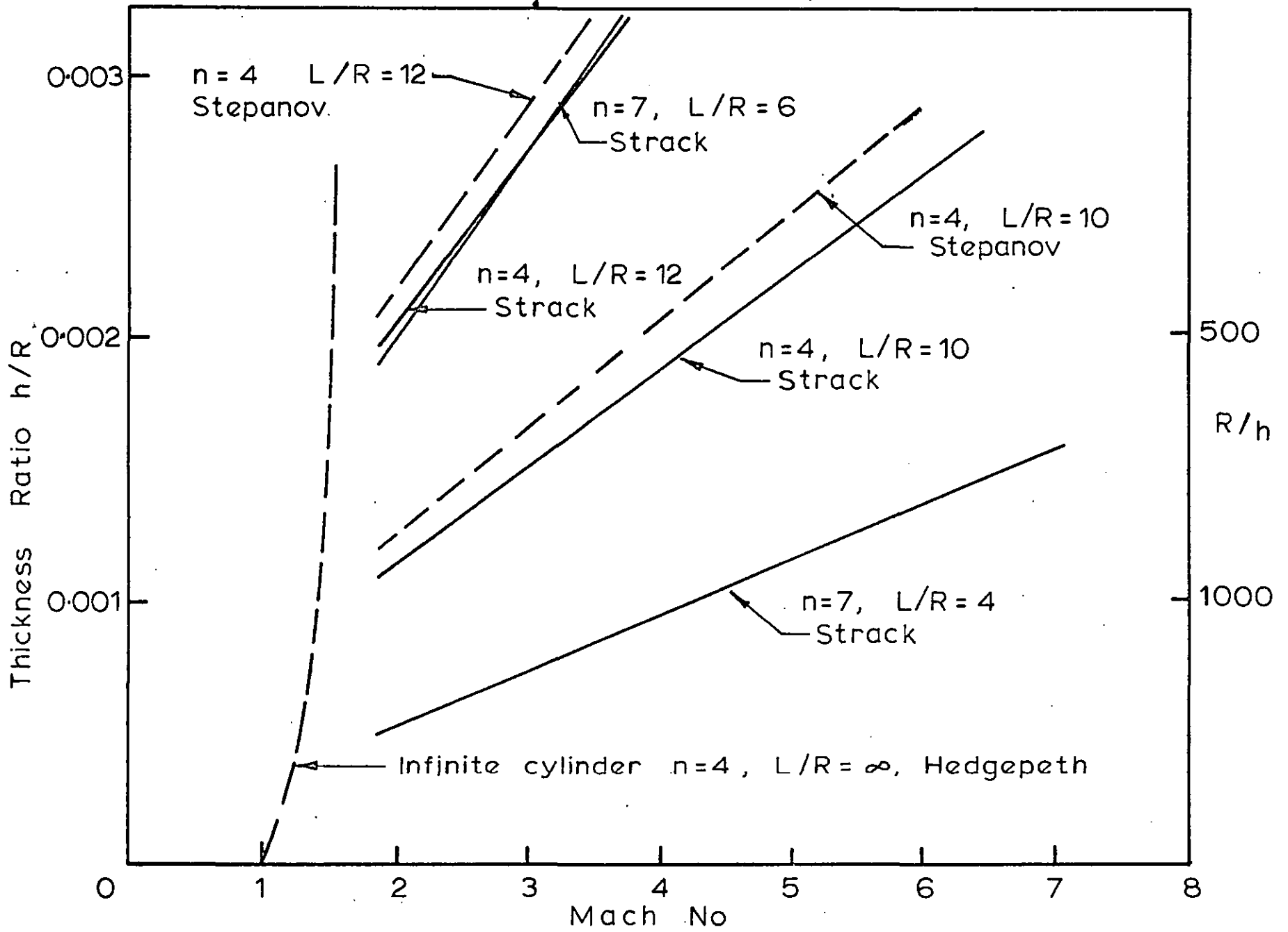

FIG. 15. COMPARISON OF FLUTTER BOUNDARIES OF AN EMPTY STEEL CYLINDER. (REF. 30).

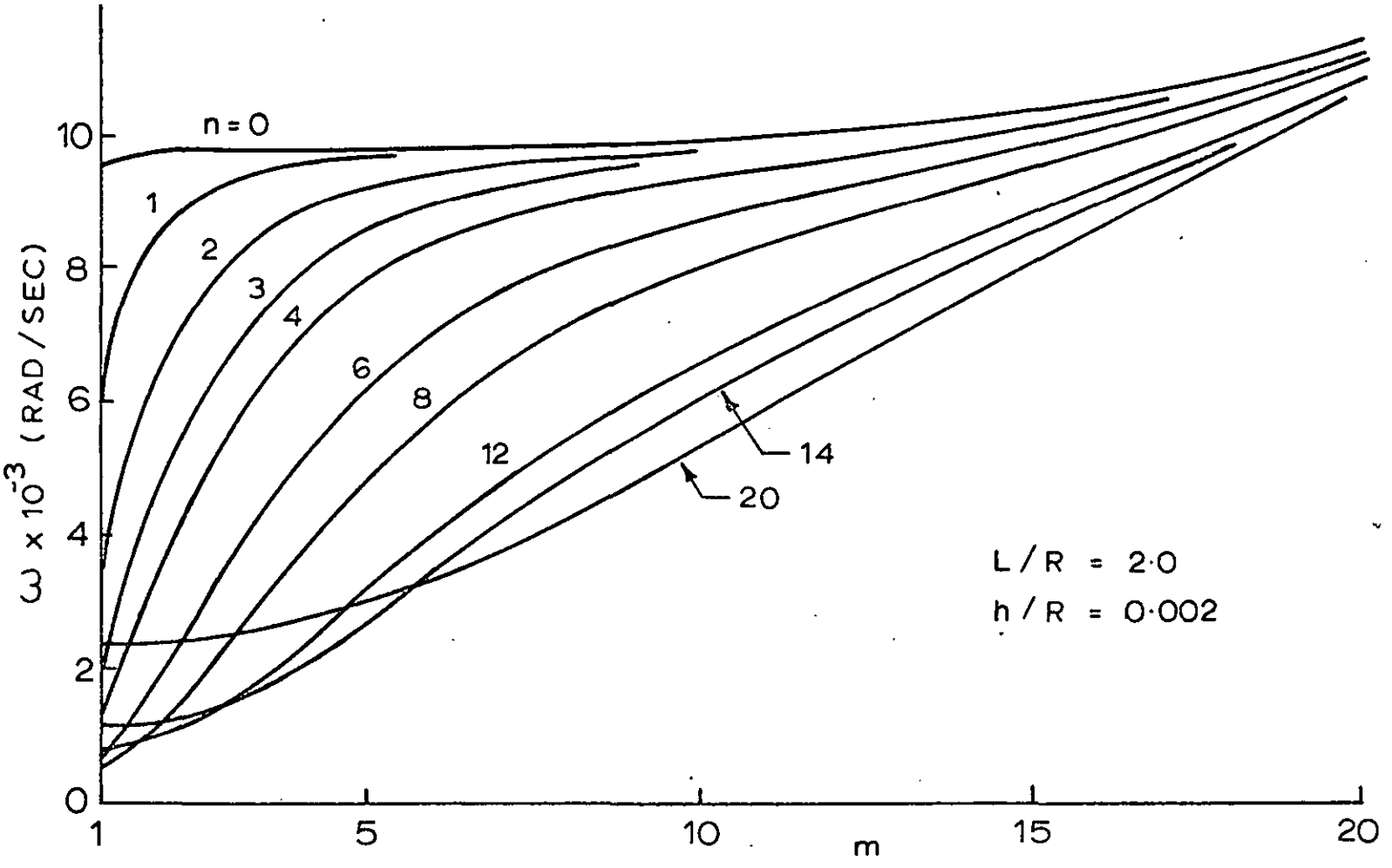

FIG. 16 FREQUENCY VERSUS LONGITUDINAL MODE NUMBER FOR AN ALUMINIUM CYLINDRICAL SHELL. (REF. 35)

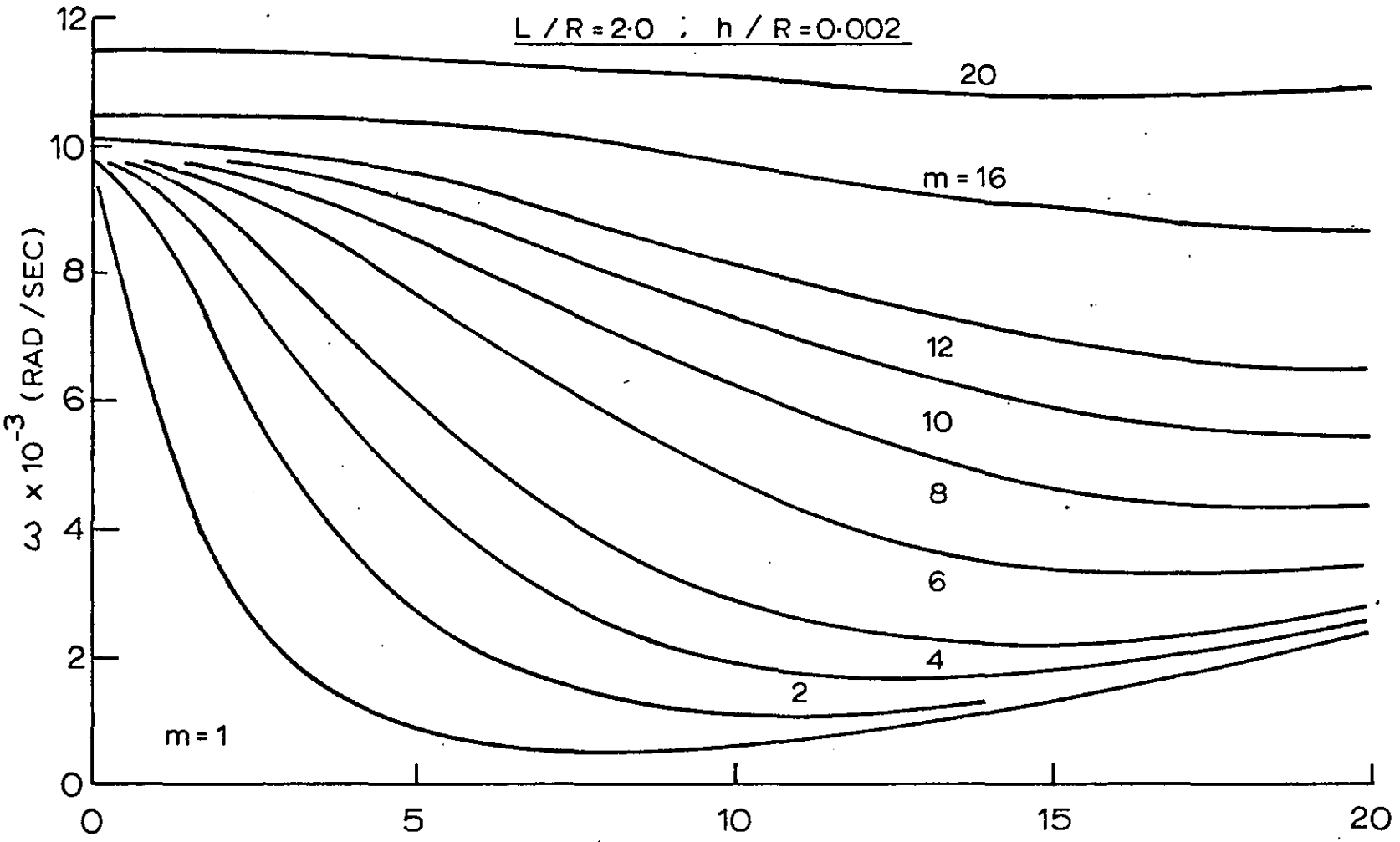

FIG. 17 FREQUENCY VERSUS CIRCUMFERENTIAL MODE NUMBER FOR AN ALUMINIUM CYLINDRICAL SHELL. (REF. 35)

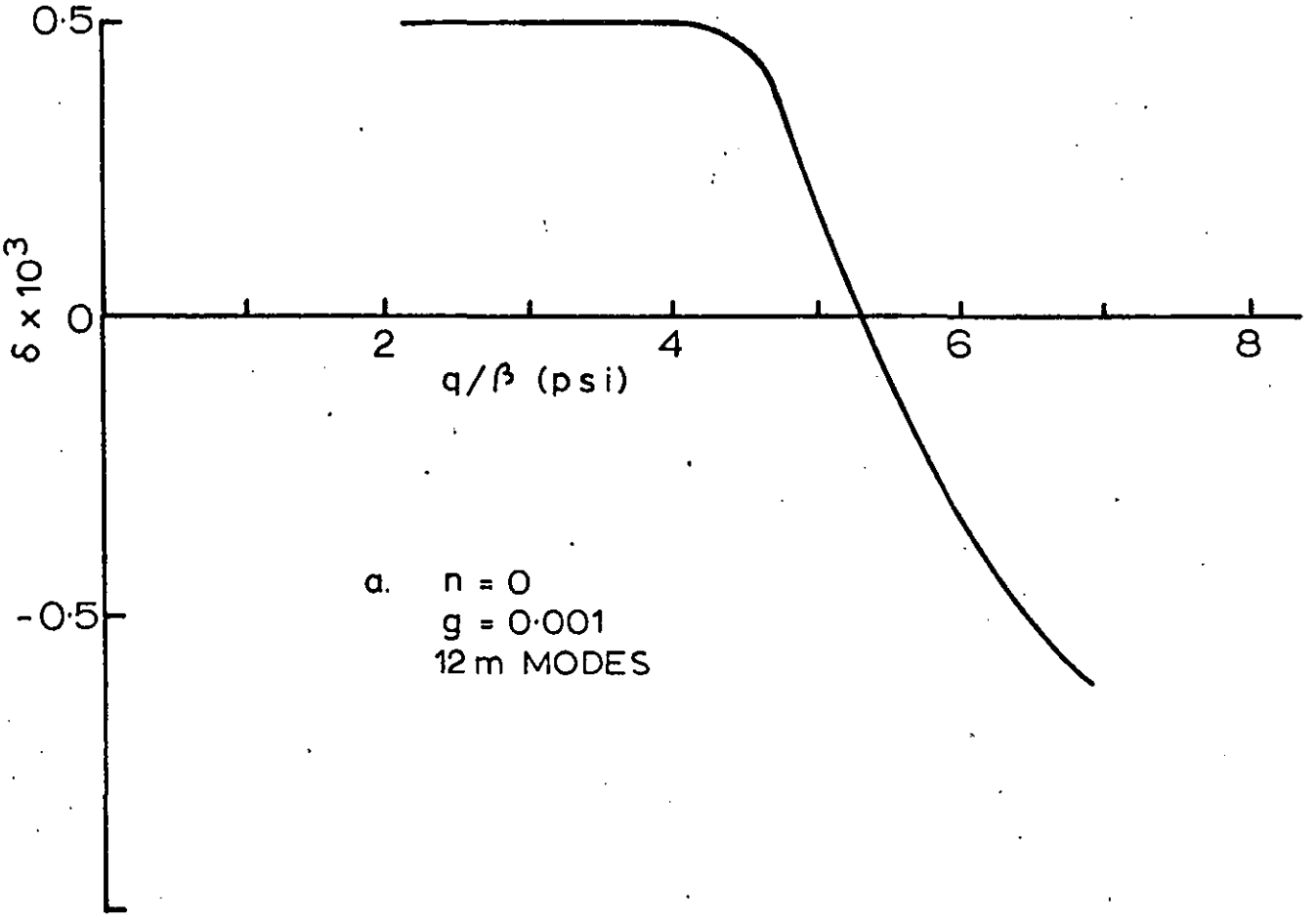

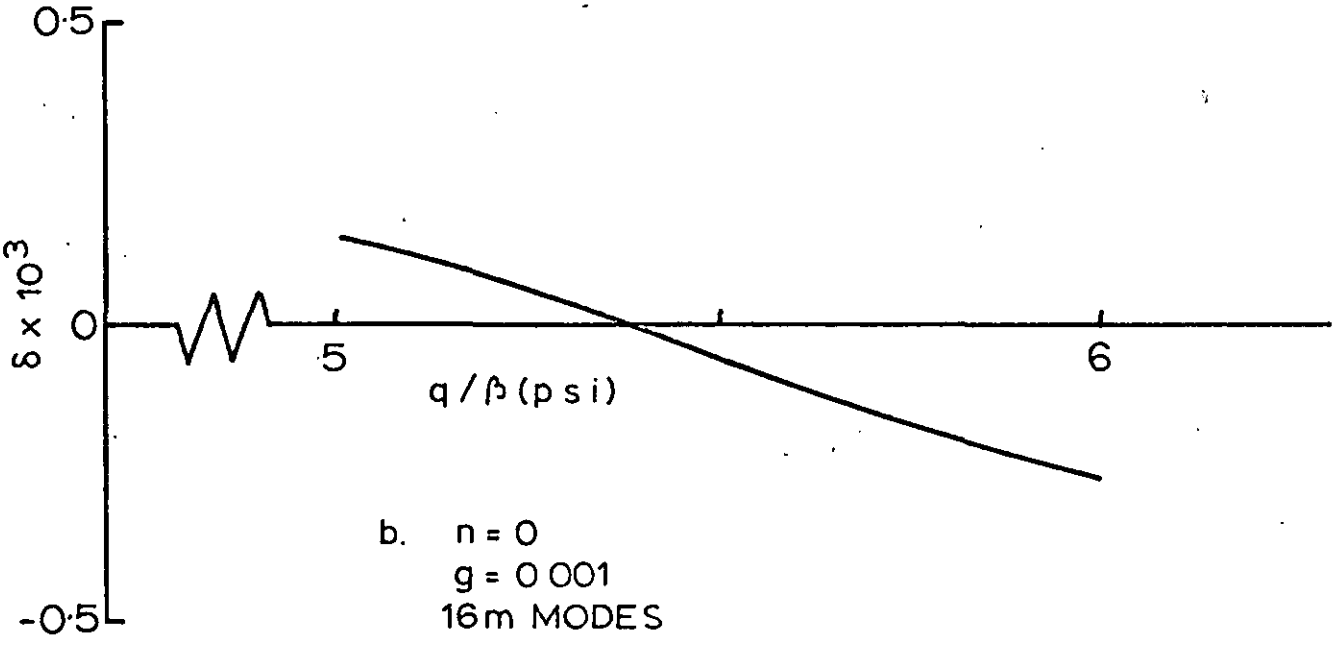

FIG. 18 DAMPING RATIO VERSUS REDUCED DYNAMIC PRESSURE FOR LOW 'n' CASE FOR AN ALUMINIUM CYLINDRICAL SHELL. (REF. 35)

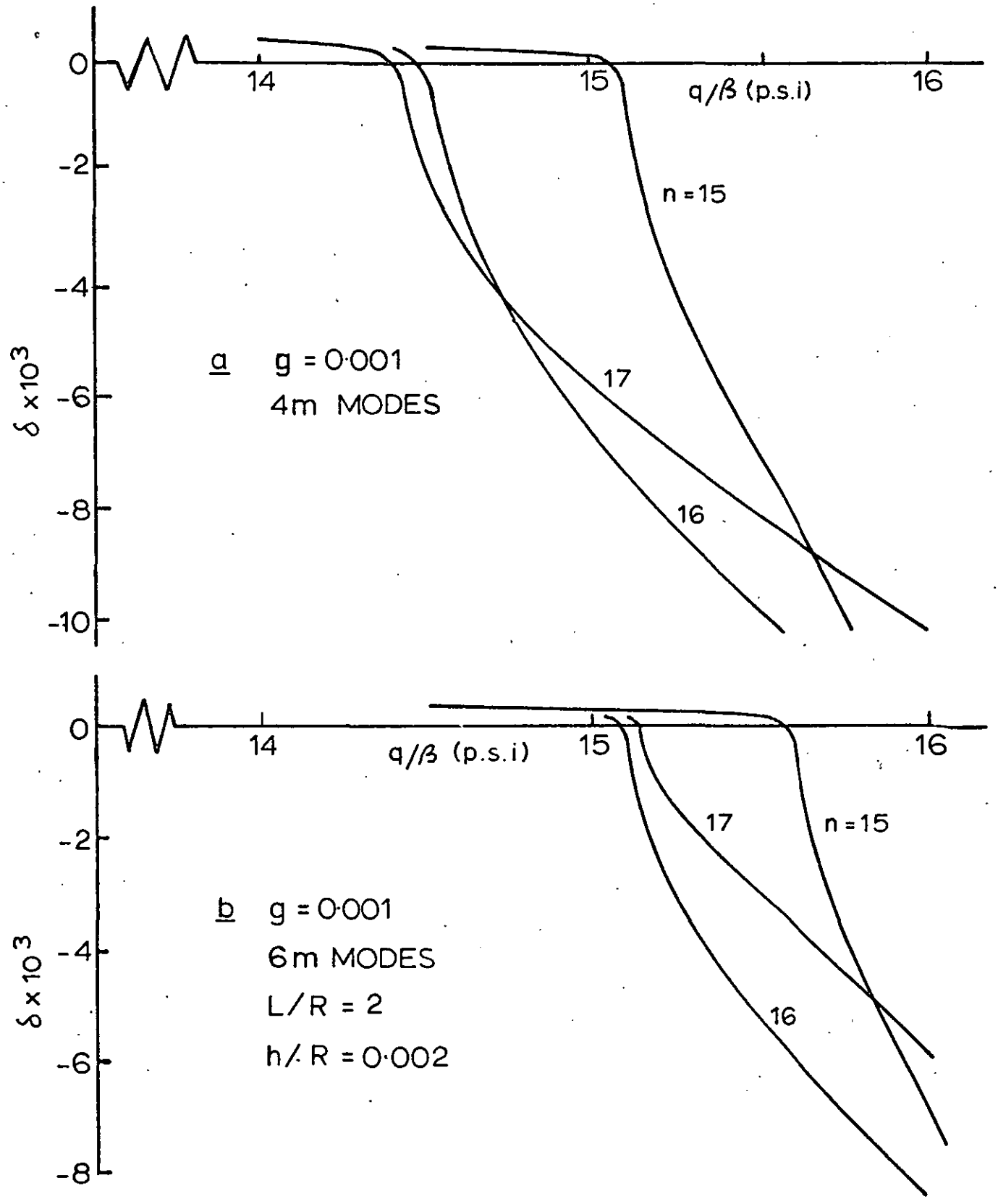

FIG. 19. DAMPING RATIO VERSUS REDUCED DYNAMIC PRESSURE FOR HIGH-n, FOR AN ALUMINIUM CYLINDRICAL SHELL. (REF. 35)

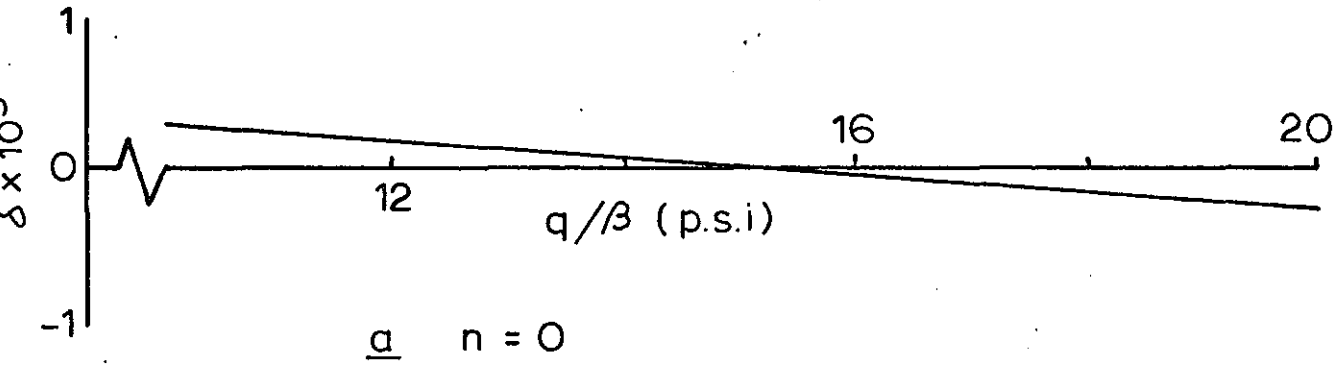

a n = 0
g = 0·01
16 m MODES

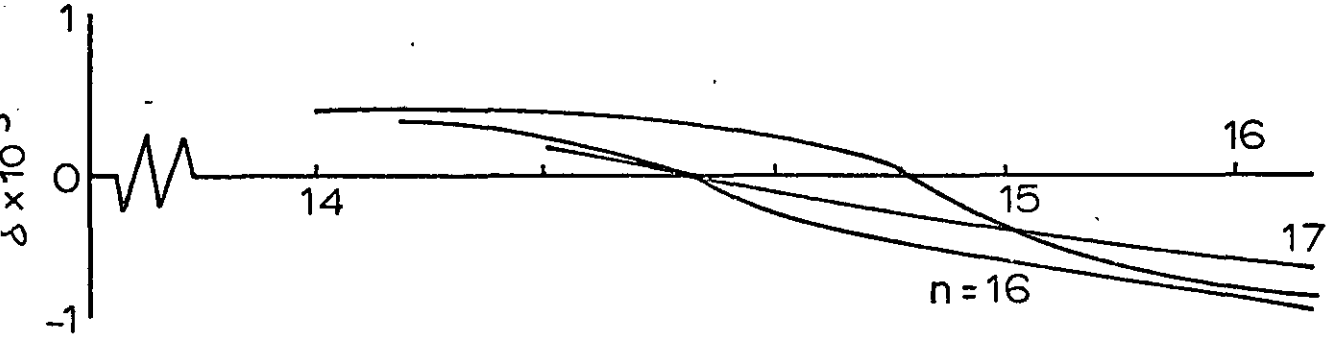

b g = 0·01, L/R = 2
4 m MODES, h/R = 0·002

FIG. 20. DAMPING RATIO VERSUS REDUCED DYNAMIC PRESSURE FOR MODERATE STRUCTURAL DAMPING FOR AN ALUMINIUM CYLINDRICAL SHELL. (REF. 35).

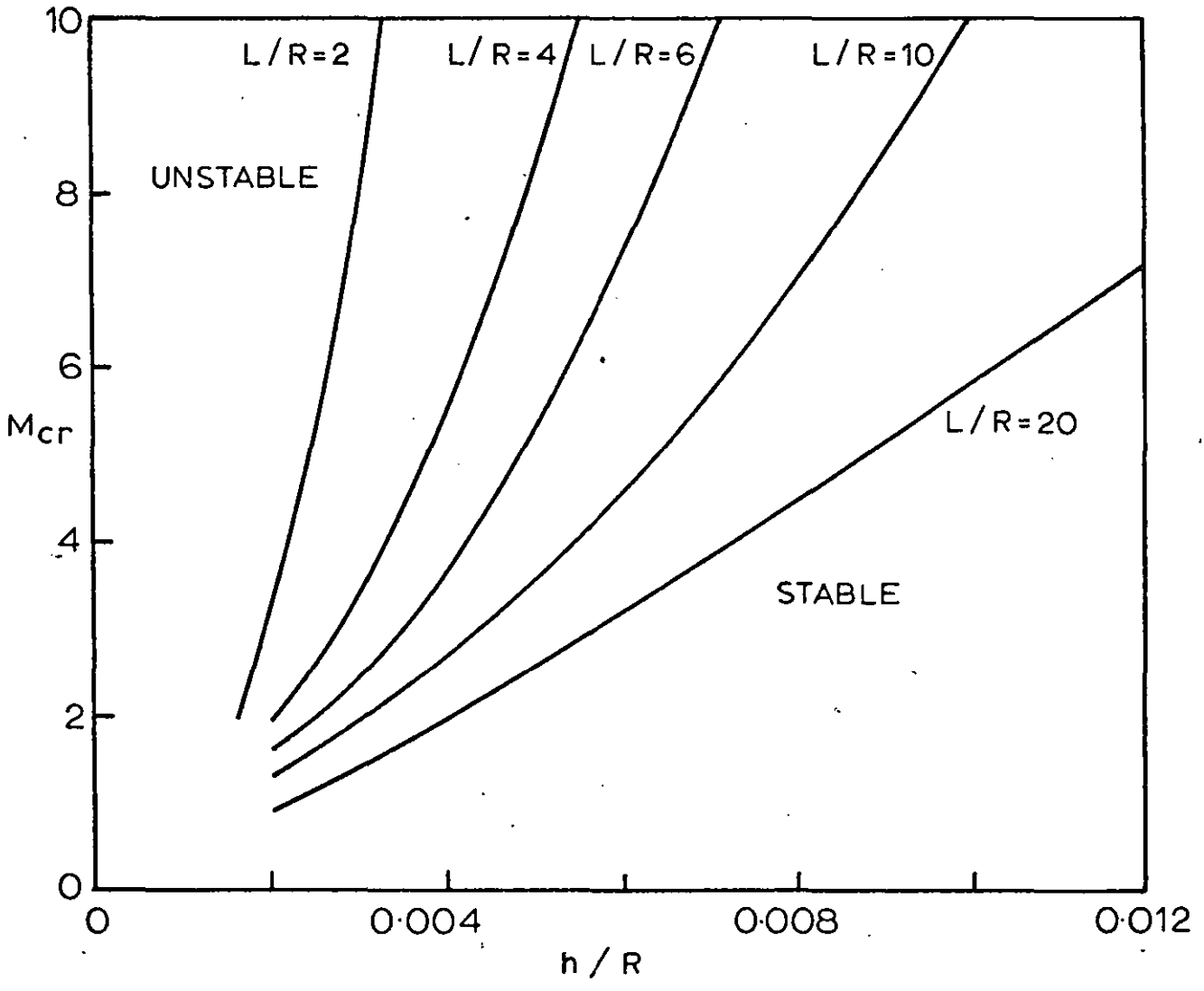

FIG. 21 FLUTTER BOUNDARY FOR STEEL SHELLS AT SEA LEVEL. (REF. 71).

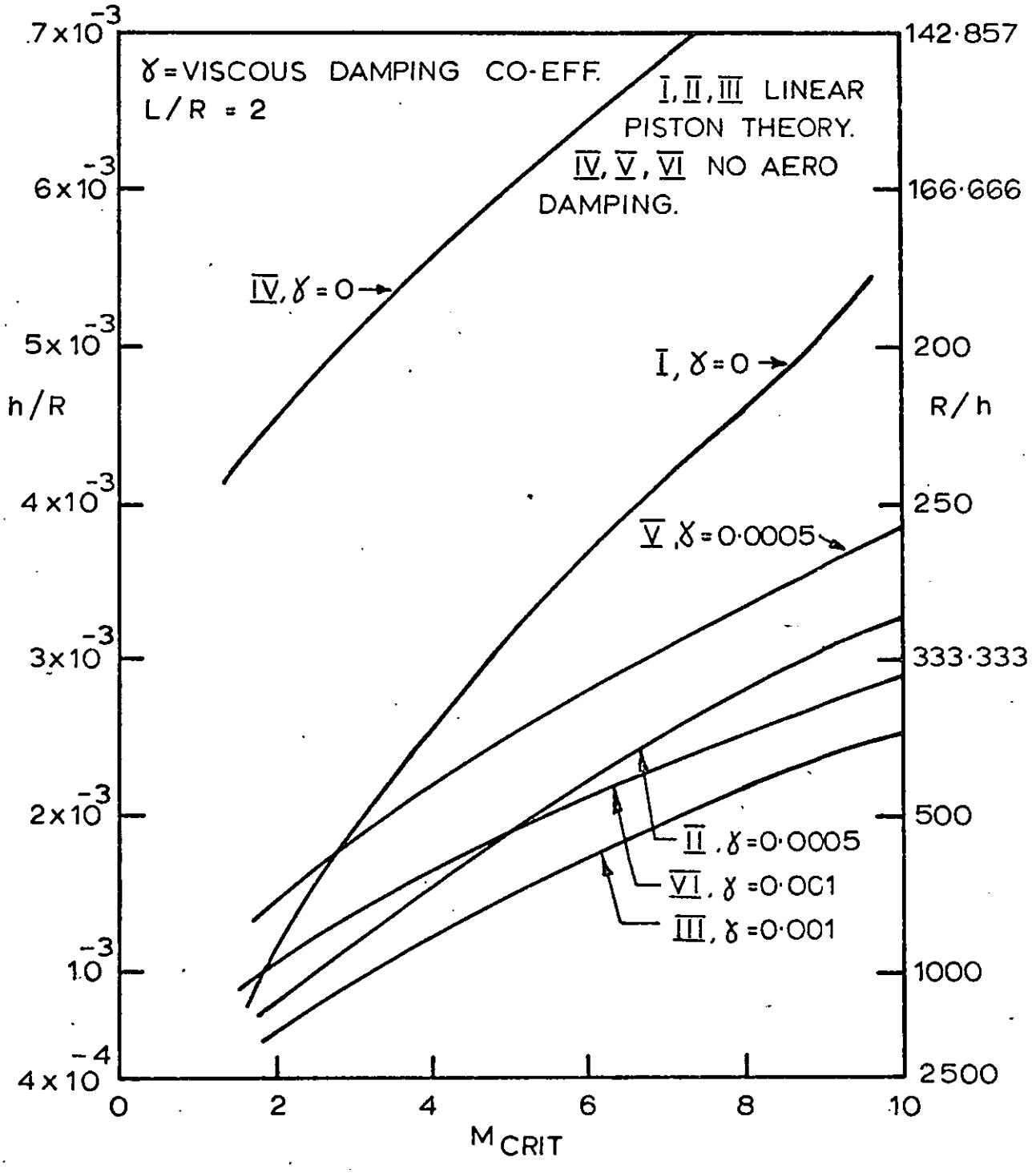

FIG. 22 FLUTTER BOUNDARIES FOR A SIMPLY SUPPORTED UNPRESSURISED, COPPER CYLINDRICAL SHELL AT 50,000 FT. ALTITUDE FOR VARIOUS DAMPING CO-EFFICIENTS. (REF. 42)

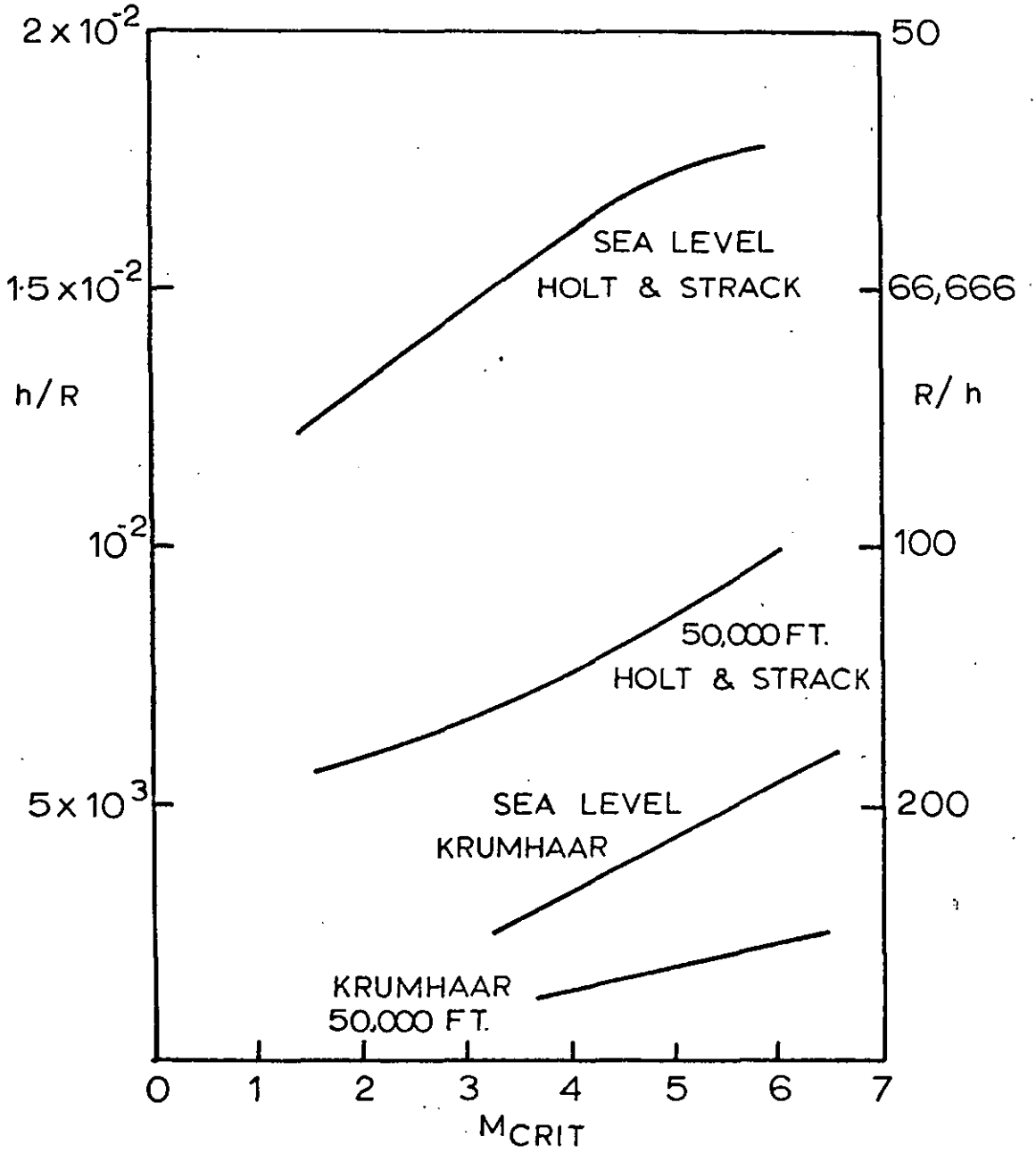

FIG. 23 COMPARISON OF THE FLUTTER BOUNDARIES FOR SIMPLY SUPPORTED UNPRESSURISED STEEL CYLINDERS WITH L/R=4 (REF. 42)

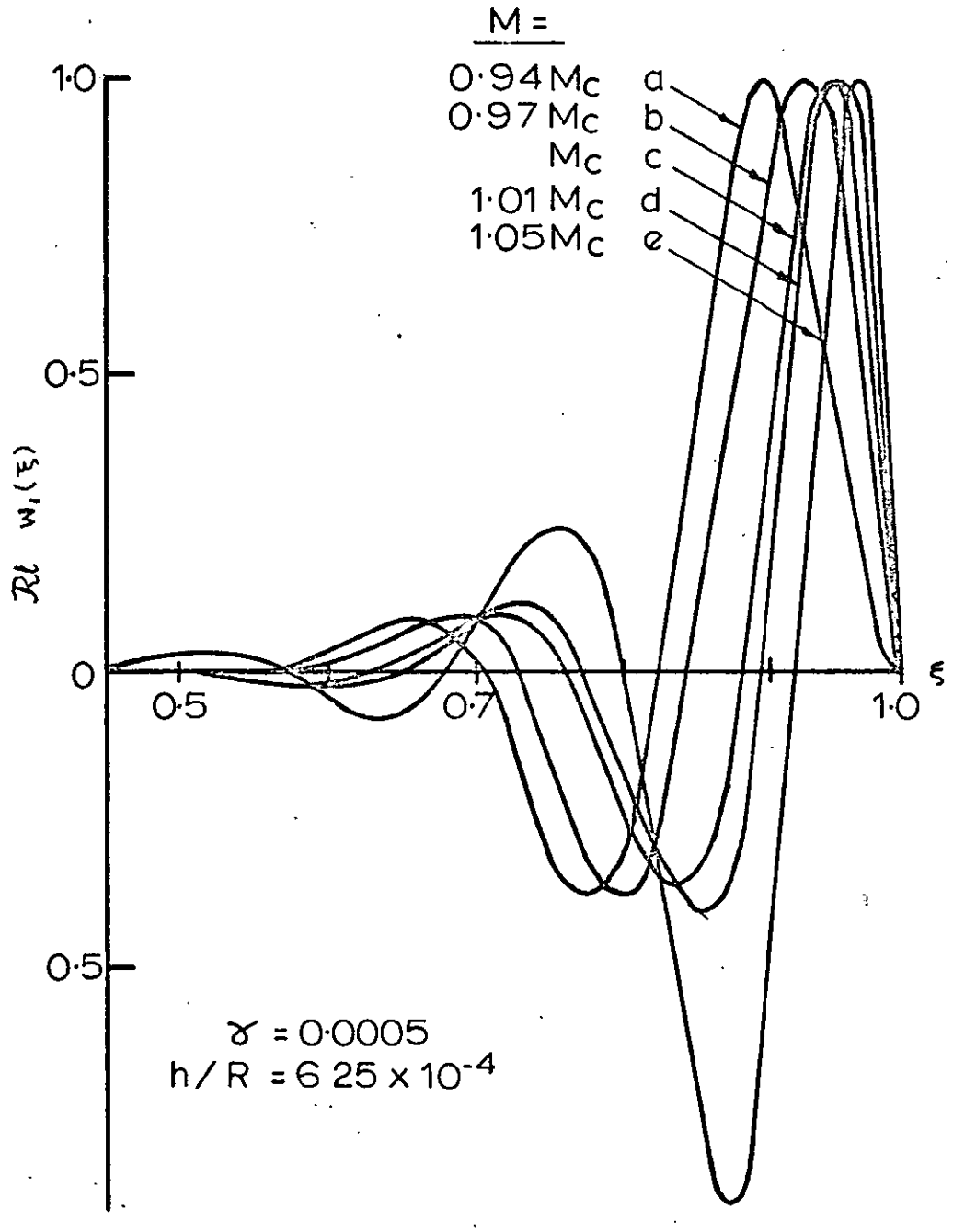

FIG. 24. REAL PARTS OF THE MODE SHAPES FOR DIFFERENT MACH NUMBERS. (REF. 135)

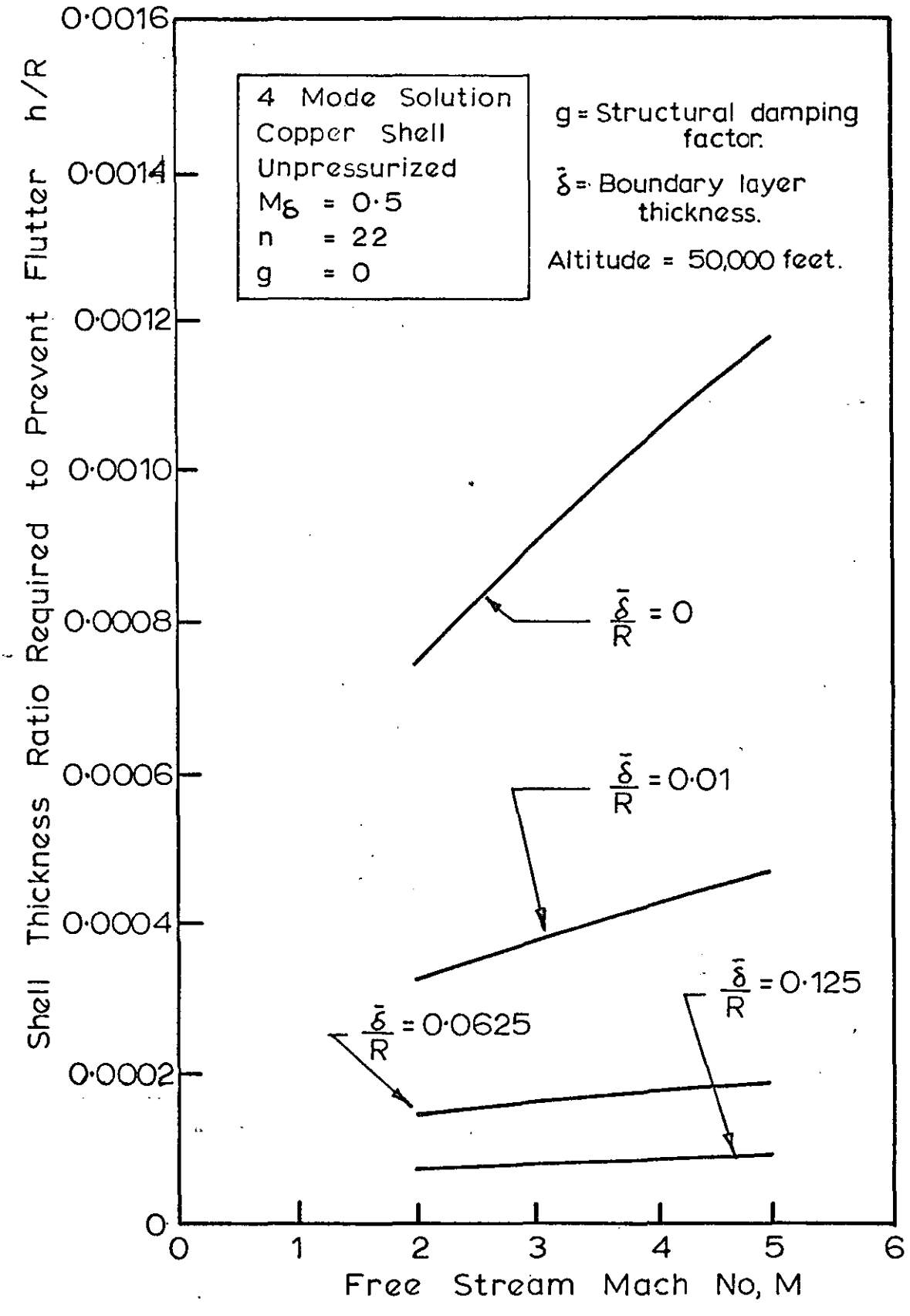

FIG. 25. INFLUENCE OF BOUNDARY LAYER THICKNESS ON THE FLUTTER BOUNDARY. (REF. 65).

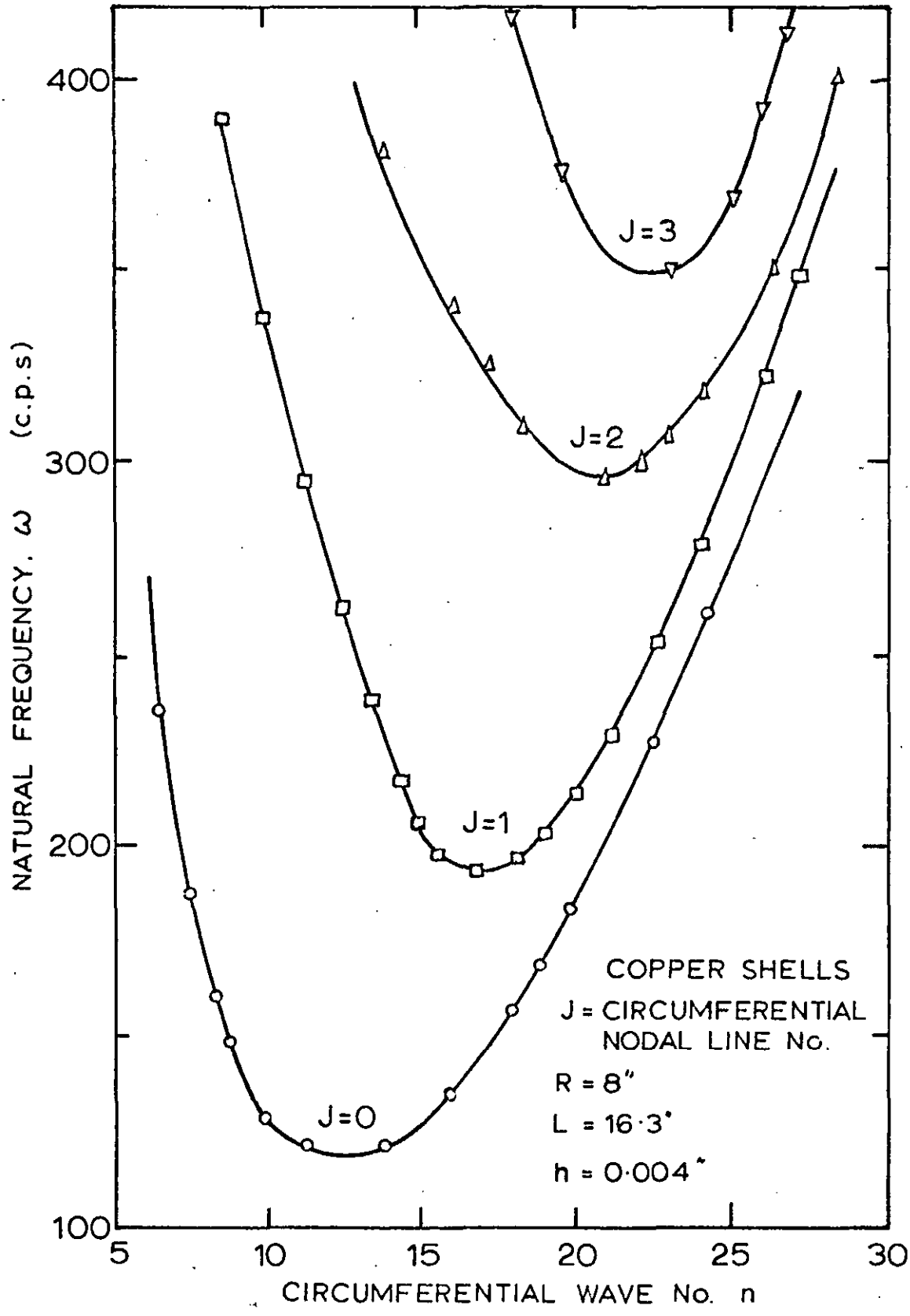

FIG. 26. FREQUENCY SPECTRUM FOR AN UNSTRESSED CIRCULAR CYLINDRICAL SHELL. (REF. 86).

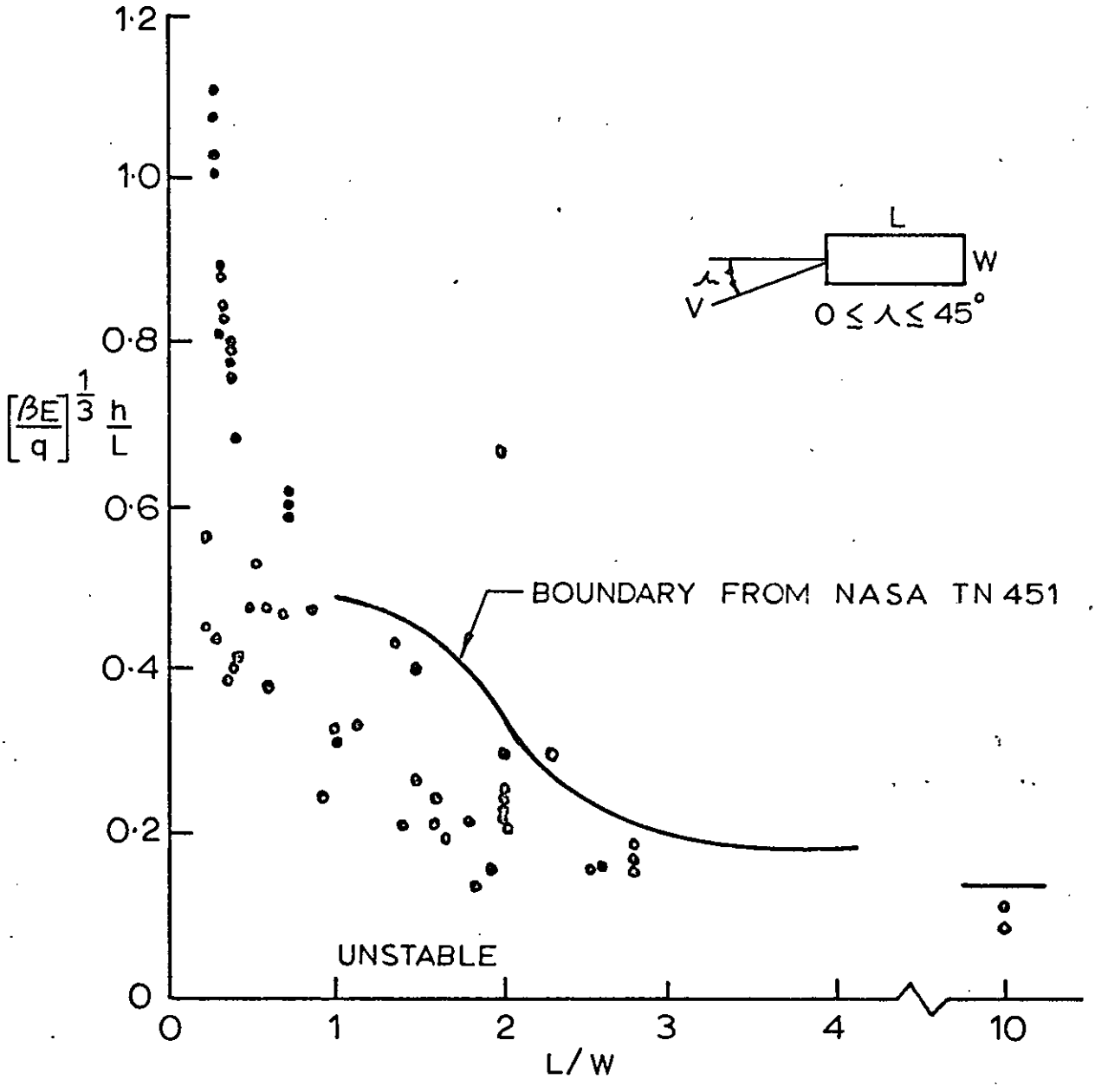

FIG. 27. PANEL FLUTTER PARAMETER VERSUS LENGTH/WIDTH RATIO. (REF. 51).

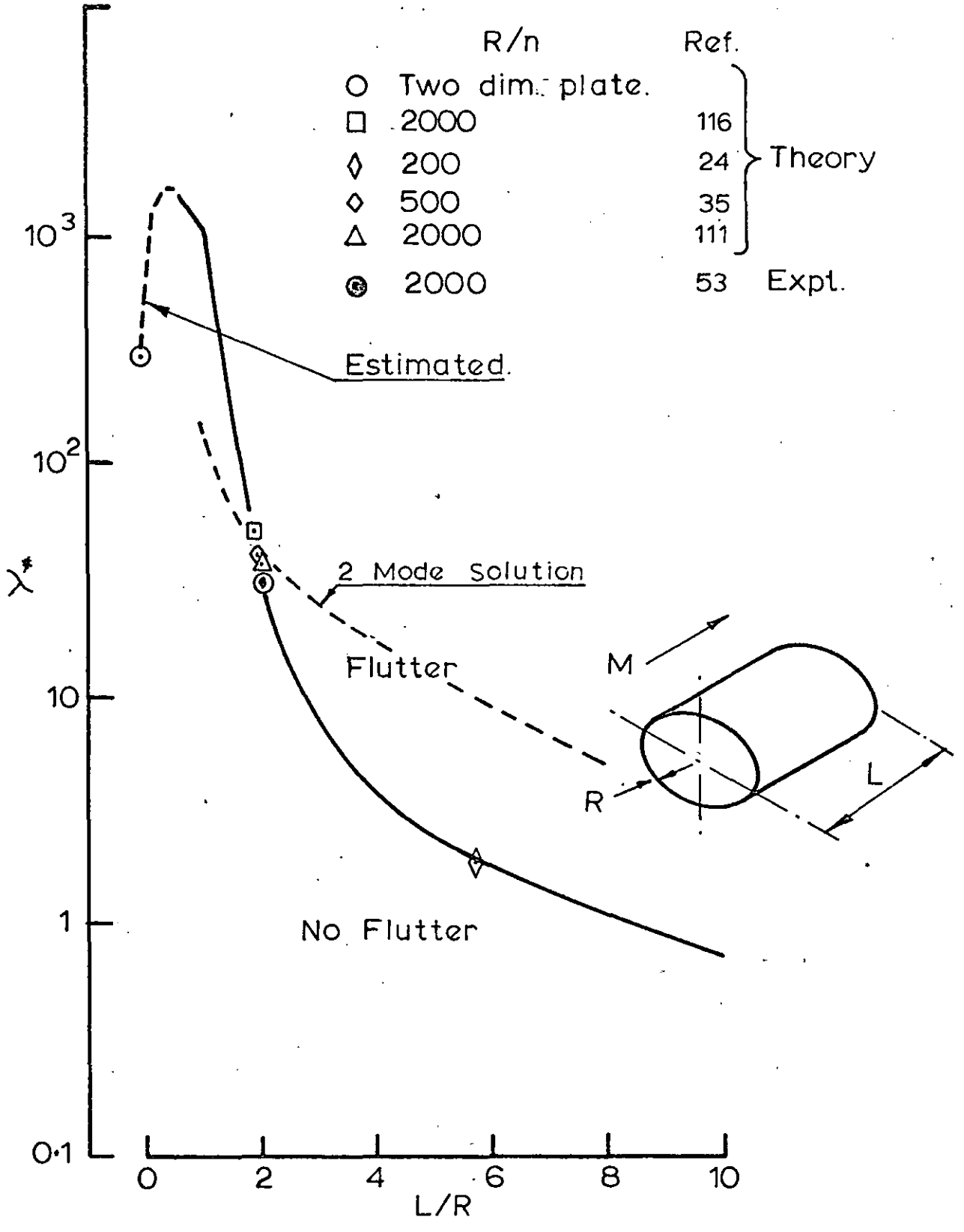

FIG. 28. FLUTTER BOUNDARIES FOR SIMPLY SUPPORTED UNSTIFFENED CYLINDERS.

(REF. 141).

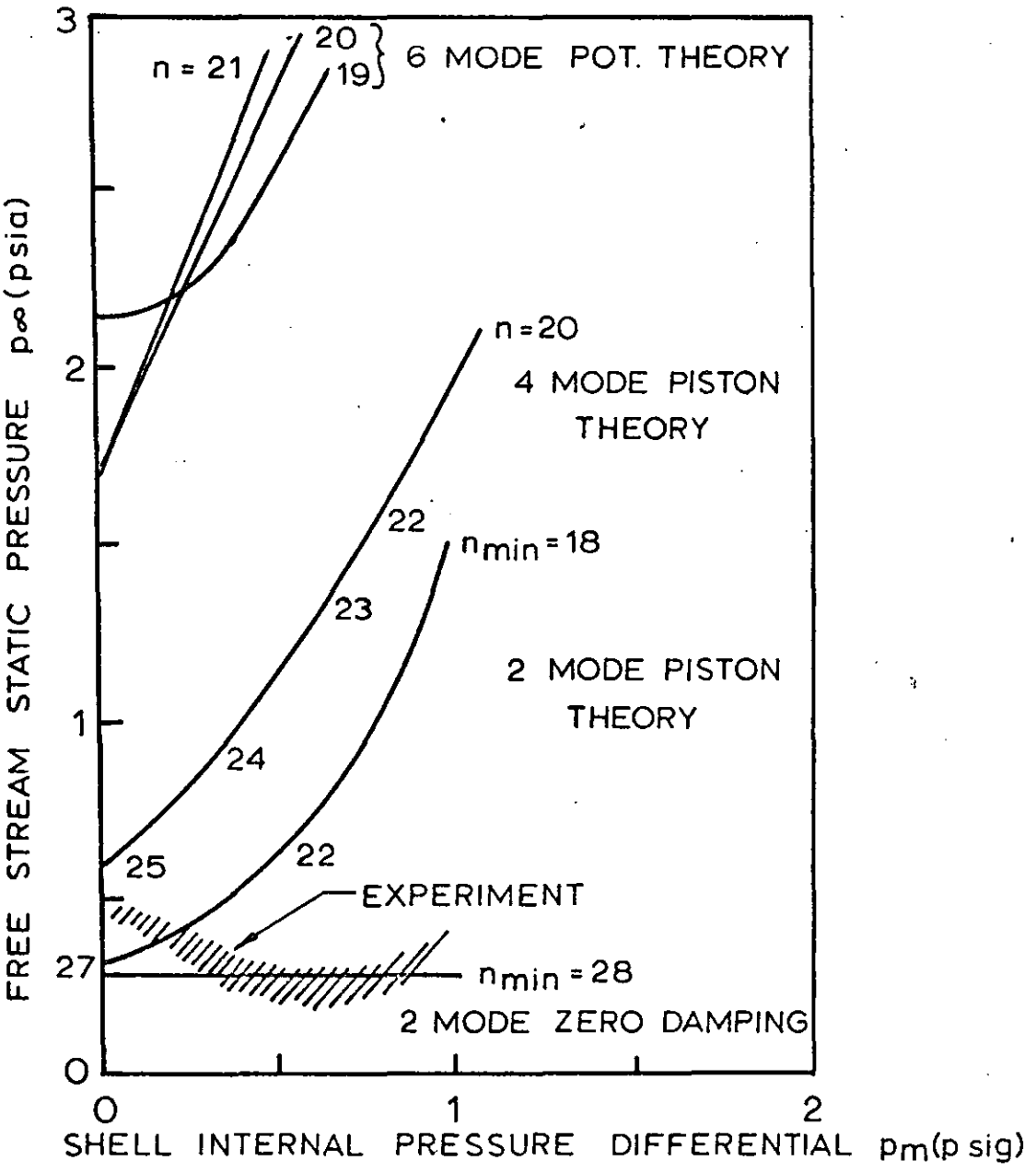

FIG. 29 FLUTTER BOUNDARIES FOR A CYLINDRICAL SHELL AT M=3·0 (ZERO END LOAD). (REF. 116)

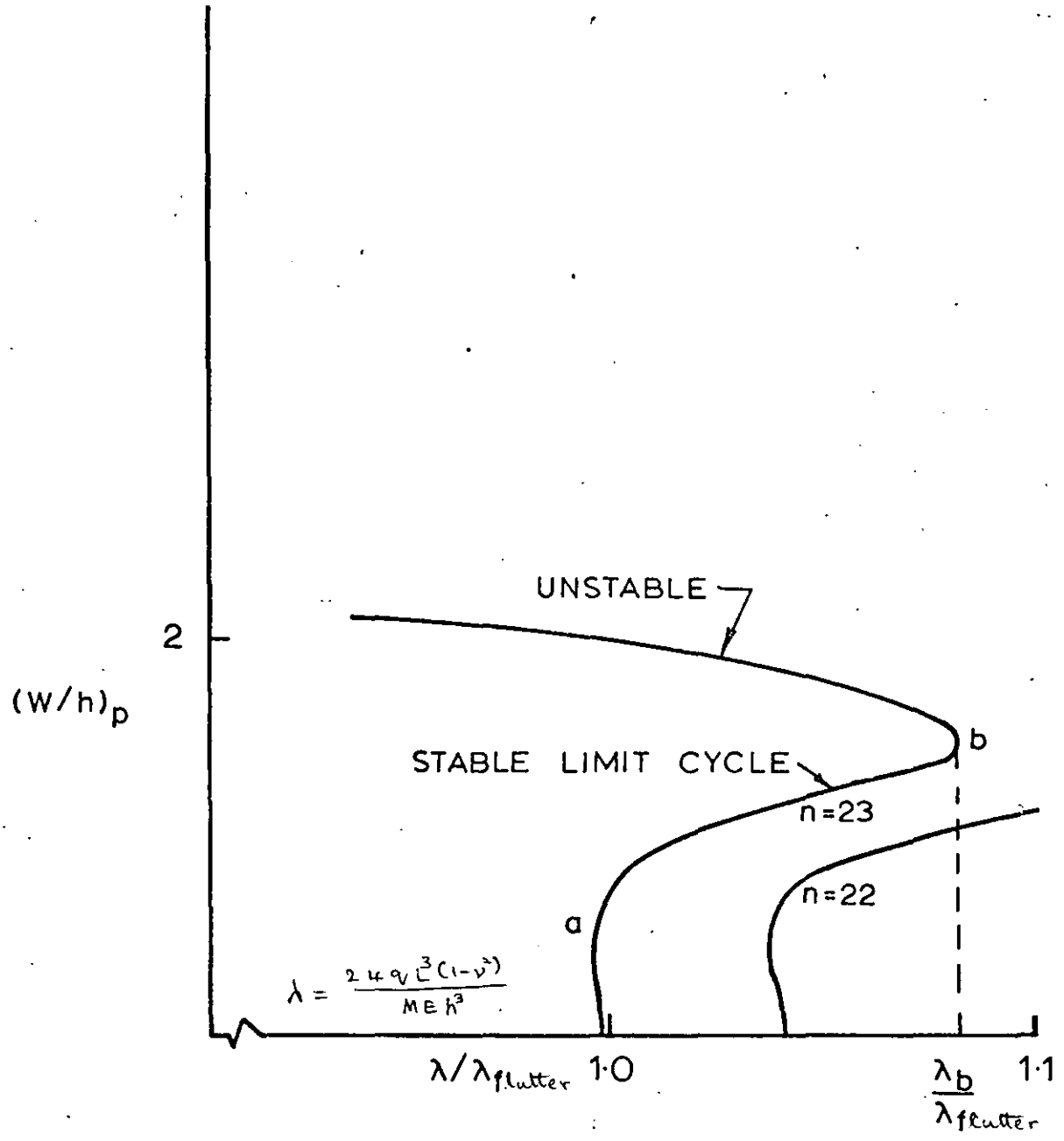

FIG. 30 LIMIT CYCLE AMPLITUDE VERSUS DYNAMIC PRESSURE. (REF. 117)

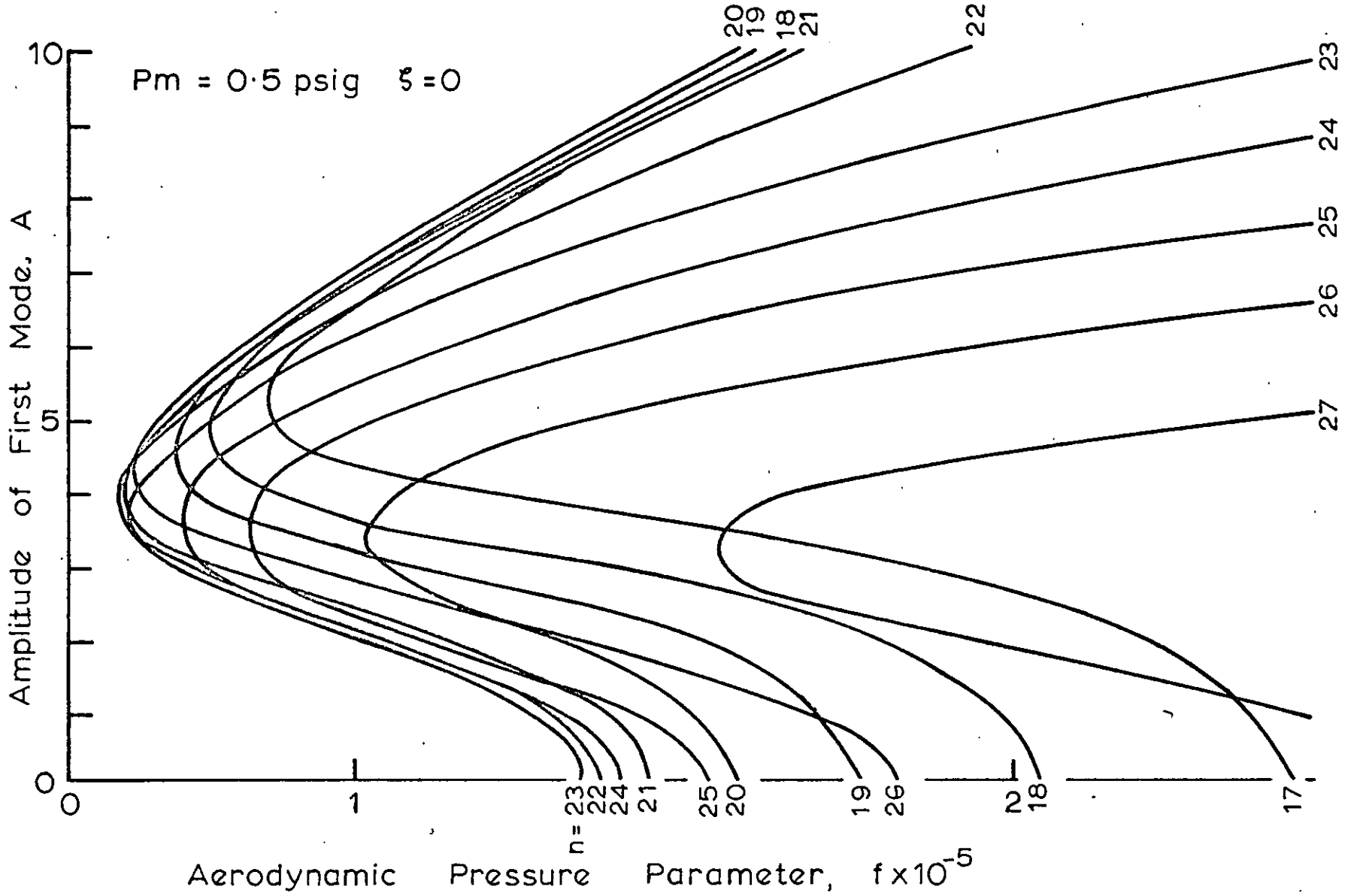

FIG. 31. LIMIT CYCLE AMPLITUDES FOR VARIOUS VALUES OF 'n'. (REF. 115).

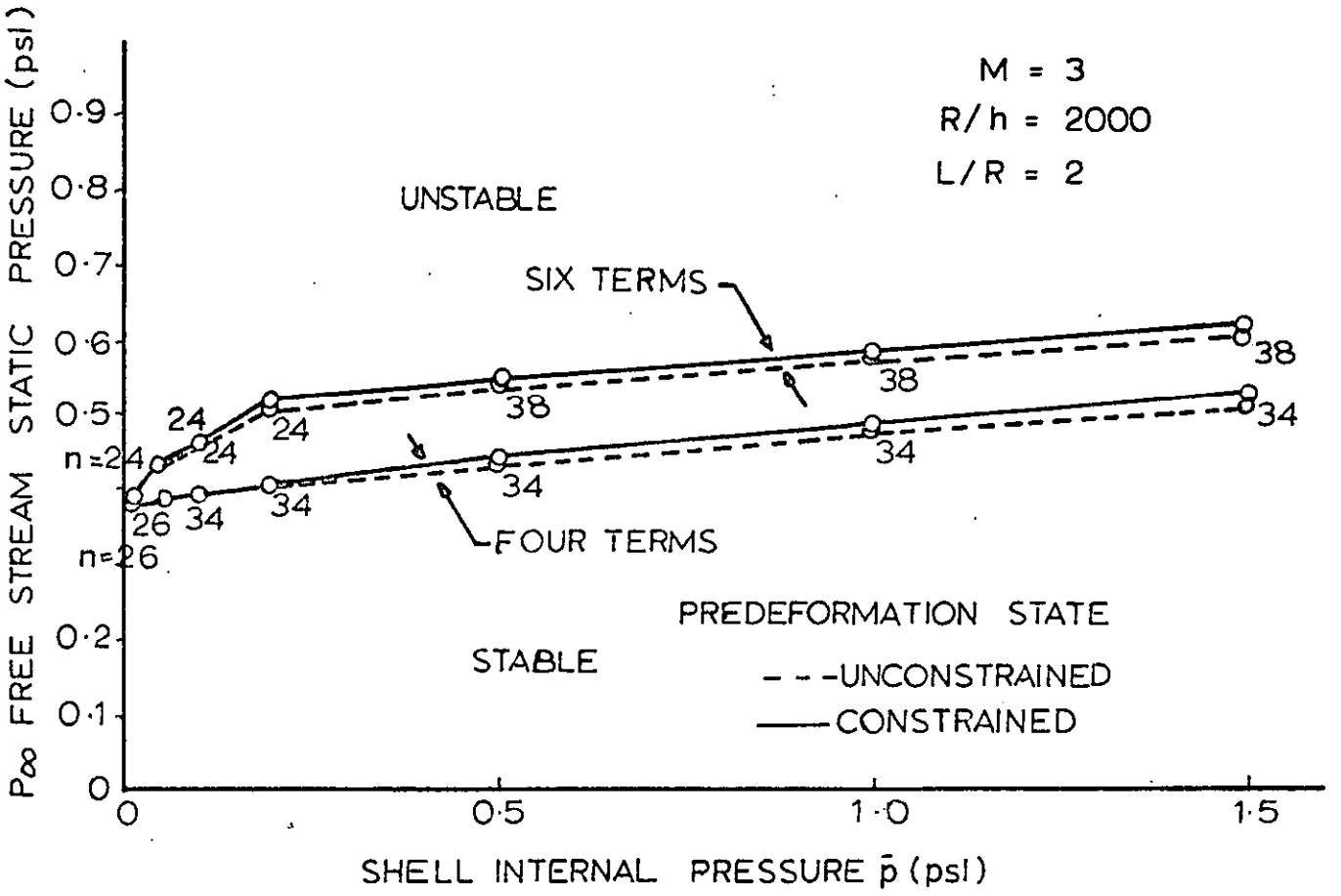

FIG. 32. FLUTTER BOUNDARIES FOR A COPPER CYLINDER. (ZERO TRACTION BOUNDARY CONDITIONS). (REF. 111).

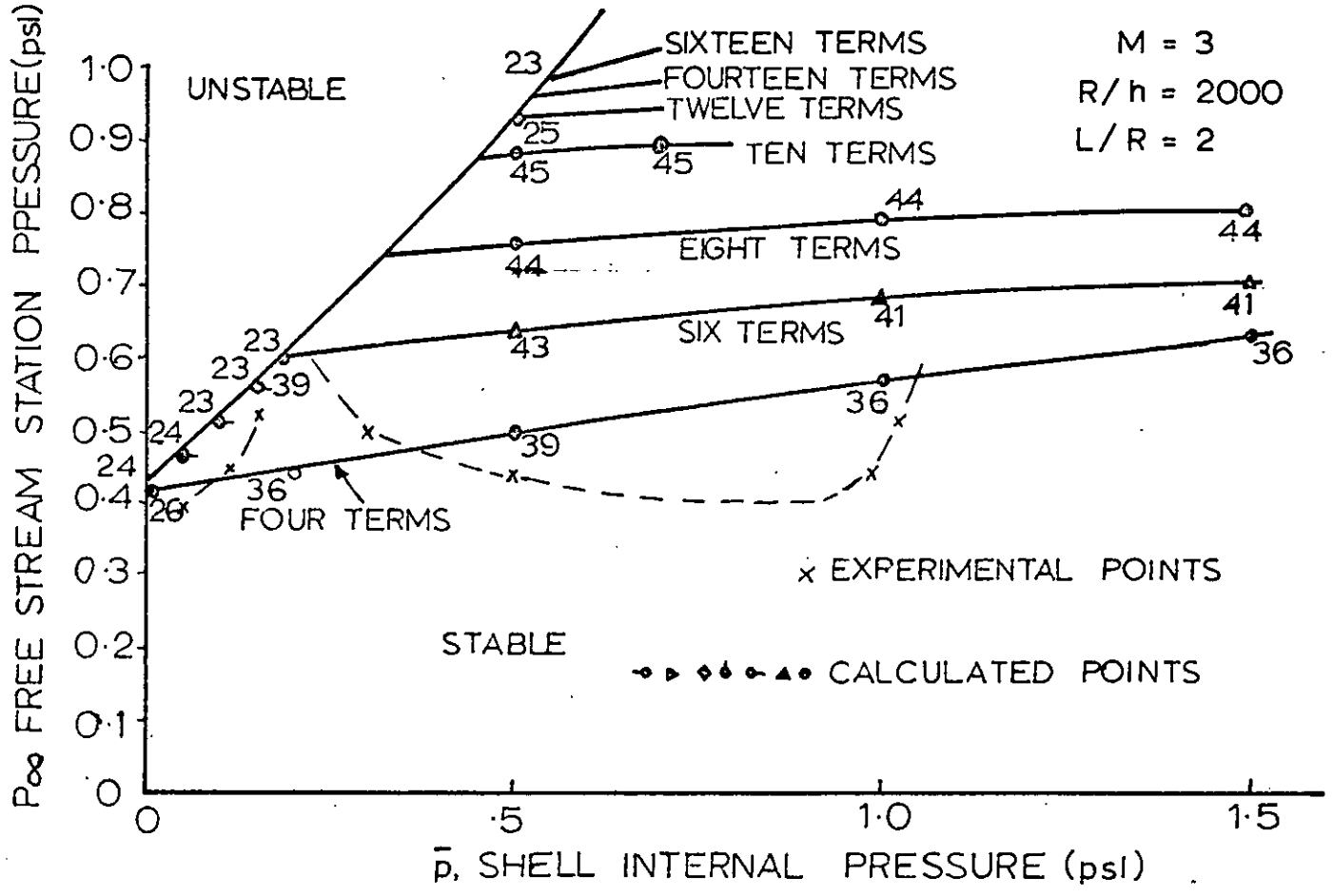

FIG. 33. FLUTTER BOUNDARIES FOR A COPPER CYLINDER. (CLASSICAL BOUNDARY CONDITIONS). (REF. 111).

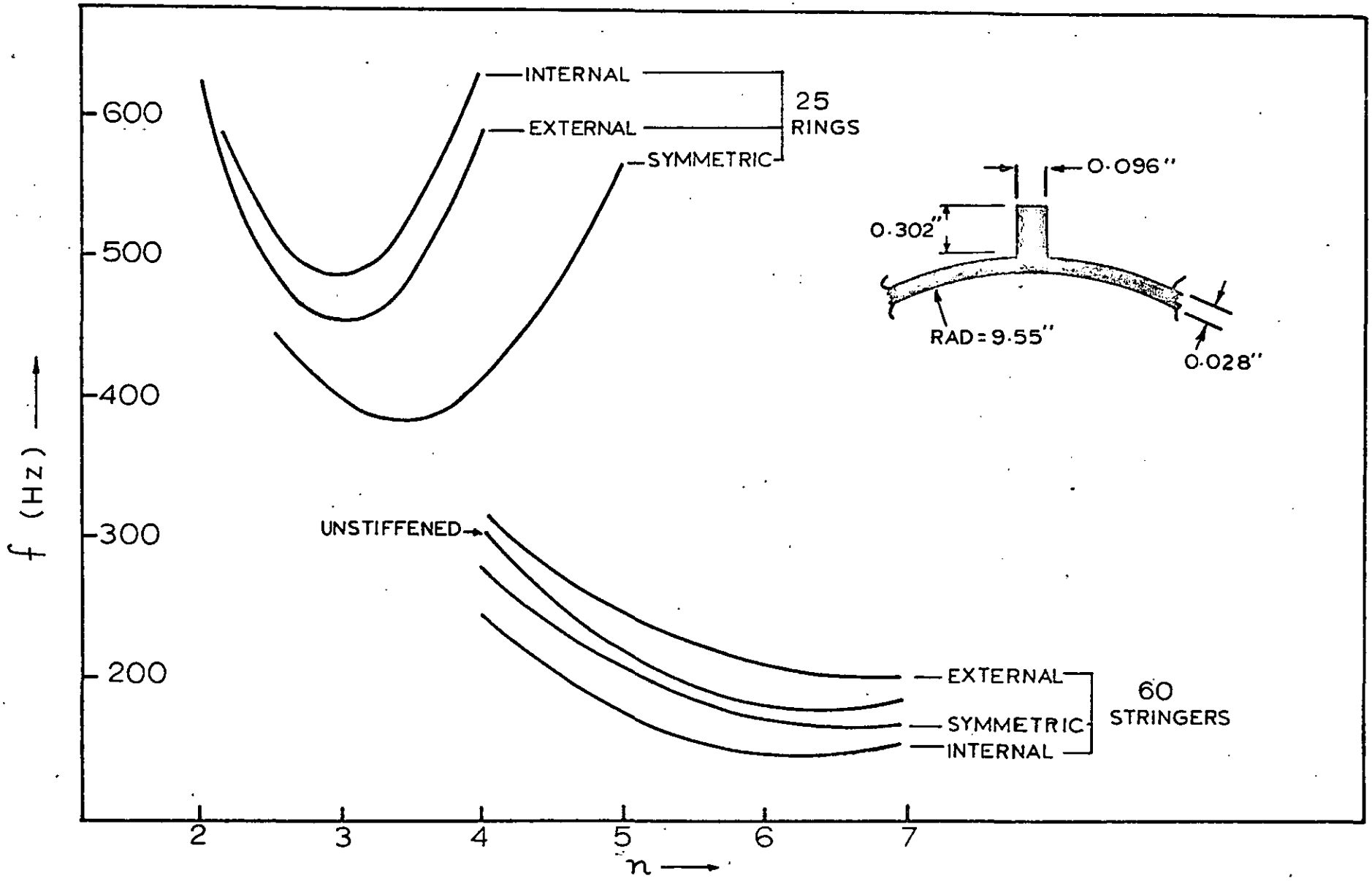

FIG. 34 EFFECT OF STIFFENER CONFIGURATION

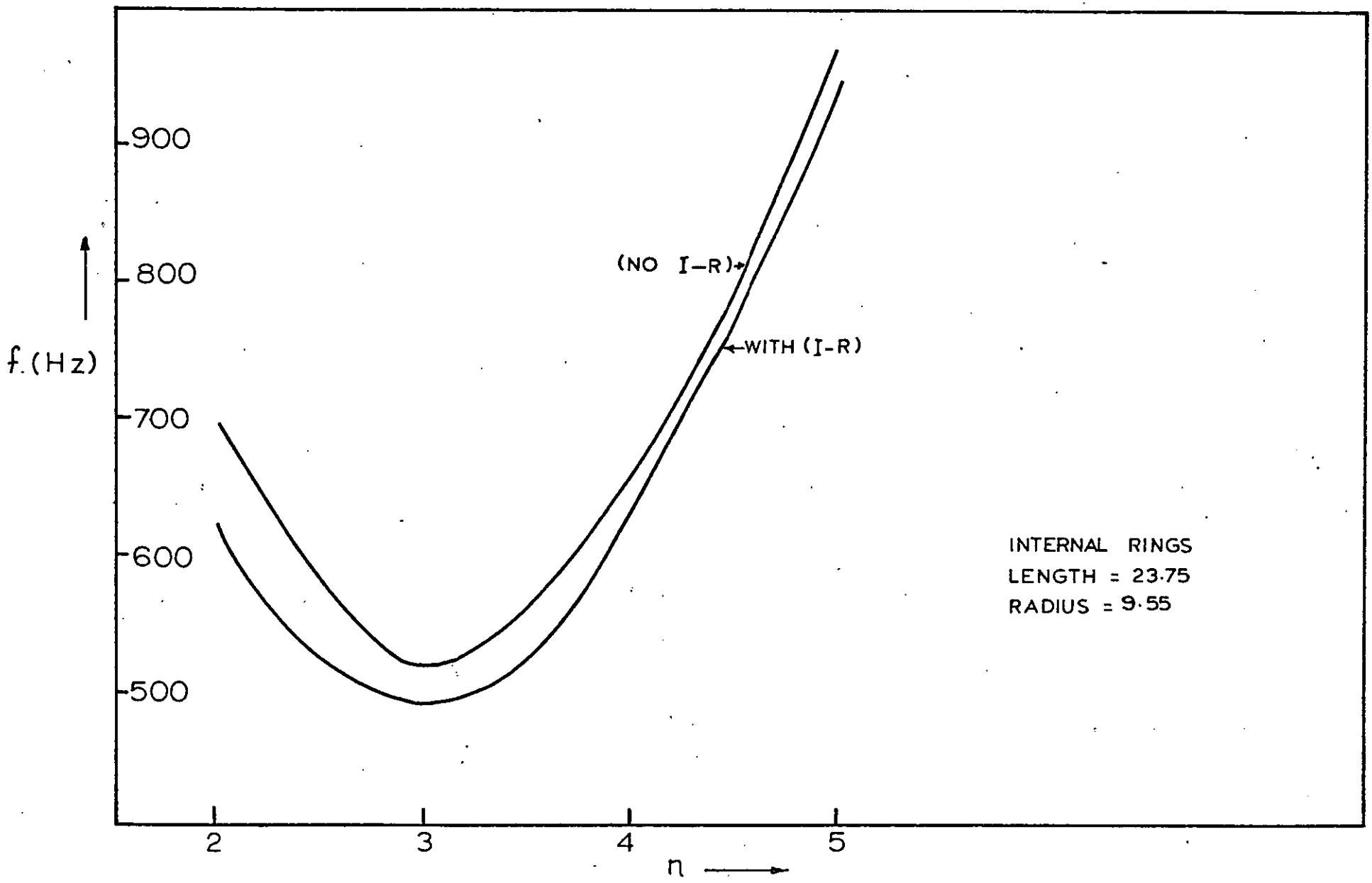

FIG. 35 EFFECT OF INPLANE (I) AND ROTARY (R) INERTIA

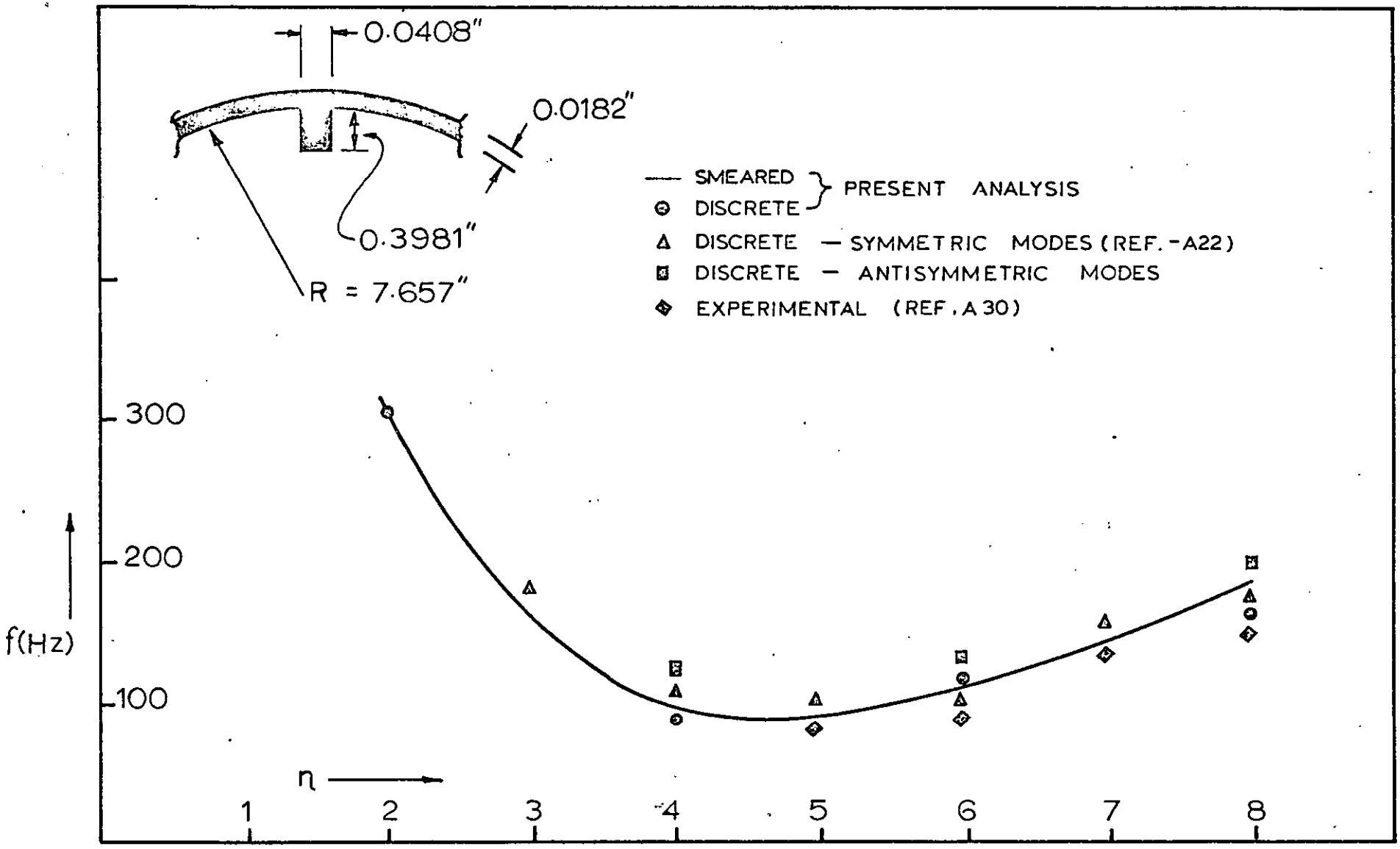

FIG. 36 EFFECT OF DISCRETE AND SMEARED STIFFENING

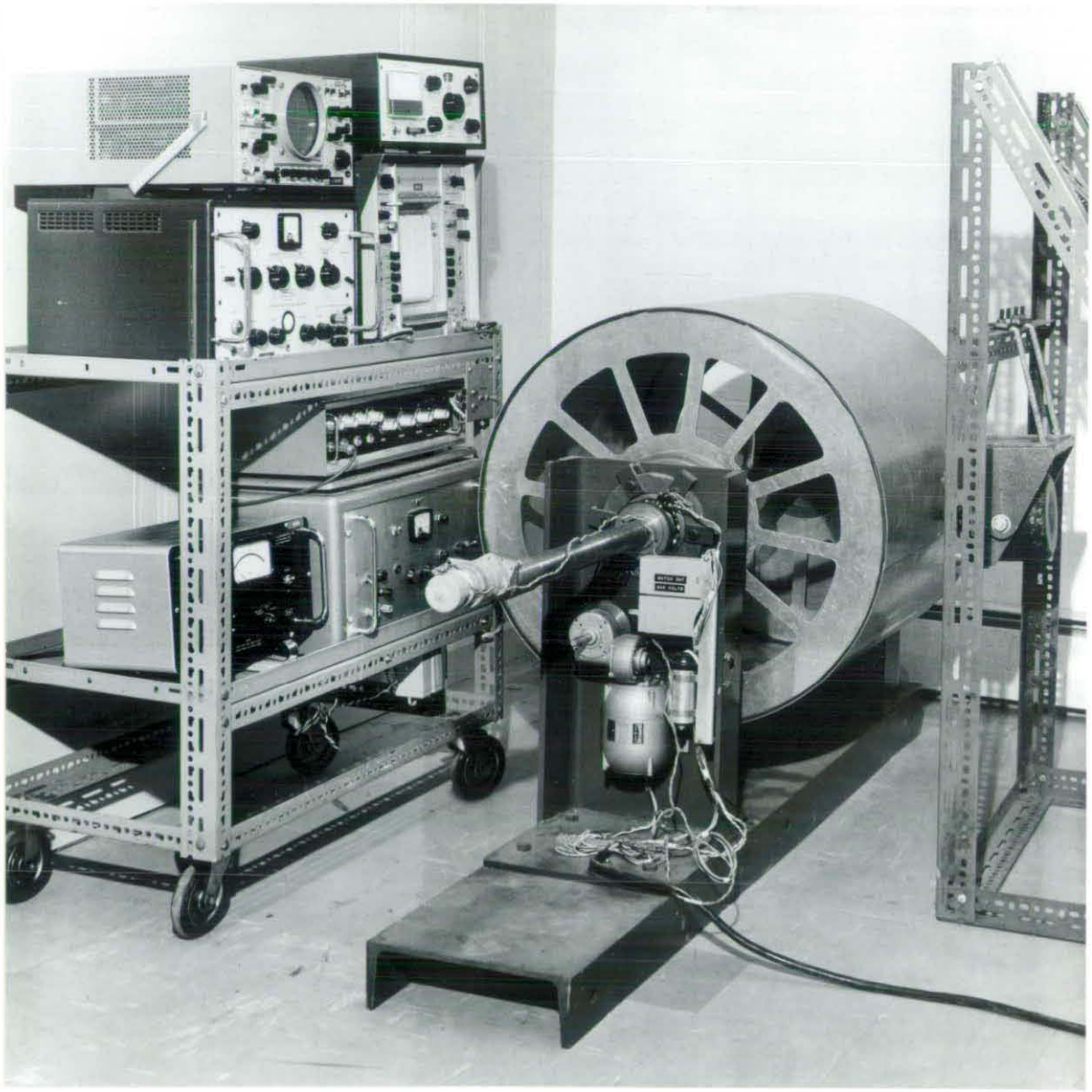

FIG. 37 EXPERIMENTAL SET-UP

FIG. 38 INSTRUMENTATION

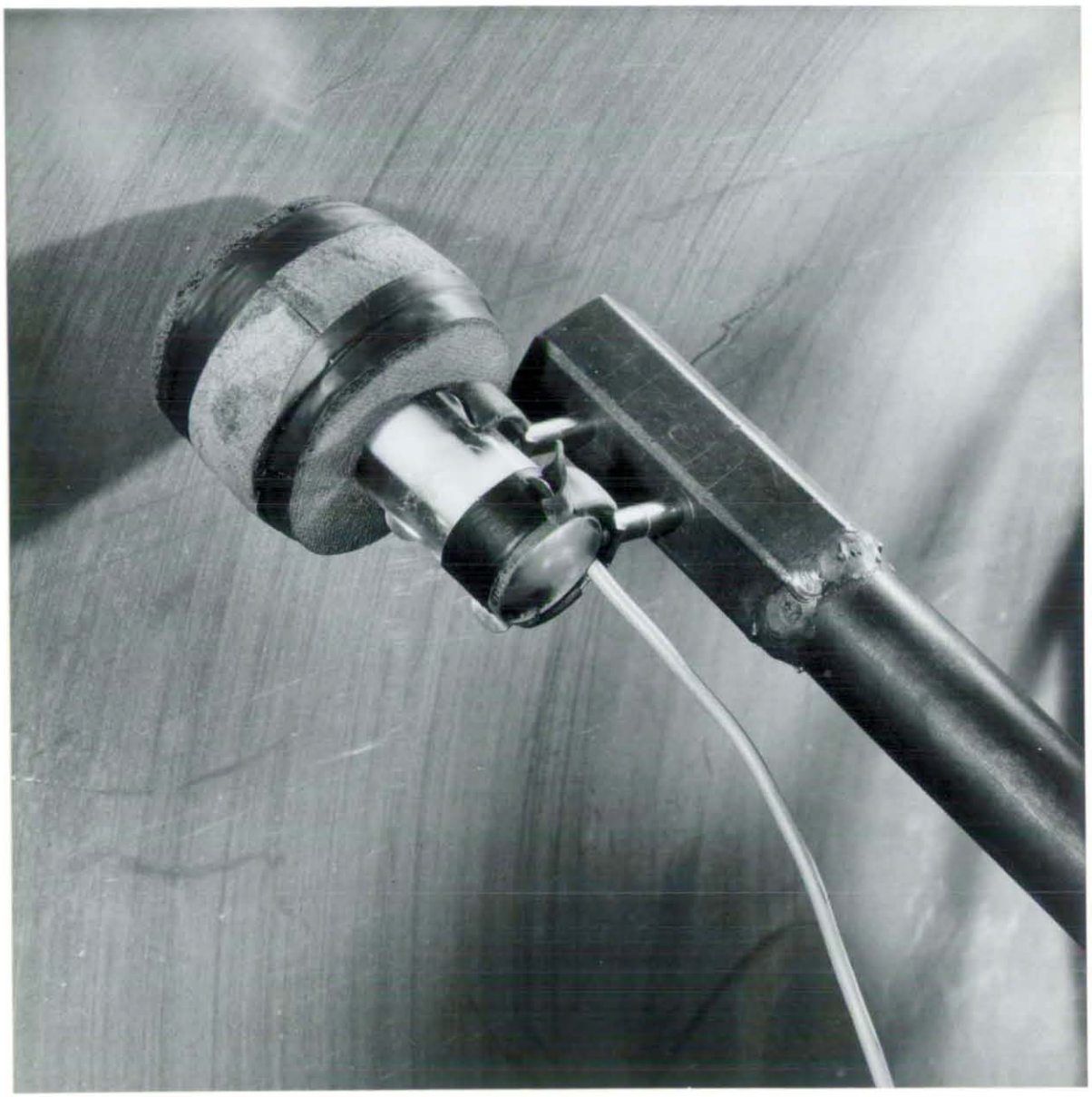

FIG. 39 MICROPHONE INSTALLATION

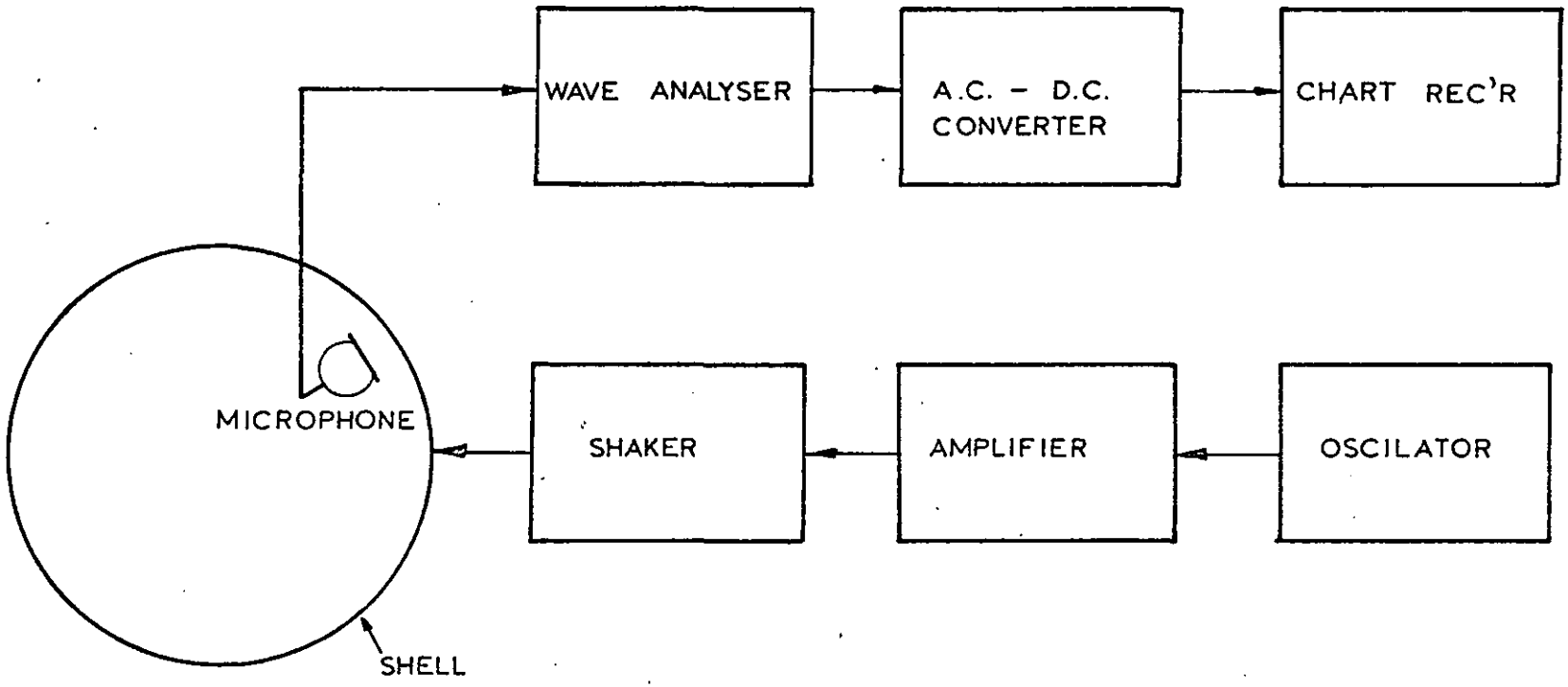

FIG. 40 SCHEMATIC DIAGRAM OF SHELL INSTRUMENTATION

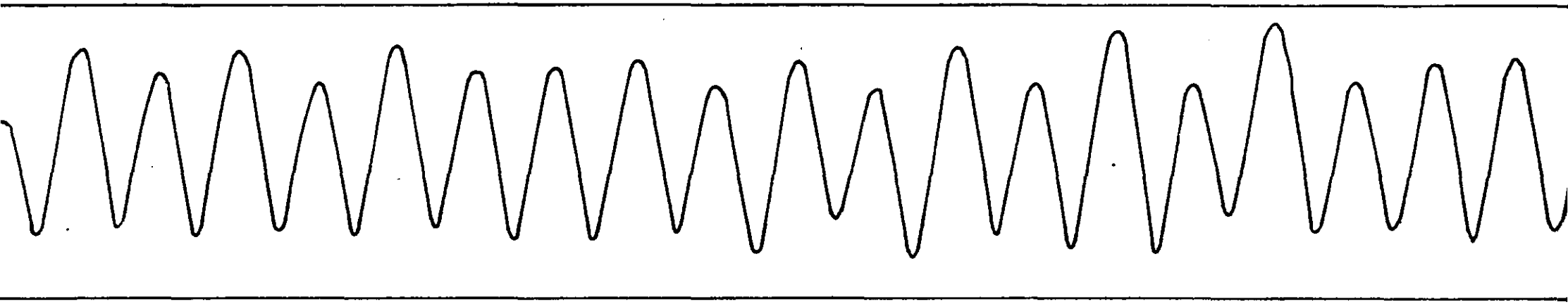

$f = 258 (Hz)$

$n = 10$

FIG. 41 TYPICAL CIRCUMFERENTIAL EXPERIMENTAL MODE SHAPE

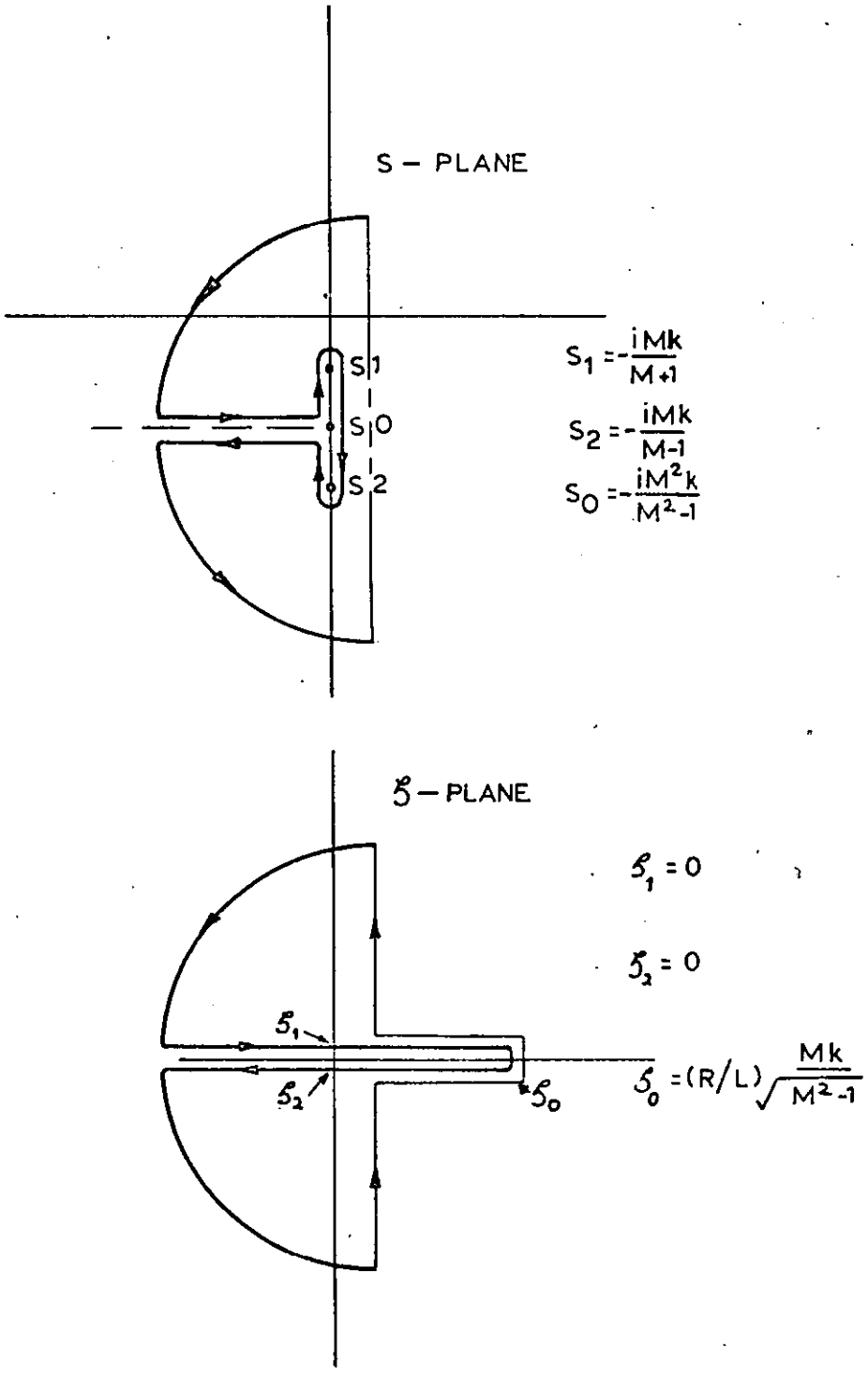

FIG.42 INTEGRATION CONTOUR.

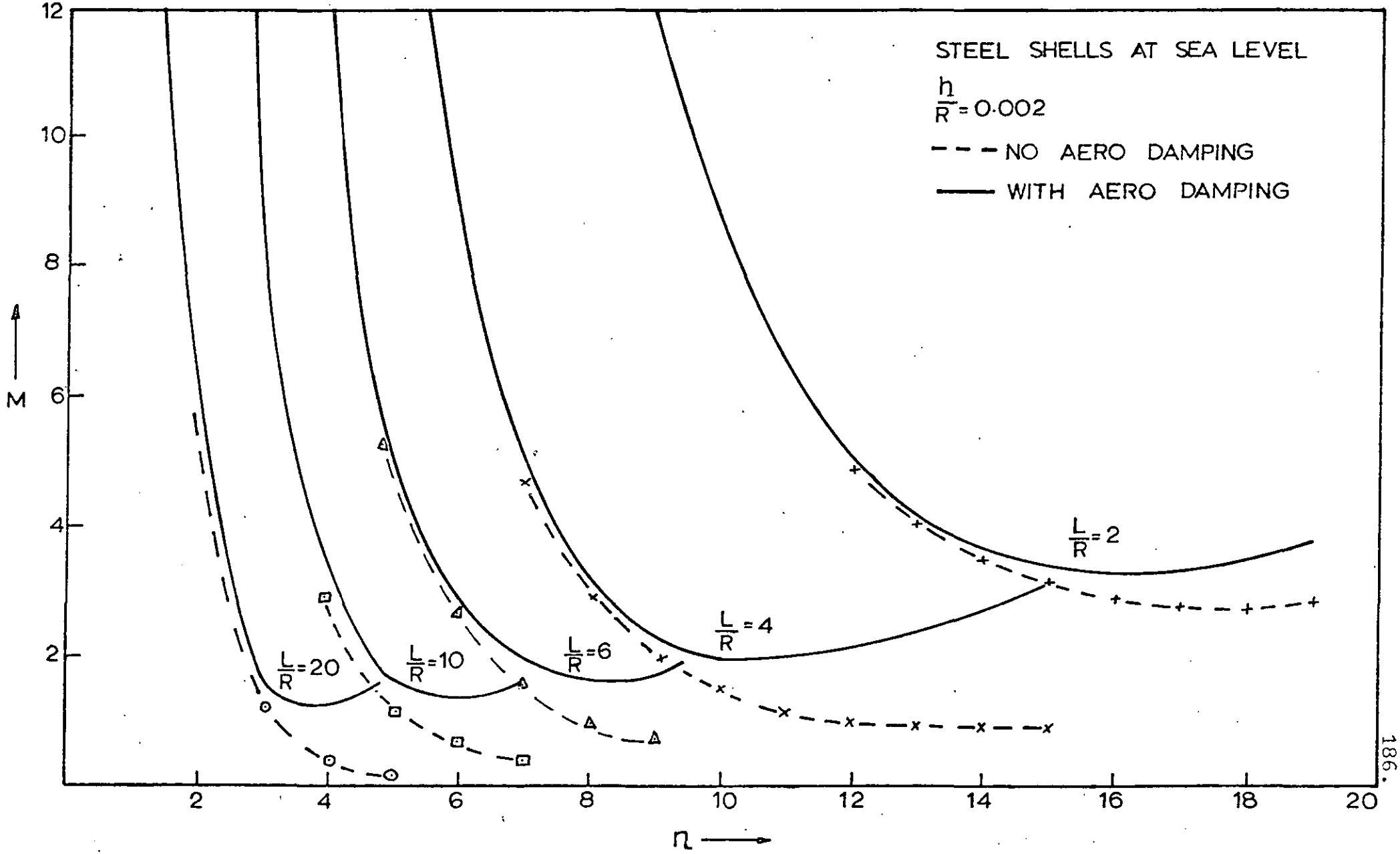

FIG. 43 VARIATION OF CRITICAL MACH NUMBERS WITH CIRCUMFERENTIAL MODE NUMBER

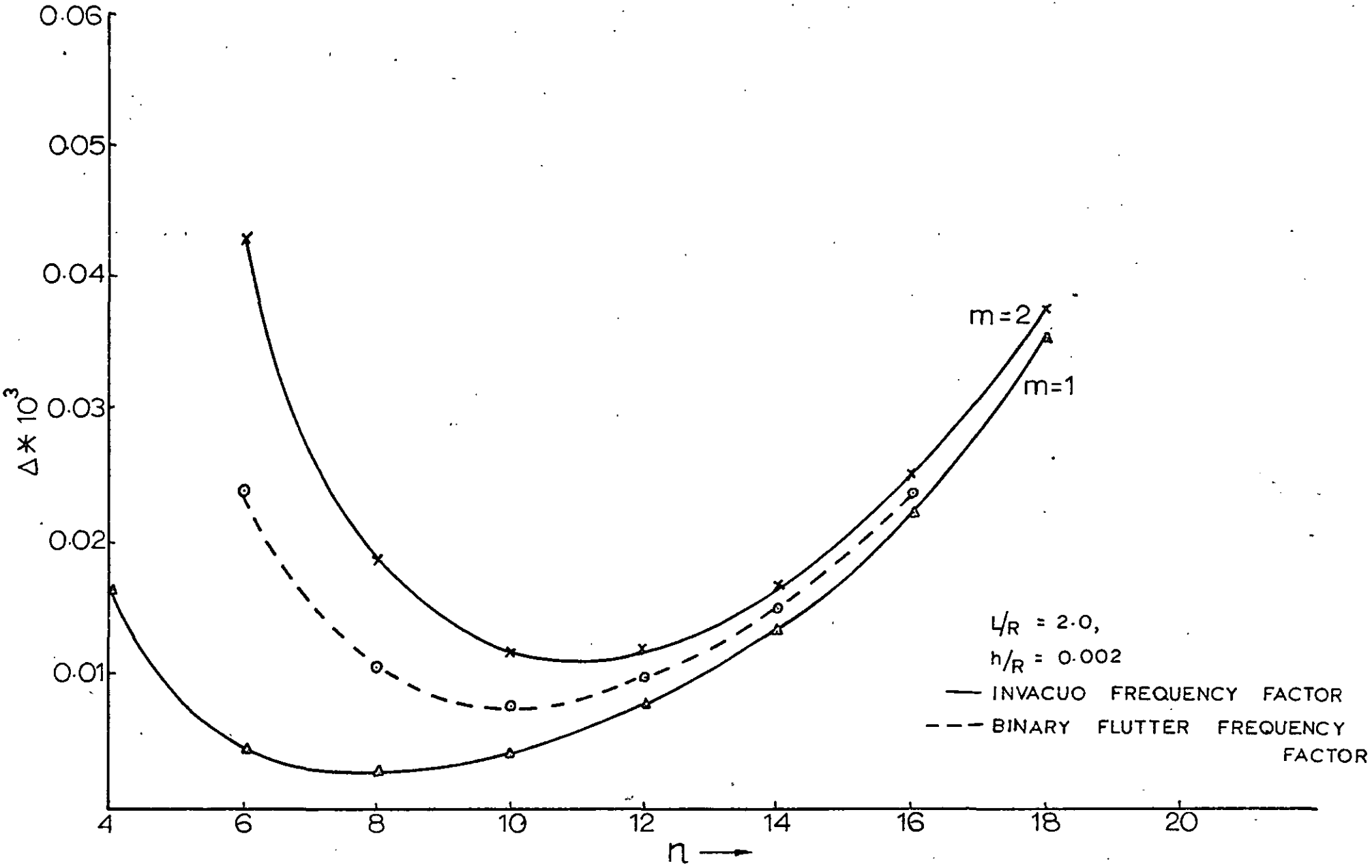

FIG. 44 COMPARISON OF INVACUO NATURAL FREQUENCY AND FLUTTER FREQUENCY FACTORS

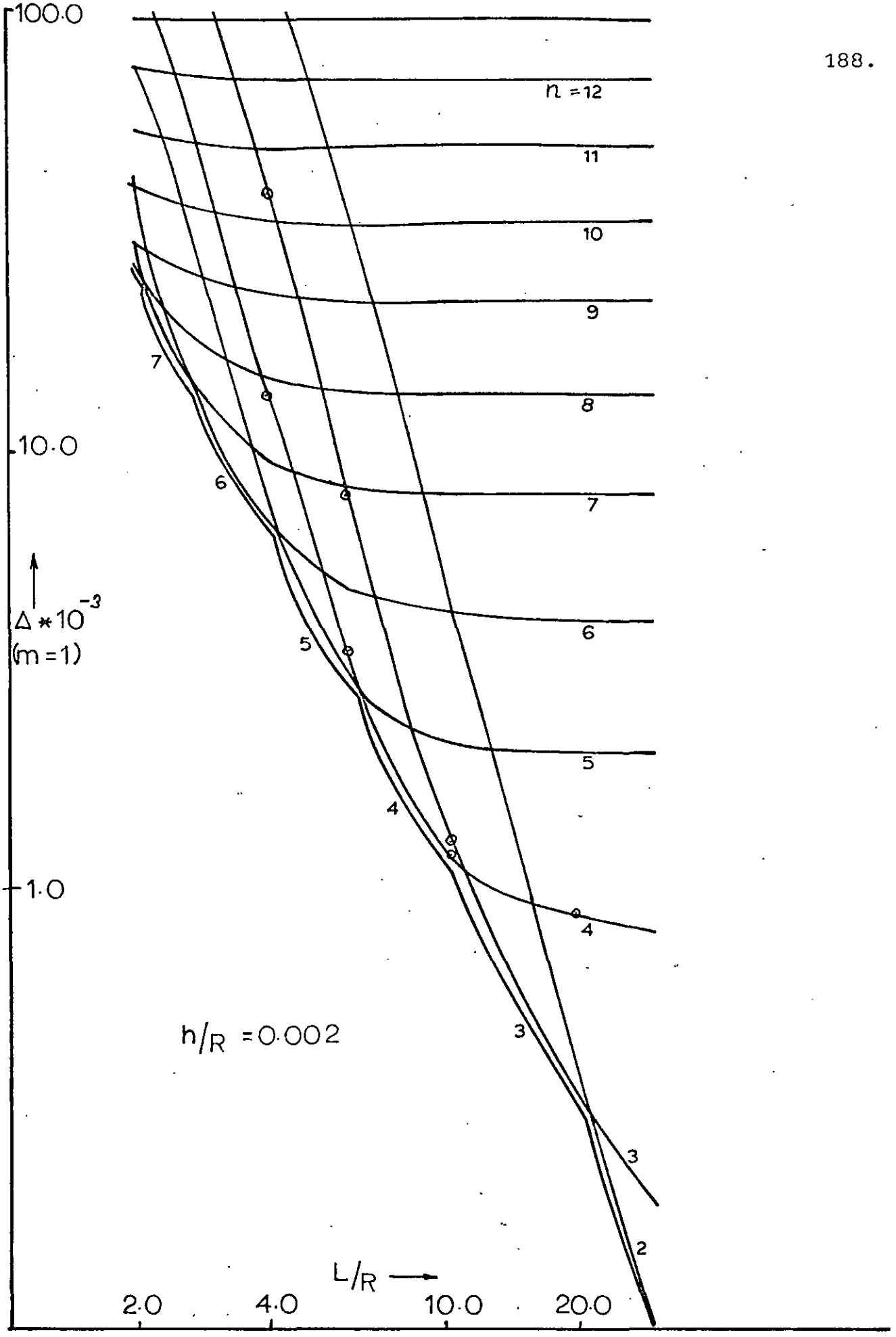

FIG. 45 INVACUO-NATURAL FREQUENCY ENVELOPE FOR A SIMPLY SUPPORTED CYLINDRICAL SHELL

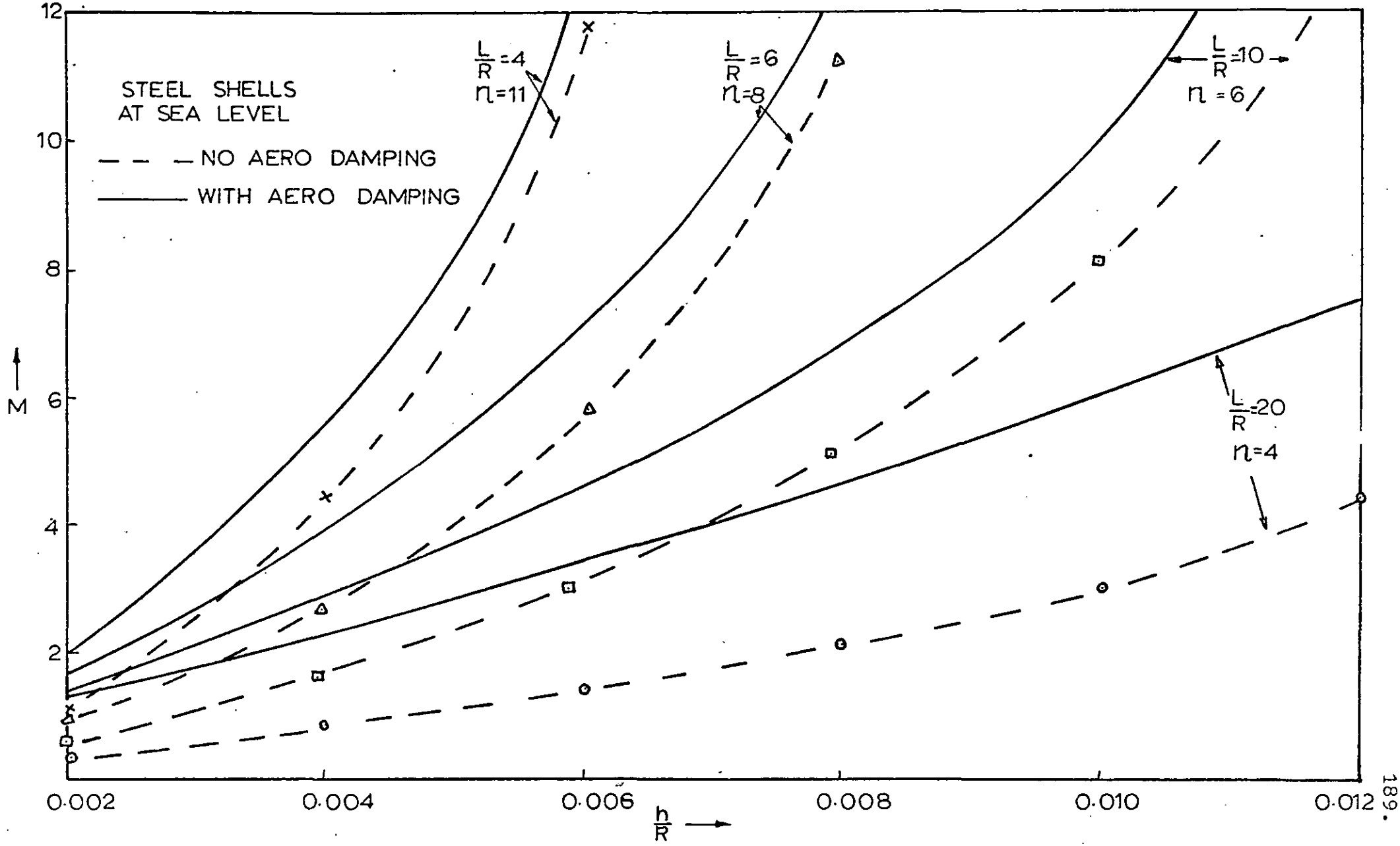

FIG. 46 FLUTTER BOUNDARIES USING LINEAR PISTON THEORY IN A BINARY ANALYSIS

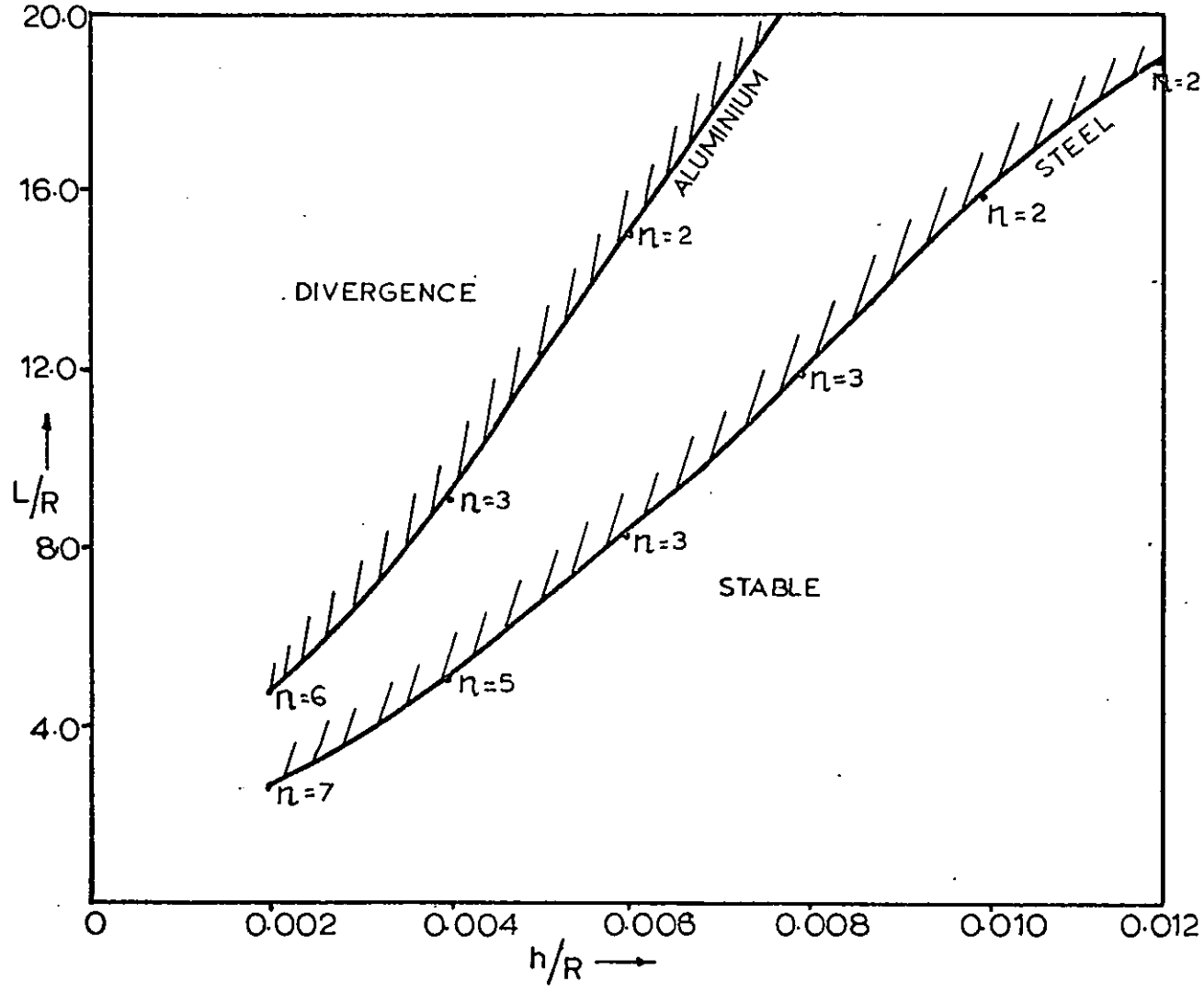

FIG.47 SINGLE DEGREE OF FREEDOM DIVERGENCE BOUNDARIES

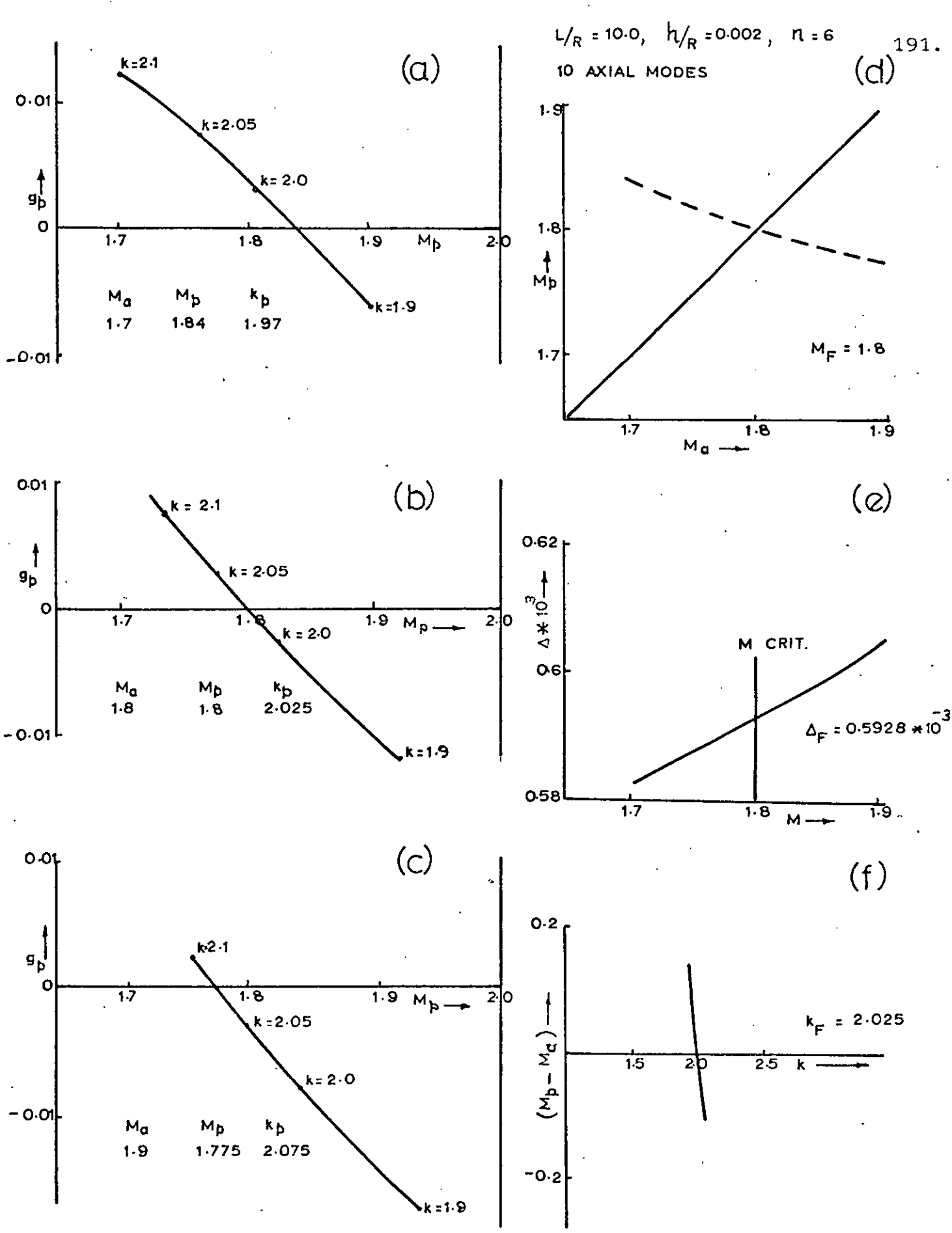

FIG. 48 TYPICAL U—g PLOTS TO DETERMINE THE CRITICAL FLUTTER PARAMETERS OF A CYLINDRICAL SHELL